AN EXAMINATION OF TRAUMATIC MANDIBULAR FRACTURE USING THREE-DIMENSIONAL FINITE ELEMENT ANALYSIS

GLADSTONE ATHELSTONE EZRA BURKE

A thesis submitted in partial fulfilment of the requirements of
Birmingham City University
for the degree of Doctor of Philosophy

August 2014

Faculty of Health, Birmingham City University

TABLE OF CONTENTS

Gladstone Athelstone Ezra Burke

Title

AN EXAMINATION OF TRAUMATIC MANDIBULAR FRACTURE USING THREE-DIMENSIONAL FINITE ELEMENT ANALYSIS

Abstract

The pattern of mandibular fractures is related to the magnitude, direction and duration of impact, which are features of the mechanism of injury. The multiplicity of injury mechanisms makes it difficult to determine if an anatomical sub-site has a greater propensity to fracture.

Traditionally biomechanical investigations on bony structures have involved cadaveric mechanical testing which is expensive, labour intensive and ethically questionable. Computer trauma modelling using three-dimensional finite element analysis has the advantage of avoiding such investigations. Such models have potential use in the medico-legal and forensic fields where they may aid in the determination of proximate and ultimate causation of injuries.

The main objectives of this research were threefold. Firstly, to develop a three-dimensional finite element model (3DFEM) of the adult human mandible, capable of simulating traumatic mandibular fracture resulting from impacts at various sites and angulations. Secondly, to use the 3DFEM to predict fracture sub-sites and temporal occurrence of mandibular fractures in a simplified traumatic simulation. Finally, the model was applied to possible clinical scenarios.

METHOD

A computed tomographic scan of the facial skeleton of a 17 yr-old male was used as a data source for the production of the finite element model. Finite element meshes were generated from the 3D reconstructed data. The assembled mandibular model was composed of 1183976 linear tetrahedral elements and 250523 nodes. The applied material properties were derived from the literature.

Finite element simulations were performed with the mandible loaded at various sites (symphysis, parasymphysis, body, angle and ramus) with varying angulations. Von Mises stress was used as a failure criterion. Static and dynamic 3D-finite element analyses of simplified loading situations were undertaken in order to predict the anatomical sub-site and temporal occurrence of fractures. The effect of localized changes in material properties was also modelled.

RESULTS

A 3DFEM of a human mandible was produced which allowed the examination of mandibular fracture under experimental loading conditions. Each load produced a unique cortical stress “signature”. In simplified trauma situations, non-linear dynamic analyses were able to give the disposition and temporal occurrence of fractures. The model did not simulate all patterns of mandibular fracture. Several patterns, especially those, which are encountered clinically, are due to indirect contacts with other parts of the facial skeleton, which was not modelled in the simulations. The modelled fracture patterns and loads were similar to those encountered in mechanical testing of cadaveric mandibles published in the literature.

CONCLUSION

A 3DFEM used to study mandibular fracture was developed. The model was capable of studying the effect of impact magnitude, direction and duration on the mandibular fracture pattern. Although this was a simplified model, the principles involved in modelling bony fractures on a macroscopic scale may be of use in larger models of the facial skeleton. This would be of even greater clinical value. The mandibular model itself has the potential to provide useful biomechanical information for use in the forensic sciences and medico-legal practice.

Acknowledgements

I should like to say thank you to the following people:

Professor Betsy Dumont of the Department of Biology, University of Massachusetts, Amherst, the doyen of biological three-dimensional finite element analysis, for introducing me to the field and giving advice on how to approach this research area.

I would also like to thank my supervisors Professors Robert L Ashford and Clive E Neal – Sturgess for arranging the facilities to embark on research in an area new to the Faculty of Health, also, Mr Aaron Latty (Strand7®, UK), Mr Carl Hitchens (formerly of Materialise, UK) and Mr Paul Booth (formerly of Birmingham City University) for providing access to software.

I also greatly appreciate those patients who gave consent for their radiographs to be used in this thesis. And finally, special thanks to the late Bruce Elson, formerly Principal Lecturer at Birmingham City University for facilitating this project.

Published material related to thesis

The contents of some of this thesis (principally Phase IIIa results) have been accepted for presentation at the XXV Congress of the International Society of Biomechanics in Glasgow, UK, July 2015. Copyright is assumed by ISB 2015 for publication of the abstracts on their website and Book of Abstracts.

LIST OF CHAPTER CONTENTS

LIST OF FIGURES

LIST OF TABLES

LIST OF GRAPHS

LIST OF EQUATIONS

Abbreviations

$\mu\varepsilon_{vm}$	von Mises micro strain
3DFEA	Three-dimensional finite element analyses
3DFEM	Three-dimensional finite element model
A_m	Muscle cross-sectional area
ASCII	American Standard Code for Information Interchange
CAD	Computer-aided design
CAM	Computer-aided modelling
CBCT	Cone-beam computed tomography
CR_m	Muscle contraction ratio
CT	Computed tomography
DICOM	Digital Imaging and Communications in Medicine
E_f	Final energy
E_{fr}	Frictional energy
E_i	Initial energy
E_{km}	Kinetic energy of the mandible
E_s	Strain energy
F_m	Muscular force
F_v	Resultant muscle force vectors
GPa	Giga Pascals
HU	Hounsfield Units
ICD	International Statistical Classification of Diseases and Related Health Problems
IGES	Initial Graphics Exchange Specification
JPEG	Joint Picture Expert Group
K	Skeletal muscle constant

KE	Kinetic Energy
MeSH	Medical Subject Heading
MPa	Mega Pascals
MRI	Magnetic resonance imaging
n	Total number of subjects in study
NLM	National Library of Medicine
NURBS	Non-uniform Rational B-Spline
OPCS	Office of Population Censuses and Surveys
r	Number of subjects with outcome
R_c	Resultant of orthogonal components
ROI	Region of interest
STL	Standard Tessellation Language
TMJ	Temporomandibular joint
v_f	Final velocity
v_i	Initial velocity
VM	von Mises
VRML	Virtual reality mark-up language
WHO	World Health Organization
W_{net}	Net work
ΔE_{kf}	Difference in kinetic energy of the fist
ε_1	Maximum principal strain
ε_3	Minimum principal strain
ε_{lat}	Lateral strain
ε_{long}	Longitudinal strain
ε_{vm}	von Mises strain
ε_y	Estimated yield strain

$\dot{\varepsilon}$	Strain rate
σ	Stress vector
σ_1	Maximum principal stress
σ_3	Minimum principal stress
σ_c	Compressive stress
σ_{max}	Maximum stress
σ_t	Tensile stress
σ_{VM}	Von Mises stress

Orientation of the mandible

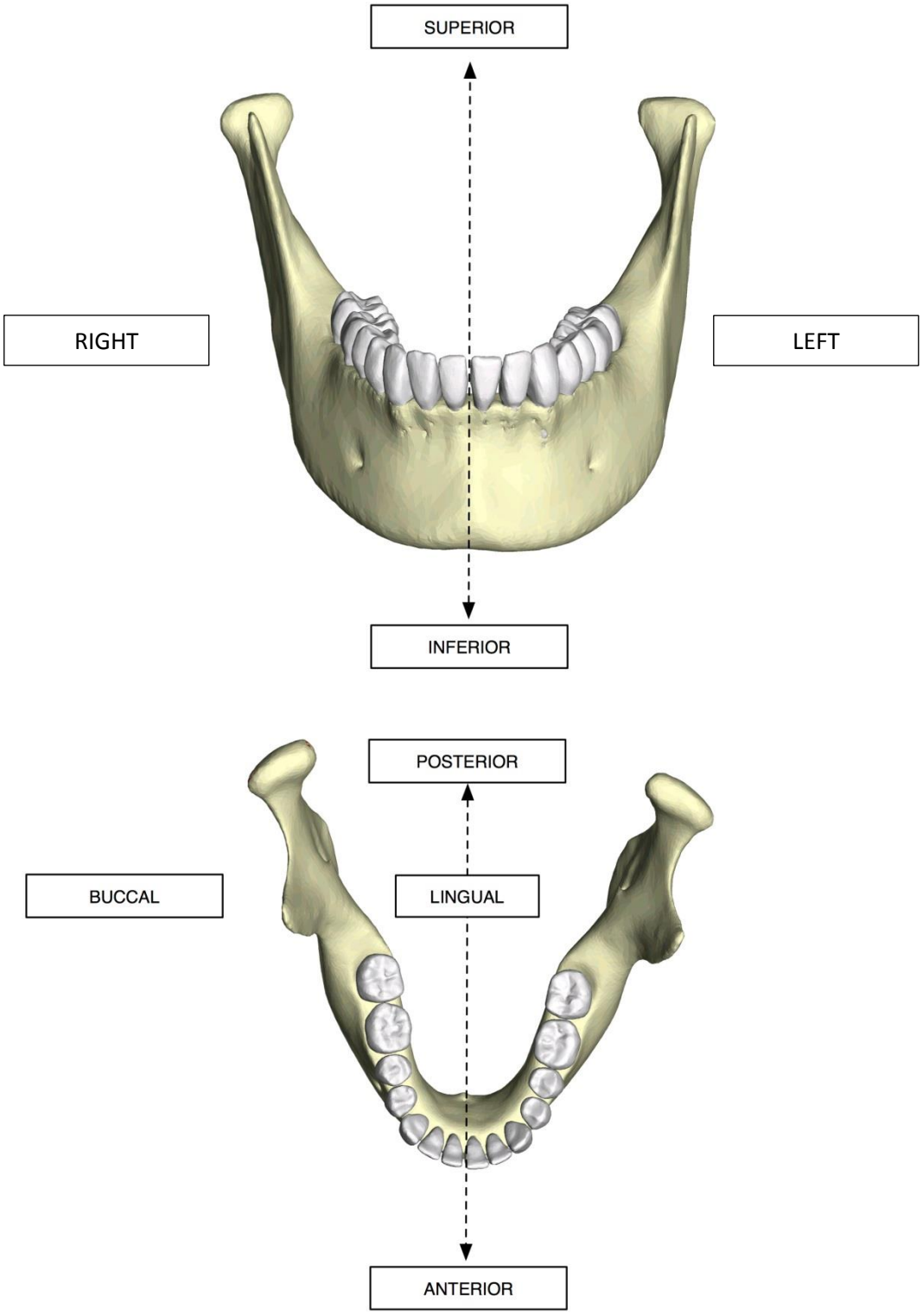

Chapter 1 Introduction

1.1 Research area

The aim of this thesis is to research the application of a computational method, namely three-dimensional finite element analysis (3DFEA), to mandibular biomechanics, with particular emphasis on the evolution and examination of fractures resulting from physical trauma.

Until fairly recently, most information regarding the response of the mandible to traumatic loading was derived from laboratory experiments involving cadaveric material or anthropometric dummies. The experiments of Nahum, (1975) and Schneider et al. (1974) provide data which is still used today to derive tolerance thresholds for mandibular bone.

Mechanical laboratory studies, whether using animals, human cadavers or dummies, have proved to be expensive, difficult to conduct with a great deal of precision or accuracy, and of dubious value biomechanically when compared to live human cases. Additionally, in many societies ethical issues preclude physical traumatic experimentation of humans and animals. As a consequence, mechanical laboratory studies are currently the gold standard for investigation of fracture thresholds in humans.

Finite element analysis was developed as a computational technique by Courant in the 1940s and applied by Turner, Clough, Martin and Topp in the late 1950s to study material stiffness. Initially its use was limited to the automotive, aeronautical, nuclear, and defence industries to evaluate stress or temperature distribution in mechanical components; perform deflection, vibration and fatigue analyses; and kinematic and/or dynamic responses of components in failure prediction. The relatively large computing

power required at the time limited its widespread use. Today the declining cost of computing means that such analyses may be performed on relatively low cost personal computers. 3DFEA is now used in the biological sciences to study extant and extinct organisms. It is possible to model the distribution of stress, strain and deformation throughout anatomical structures. Currently 3DFEA is not routinely used in medical or forensic practice. The lengthy modelling process and long computation times have limited its utility. However, the potential for measuring biological performance in modelled traumatic situations is appealing.

Head impact biomechanical simulations using 3DFEA have been used in the past as forensic tools for reconstructing brain injuries (Motherway et al., 2009) and as part of expert witness evidence in medico-legal cases (De Santis Klinich, K.D., and Hulbert, G. M., 2002), however, as of yet, no mandibular models have been produced and used with the same effect.

This thesis will aim to study structural performance of the mandible with the main aspect being structural failure resulting in fracture. The results required to do this will include the effect of magnitude, direction, duration and physical geometry of impact forces on the geometry and severity of mandibular injuries.

1.2 Research relevance

As previously mentioned, the majority of mechanical tests on biological structures are undertaken in the laboratory setting. The tissues of explanted human or animal tissue must undergo complex preparation procedures before being fit for investigation. This may affect the ability of the tissues to satisfactorily reproduce the in vivo response. There are additional issues when the biomechanical responses required relate to tissues which have unique or rare properties. In such cases there will be insufficient material to

test mechanically. At present, logical extrapolation of current normal data offers the only solution.

Computer modelling of biological structures may be a solution to these problems. If a suitable model could be produced that was capable of replicating the response of the mandible under certain conditions then there would be little need for human or animal models. With the ability to change material properties and model rare conditions there would be supporting evidence for theoretical extrapolations. There would also be a commensurate reduction in time and expense, making the modelling of multiple scenarios a possibility, aiding the determination of potential mechanisms of injury.

1.3 Research application

The mandible is the second most commonly fractured bone in the facial skeleton. The leading cause of fracture is mechanical impact. The most commonly reported impact sources are interpersonal violence, road traffic accidents, falls and sporting injuries, although the relative frequencies of each source vary between studies. In many situations where bodily injuries result there may appear to be a straightforward relationship between the assumed mechanism and the resulting injuries found on examination. However, the assumed cause of injuries is open to misinterpretation, with similar injury patterns found on routine investigations resulting from different mechanisms and vice versa (Gordon and Shapiro, 1975).

In the field of forensic science the elucidation and prediction of the biomechanics of the mandible can aid the understanding of fracture mechanisms resulting from physical trauma. Results such as the derivation of relative fracture thresholds are particularly important.

Medical expert witnesses are frequently asked questions regarding the likelihood of a particular mechanism of injury, or the magnitude of force required to produce the injury. Biomechanical data may be used to support or refute a potential mechanism of injury in addition to being used to produce computer simulations which may be used to explain a mechanism of injury to a jury.

At present, few authors have published finite element studies attempting to simulate traumatic impacts on the mandible. Models have described the stress distribution on the mandibular cortex; however, fracture patterns and temporal occurrence have not been modelled. The effects of muscles, teeth, material properties and strain rate have also not been modelled. This research hypothesizes that these deficiencies may be addressed by producing a model that can simulate the biomechanical behaviour of the mandible under load and predict the occurrence of fractures in laboratory and selected clinical situations.

The finite-element method, has been successfully used to study stress, strain and material fracture in the field of engineering, and theoretically may be used to model fractures in biological structures. This is based on the premise that the laws of physics and Newtonian mechanics are universal. As the veracity of this premise has yet to be disproved, one might hypothesize that the research goal is possible, subject to the availability of the required input parameters.

The initial model which this thesis aims to produce and test should be relatively rudimentary, relying on simplified analyses. The final model should be scalable and allow investigation beyond the scope of the initial research area.

1.3.1 Possible research scenarios

Examples of scenarios envisaged for this research include two cases presented below.

a) A dentist extracted a right molar tooth in a young man. Apparently the procedure was routine and completed without complication. A week later the patient complained of a pain in the contralateral parasymphysis of the mandible. After radiographic examination of the area, it was found that there was an ectopic tooth with a minimally enlarged follicle in the area of the fracture. The patient decided to take legal action and an expert witness was asked to provide information on whether the dentist had used excessive force or improper technique during the extraction or whether the ectopic tooth had made the mandible susceptible to fracture.

b) Forensic science deals with the relationship between medicine and law, and whilst much of the work is performed post mortem (Gordon and Shapiro, 1975) the ability to demonstrate the correlation between an assault weapon and injury in live patients is often the requirement of an expert witness. At their best, an expert can only suggest a possible cause of an injury and differentiating between assaults with a foot, a fist, an elbow, a forehead or indeed any other blunt or sharp weapon resulting in a mandibular fracture may be difficult. Any additional supporting evidence would strengthen an opinion.

For the expert witnesses to give the court relevant information, the data required would include:

- The nature of the impacting object
- An estimation of the applied force
- An estimation of the expected strength of a normal mandible
- An estimation of the expected strength of the affected mandible

- A determination of the risk of fracture

The research will be expected to provide sufficient information to answer these questions. The two cases will be reviewed at the end of the research to see how well the research has satisfied these requirements.

1.4 Expected research results

The results of this research will provide data on the forces, displacements, stresses, strains and strain rates associated with mandibular deformation and failure. These values may be used as a measure of performance. Performance is a term borrowed from engineering, but frequently applied to biological systems. It refers to the mechanical efficiency or strength of a specific system. In reference to biological structures such as bone it can refer to the stress which can be withstood without deformation (which may cause system failure) or catastrophic material failure.

The applied use of this research will be to provide a problem-solving environment in which traumatic mechanisms of injury may be investigated whilst changing individual variables such as material properties (local or general), or uncommon conditions resulting in bony failure due to changes in the structural properties of bone, may be studied.

1.5 Research scope

The scope of this research will be limited. This will be necessary due to time and resource constraints. Financial constraints arise from two sources. Firstly, if this research is to be of value to forensic scientists or clinicians undertaking medico-legal work it should be based on equipment that would be within the budget of such professionals. Therefore modest computing equipment is to be used. Whilst software may be

prohibitively expensive if purchased outright, most companies have more reasonable licence leasing schemes at a reduced cost.

Simplified loading scenarios will be examined. Impacts will only be examined in the horizontal plane and the number of impact sites will be reduced. As a consequence of this, it is not expected that all mandibular fracture patterns will be modelled as these may have an indirect contact component. However, most previous mandibular cadaveric laboratory experiments (the current gold standard) should be capable of reproduction. This should also allow a level of model validation.

Finally, the model produced will be an idealized generic model rather than a patient-specific model, thus generalized conclusions will be drawn, however, the level of generalization will not be so broad as to reduce the value of the research.

1.6 List of chapters

This thesis is divided into six chapters. This chapter has introduced the research area and discussed its relevance. The research scope has also been discussed. Chapter 2 reviews the literature associated with this thesis. It is divided into three sections. The first section discusses the mechanical laboratory studies which the product of this thesis aims to replace. The third section looks at the pattern of fractures encountered clinically. Clinical experience is what most medical expert witnesses will draw upon when determining whether an injury fits a particular mechanism and therefore the prevalence of sub-site fractures, the multifocal mandibular fracture pattern and the effect of localized changes in material properties such as un-erupted third molar teeth, are discussed. A second purpose of this section is to provide a form of clinical validation for the research findings. The intervening second section discusses previous attempts to bridge the gap between laboratory experiments and clinical findings using 3DFEA.

Information gained from this section will also inform Phase Ia of the research –the production of the 3DFEA model.

Chapter 3 describes the methodology to be used throughout the research. Any deviations from the methodology are described in chapter 4 which describes the six research phases undertaken. Research findings and conclusions are found in chapter 5. The thesis itself ends at chapter 6 where limitations and future research are discussed. The bibliography and appendices appear in their respective sections after chapter 6. The appendices contain information regarding the use of the companion disc in addition to basic information on mandibular anatomy, mandibular fracture classifications and engineering principals that will aid the understanding of the thesis. Tabulated raw data from analyses and review protocols are also present. The thesis structure is given in figure 1.1

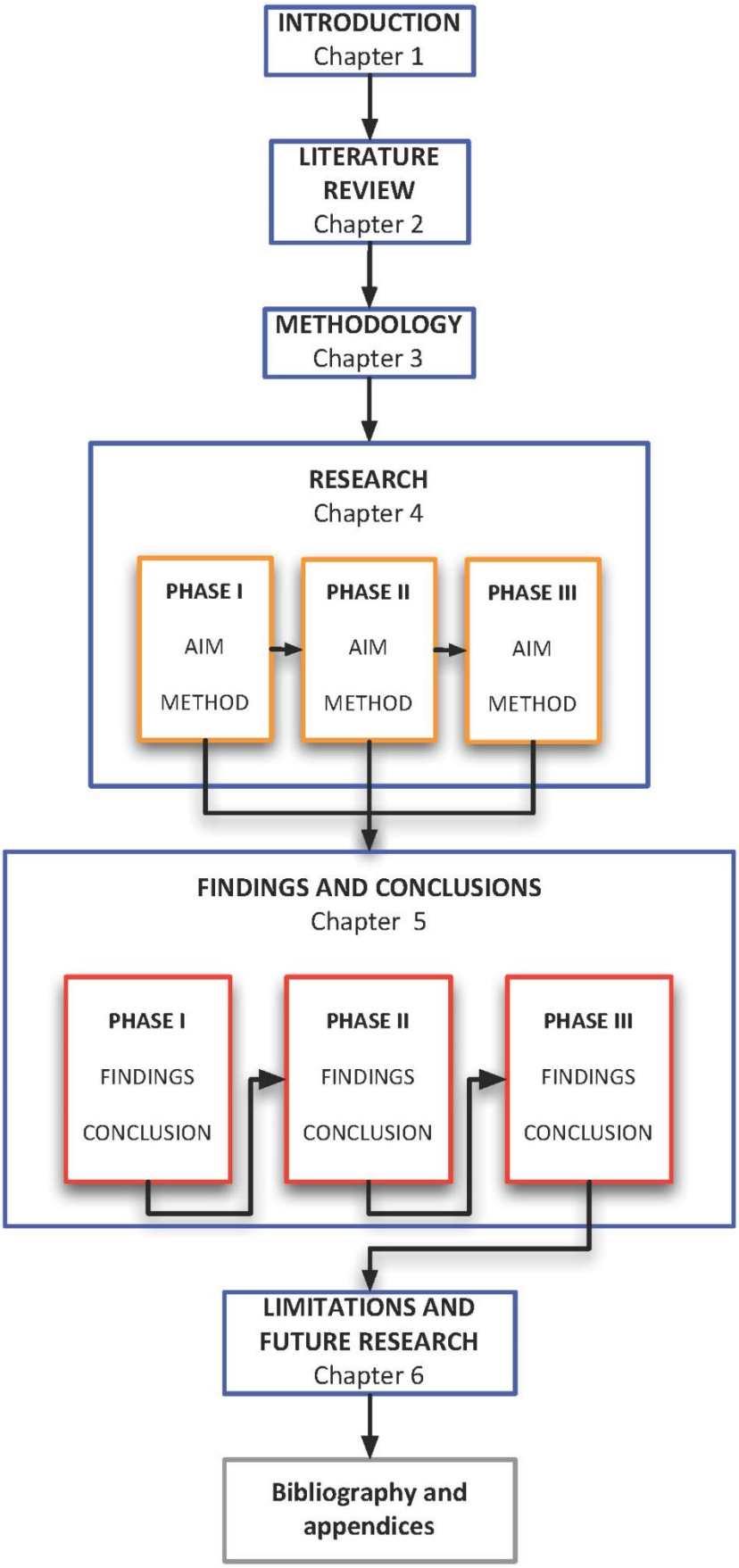

Figure 1.1 Thesis structure

Chapter 2 Literature review

2.1 Structure

This research aims to occupy an area between cadaveric laboratory study of mandibular fractures and epidemiological findings of clinical cases resulting from trauma using the computer modelling technique of three-dimensional finite element analysis. As such the relevant literature is drawn from three areas (see diagram below).

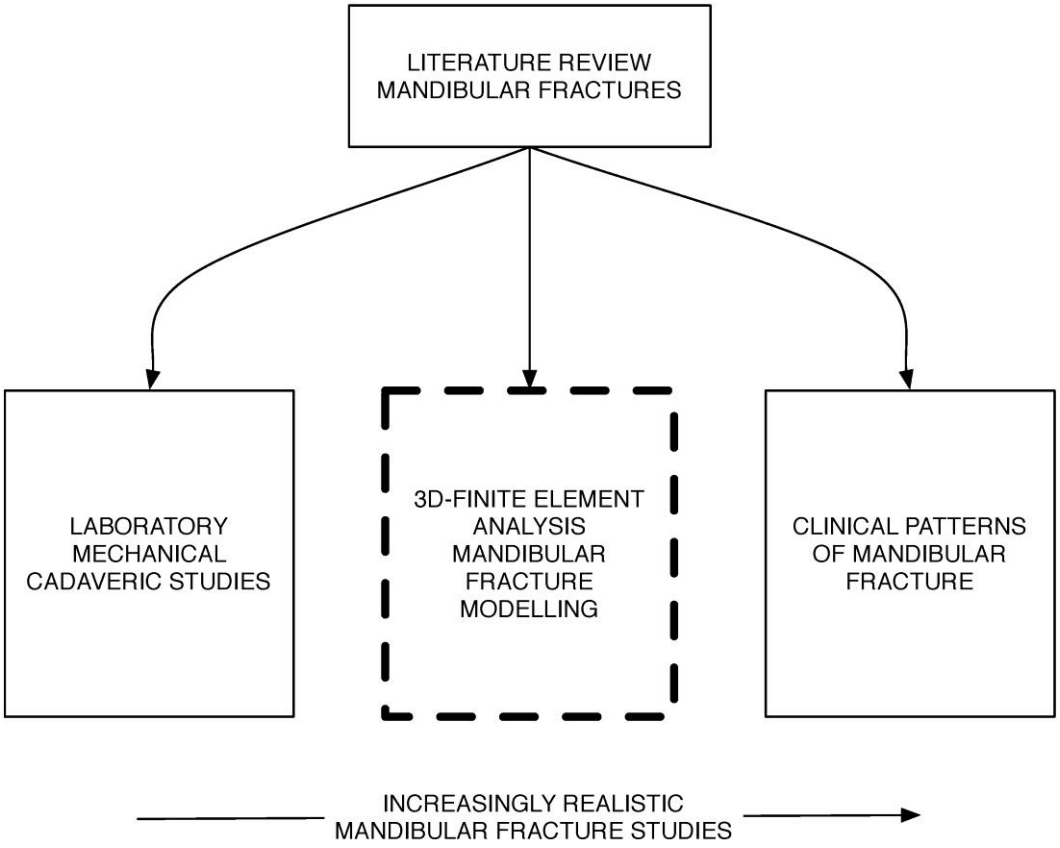

Figure 2.1 The structure of the literature review

2.2 Laboratory mechanical cadaveric studies of mandibular fracture

Several authors have been instrumental in the elucidation of the dynamic responses of the mandible. The pioneering studies of Swearingen (1965), Hodgson (1967), Nahum (1968), Schneider et al. (1974), Reitzik et al. (1978), Huelke et al. (1983), and Unnewher et al (2003) are well-known. They are frequently quoted in the literature when information regarding mandibular deformation and fracture tolerance is required. Several of these studies are discussed below along with their weaknesses. Whilst there are other published studies, the principles of mechanical material testing are grossly similar. Methods of measuring strain and the determination of fracture may have improved but mechanical tests suffer from the limitations of using cadaveric material and therefore little is to be gained from more extensive discussion.

2.2.1 Animal cadaveric studies

Reitzik, et al. (1978) performed a mechanical analysis comparing the forces required to fracture the mandible of *Cercopithecus aethiops* (vervet monkey) through the region of the anatomical angle when third molar teeth were either present or absent. The source population was 10 monkeys with third molar teeth present and 10 without.

No note was made of the degree of eruption of the third molar teeth or the presence of pathology. It does not appear that these details formed part of any exclusion criteria for cases or controls. It was also noted that the age of the monkeys was unknown. The monkeys without third molars could have been much younger, with no evidence of third molar growth or older with congenitally missing third molars. No details of the medical or nutritional status of the monkeys were known. With such small sample sizes, these details could significantly affect the validity of the study, making a direct clinical correlation difficult.

The specimens were stored at minus 30 degrees Celsius for an unspecified period before being thawed and having the soft tissue removed. After halving, forty hemi-mandibles were available.

In order to perform loading the entire ascending ramus of each hemi-mandible was embedded in an acrylic block. This block was angled at 45 degrees to the lower border of the mandible. A tensile force was applied by means of a wire loop placed around the mandible distal to the canine tooth. The loop was mounted in an Instron tensiometer. As a result all fractures occurred at the angle of the mandible. The authors concluded, “Under the experimental conditions used, monkey mandibles containing un-erupted third molars fractured at approximately 60% of the force required to fracture the mandible containing erupted third molars” (Reitzik et al., 1978).

The authors were very clear in their conclusions that these results were applicable only under the experimental conditions i.e. when applied to the mandibles of vervet monkeys loaded in a particular fashion. Monkeys have a different mandibular geometry and their bones have different material properties to humans. The manner of mandibular loading was different to that which would occur under any clinical condition in a human. In normal function, it would be difficult to deform the mandible to a degree sufficient to fracture without first bodily moving the mandible before the maxillary teeth were contacted.

The authors reviewed the literature and concluded that the storage of the mandible at minus 30 degrees Celsius had no effect on the mechanical properties of bone (Chamay, 1970 and Sammarco, et al., 1971). Bearing in mind the use of a hemi-mandible; the abnormal loading pattern; the absent effect of the mandibular condyles; the lack of differentiation between the degree of eruption of the third molar teeth; the lack of knowledge of the age and nutritional state of the monkeys; it cannot be said that, in

isolation, this study is strong evidence that the non-pathological third molar tooth significantly reduces the resistance of the angle of the mandible to fracture in the clinical situation in humans. Despite this, a majority of authors who have published on the effect of third molar teeth on mandibular angle fractures have quoted this paper as evidence in support of their theories on clinical findings (see section 2.6).

2.2.2 Human cadaveric studies

Nahum (1974) studied the impact tolerance of the mandible in an attempt to simulate clinical trauma conditions. Both embalmed and unembalmed specimens were used. A drop-weight assembly was used to impact various locations of the mandible with varying forces. The impact area was composed of a one inch squared circular disk made of crushable nickel foam.

The temporomandibular joints were approximated using semi-rigid fixation. The joints were pinned at the free ends. To avoid potential instability on symphyseal loading, anterior/submental-vertical impacts were chosen. Lateral impacts were in the region of the body of the mandible. In total, eight specimens were used for lateral impacts and nine were used for symphyseal impacts.

As is clear from the research, the number of specimens studied was relatively small. There was no standardization possible in terms of specimen age, gender, pre-morbid state, size and shape, making interpretation of the results difficult. Nahum claimed that embalming had little effect on the results, but this was difficult to determine with so few specimens. One point that was noted was that the thickness of the overlying tissues had a significant effect on the genesis of fractures, with the force required to fracture the mandible being significantly less when no soft-tissue was present.

Unnewehr et al. (2003) aimed to determine the fracture properties of the human mandible. They used a total of seven adult human mandibles (five male, two female). In contrast to Nahum, Unnewehr et al. exarticulated the mandible, removed the soft tissue and stored the specimen at minus 18 degrees. Before testing, the specimens were rehydrated in 0.9% saline for 1 hour. A 20kg mass suspended from the coronoid process was used to represent occlusal force. Semi-rigid elastic fixation was applied at temporomandibular joints in order to better simulate the physiological state. Impacts were produced by a pendulum mass. No details of the impact surface area were given. All specimens were subjected to a low force impact before each high force impact experiment in an attempt to eliminate the effect of micro-fractures. Cortical deformation was measured with strain gauges. They authors noted that the properties of the temporomandibular joint were crucial in the generation of fractures. They also felt that the lack of soft-tissue had little effect the fracture thresholds. In terms of the study of the biomechanics of the mandible, the use of the strain gauges was an improvement on the studies by Nahum; however, the readings were limited to the position of the gauges.

In general, all authors found that patterns of fracture were fairly constant, regardless of age, gender and mandible size. This might be due to the same form of impacts being studied. The range of fracture thresholds varied significantly between authors.

Whilst these studies (and those that followed them) have provided data for forensic and medico-legal use, they have limitations. As may be seen, there can be no consistency in bone material properties, mandibular size, and impact site between two specimens.

Author	Year	Impact direction (site)	Fracture threshold (N)
Hodgson	1967	Various	1598-2664
Nahum	1968	Antero-posterior (symphyseal) Lateral	1890-4120 820-3400
Schneider et al.	1974	Antero-posterior (symphyseal) Lateral	1780 890
Huelke et al.	1968	Antero-posterior (symphyseal) Lateral	2442-3996 1332-3330
Unnewehr et al.	2003	Antero-posterior (symphyseal) Lateral	2465-3122 633-763

The study of rare conditions such as the osteogenesis imperfecta (brittle bone disease) or the effect of lesions within the bone on fracture thresholds cannot be determined with any confidence from these studies. The ability to study a change in any single variable is made difficult by the fact that no two mandibles are the same and large numbers of cadaveric specimens are difficult to acquire. These studies are not suitable for simulating clinical situations; however, they do provide information that has been extrapolated to answer clinical and forensic questions. How effective they are at doing this is debatable due to the small numbers of specimens in the laboratory studies and the large number of uncontrollable variables.

2.3 Three dimensional finite element analysis in the study of the mandible

2.3.1 Introduction

The biological modelling literature is sparsely populated with 3DFEA mandibular models aimed at the study of fractures, therefore this literature review includes 3DFEA studies not directly related to the study of fractures but which have a direct influence on the first phase of the research i.e. the production of the finite element model.

2.3.2 Literature search strategy and aim

A search of electronic databases was performed to identify studies employing 3DFEA to study the mandible in relation to fracture or trauma.

2.3.3 Eligibility criteria

Studies suitable for review included 3DFEA related to mandibular trauma which required the production of a model of at least a hemi-mandible. A hemi-mandible was defined as a portion extending from the mandibular symphysis to the mandibular angle, including the whole ascending ramus and condyle. All studies should have been published in peer-reviewed journals. Studies were not limited with regard to study date, however, it was understood that three-dimensional studies related to the mandible before 1994 were unlikely to be found. The studies were limited to human subjects and to the English language.

2.3.4 Information sources

Ovid Medline®, Embase® and PubMed® databases were interrogated. Exclusion criteria are summarized in table 2.1. The Medical Subject Heading (MeSH) terms employed in the search are outlined in table 2.2. Manual searching was employed when appropriate references were listed in retrieved articles.

Exclusion criteria
Studies employing two-dimensional finite element analysis
Studies modelling less than a hemi-mandible
Studies unrelated to trauma or mandibular trauma
Studies not published in the English language
Review articles which contained no actual finite element analysis
Papers reporting only clinical outcomes
Studies using the same model in multiple publications

Table 2.1 Exclusion criteria for literature review.

2.3.5 Search

Electronic Databases	No. Hits per Database
Database: Ovid MEDLINE(R) In-Process and Other Non-Indexed Citations and Ovid MEDLINE(R) <1946 to Present>, Ovid OLDMEDLINE(R) <1946 to 1965>, Embase Classic+Embase <1947 to 2014 April 08>Search Strategy: "finite element".mp. [mp=ti, ab, ot, nm, hw, kf, px, rx, ui, an, sh, tn, dm, mf, dv, kw] (35372) mandible.mp. [mp=ti, ab, ot, nm, hw, kf, px, rx, ui, an, sh, tn, dm, mf, dv, kw] (123964) trauma.mp. [mp=ti, ab, ot, nm, hw, kf, px, rx, ui, an, sh, tn, dm, mf, dv, kw] (415895) fracture.mp. [mp=ti, ab, ot, nm, hw, kf, px, rx, ui, an, sh, tn, dm, mf, dv, kw] (410304) limit to English language	105
Database: PubMed Search Strategy: finite and element and mandible (trauma or fracture) and bone Query Translation: finite[All Fields] AND ("elements"[MeSH Terms] OR "elements"[All Fields] OR "element"[All Fields]) AND ("mandible"[MeSH Terms] OR "mandible"[All Fields]) AND ("injuries"[Subheading] OR "injuries"[All Fields] OR "trauma"[All Fields] OR "wounds and injuries"[MeSH Terms] OR ("wounds"[All Fields] AND "injuries"[All Fields]) OR "wounds and injuries"[All Fields]) AND ("fractures, bone"[MeSH Terms] OR ("fractures"[All Fields] AND "bone"[All Fields]) OR "bone fractures"[All Fields] OR "fracture"[All Fields])	90
Total	195

Table 2.2 Electronic databases, search strategy, medical subject headings (MeSH) and results.

2.3.6 Study selection

Papers were reviewed concerning reproducibility of the study, accuracy of the finite element model and conclusions drawn. Reproducibility factors included those study details that would allow a researcher to produce similar results. The factors related to reproducibility and model accuracy are shown in table 2.3.

Model accuracy	**Study reproducibility**
Mesh convergence	Analysis type
Mesh quality	Geometry acquisition
Validation	Element type
	Element resolution
	Mechanical behaviour
	Boundary conditions
	Outcome variables

Table 2.3 Factors for study review.

2.3.7 Search strategy results

The search resulted in 195 abstracts of which, 82 were potentially relevant. Once duplicated entries were removed, 44 articles were retrieved and examined in full. Seven papers were rejected and a single paper was obtained from the reference list of articles retrieved. A summary of the articles selected for review are found in Table 2.4.

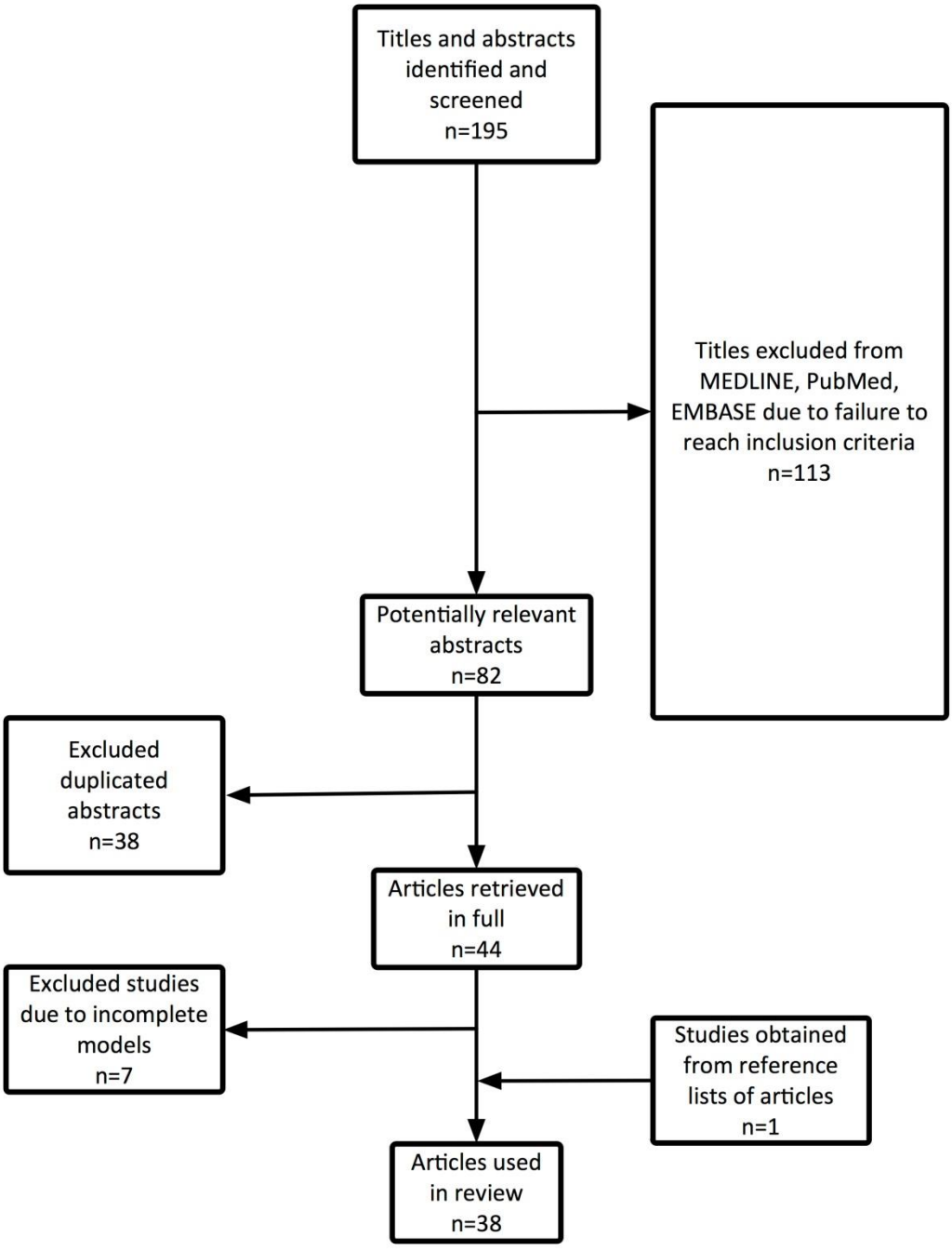

Figure 2.2 Search strategy for mandibular finite element studies related to fracture or trauma.

Investigators	*Analysis type*	*Geometry*	*Element type*	*Element/ node resolution*	*Mechanical Behaviour*	*Mesh Convergence*	*Mesh Quality*	*Restraints*	*Validation*	*Outcome variable*	*Study area*
Murakami, et al., 2013*	Static*	CBCT	TET;TRI	100218; 15927/22288	Isotropic, linearly elastic, homogeneous	NS	NS	Superior condyles. 111,111	NS	σ_{VM}	Osteosynthesis (prophylactic)
Narra, et al., 2014	Static*	CT	TET10	NS	Orthotropic, linearly elastic, homogeneous	NS	NS	Superior condyles, 111,000	NS	σ_{VM}	Reconstruction
Bezerra, et al., 2011	Dynamic	CBCT	TET/TRI	524927 (Max - bone)	Isotropic, linearly elastic, homogeneous	NS	NS	Posterior superior condyle, 111,111	NS	σ_{VM}	Third molar removal
Ertem, et al., 2013	Static*	CT (Cadaver)	NS	141411/30319, 145675/31019, Hemi-mandible	NS	NS	NS	Superior condyles, 111,000	NS	σ_1, σ_3,ε_1, ε_3	Reconstruction
Li, et al., 2013	Static*	CT	TET10	9285/46301, 9023/32345	Isotropic, linearly elastic, homogeneous (Model only cortical bone)	Reference made to convergence studies by other authors	NS	Superior condyles. 111,111	NS	σ_{VM}	Reconstruction
Vajgel, et al., 2013	Static*	CT	TET	640137/451532	Orthotropic, linearly elastic, homogeneous	NS	NS	Superior condyles, 111,111	NS	σ_{VM}	Osteosynthesis
Lei, et al., 2012	Dynamic	CT (Chinese Virtual Human)	HEX8	26644/27522	Isotropic, linearly elastic, homogeneous	NS	NS	Superior condyles. 111,011	NO	σ_{VM}	Trauma
Savoldelli, et al., 2012	Static*	CT	TET	40831	Isotropic, linearly elastic, homogeneous	NS	NS	Muscles of mastication and TMJ modelled	YES	σ_{VM}, displacement	TMJ examination
Murakami, et al., 2011	Static*	CAD/CAM	HEX8	NS	Isotropic, linearly elastic, homogeneous	NS	NS	Superior condyles, 111,000 (Cadaveric model constrained over entire ramus, condyle and coronoid process)	Experimental cadaveric model constrained in different manner to FE model, therefore not valid	σ_{VM}	Mandibular resection
Mesnard, et al., 2011[d]	Static*	Solid CAD model of polymeric replica of human mandible	TET4	71280	Isotropic, linearly elastic, homogeneous	Reference made to convergence studies by other authors	NS	Superior condyles, 111,000	Indirect, against the work of other authors but different study	ε_{VM}	TMJ prosthesis
Boccaccio, et al., 2011*	Static*	CT of synthetic model (NURBS)	TET4	100000 (including distraction device)	Isotropic, linearly elastic, homogeneous	NS	NS	Ramus	NS	σ_{VM}	Distraction
Ammar, et al., 2011	Static*	CBCT	TET4	NS. Final analysis only used a section of the initial model	Isotropic, linearly elastic, homogeneous	NS	NS	NS	NS	σ_{VM}	Orthodontic movement
Gaball, et al., 2011*	Static*	CT (IGES)	NS	NS	Referred to Lovald et al., 2009	Regional – at area of investigation.	NS	Superior condyles, 111,000	NS	σ_{VM}, ε_1	Osteosynthesis
Kimsal, et al., 2011	Static*	CT	NS	75407-101029 (including osteosynthesis plates)	Isotropic, linearly elastic, homogeneous	Regional – at area of investigation. Convergence within "a few % points"	NS	Referred to Lovald et al, 2009	NS	σ_{VM}, σ_1, ε_1	Osteosynthesis
(Ramos, et al., 2011[d]	Static*	Solid CAD model of polymeric replica of human mandible	TET4	71280	Isotropic, linearly elastic, homogeneous	Reference made to convergence studies by other authors	NS	Incisor teeth fixed, 111,000	Model previously used and validated by Mensard, 2006	ε_{VM}	TMJ prosthesis

Investigators	*Analysis type*	*Geometry*	*Element type*	*Element/ node resolution*	*Mechanical Behaviour*	*Mesh Convergence*	*Mesh Quality*	*Restraints*	*Validation*	*Outcome variable*	*Study area*
Tang, et al., 2012	Dynamic	CT (Chinese Virtual Human)	TET HEX	275216/1387101 30024 TET 245192 HEX	Isotropic, linearly elastic, homogeneous	NS	Maximum element aspect ratio	Condyles, 111,000	NS	Kinetic Energy Stress	Trauma
Choi, et al., 2010	Static*	CT	NS	NS	NS	NS	NS	Superior condyles, 111,000	NS	Maximum equivalent stress	Osteosynthesis
Szucs, et al., 2010*	Static*	CBCT	TET	742412/148181	Linearly elastic	NS	NS	Molar teeth	NS	σ_{VM}, σ_1, σ_3	Third molar removal
Wang, et al., 2010	Static*	CT	TET10	235000/375000	Isotropic, linearly elastic, homogeneous	NS	NS	Superior condyles, 111,000	NS	σ_{VM}	Osteosynthesis
Ming-Yih, et al., 2010	Static*	CT	TET10	353626/67837	Isotropic, linearly elastic, homogeneous	YES – midline displacement (5%)	NS	Condyle seat	NS	σ_{VM}	Osteosynthesis
Ji, et al., 2010	Static*	CT	NS	NS	Isotropic, linearly elastic, homogeneous	NS	NS	Superior condyles, 111,000	NS	σ_{VM}	Osteosynthesis
Lovald, et al., 2009(1)[γ]	Static*	CT(IGES)	TET	47525/72899	Orthotropic, linearly elastic, homogeneous	Regional– at area of investigation. Convergence within "a few % points"	NS	Superior condyles, 111,111	NS	ε_1, σ_1, σ_{VM}	Osteosynthesis
Lovald, et al., 2009(2)[γ]	Static*	CT (IGES)	TET10	125295/189497	Orthotropic, linearly elastic, homogeneous	Regional– at area of investigation. Convergence within "a few % points"	NS	Superior condyles, 111,000	NS	ε_1, σ_1, σ_{VM}	Osteosynthesis
Parascandolo, et al., 2010	Static*	VRML triangulation of surface model	QUAD	4560	Anisotropic properties claimed but no data given on how achieved	NS	NS	Spring elements on condylar heads active in compression only	NS	σ_c, σ_t	Osteosynthesis
Schuller-Götzburg, et al., 2009	Static*	Sectioned mandible photographed and traced	HEX8	20000	Isotropic, linearly elastic, homogeneous	NS	NS	NS	NS	σ_{VM}	Osteosynthesis/ Reconstruction
Sugiura, et al., 2009	Static*	CT, axial scans traced.	HEX8	4713-4993/6789-7255	Isotropic, linearly elastic, homogeneous	NS	NS	Superior condyles. 111,111	NS	σ_c, σ_t,σ_{VM}	Osteosynthesis
Kavanagh, et al., 2008	Static*	CT (altered)	TET	35300/8340	Isotropic, linearly elastic, homogeneous	NS	NS	Superior condyles, 111,000	NS	σ, Displacement	Osteosynthesis
Arbag, et al., 2008[α]	Static*	CT (dried skull), axial scans traced.	HEX20	NS (mirrored hemi-mandible)	Isotropic, linearly elastic, homogeneous	NS	NS	Superior condyles, 111,000	NS	Displacement	Osteosynthesis
Kromka & Milewski, 2007	Static*	NS	NS	NS	NS	NS	NS	Different constraints for mechanical and FE set-up	Mechanical validation not achieved	ε_1, ε_2	Osteosynthesis
Korkmaz, 2007	Static*	CT (dried skull), axial scans traced.	NS	NS	NS	NS	NS	NS	NS	ε_1	Osteosynthesis
Boccaccio, et al., 2007	Static*	CT of synthetic model (VRML)	HEX8	17767	Isotropic, linearly elastic, homogeneous	NS	NS	Ramus	NS	σ_{VM}	Distraction osteogenesis
Korkmaz, 2007(2)[α]	Static*	CT (dried skull), axial scans traced.	HEX20	NS (mirrored hemi-mandible)	Isotropic, linearly elastic, homogeneous	NS	NS	Superior condyles, 111,000	NS	Displacement	Osteosynthesis

Investigators	*Analysis type*	*Geometry*	*Element type*	*Element/ node resolution*	*Mechanical Behaviour*	*Mesh Convergence*	*Mesh Quality*	*Restraints*	*Validation*	*Outcome variable*	*Study area*
Knoll, et al., 2006	Static*	NS	NS	NS	Isotropic, linearly elastic, homogeneous	NS	NS	NS	NS	σ_{VM}	Osteosynthesis
Choi, et al., 2005	Static*	Traced sectioned cortical bone outlines	HEX	258/1635	Transversely isotropic, linearly elastic, homogeneous	NS	NS	NS	Comparison	σ_c, σ_t	Occlusion
Gallas Torreira & Fernandez, 2004[β]	Dynamic	Surface mesh obtained from 3rd party	TET	30119/7073	Isotropic, linearly elastic, homogeneous	NS	NS	NS	NS	σ_{VM}	Trauma
Cox, et al., 2003	Static*	Commercial model	HEX8	NS Hemi-mandible used	Regionally orthotropic, linearly elastic, homogeneous	NS	NS	Superior condyles, 111,000	NS	σ_{VM}	Osteosynthesis
Fernández, et al., 2003[β]	Static*	NS	TET4	NS	Isotropic, linearly elastic, homogeneous	NS	NS	Superior condyles	NS	σ_{VM}	Osteosynthesis
Wagner, et al., 2002	Static*	Traced axial CT scans	NS	NS	NS	NS	NS	Mandibular joint, 111,000	NS	σ_{VM}	Osteosynthesis

Table 2.4 Summary of the characteristics of 3DFEA studies

Tri	Triangular elements
Tet	Tetrahedral elements with unknown node number
Tet4	Tetrahedral elements with four nodes (linear element)
Tet10	Tetrahedral elements with ten nodes (quadratic element)
Hex	Hexahedral elements with unknown node number
Hex8	Hexahedral elements with eight nodes (linear element)
Hex20	Hexahedral elements with twenty nodes (quadratic element)
NS	Not specified in text as to whether
Static*	Not specified but assumed from methodology
ε_1	First principal strain
ε_3	Third principal strain
σ_{VM}	von Mises stress
σ_c	Compressive stress
σ_t	Tensile stress
σ_3	Third principal stress
σ_1	First principal stress
Constraints	$x_t y_t z_t, x_r y_r z_r$ where a value of 1 implies restriction and 0 implies free movement. t=translation and r=rotation

Studies, which have used the same model, have similar superscript

2.3.8 Review of modelling techniques used - general conclusions

Table 2.5 shows the breakdown of biological studies employing 3DFEA mandibular models to study the management of fractures and traumatic injuries.

Area of study	**No. articles**
Osteosynthesis	21
Third molar removal in relation to fracture	2
Mandibular reconstruction	4
Temporomandibular joints	3
Mandibular trauma	3
Distraction osteogenesis	2
Orthodontic treatment	1
The study of dental occlusion	1

Table 2.5 Areas of mandibular study employing finite element analysis.

2.3.8.1 Analysis type

Study analyses were either static or dynamic, although in many cases this was not explicitly stated and was inferred from the methodology. Linear mechanics were used throughout all studies.

2.3.8.2 Geometry

Accurate geometry is essential to reproduce the characteristics of the system under investigation and most of the studies performed within the last 8 years utilized clinical CT scans, either conventional or cone-beam (CBCT). How the data was used varied between studies. CT data of plastic models has been used (Mesnard, et al., 2011; Boccaccio, et al., 2011), as well as dried skulls (Arbag, et al., 2008; Korkmaz, et al., 2007), cadavers (Ertem, et al., 2013), and lately, three-dimensional reconstructions directly from either clinical conventional CT (Narra, et al., 2014; Li, et al., 2013; Vajgel, et al., 2013; Savoldelli, et al., 2012; Gaball, et al., 2011; Kimsal, et al., 2011; Choi, et al., 2010), or CBCT data (Murakami, et al., 2014; Bezerra, et al., 2013; Anmar, et al., 2011; Szucs, et al., 2010). Those techniques which utilized micro CT (μCT) examination of dried skulls were able to re-produce hard tissue most accurately; however, this level of ionizing radiation exposure is not used clinically.

2.3.8.3 Element type

Finite elements are mathematical representations of simple shapes that can be used to convert forces, displacements and stiffness into values of stress and strain (Adams, 2008). They generally have 3 forms; line, shell and solid. The most common solid elements used in biological 3DFEA are tetrahedral, hexahedral or occasionally pentahedral.

Few of the authors gave justification for their element choice. In the case of earlier studies this may have been due to the lack of element choice with analysis software.

2.3.8.4 Element resolution

Element resolution is vital to the accuracy of the solution. A wide range of element resolutions were used for similar studies, ranging from 4500 to 740000. Whether a model has sufficient resolution to give a mathematically accurate solution may be confirmed with a convergence study. Some authors assumed that once a model had converged at one element resolution, then all roughly similar models with the same resolution would also result in a converged solution (Mesnard, et al., 2011). This is not always true, making comparison between studies difficult. The required resolution to produce an accurate result is dependent on the answer being sought, the element type chosen and the individual geometry.

2.3.8.5 Boundary conditions

Boundary conditions, i.e. loads, restraints and contacts, are idealized representations of modelled and non-modelled parts of a system (Adams, 2008). The correct application is therefore critical to the accuracy of any analysis. Loads may be applied to model nodes directly as forces or to elements as pressure, or to the whole body as accelerations and velocity.

Restraints are used to eliminate unwanted degrees of freedom in a model. In most mandibular models reviewed, the superior condylar heads were restrained, simulating the effect of the temporomandibular joint (TMJ). One of the unwanted effects of the restraints is to produce areas of high stress and strain locally. None of the authors made reference to this effect when interpreting their results.

2.3.9 Review of studies

Mandibular 3DFEA models have been used frequently used to study plate osteosynthesis in the management of trauma. These studies have concentrated on

either an assessment of the ideal positioning of the plates or determining whether a plate is able to bear a specific load without failure.

An early study by Wagner, et al. (2002) involved the biomechanical behaviour of the mandible and plate osteosynthesis in the treatment of condylar fractures. The authors constructed a finite element model utilizing the traced cortical outlines from axial CT scans and CAD/CAM software to produce a three-dimensional model. Using only the outer cortical outline, sub-cortical structure could not be reproduced. Cancellous bone was not modelled. No details of element resolution were given. Material properties (unspecified) were applied following the conversion of CT Hounsfield units into density values and then into the elastic modulus. This process required calibration, but no mention of this was made in the paper. The boundary conditions included temporalis, masseter and medial pterygoid muscles. These were modelled as load vectors bilaterally. It was not possible from the description to determine whether the muscle forces were applied as single resultant vectors applied to a point on the mandibular cortex or whether the load was split over the anatomical insertion point of each muscle. Displacement constraints were placed in the mandibular joint. The authors stated that lateral pterygoid was not modelled due to its direction of action. The outcome measure of the study was von Mises stress in the osteosynthesis plate and the mandible.

Cox, et al. (2003) also studied osteosynthesis plates, this time comparing resorbable polymer plates and screws for fixation of fractures. To produce the mandibular geometry, a meshed surface model was purchased and its dimensions were compared to a plastic replica mandible. The surface accuracy of the model was therefore limited by the accuracy of the plastic replica. The cortical thickness was determined from cortical measurements taken at six points from the axial CT scans of an unrelated patient. These were transposed to the model geometry. Unlike the study of Wagner, et al. (2002) these

authors modelled cancellous bone volume. This was defined as the space deep to the cortex. The mandibular canal was not modelled in either cortical or cancellous bone. The authors assigned orthotropic properties to three different areas of the cortical bone in the model. This theoretically improved the accuracy of the material properties. It was postulated that the model would have been more accurate if the bone was assigned "gradual and continuously changing local orthotropic properties in hundreds or thousands of micro-regions around the mandibular arch" (Cox, et al., 2003). Cancellous bone was modelled as isotropic despite being highly anisotropic. No details of model element resolution or mesh convergence were given, making assessing model accuracy difficult. With no comparison of results available, it is difficult to determine whether the use of orthotropic cortical bone properties was an improvement over the use of isotropic properties either mechanically or clinically. In addition, the solution time was not given, making it difficult to determine whether the accuracy improvement/processing time ratio would make the change unreasonable.

The 3DFEA model produced by Lovald, et al. (2009) was an incrementally better model from an anatomical point of view. Clinical CT data was reconstructed to produce the geometry using IGES line contours, which were subsequently "skinned" to produce volumes. The final volume mesh contained over 125000 quadratic tetrahedra. Mesh convergence was achieved within "a few percentage points" according to the authors. Regional orthotropic material properties were assigned in 12 cortical bone volumes, an increase over the model of Cox, et al. (2003), however, both buccal and lingual cortices used the same values of elastic modulus in contrast to the natural situation (Schwartz-Dabney and Dechow, 2003). In line with other studies, translational restraints were placed on the condylar heads. These were sufficiently distant from the area of interest to make little difference to the interpretation of the results. Muscle force vectors were applied (after Korioth, et al. (1992)) to produce incisal and unilateral molar loading

conditions. This complex model enabled the evaluation of osteosynthesis plates under simulated loading conditions. The main problem with the modelling technique was that the analysis was performed statically whereas the true loading condition would be dynamic. No mechanical model validation was performed.

Many other authors have investigated the use osteosynthesis plates using 3DFEA using mandibular models, including Korkmaz, et al. (2007); Kromka, et al. (2007); Arbag, et al. (2008); Kavanagh, et al. (2008); Schuller-Götzburg, et al. (2009); Lovald, et al. (2009); Parascandolo, et al. (2010); Ji, et al. (2010); Ming-Yih, et al. (2010); Wang, et al. (2010); Choi, et al. (2010); Kimsal, et al. (2011); Gaball, et al. (2011); Vajgel, et al. (2013); and Murakami, et al. (2014). The most advanced of these studies, have produced their mandibular geometry directly from conventional or cone-beam CT scans of the mandible. No authors attempted to assign anisotropic properties to the mandible. Few authors have segmented the mandibular teeth in their analyses, even when the teeth were used to load the mandible.

The work of Ashman and Van Buskirk (1987) suggested that mandibular bone might be reasonably considered to behave orthotropically and as previously stated, it was assumed that the regionally orthotropic models of Lovald, et al. (2009) and Vajgel, et al. (2013) would provide greater accuracy, although little evidence has been found to support this in clinical studies. Lovald, et al. (2009) and Kimsal, et al. (2011) stated that mesh convergence had been reached at element resolutions ranging from 75000-125000 for their mandibular models despite using linear rather than quadratic tetrahedra. These would appear to be very low element resolutions, compared to other authors who used the same modelling technique (Vajgel, et al., 2013), for models that were anatomically quite detailed.

All analyses reviewed to this point were performed statically, despite the fact that they were used to study situations that were clearly dynamic in nature.

The paper of Gallas Torreira and Fernandez, (2004) described one of the first attempts to study traumatic insults to the mandible using dynamic 3DFEA. This paper gave few details on how the geometry was modelled; except that it was obtained from the work of a third party who laser scanned an object and used a CAD/CAM application to produce a digital model. It was not stated how sub-cortical structures were modelled. The individual teeth were not modelled as separate volumes. The model was composed of 30119 tetrahedra with 7073 nodes. No convergence details or mesh quality measures were mentioned. The temporomandibular joints were modelled with a "unilateral contact condition on the upper surface of the condyles within the glenoid fossa" (Gallas Torreira and Fernandez, 2004). No muscles were modelled or equivalent forces applied to the model. Isotropic model properties were used for both cortical and cancellous bone. The load chosen for the analysis was $1x10^{7}Nm^{-2}$, which was large enough to produce a fracture (Krüger, 1986); however, the use of a load that by definition would be outside the elastic limit of bone would seem to preclude the use of linearly elastic mechanics. The model was examined after an impact of one second. This seems a long contact time for an impact as a result of inter-personal violence. One would normally consider this to be in the order of milliseconds. Two impact scenarios were analysed, symphyseal and body. Von Mises stress was used as the indicator of bone failure. The authors felt that their study verified clinical observations by identifying potentially weak areas of the mandibular geometry such as the condylar neck and the mandibular angles. Despite being a dynamic analysis, no information was given regarding the temporal appearance of areas of high stress. If areas of high stress were to be associated with the appearance of fractures then the temporal appearance of stress would give information concerning the fracture order.

The second dynamic 3DFEA study related to mandibular trauma was produced by Tang, et al. (2011) in order to investigate ballistic injuries to the human mandible. This study was related to a previous study of the same authors, which modelled ballistic injuries in the pig mandible. The Chinese Visible Human (chinesevisiblehuman.com) formed the digital dataset for the mesh. Cortical and cancellous bone was modelled but teeth and associated structures were omitted, suggesting that the dataset was altered during 3D reconstruction. No muscles were modelled. The final volume mesh was composed of a mixture of tetrahedral and hexahedral elements. The resolution was 275216 elements and 1387101 nodes. Constraints were placed in the superior condylar regions, as in most papers. This paper was the first to mention a mesh quality assessment, ensuring that the maximum element ratio of the mesh did not exceed five. As high velocity impacts were being studied, the full simulation time was 500μs resulting in a computation time of 38-40 hours on a well-specified computer.

A similar paper from the same institution investigated blast injuries to the mandible (Lei, et al., 2012). The general modelling technique was the same; however, the model had a much lower element resolution. Von Mises stress was used as the indicator of failure. Stress and strain patterns in their study had different patterns both spatially and temporally. In acknowledging the limitations of their study, the authors noted the use of isotropic, homogeneous properties, the lack of validation and verification due to ethical and practical reasons. They argued that the results of their previous study of gunshot injuries to a pig mandible (Chen, et al., 2010) using 3DFEA produced results that were considered accurate and that as this study utilised the same technique, and as the model had similar material properties, the results should also be considered accurate. This might not be as reasonable a conclusion as it appears as the mechanisms of injury were different (i.e. rifle shot vs. blast injury) meaning that the model was loaded in a different manner and the geometry of the mandible in both cases differed significantly.

The final study related to trauma is that of Bezerra, et al. (2014). The aim of the study was to determine whether erupted third molars weaken the mandible, when subjected to impacts in the symphyseal region. Mandibular geometry was reproduced using CBCT scans of a normal mandible. The 3DFEA mesh was constructed by separating 'masks' of mandibular structures using a thresholding technique whereby pixels of pre-defined Hounsfield values were eliminated from the axial scans. The masks were then reconstructed, producing a 3D model where each voxel was directly converted into a finite element. One drawback of this technique is that the resolution of the resulting model was determined by the resolution of the scan. Tetrahedral elements and triangular elements were used, although it is not clear where the 2-dimensional triangular elements were used. Material properties were once again to isotropic and linearly elastic. 524927 elements were used in constructing the bony structures. Masticatory muscles were reproduced using spring elements and condyles were constrained in all degrees of freedom at the most posterior superior part of the condyles rather than the more traditional position of the superior condylar head. The load was applied perpendicular to the frontal plane. Closer examination of the *Bezerra* study shows a flaw of the voxel-transformation technique which could affect the analysis results. The mandibular model showed that the teeth were incompletely segmented, fused to each other. This meant that in terms of action the teeth acted as a single unit rather than individually. Therefore, the influence of the erupted third molar was not examined in isolation and the conclusion of the analysis results could be in doubt. Whether a dentition with sufficiently tight contact points or significant crowding would produce the same effect as the FEA model remains untested.

2.3.10 Conclusions

The preceding review gave a useful insight into modelling techniques previously used by authors studying the mandible in clinical situations. In evaluating the techniques used it would seem that modelling traumatic injuries to the mandible should be theoretically possible. The following points should be observed when producing a suitable 3DFEA model.

1. Static or dynamic analyses may be used; however, the research question must be appropriately phrased.
2. CT scans seem to be the best source of data to reproduce the geometry of the mandible most accurately. Of the choice of conventional clinical CT, cone-beam CT and μCT, the best resolution would be gained from a μCT scan; however, this would require a dried human skull.
3. Element resolution is important to calculation accuracy. The final resolution should be decided following a mesh convergence study if the analysis software does not perform this automatically. Although only a single study used a mesh-quality parameter this is to be recommended to ensure accuracy of the mesh.
4. The use of either isotropic or orthotropic properties for cortical bone may be used; however, no real benefit of one over another has been shown in a study.
5. Although all studies reviewed used linear mechanics and claimed that results were comparable with clinical situations. This may not be the case in non-linear situations such as bony fracture.
6. In most studies, condyles were restrained on the superior surface of the head. This has widely been accepted as a reasonable approximation of the temporomandibular joint as long as the restrained area is away from the area under investigation.

7. Outcome variables such as von Mises stress may be a reasonable first approximation of failure for a material such as bone that can fail in a ductile or quasi brittle manner.
8. Validation of models using human subjects is not possible due to ethical considerations; however, experimental mechanical studies, comparison and trend studies are still possible.

2.4 Clinical patterns of mandibular fracture

2.4.1 The prevalence of mandibular sub-site fractures: Introduction and rationale

The mandible is the largest and strongest bone of the facial skeleton (Haug, et al., 1990; Hogg and Horswell, 2006; Vetter, et al., 1991; Oikarinen, et al., 1993), and been and after the nasal bones is the second most traumatically injured bone in the adult facial skeleton.

Mandibular fractures may be uni- or multifocal. There is little consensus regarding which site fractures most frequently. The predominant fracture site has been variously identified as the condyle (Al Ahmed, et al., 2004; Bormann, et al., 2009; Brasileiro and Passeri, 2006; Christiaens and Reychler, 2002; de Matos, et al., 2010), the angle (Antoun and Lee, 2008; Anyanechi and Saheeb, 2011; Ogundare, et al., 2003), the body (Adebayo, et al., 2003; Adekeye, 1980; Adi, et al., 1990; Chambers and Scully, 1987; Mwaniki and Guthua, 1990), and parasymphysis (Abdullah, et al., 2013; Goldberg and Williams, 1969). Fracture sub-site preference might be due to an inherent weakness associated with the mandibular geometry, the material properties, the traumatic aetiology or a combination of the three.

2.4.1.1 Objective

To review the existing, peer-reviewed literature which reported the prevalence of mandibular fractures with the aim of determining which anatomical fracture sub-site featured predominantly.

2.4.1.2 Method

A protocol for the analysis and the study inclusion criteria were devised before the data collection phase. The protocol may be found in appendix 17.

2.4.1.2.1 Eligibility criteria

Eligible studies were prospective or retrospective, reporting the prevalence of non-pathological fractures of the mandible in humans. Such cases presenting to medical establishments for either surgical or non-surgical treatment must have been consecutive patients within a defined time period.

2.4.1.2.2 Information sources

Electronic and manual literature searches were performed to identify studies reporting the incidence of mandibular fractures. Ovid Medline, Embase, PubMed, Scirus and Scopus databases were interrogated. The Medical Subject Heading (MeSH) terms employed are outlined in table 2.6. The search was limited between the years 1963 and 2013 and to human subjects when such options were available in the database. No language restrictions were employed. Manual searching was employed when appropriate references were found in retrieved articles.

2.4.1.2.3 Study selection

An eligibility assessment was performed by a single reviewer. It was realized that this could introduce bias and errors so in an attempt to reduce the errors the eligibility assessment was performed on four occasions separated by three months. Journal abstracts were reviewed for all search results where they were available. In cases where there was no abstract and the title was not clear with respect to the exclusion criteria, a decision whether or not to exclude the article was made following retrieval. All papers

selected must have classified mandibular fracture according to the Dingman and Natvig classification. Figure 2.3 shows the anatomical boundaries used for classification of sub-sites.

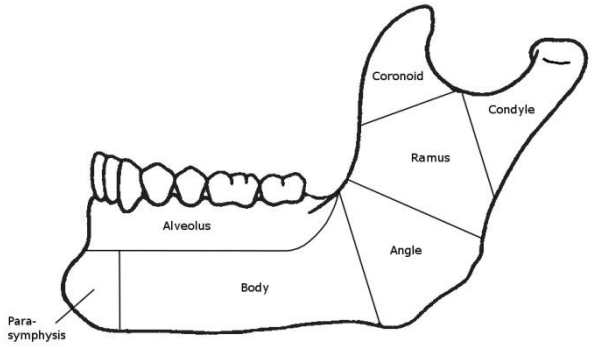

Figure 2.3 The fracture sub-site classification used for the meta-analysis. The ramus was combined with the coronoid process forming the ascending ramus for analysis purposes.

Qualitative and quantitative data were entered into a spreadsheet (Excel 2010, Microsoft©). Authors, publication date, site and relative frequency of mandibular fracture, age group studied, study type, study period and country of study origin were recorded from articles included in the study. Where a study was not specifically related to mandibular fractures, but contained sufficient related raw data, this was extracted and frequencies calculated manually. Authors were also contacted to provide clarification on their data where this was not clear in the published article. The retrieved articles that were deemed suitable for meta-analysis were analysed using StatsDirect®. Bias was assessed using a funnel plot (Sterne and Egger, 2001). Evidence of asymmetry was based on $p<0.05$. Heterogeneity statistics (non-combinability statistics), Cochran Q and I^2 (Higgins and Thompson, 2002; Higgins, et al., 2003), were also calculated. A prevalence meta-analysis was performed. Other papers pertinent to mandibular fracture

sub-sites, but using a classification unsuitable for the meta-analysis were also reviewed for other information that was related to mandibular fracture patterns (see section 2.5).

Search Strategy		*No. Hits per Database*
Database: Ovid MEDLINE(R) In-Process and Other Non-Indexed Citations and Ovid MEDLINE(R) <1946 to Present>, Ovid OLDMEDLINE(R) <1946 to 1965>, Embase Classic+Embase <1947 to 2013 March 29> **Search Strategy:** **((mandible or mandibular) and fracture and trauma).mp. [mp=ti, ab, ot, nm, hw, kf, ps, rs, ui, an, sh, tn, dm, mf, dv, kw] (1942)** **Limit to human (1664)** **Limit to yr= "1963- Current" (1663)** **remove duplicates (1130)**		1130
Database: PubMed **Search Strategy: ((mandible or mandibular) and fracture and trauma)** **Query Translation:** **(("mandible"[MeSH Terms] OR "mandible"[All Fields]) OR ("mandible"[MeSH Terms] OR "mandible"[All Fields] OR "mandibular"[All Fields])) AND (("fractures, bone"[MeSH Terms] OR ("fractures"[All Fields] AND "bone"[All Fields]) OR "bone fractures"[All Fields] OR "fracture"[All Fields]) AND ("injuries"[Subheading] OR "injuries"[All Fields] OR "trauma"[All Fields] OR "wounds and injuries"[MeSH Terms] OR ("wounds"[All Fields] AND "injuries"[All Fields]) OR "wounds and injuries"[All Fields]))**		6604
Scirus	(mandible or mandibular)AND (fracture or fractures) in title	6
Scopus	(mandible or mandibular)AND (fracture or fractures) in title	771
Total		8511

Table 2.6 Search strategies employed in the prevalence meta-analysis.

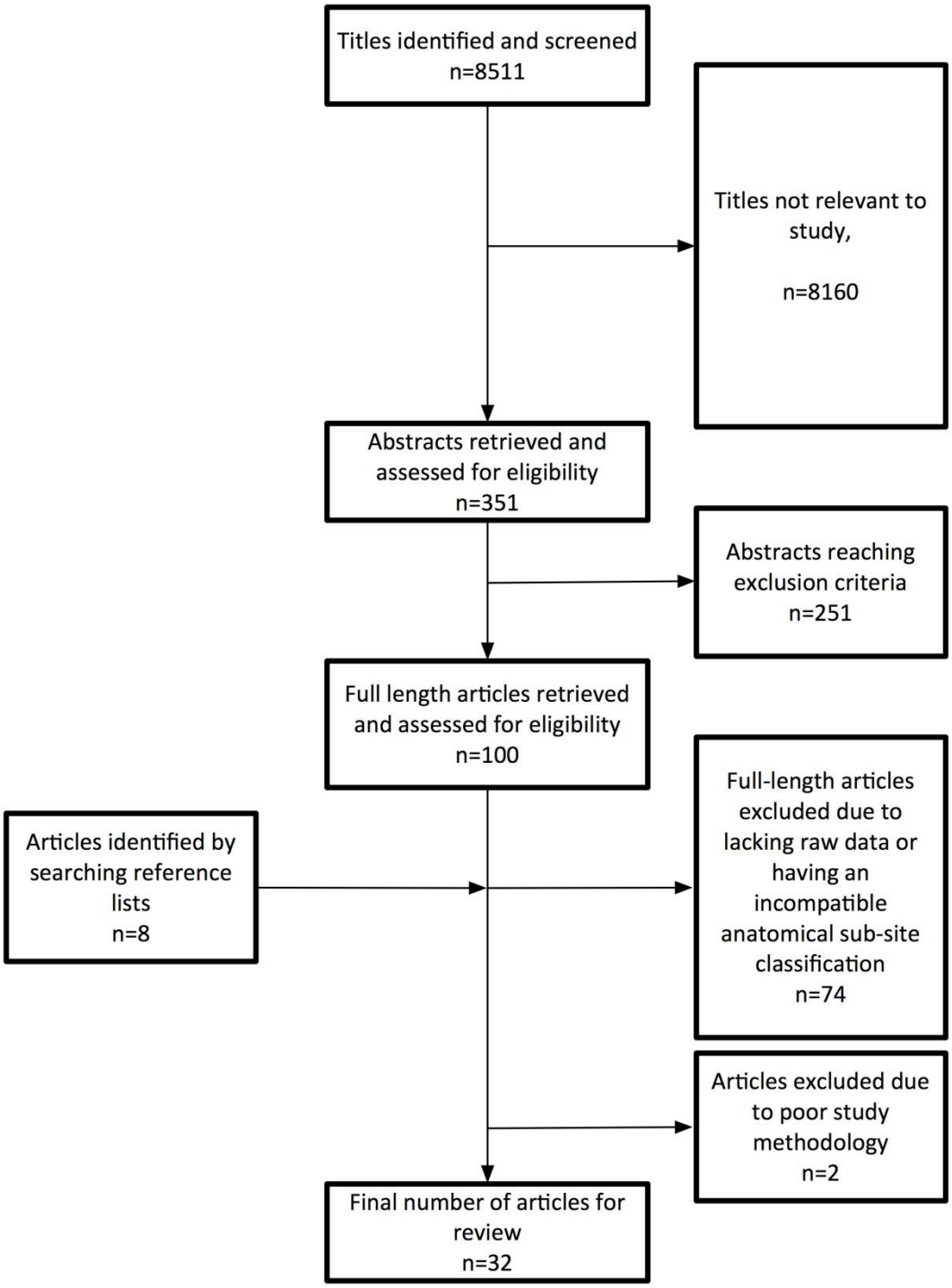

Figure 2.4 Flow chart of selection process for article review.

2.4.1.3 Results

The search strategy outlined in the method yielded 8511 studies, which were initially identified for examination. After applying the selection process Figure 2.4, of the 351 full-length articles retrieved, 251 did not meet the exclusion criteria (see appendix 20) 100 articles remained which were fully assessed. Thirty-two studies were deemed suitable for meta-analysis. Of the 32 studies included, 2 had a very small sample size. The study by Le, et al. (2001) was confined to facial fractures presenting in domestic violence victims who presented to the emergency room where the fist was the most common means of assault. In this study there were only 30 mandibular fractures in total. The second study (Oji, 1998) only included 42 mandibular fractures.

A large multicentre study which included 5196 mandibular fractures (Boole, et al., 2001) was excluded due to the methodology. In this study of active duty army soldiers the number of fractures at mandibular sub-sites was retrieved from an army database which included all body injuries, however, the authors did not verify the data in any way i.e. neither radiographs or medical notes were reviewed. The study by Copcu, et al. (2004) was also excluded as they did not include patients treated under local anaesthesia in an area of the world where this is a common treatment modality for minimally displaced fractures. These fractures were most likely to have been condylar fractures. The exclusion of such fractures would have significantly altered their results. Two authors contacted provided clarification of their results (Eskitaşcıoğlu, et al., 2013; Zachariades, et al., 1990).

Articles assessed for meta-analysis eligibility													
	Anatomical site and relative frequency of mandibular fractures (% is the superior number, r is the inferior number)												
Authors	**Condyle**	**Ramus**	**Angle**	**Body**	**Parasymphysis**	**Symphysis**	**Alveolus**	**Coronoid**	**Age range**	**Number of cases/fractures**	**Study Period**	**Study type**	**Country**
Abdullah, et al., 2013	22.2 42	1.1 2	17.5 33	15.9 30	29.6 56	6.4 12	5.8 11	1.6 3	All	*/189	2007-2011	Retrospective	Saudi Arabia, Riyadh
Adebayo, et al., 2003	5.8 27	4.7 22	18.5 86	51 238	* *	12.3 57	7.3 34	1 1	5y-65y	443/465	1991-2000	Retrospective	Nigeria, Kaduna
Adekeye, 1980	11 *	* *	16 *	47 *	26 *	* *	* *	1 *	All	*/1615	1973-1978	Prospective	Nigeria, Kaduna
Adi, et al., 1990†	26.1 165	3.6 23	19.5 123	26.3 166	19.1 121	PS PS	3.5 22	1.9 12	All	378/632	1977-1985	Retrospective	Scotland, Dundee
Ajagbe, et al., 1977	20 *	* *	15 *	51 *	0 *	13 *	* *	1 *	All	*/152	1965-1975	Retrospective	Nigeria, Ibadan
Aksoy, et al., 2002	15.3 *	1.8 *	15.3 *	10.0 *	36.5 *	21.2 *	* *	* *	All	417/*	1994-2001	Retrospective	Turkey, Ankara
Al Ahmed, et al., 2004	25.3 38	4.0 6	23.3 35	20.0 30	18.0 27	PS PS	8.0 12	1.3 2	All	*/150	1999-2002	Retrospective	UAE, Sharjah
Al-Aboosi & Perriman, 1976	24.1 33	0.7 1	16.1 22	13.9 19	33.6 46	11.7 16	* *	* *	NS	100/137	1965-1970	Retrospective	Iraq, Baghdad
Al-Khateeb & Abdullah, 2007	12.2 33	4.1 11	17.4 47	39.6 107	* *	15.6 42	10.0 27	1.1 3	All	203/270	1995-2003	Retrospective	UAE
Anderson, 1995	41.7 20	* *	* *	22.9 11	10.4 5	8.3 4	16.7 8	* *	NS	33/48	1983-1992	Retrospective	Scotland, Edinburgh
Andersson, et al., 1984	43.3 406	1.7 16	13.5 126	23.2 217	11.8 110	PS *	5.0 47	1.5 14	All	795/936	1978-1980	Retrospective	Sweden, Stockholm
Ansari, 2004	27.2 325	0.3 4	18.3 218	30.5 364	* *	23.2 277	* *	0.5 6	All	/*1194	1987-2001	Retrospective	Iran, Hamedan
Anyanechi & Saheeb, 2011	27.1 *	* *	31.3 *	12.7 *	6 *	22.9 *	* *	* *	15y-42y	73/*	2005-2008	Prospective	Nigeria, Calabar
Antoun & Lee, 2008	25.5 75	2.4 7	35.0 103	13.9 41	17.3 51	5.8 17	* *	* *	All	*/294	1996-2006	Retrospective	New Zealand

Authors	Condyle	Ramus	Angle	Body	Parasymphysis	Symphysis	Alveolus	Coronoid	Age range	Number of cases/fractures	Study Period	Study type	Country
Arvind, et al., 2013	CC *	* *	* U	* U	PS *	* U	* *	CC *	6y-16y	U/U	2008-2012	Retrospective	India, Nadu
Bamjee, et al., 1996	14.2 48	3.6 12	32.8 111	19.2 65	22.2 75	7.4 25	* *	0.6 2	<18y	*/338	1989-1992	Retrospective	South Africa, Johannesburg
Bataineh, 1998	14.1 59	22.7 95	24.8 104	32 134	* *	4.1 17	* *	2.4 10	All	584/419	1992-1997	Retrospective	Jordan
Bither, et al., 2008	16.7 81	5.4 26	19.8 96	13.6 66	39.3 191	1.4 7	3.3 16	0.6 3	3y-67y	324/486	2003-2007	Retrospective	India, Maharashtra
Boole, et al., 2001	23.3 716	4.5 140	35.6 1096	12.7 392	PS PS	20.1 620	2.7 84	1 30	All	2344/3078	1980-1998	Retrospective	Honolulu, Hawaii
Bormann, et al., 2009	41.8 291	2.4 17	20.3 141	14.5 101	20.7 144	PS *	* *	0.3 2	10y-96y	444/696	2000-2005	Retrospective	Germany
Brasileiro & Passeri, 2006	28.8 162	2.3 13	20.1 113	23.7 133	* *	24.7 139	* *	0.4 2	All	423/562	1999-2004	Retrospective	Brazil, Sao Paulo
Breeze, et al., 2011	9.4 10	RA *	24.8 26	29.2 31	* *	36.8 39	* *	* *	All	60/106	2004-2009	Retrospective	Birmingham, UK
Chambers & Scully, 1987	16.5 29	9.1 16	22.7 40	27.8 49	10.2 18	10.8 19	* *	2.8 5	NS	124/176	1944-1945	Retrospective	India, Trimalgherry-Deccan
Christiaens & Reychler, 2002	30.6 436	2.3 33	15.6 223	24.8 353	16.7 238	8.6 123	* *	1.3 19	All	1198/1425	2000-2002	Retrospective	Brazil, Belo Horizonte
Copcu, et al., 2004	18.7 20	3.7 4	23.4 25	26.2 28	19.6 21	PS PS	6.5 7	1.9 2	All	218/107[γ]	1996-2002	Prospective	Turkey, Izmir
de Matos, et al., 2010	28.3 57	4.0 8	18.4 37	24.9 50	* *	22.4 45	* *	2 4	All	126/201	2002-2005	Retrospective	Brazil, Sao Paulo
Dongas & Hall, 2002	24.1 *	1.8 *	32 *	17.7 *	15.6 *	3.6 *	2.1 *	1.5 *	All	251/385Π	1993-1999	Retrospective	Australia, Tasmania
Elgehani & Orafi, 2009	18.6 124	2.0 13	21.8 145	19.2 128	27.0 180	5.6 37	4.4 29	1.4 9	8mnth-72y	493/666Δ	2000-2006	Retrospective	Benghazi, Libya
Ellis 3rd, et al., 1985	29.1 910	2.7 85	23.3 729	32.9 1029	PB *	8.7 272	1.1 34	2.1 65	NS	1946/3124	1974-1983	Retrospective	Scotland, Canniesburn
Emshoff, et al., 1997†	39.5 117	4.7 14	13.9 41	24.3 72	NC	17.2 51	* *	0.3 1	4y-74y	712/296	1984-1993	Retrospective	Austria, Innsbruck
Eggensperger Wymann, et al., 2008	11.5 3	* *	23.1 6	34.6 9	30.8 8	PS *	* *	* *	All	*/26	2000-2002	Retrospective	Switzerland, Bern
Eskitaşcıoğlu, et al., 2009	19.2 64	1.5 5	10.5 35	13.2 44	34.8 116	9.0 30	11.7 39	* *	0y-16y	235/333	1987-2007	Retrospective	Turkey, Kayseri

Authors	Condyle	Ramus	Angle	Body	Parasymphysis	Symphysis	Alveolus	Coronoid	Age range	Number of cases/fractures	Study Period	Study type	Country
Eskitaşcıoğlu, et al., 2013	19.7 215	2.5 27	16.7 182	19.7 215	28.6 312	7.3 80	5.0 55	0.4 4	17yr- 90yr	753/1090	1992- 2011	Retrospective	Turkey, Kayseri
Ferreira, et al., 2004	31.0 211	7.3 50	16.0 109	13.2 90	13.1 89	7.9 54	11.2 76	0.3 2	<18yr	521/681	1993- 2002	Retrospective	Portugal, Porto
Fasola, et al., 2003	3.9 2	* *	11.8 6	60.8 31	PS *	23.5 12	* *	* *	All	*/51	1984- 1998	Retrospective	Nigeria, Ibadan
Fridrich, et al., 1992	26 *	2.2 *	26.7 *	11.3 *	23.6 *	PS PS	1.1 *	1.3 *	All	1067/1515П	1979- 1989	Retrospective	USA, Iowa
Gandhi, et al., 2011	14.4 69	0.6 3	18.4 88	9.8 47	* *	49.5 237	7.3 35	* *	All	324/479	2006- 2010	Retrospective	India, Punjab
Ghodke, et al., 2013	38.8 19	* *	6.1 3	22.5 11	20.4 10	10.2 5	* *	2.0 1	1yr- 70yr	35/49	2008- 2009	Prospective	India, Aurangabad
Glazer, et al., 2011	44.7 38	* *	21.2 18	8.2 7	25.9 22	* *	* *	* *	All	61/85	1993- 2010	Retrospective	Israel, Be'er-Sheva
Goldberg & Williams, 1969	13.4 41	1.6 5	26.6 81	20.3 62	27.5 84	10.5 32	* *	* *	NS	202/305	1964- 1967	Retrospective	USA, Harlem
Hall & Ofodile, 1991	11.9 21	2.8 5	22.2 39	46.0 81	10.3 18	4.0 7	2.8 5	* *	NS	116/176	1984- 1987	Retrospective	USA, New York
Hall, 1972	36.2 42	* *	* *	63.8 74	* *	* *	* *	* *	<16yr	*/116	1956- 1969	Retrospective	Australia, Melbourne
Hallmer, et al., 2010	32.9 143	6.0 26	16.8 73	37.3 162	PB PB	5.8 25	* *	1.2 5	All	*/434	1993- 2003	Retrospective	Sweden, Malmö
Hill, et al., 1984	13.9 *	2.8 *	33.3 *	38.9 *	8.3 *	* *	* *	2.8 *	All	214/*	1979- 1983	Prospective	UK, Bradford
Hung, et al., 2004	23.6 30	1.6 2	30.7 39	28.3 36	* *	15.7 20	* *	* *	6yr- 64yr	85/127	1997- 2001	Retrospective	New York, USA
Iida, et al., 2001	33.6 507	3.8 57	21.7 327	10.4 152	21.7 327	8.6 129	* *	0.6 9	All	955/1508	1981- 1996	Retrospective	Japan, Osaka
Iida, et al., 2003	38.1 135	2.8 10	21.8 77	34.2 121	PB *	2.0 7	* *	1.1 4	All	226/354	1997- 2001	Retrospective	Germany, Heidelberg
Imahara, et al., 2008	21.2 *	6.5 *	13.9 *	12.1 *	PS *	16.6 *	4.7 *	0.9 *	0-18yr	*/4169П	2001- 2005	Retrospective	USA
Infante Cossio, et al., 1994	43.3 43	0 *	20.3 20	12.3 12	* *	24.3 24	* *	0 *	<16y	59/99	1988- 1990	Retrospective	Spain, Seville
Joshi, et al., 2013	40.8 40	4.1 4	5.1 5	14.3 14	24.5 24	PS *	10.2 10	1.0 1	1y-15y	*/98	2005- 2010	Retrospective	Maharashtra, India

Authors	Condyle	Ramus	Angle	Body	Parasymphysis	Symphysis	Alveolus	Coronoid	Age range	Number of cases/fractures	Study Period	Study type	Country
Kadkhodaie, 2006	25.6 790	1.3 40	16.4 506	30.5 942	16.7 515	4.9 151	4.3 133	0.4 12	All	*/3089	2001-2004	Retrospective	Iran, Gilan
King, et al., 2004	18 *	10.3 *	26.9 *	25.6 *	19.2 *	* *	0 *	* *	All	134/225	7 years	Retrospective	USA, Illinois
King, et al., 2004	23.5 *	6.3 *	10.9 *	10.9 *	45.3 *	* *	3.1 *	* *	All		7 years	Retrospective	USA, Illinois
King, et al., 2004	2.8 *	11.1 *	5.6 *	36.1 *	44.4 *	* *	0 *	* *	All		7 years	Retrospective	USA, Illinois
King, et al., 2004	34.4 *	0 *	9.4 *	25 *	28.1 *	* *	3.1 *	* *	All		7 years	Retrospective	USA, Illinois
King, et al., 2004	50 *	0 *	0 *	12.5 *	37.5 *	* *	0 *	* *	All		7 years	Retrospective	USA, Illinois
Kiong, et al., 2007	17 *	1 *	12 *	27 *	20 *	13 *	10 *	* *	<15y	*/*	2002-2003	Retrospective	Malaysia, Johor Bahru
Kyrgidis, et al., 2013	34.2 460	* *	22.4 301	30.0 376	15.5 208	PS *	* *	* *	All	795/1345	1998-2008	Retrospective	Greece, Thessaloniki
Le, et al., 2001	32.0 8	4.0 1	28.0 7	12.0 3	16.0 4	PS *	8.0 2	0 *	All	*/25	1992-1996	Retrospective	USA, Oregon
Lee & Chou, 2010	15.6 *	0 *	50 *	3.1 *	* *	28.1 *	* *	3.1 *	All	21/*	1996-2006	Retrospective	New Zealand, Christchurch
Lee, 2009	24.8 358	3.5 51	33.7 486	15.3 221	16.2 234	6.4 92	* *	* *	2y-95y	1045/1442		Retrospective	New Zealand, Christchurch
Lee, et al., 2010	15.6 5	0 0	50.0 16	3.1 1	* *	28.1 9	* *	3.1 1	All	21/32	2003-2007	Retrospective	Korea, Jeju
Lindqvist, et al., 1986	68 *	1 *	5 *	11 *	11 *	* *	4 *	0 *	All	93/*	1981-1983	Retrospective	Finland, Helsinki
Linn, et al., 1986	55.1 38	1.5 1	13 9	8.7 6	15.9 11	5.8 4	* *	* *	All	*/69	1971-1978	Retrospective	Netherlands
Madhi & Ali, 2013	6 6	4 4	33 33	42 42	3 3	11 11	* *	1 1	All	*/100	2005-2006	Retrospective	Iraq, Baghdad
Madhi & Ali, 2013	18.7 28	6.7 10	27.3 41	17.3 26	21.3 32	7.3 11	* *	1.3 2	All	*/150	1995-1996	Retrospective	Iraq, Baghdad
Martins, et al., 2011	22.1 33	1.4 2	18.5 27	15.1 22	26.0 38	14.4 21	2.1 3	0 0	All	95/146	2007-2008	Retrospective	Brazil, Rio de Janeiro
Mijiti, et al., 2014	19.9 125	6.7 42	12.3 77	35.2 221	PS *	19.9 125	5.1 32	0.8 5	0-91y	*/627	2006-2010	Retrospective	Xinjiang, China

Authors	Condyle	Ramus	Angle	Body	Parasymphysis	Symphysis	Alveolus	Coronoid	Age range	Number of cases/fractures	Study Period	Study type	Country
Müller, 1969	28 *	3 *	26 *	43 *	* *	* *	* *	* *	All	*/2582	1961-1966	Retrospective	Germany, Halle
Muñante-Cárdenas, et al., 2010	43.2 60	1.4 2	15.1 21	15.1 21	18.7 26	6.5 9	* *	* *	<16y	112/139	1999-2008	Retrospective	Brazil, Sao Paulo
Mwaniki & Guthua, 1990	3 *	4.9 *	26.5 *	42.2 *	* *	20.5 *	3 *	* *	All	*/*	1984-1986	Retrospective	Kenya, Nairobi
Ogundare, et al., 2003	16.6 *	2.2 *	36.3 *	21.2 *	17.8 *	4.3 *	1 *	* *	All	*/*	1990-1999	Retrospective	Washington DC
Oji, 1998	31.0 13	* *	11.9 5	21.4 9	14.3 6	9.5 4	11.9 5	0 *	<11y	*/42	1985-1996	Retrospective	Nigeria, Enugu
Oji, 1999	26 *	2.1 *	17.4 *	36.2 *	15.3 *	* *	2 *	0.2 *	All	481/900	1985-1995	Retrospective	Nigeria, Enugu
Ólafsson, 1984	32.6 124	3.4 13	20.3 77	28.2 107	* *	12.4 47	1.6 6	1.6 6	All	238/380	1970-1979	Retrospective	Iceland, Reykjavik
Olasoji, et al., 2002	11.4 31	* *	4.4 12	56.8 155	7.3 20	20.1 55	* *	0 *	1y-62y	203/273	1996-1999	Prospective	Nigeria, Maiduguri
Olson, et al., 1982	29.1 *	1.7 *	24.5 *	16 *	22 *	PS *	3.1 *	1.3 *	All	580/8	1972-1978	Retrospective	USA, Iowa
Ortakoğlu, et al., 2004	26.1 42	1.86 3	17.4 28	30.4 49	PS PS	24.2 39	* *	* *	*	126/161	1994-1999	Retrospective	Turkey, Ankara
Qudah, et al., 2005	38.4 83	11.6 25	13.9 30	16.2 35	18.1 39	* *	* *	1.9 4	All	203/216	1993-2002	Retrospective	Jordan, Irbid
Qudah, et al., 2005	15.3 104	20.9 142	24.7 168	31.8 216	4.6 31	* *	* *	2.8 19	All	497/680	1993-2002	Retrospective	Jordan, Irbid
Ramli, et al., 2008	11.4 5	* *	29.5 13	18.2 8	31.8 14	9.1 4	* *	* *	All	*/44	2004-2005	Retrospective	Malaysia, Kuala Lumpur
Sakr, et al., 2006	19.1 142	1.5 11	22.1 164	21.1 157	21.5 160	8.2 61	5.4 40	1.1 8	All	509/743	1991-2000	Retrospective	Egypt, Alexandria
Salem, et al., 1968	21.0 169	4.2 34	21.3 171	15.4 124	15.9 128	13.3 107	8.0 64	0.7 6	All	523/803	1966-1967	Retrospective	USA, California
Sane, et al., 1988	43.1 28	1.5 1	27.7 18	10.8 7	6.2 4	6.2 4	* *	4.6 3	All	*/65	1981-1985	Retrospective	Finland, Helsinki
Sasaki, et al., 2012	26. 239	2.9 26	23.8 217	13.6 124	* *	32.4 295	* *	1.0 9	All	*/910	2000-2004	Retrospective	Japan, Tokyo

Authors	Condyle	Ramus	Angle	Body	Parasymphysis	Symphysis	Alveolus	Coronoid	Age range	Number of cases/fractures		Study Period	Study type	Country
Sawhney & Ahuja, 1988	22 *	1 *	24 *	20 *	* *	33 *	* *	0 *	2y-80y	123/*		1982-1983	Retrospective	India, Chandigarh
Schön, et al., 2001	9.1 14	5.2 8	42.9 66	26.0 40	16.2 25	PS *	* *	0.6 1	All	114/154		1995	Retrospective	Australia, Townsville
Schuchardt, et al., 1966	24 *	4 *	20 *	52 *	* *	* *	* *	* *	All	922/*		1958-1963	Retrospective	Germany, Hamburg
Simsek, et al., 2007	15.9 40	3.6 9	27.4 69	29.0 73	* *	22.6 57	1.6 4	* *	3y-79y	210/252		1991-2000	Retrospective	Turkey, Ankara
Simsek, et al., 2007	18.9 197	3.9 41	27.6 287	23.1 240	* *	25.7 268	0.8 8	* *	3y-87y	665/1041		1991-2000	Retrospective	USA, Virginia
Stylogianni, et al., 1991	46.3 57	1.6 2	5.7 7	38.2 47	* *	* *	8.1 10	* *	All	92/123		1980-1987	Retrospective	Greece, Athens
Subhashraj, et al., 2007	18.8 96	4.7 24	11.7 60	8.2 42	30.5 156	10.5 54	11.1 57	4.5 23	All	*/512		1999-2005	Retrospective	India, Chennai
Subhashraj, et al., 2008	22.1 98	2.7 12	11.5 51	5.9 26	35.2 156	10.4 46	10.8 48	1.4 6	6y-89y	238/443		2000-2004	Retrospective	India, Chennai
Thorén, et al., 1992	76.0 *	0 *	4.0 *	0 *	* *	8.0 *	12.0 *	* *	0y-5y	19	157/220	1980-1989	Retrospective	Finland, Helsinki
Thorén, et al., 1992	63.6 *	0 *	3.6 *	9.1 *	* *	18.2 *	5.4 *	* *	6y-9y	38		1980-1989	Retrospective	Finland, Helsinki
Thorén, et al., 1992	63.8 *	1.7 *	8.6 *	10.3 *	* *	12.1 *	3.4 *	* *	10y-12y	41		1980-1989	Retrospective	Finland, Helsinki
Thorén, et al., 1992	50 *	3.7 *	17.1 *	11 *	* *	15.5 *	2.4 *	* *	13y-15y	59		1980-1989	Retrospective	Finland, Helsinki
Thorén, et al., 2009	60.8 236	1.5 6	10.3 40	7.2 28	PS *	20.1 78	* *	* *	NS	*/388		1993-2002	Retrospective	Finland, Helsinki
van Beek & Merkx, 1999	46.1 610	1.9 25	13.6 180	38.4 509	* *	* *	* *	* *	All	822/1324		1960-1974	Retrospective	Netherlands
van Beek & Merkx, 1999	44.8 532	2.8 33	13.7 163	38.7 459	* *	* *	* *	* *	All	707/1187		1975-1987	Retrospective	Netherlands
Van Hoof, et al., 1977	46.4 583	1.2 15	14.1 177	10.2 128	14.2 178	13.2 166	* *	0.7 9	All	797/1256		1960-1974	Retrospective	Netherlands
Venugopal, et al., 2010	24.7 80	* *	12.7 41	11.1 36	51.5 167	* *	* *	* *	14y-65y	108/324		2004-2008	Retrospective	India, New Delhi

Authors	Condyle	Ramus	Angle	Body	Parasymphysis	Symphysis	Alveolus	Coronoid	Age range	Number of cases/fractures	Study Period	Study type	Country
Walden, et al., 1956	19.0 136	5.0 36	23.6 169	42.1 301	* *	9.2 66	0.1 7	* *	All	466/715	1950-1954	Retrospective	USA, New York
Yamamoto, et al., 2010	55.9 280	2.4 12	6.2 31	12.2 61	* *	17.0 85	6.4 32	* *	All	*/501	1981-2007	Retrospective	Japan, Nara
Yamamoto, et al., 2011	38.2 34	4.5 4	13.5 12	10.1 9	* *	27.0 24	4.5 4	2.2 2	All	62/89	1982-2008	Retrospective	Japan, Nara
Zachar, et al., 2013	21.2 *	* *	33.4 *	19.6 *	13.2 *	PS *	5.7 *	6.9 *	All	391/618	2001-2011	Retrospective	Afghanistan
Zachariades, et al., 1983	21 *	8.9 *	* *	32.3 *	* *	26.6 *	10.1 *	1.2 *	All	694/*	1970-1980	Retrospective	Greece, Athens
Zachariades, et al., 1983[α]	42.3 44	RA *	21.1 22	25.0 26	* *	11.5 12	* *	* *	All	62/104	1970-1980	Retrospective	Greece, Athens
Zachariades & Papavassiliou, 1990[α]	26 65	4.4 11	6.8 17	16 40	* *	17.2 43	29.6 74	* *	<14y	*/250	1960-1984	Retrospective	Greece, Athens
Zachariades & Papavassiliou, 1990[α]	23.9 1155	7.4 360	15.4 747	21.1 1021	* *	23.5 1141	8.6 414	* *	All	*/4838	1960-1984	Retrospective	Greece, Athens
Zachariades & Papavassiliou, 1990[α]	23.8 1140	7.3 349	15.4 736	20.5 968	* *	23.6 1129	8.5 406	1.1 52	NS	*/4780	1960-1984	Retrospective	Greece, Athens
Zhou, et al., 2013	54.2 156	0.3 1	7.6 22	14.9 43	* *	21.5 62	1 3	0.3 1	<18y	192/288	2000-2009	Retrospective	China, Wuhan
Zix, et al., 2011	42.7 303	0.7 5	12.3 87	7.5 53	PS PS	34.7 246	* *	1.8 13	16y-97y	420/709	2000-2007	Retrospective	Switzerland, Bern

Table 2.7 ***Articles assessed for meta-analysis eligibility. Shaded studies were excluded from the meta-analysis.***

KEY. PS=Parasymphysis and symphysis combined in study; PB=parasymphysis and body combined in study; RA=ramus and angle combined in study. CC, condyle and coronoid combined in study. *=No data in study. †=Classification into anterior and posterior body. NC= not in classification. α= Studies derived from same dataset. U = unclear from data given. NS= not specified in study. γ= only single site fractures included. ∆, one study was excluded due to the inability to identify the fracture type as the mandible was lost in gunshot wound. Studies with multiple data sets are recorded under the same author and the same year. Π= Raw data as presented in study did not match author calculations.

2.4.1.3.1 Summary of studies deemed suitable for meta-analysis

The table below shows the tabulated event data for the 32 studies used in each meta-analysis. The value ***n*** represents the total number of fractures reported in the study and ***r*** represents the number of fractures of the required outcome i.e. fracture sub-site.

Author	Condyle		Ascending ramus		Angle		Body		Parasymphysis		Alveolus	
	r	*Total (n)*	*r*	*Total (n)*	*r*	*Total (n)*	*r*	*Total (n)*	*r*	*Total (n)*	*r*	*Total (n)*
Abdullah, et al., 2013	42	189	5	189	33	189	30	189	68	189	11	189
Adebayo, et al., 2003	27	465	23	465	86	465	238	465	57	465	34	465
Adi, et al., 1990	165	632	35	632	123	632	166	632	121	632	22	632
Al Ahmed, et al., 2004	38	150	8	150	35	150	30	150	27	150	12	150
Al-Khateeb and Abdullah, 2007	33	270	14	270	47	270	107	270	42	270	27	270
Andersson, et al., 1984	406	936	30	936	126	936	217	936	110	936	47	936
Bither, et al., 2008	81	486	29	486	96	486	66	486	198	486	16	486
Elgehani, et al., 2009	124	665	22	665	145	665	128	665	217	665	29	665
Ellis, et al., 1985	910	3124	150	3124	729	3124	1029	3124	272	3124	34	3124
Eskitaşcıoğlu, et al., 2009	64	333	5	333	35	333	44	333	146	333	39	333
Eskitaşcıoğlu, et al., 2013	215	1090	31	1090	182	1090	215	1090	392	1090	55	1090
Ferreira, et al., 2004	211	681	52	681	109	681	90	681	143	681	76	681
Gandhi, et al., 2011	69	479	3	479	88	479	47	479	237	479	35	479
Hall and Ofodile, 1991	21	176	5	176	39	176	81	176	25	176	5	176
Joshi, et al., 2013	40	98	5	98	5	98	14	98	24	98	10	98
Kadkhodaie, 2006	790	3089	52	3089	506	3089	942	3089	666	3089	133	3089
Le, et al., 2001	8	25	1	25	7	25	3	25	4	25	2	25
Martins, et al., 2011	33	146	2	146	27	146	22	146	59	146	3	146
Mijiti, et al., 2014	125	627	47	627	77	627	221	627	125	627	32	627
Oji, 1998	13	42	0	42	5	42	9	42	10	42	5	42
Olafsson, 1984	124	380	19	380	77	380	107	380	47	380	6	380
Sakr, et al., 2006	142	743	19	743	164	743	157	743	221	743	40	743
Salem, et al., 1968	169	803	40	803	171	803	124	803	235	803	64	803
Simsek, et al., 2007 (a)	40	252	9	252	69	252	73	252	57	252	4	252
Simsek, et al., 2007 (b)	197	1041	41	1041	287	1041	240	1041	268	1041	8	1041
Subhashraj, et al., 2007	96	512	47	512	60	512	42	512	210	512	57	512
Subhashraj, et al., 2008	98	443	18	443	51	443	26	443	202	443	48	443
Walden, et al., 1956	136	715	36	715	169	715	301	715	66	715	7	715
Yamamoto K et al. 2010	280	501	12	501	31	501	61	501	85	501	32	501
Yamamoto, et al., 2011	34	89	6	89	12	89	9	89	24	89	4	89
Zachariades, et al., 1990	1155	4838	360	4838	747	4838	1021	4838	1141	4838	414	4838
Zhou, et al., 2013	156	288	2	288	22	288	43	288	62	288	3	288

Table 2.8 Tabulated event data.

2.4.1.3.2 Bias assessment

The bias assessment plots show sub-site fracture prevalence on the horizontal axis as a proportion, and the precision of the estimated effect on the vertical axis. The precision is the inverse of the standard error. As may be seen, the "funnel" is inverted with a precision of zero on the vertical axis inferiorly. Each study is represented by a red dot. The least precise studies are found at the bottom of the plot. The orange vertical line which lies between the 95% confidence interval curves (blue) represents the overall prevalence estimate. In cases where there is no significant bias the funnel plot is symmetrical about the overall prevalence estimate line (Higgins, et al., 2003). The funnel plot for the mandibular condyle is shown in section 2.4.1.3.4.; the remaining funnel and Forest plots are found in appendix 7. As visual assessment of asymmetry, and hence bias, is difficult and somewhat unreliable, statistical bias assessments were undertaken. The null hypothesis for Egger's test is that the funnel plot is symmetrical, with the alternate being funnel asymmetry. The value of P for Egger's test was less than 0.05 for fractures of the parasymphysis and alveolus and therefore there was evidence to reject the null hypothesis and accept the alternate at the 5% level of significance. Therefore these studies showed significant bias.

	Condyle	**Ascending ramus**	**Angle**	**Body**	**Parasymphysis**	**Alveolus**
Non-combinability of studies						
Cochran Q	910.0045 (df = 31) P < 0.0001	308.5647 (df = 31) P < 0.0001	386.679809 (df = 31) P < 0.0001	1156.094052 (df = 31) P < 0.0001	1460.611714 (df = 31) P < 0.0001	604.6960 (df = 31) P < 0.0001
I^2 (inconsistency)	96.6% (95% CI = 96.1% to 97%)	90% (95% CI = 87.3% to 91.8%)	92% (95% CI = 90.1% to 93.3%)	97.3% (95% CI = 97% to 97.6%)	97.9% (95% CI = 97.6% to 98.1%)	94.9% (95% CI = 94% to 95.6%)
Bias indicators						
Egger	1.094624 (95% CI = -3.0424 to 5.2317) P = 0.5929	1.626406 (95% CI = -0.4968 to 3.7496) P = 0.1282	0.5098 (95% CI = -2.1569 to 3.1765) P = 0.699	-0.0672 (95% CI = -4.9468 to 4.8123) P = 0.9777	6.0081 (95% CI = 1.9948 to 10.0215) P = 0.0047	3.9679 (95% CI = 1.8524 to 6.0833) P = 0.0006

Table 2.9 Combined bias calculations for each mandibular sub-site.

In addition to the meta-analysis data, the forest plots give a graphical representation of the results of the meta-analysis. For the 32 studies, the authors are displayed on the left and the estimated prevalence with the associated confidence interval is displayed on the right as a proportion. The study prevalence is represented by a blue square and its associated confidence interval by the associated horizontal line. The overall combined prevalence is indicated by the orange diamond. An assessment of the variation between the study estimates was made.

2.4.1.3.3 Heterogeneity

Although Cochran Q aims to determine the degree of heterogeneity (i.e. whether there are real differences between study results), its calculation method (chi-squared distribution with k-1 degrees of freedom) renders it susceptible to error due to the number of studies. The number of studies included was relatively high and therefore the effects should have been minimized. Nevertheless, it was included so that the inconsistency (I^2) could be calculated. I^2 does not depend on the number of studies and has values between 0% and 100%, with a value of 0% representing no heterogeneity (Higgins, et al., 2003). The null hypothesis for this test is that homogeneity existed, with the alternate being that heterogeneity was present. Significant heterogeneity is suggested if $I^2 \geq 50\%$. It may be seen that there was significant statistical heterogeneity present amongst the studies of all analyses and therefore the random effects model was considered to be the most appropriate, despite giving a slightly less accurate combined effect size with a wider confidence interval. The fixed effect results may be found in appendix 7 for comparison.

2.4.1.3.4 Condyle

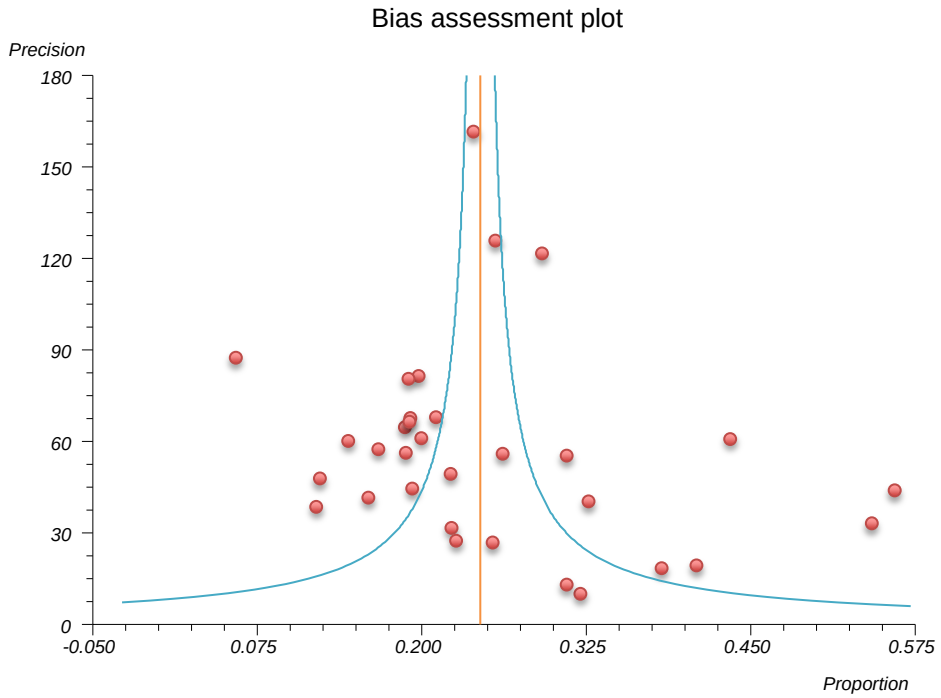

Graph 2.1 Condyle bias assessment plot.

Author	Effect Size (Proportion) and 95% Confidence Interval (exact)			% Weight
	Point Estimate	Lower Limit	Upper Limit	Random
Abdullah, et al., 2013	0.222222	0.165099	0.288274	3.027431
Adebayo, et al., 2003	0.058065	0.03861	0.083359	3.253832
Adi, et al., 1990	0.261076	0.227225	0.297176	3.298634
Al Ahmed, et al., 2004	0.253333	0.18593	0.330744	2.938277
Al-Khateeb and Abdullah, 2007	0.122222	0.085645	0.167346	3.137604
Andersson, et al., 1984	0.433761	0.401728	0.466211	3.340272
Bither, et al., 2008	0.166667	0.134617	0.202835	3.261072
Elgehani, et al., 2009	0.186466	0.157557	0.218189	3.304926
Ellis, et al., 1985	0.291293	0.275402	0.307576	3.402894
Eskitaşcıoğlu, et al., 2009	0.192192	0.151273	0.238684	3.18895
Eskitaşcıoğlu, et al., 2013	0.197248	0.174009	0.222133	3.35271
Ferreira, et al., 2004	0.309838	0.275261	0.346073	3.307765
Gandhi, et al., 2011	0.14405	0.113839	0.178734	3.258725
Hall and Ofodile, 1991	0.119318	0.075398	0.176593	3.001533
Joshi, et al., 2013	0.408163	0.309923	0.512107	2.732374
Kadkhodaie, 2006	0.255746	0.240436	0.27152	3.402584
Le, et al., 2001	0.32	0.149495	0.535001	1.738882
Martins, et al., 2011	0.226027	0.160983	0.302523	2.926851
Mijiti, et al., 2014	0.199362	0.168769	0.232816	3.297625
Oji, 1998	0.309524	0.176221	0.470861	2.15996
Olafsson, 1984	0.326316	0.279373	0.37599	3.216885
Sakr, et al., 2006	0.191117	0.163445	0.221266	3.317652
Salem, et al., 1968	0.210461	0.182749	0.240316	3.325812
Simsek, et al., 2007 (a)	0.15873	0.115885	0.209811	3.118664
Simsek, et al., 2007 (b)	0.189241	0.165872	0.214382	3.349142
Subhashraj, et al., 2007	0.1875	0.154601	0.224055	3.269252
Subhashraj, et al., 2008	0.221219	0.183411	0.262796	3.245553
Walden, et al., 1956	0.19021	0.16207	0.220932	3.313392
Yamamoto K et al. 2010	0.558882	0.514167	0.602899	3.26589
Yamamoto, et al., 2011	0.382022	0.281	0.49113	2.677881
Zachariades, et al., 1990	0.238735	0.226779	0.251007	3.412599
Zhou, et al., 2013	0.541667	0.48221	0.600257	3.154375

Table 2.10 Condyle results.

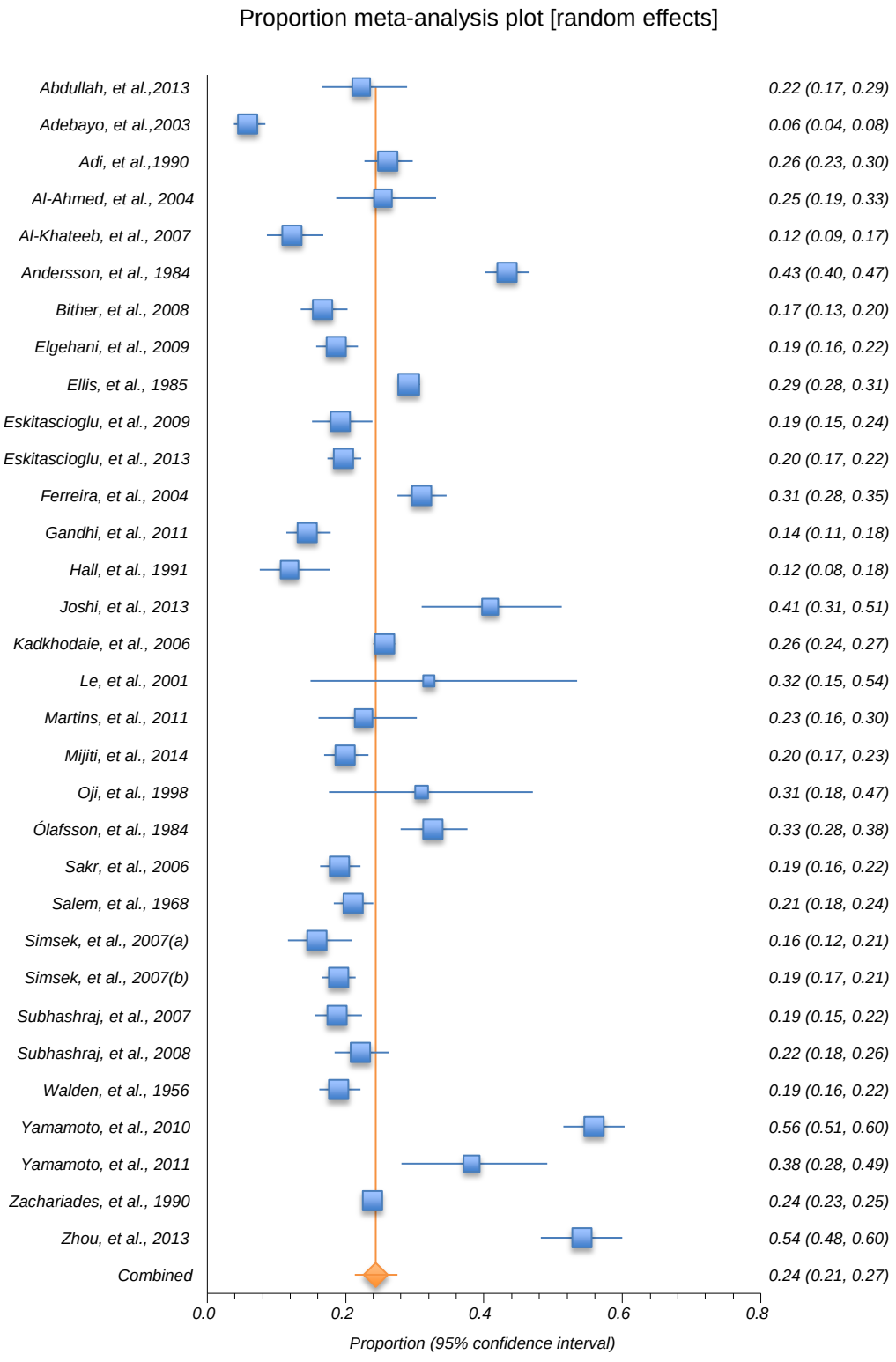

Graph 2.2 Condyle Forest plot (random effects).

2.4.1.4 Summary results

Anatomical location of fracture	*Effect size (Prevalence)*	*95% Confidence interval Random effects*	*Analysis set (k)*
Angle	**0.172**	(0.154 - 0.190)	32
Body	**0.214**	(0.181 - 0.248)	32
Condyle	**0.243**	(0.212 - 0.275)	32
Dentoalveolar	**0.053**	(0.041 - 0.068)	32
Symphyseal/Parasymphyseal	**0.247**	(0.209 - 0.287)	32
Ascending ramus	**0.040**	(0.032 - 0.049)	32

Table 2.11 Summary prevalence for mandibular fracture sub-sites.

2.4.1.5 Discussion

There are limitations to this analysis, several intrinsic to meta-analyses. Publication bias is always a problem as studies which support a particular theory regarding sub-site prevalence are more likely to be published in readily accessible journals. Other sources included, language bias, particularly concerning the English language. Even in an electronic database search, studies in the English language are more likely to be published. There may also have been some citation bias as studies were usually accompanied with an explanation for the findings and those authors that found that their studies agreed with the prevailing opinion at the time were more likely to be cited and therefore picked up on an electronic search. As suggested, multiple publication bias is a problem when authors have used the same or similar data in multiple publications. This is particularly a problem when the data of a previous analysis is later combined with newer data and published in another journal without the author specifically stating that some of the data had been previously used in publication.

Differences in methodological quality may result in heterogeneity. Many studies included non-uniform definitions as to the position of anatomical sub-sites. Although, the Dingman and Natvig classification was chosen for the study the classification itself may not have been sufficiently accurate to define the anatomical sub-site. There are

frequently different interpretations of the anatomical boundary or regions such as the condylar region, the angle of the mandible and the symphysis. This problem is accentuated when there has been tooth loss. These problems should have been minimized in the combining regions such as the parasymphysis/symphysis and the ramus/coronoid. Studies which did not use the Dingman and Natvig classification were excluded; however, these could have included pertinent information.

Most of the studies were retrospective in nature and involved a re-examination of pertinent plain radiographs of variable quality. Studies have shown that plain radiographs, particularly dental panoramic tomographs, are less accurate, less sensitive and less specific for the diagnosis of mandibular fractures when compared to computed tomography (Roth, et al., 2005; Wilson, et al., 2001); therefore the incidence of mandibular fractures, especially condylar fractures may be higher than reported. Those studies performed earlier (e.g. Walden, et al., 1956) would have diagnosed fractures using different and less accurate means i.e. from the examination of two oblique lateral views rather than the use of the dental panoramic radiograph which was became common much later on and was itself superceded by conventional or cone-beam CT in some centres.

Studies involving children were not excluded by many investigators and many authors differed in their classification of a child (e.g. Oji, 1998 (<11 years old); Ugboko, et al., 2000 (< 14 years old); Olasoji, et al., 2002 (< 15 years old)). Whether the change in mandibular form with age was significant enough to affect the prevalence of certain fractures remains unsure.

When the total number of fractures is considered, and this is irrespective of the number of fractures sustained in any single patient, it is difficult to determine which anatomical sub-site is fractured most frequently from the results of this meta-analysis as the effect

size for the condyle, parasymphysis/symphysis and angle are similar, showing significant dispersion.

Despite all of the limitations of the various forms of bias and the degree of statistical heterogeneity, one must consider the alternative method of attempting to synthesize the prevalence data found in the literature search i.e. the narrative review. Many of the same forms of bias would be present; however, as this would not be quantified in a narrative review there would be a tendency to ignore it. The strict criterion for study eligibility in the meta-analysis is an advantage that is not always present in a narrative review or if it is present, it is not formally stated. The reason for including a study in a purely narrative review may introduce a reviewer bias in a very non-transparent way that makes it difficult to interpret, whereas the meta-analysis details all studies and the procedures of inclusion and exclusion, allowing quantification of bias. Additionally, the weight given to a particular study in a narrative review is at the discretion of the author whereas the weighting system for a meta-analysis is described in the report.

In the same way that bias was addressed, so was heterogeneity. This was quantified and steps taken to minimize the effect, e.g. by the use of the random effect model. The narrative review has no common equivalent. Therefore it can be said that the use of a meta-analysis was the best way to synthesize the prevalence data.

2.4.1.6 Conclusion

The mandible has unique geometry, which result in areas inherently susceptible to fracture. It is reasonable to assume that fractures in these areas should occur more frequently than would be expected by chance alone and this should be reflected in the incidence and pattern of fractures. The meta-analysis has given some insight into areas of the mandible that are more frequently fractured with more accuracy all reported

studies thus far. It may give a suggestion that certain sites have an increased propensity over others, but gives no real indication as to the reason for this, although the mechanism of injury may be a significant factor. Where the mandibular anatomy is significantly different or integrity of the bone is compromised due to the presence of a local change in material properties, such as an un-erupted third molar tooth, the pattern of fracture may differ. No studies specifically took this factor into account when reporting prevalence. The overall prevalence of mandibular sub-site fractures therefore does not give the full picture regarding the "weak" (Halazonetis, 1968) regions of the mandible. Epidemiological prevalence studies are useful in planning treatment need and the organization of services; however, difficulties arise when using these studies to determine the "weak" areas of the mandible. Traumatic forces that result in fractures may present to a particular mandibular sub-site more than others. Those who have a more prognathic chin (i.e. have a class III skeletal base) may be expected to experience more chin trauma compared with those with a retrognathic profile (class II skeletal base) where the chin is relatively more protected by the cranio-facial skeleton. None of the articles reviewed for the meta-analysis took into account the skeletal relationship when determining the fracture sub-site frequency. What the meta-analysis does suggest is that most impacts to the mandible occur in the anterior region, which, depending on the impact force and contact area may result in fractures in the condylar region or the symphyseal/parasymphyseal region.

2.4.2 Multifocal fractures

2.4.2.1 Introduction and aim

Multifocal fractures occur at more than one site. This section aims to review the reported range of multifocality in the literature and identify consistent fracture patterns.

2.4.2.2 Method

The studies identified in section 2.4 were reviewed to determine any studies that also reported the pattern of multiple mandibular fractures.

2.4.2.3 Results

Eleven studies gave details of mandibular fracture combinations.

Author	Multifocal fracture frequency
Ferreira, et al., 2004	26.1%
Elgehani, et al., 2009	37.2%
Iida, et al., 2001	48.5%
Adebayo, et al., 2003	49.5%
Van Hoof et al., 1977	49.8%
Ellis 3rd, et al., 1985	51.4 %
Ólafsson, 1984	51.7%
Adi, et al., 1990	52.9%
Subhashraj, et al., 2008	54.6%
King, et al., 2004	67.9%
Greene, et al., 1997	69.8%

Table 2.12 Reported multifocal mandibular fracture incidences.

Five studies also gave details of the sub-site pattern of multiple fractures. None of the authors differentiated between sides concerning fracture patterns. Some common fracture patterns reported are seen in Figures 2.5 to 2.8.

Author and multifocal fracture pattern frequency									
Schön, et al., 2001	**%**	**Adekeye, 1980**	**%**	**Goldberg and Williams, 1969**	**%**	**Muñante-Cárdenas, et al., 2010**	**%**	**Copcu, et al., 2004**	**%**
Parasymphysis, angle	17	Bilateral body	58.5	Bilateral body	27	Angle, body	18.5	Angle, parasymphysis	33
Parasymphysis, subcondyle	12	Right angle, left body	19.0	Symphysis, body	7	Angle, parasymphysis	18.5	Angle, body	15
Body, subcondyle	15	Left angle, right body	9.5	Symphysis, subcondyle	3	Parasymphysis, subcondyle	18.5	Parasymphysis, subcondyle	10
Angle, body	40	Left condyle, right body	8.7	Symphysis, bilateral subcondyle	1	Symphysis, subcondyle	14.8	Bilateral subcondyle	10
		Bilateral angle	2.6	Bilateral subcondyle	2	Body, subcondyle	18.5	Body, subcondyle	7
		Bilateral condyle	1.8	Body, subcondyle	5	Body, symphysis	11	Bilateral angle	6
				Body, bilateral subcondyle	1			Angle, subcondyle	5
				Ramus and other	2			Bilateral body	4

Table 2.13 Mandibular fracture combinations reported in the literature with frequencies.

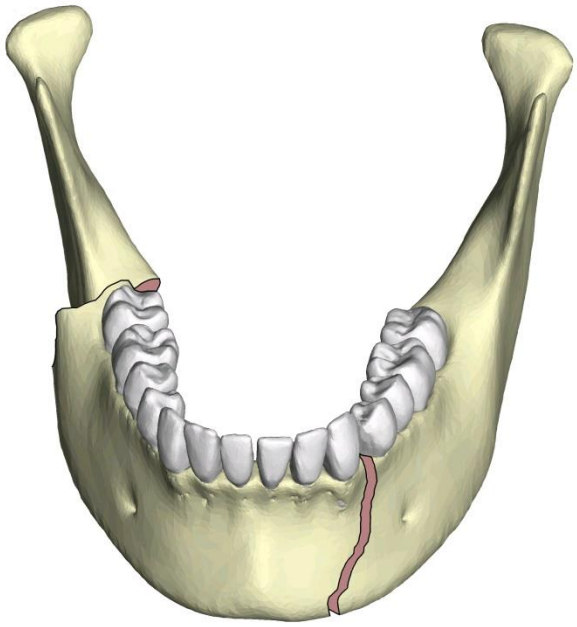

Figure 2.5 Right angle, left parasymphysis fracture combination. (Adapted from Colton, et al., 2014)

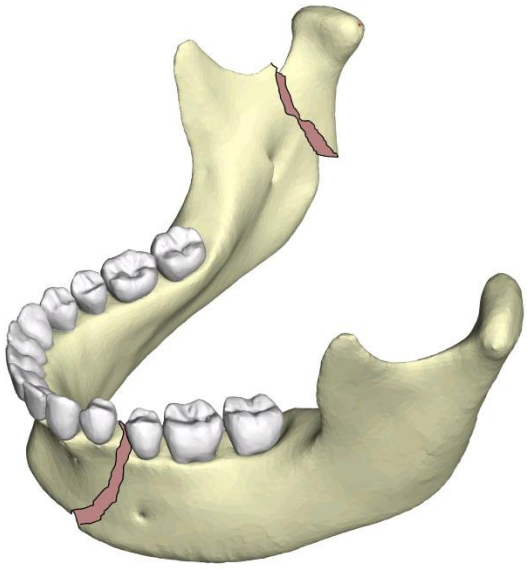

Figure 2.6 Right condyle, left parasymphysis fracture combination. (Adapted from Colton, et al., 2014)

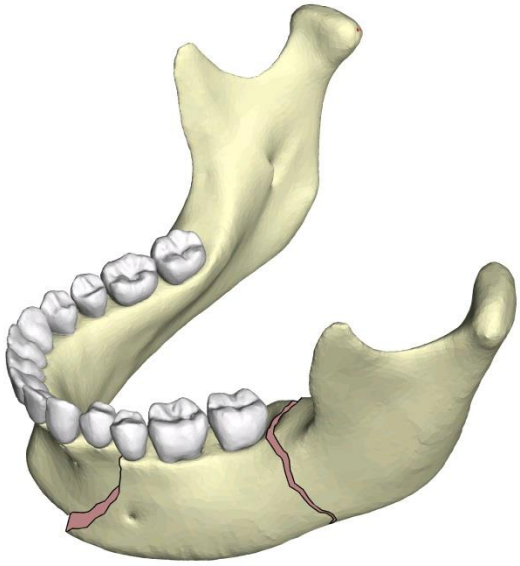

Figure 2.7 Left body condyle and left angle fracture combination. (Adapted from Colton, et al., 2014)

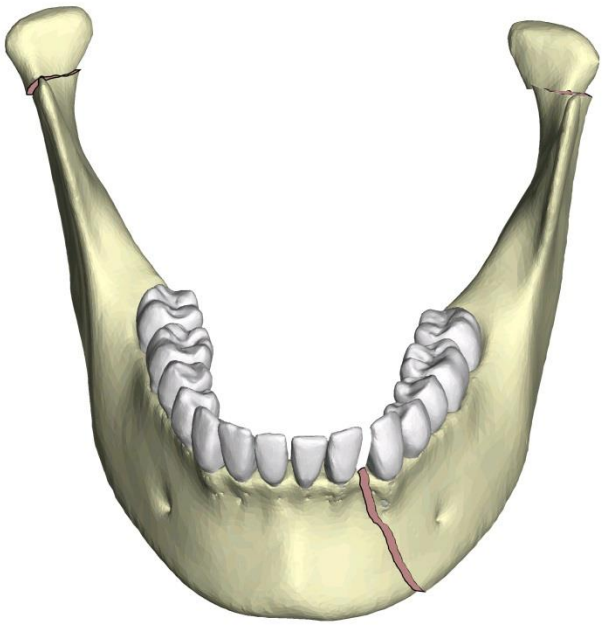

Figure 2.8 Bilateral condyles, left parasymphysis fracture combination. (Adapted from Colton, et al., 2014)

2.5.4 Discussion

Multifocal fractures of the mandible appear to be at least as common as uni-focal. The vast majority of the retrospective studies reviewed plain radiographs. Neither sagittal fractures nor sub-clinical damage such as compression fracture of the condylar head can be seen on plain radiographs and therefore are frequently undiagnosed (Rhea, et al., 1999). This suggests that the incidence of these fractures may be even higher than the 24.3% suggested in the meta-analysis (see table 2.13).

2.4.3 The effect of third molars on the incidence of angle fractures

2.4.3.1 Introduction and aim

Many papers have found that the angle of the mandible is fractured most frequently (although this was not found in the meta-analysis in section 2.4.1.4). This may be related to the presence of un-erupted or partially erupted third molar teeth. The purpose of this section was to assess the evidence for the proposition that the presence of third molar teeth increases the risk of fractures at the angle of the mandible.

2.4.3.2 Method

An electronic search of EMBASE, PubMed and MEDLINE databases was performed. The Medical Subject Headings (MeSH) and search strategies used are shown in table 2.14. The search yielded 352 articles. These were reviewed by abstract and title. The inclusion criteria included studies relating mandibular angle fractures and the presence of third molar teeth in humans. Two-hundred and ninety four abstracts were rejected due to failure to reach the inclusion criteria. There were no exclusions due to language. Once duplicate studies were removed, twenty-eight articles were available for review. The flow chart for the selection process is shown in figure 2.8.

Electronic Databases and Search Strategy	No. Hits per Database
Database: Ovid MEDLINE(R) In-Process and Other Non-Indexed Citations and Ovid MEDLINE(R) <1946 to Present>, Ovid OLDMEDLINE(R) <1946 to 1965>, Embase Classic+Embase <1947 to 2014 May 21> **Search Strategy:** **(mandible and fracture and third molar).mp. [mp=ti, ab, ot, nm, hw, kf, ps, rs, ui, an, sh, tn, dm, mf, dv, kw] (156)**	156
Database: PubMed **Search Strategy: ((mandible or mandibular) and fracture and third molar)** **Query Translation:** **("mandibular fractures"[MeSH Terms] OR ("mandibular"[All Fields] AND "fractures"[All Fields]) OR "mandibular fractures"[All Fields] OR ("mandible"[All Fields] AND "fracture"[All Fields]) OR "mandible fracture"[All Fields]) AND ("molar, third"[MeSH Terms] OR ("molar"[All Fields] AND "third"[All Fields]) OR "third molar"[All Fields] OR ("third"[All Fields] AND "molar"[All Fields]))**	196
Total	352

Table 2.14 Search strategies employed in the prevalence meta-analysis.

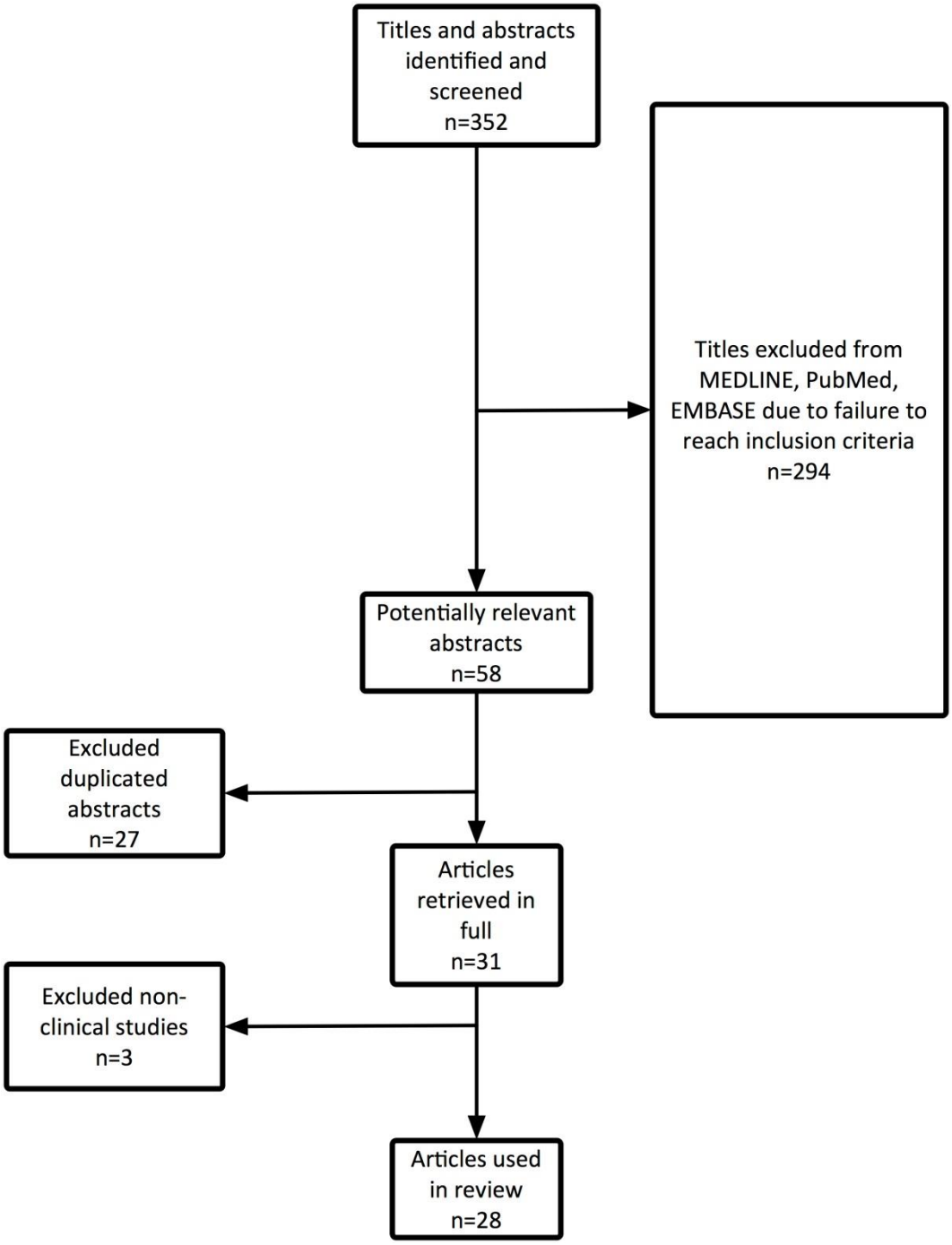

Figure 2.9 Literature review search strategy.

2.4.3.3 Results

The conclusion summaries of the studies are found in table 2.15.

2.4.3.3.1 Review of Studies

Four retrospective studies aimed to measure associations between mandibular third molar position and the risk of angle fracture (Tevepaugh and Dodson, 1995; Lee and Dodson, 2000; Fuselier, et al., 2002; Halmos, et al., 2004). These papers are of interest as they all have a common co-author, and all, in part or in entirety, utilize the cohort of patients admitted to the Grady Memorial Hospital, between January 1993 and February 1994. In the case of Tevepaugh, et al. (1995), data was used over the period January 1993 to February 1994. Lee, et al. (2000) added data, increasing the data collection period to February 1998. Fuselier, et al. (2002), added data from Parkland Memorial Hospital, Dallas, TX (period 1990 to 2000) to the data of the Tevepaugh and Lee studies, and finally, Halmos, et al., utilized the two previous data sources and added data from Massachusetts General Hospital, Boston, MA, between 1993 and 2001, to increase their sample size.

The use of the same data source in multiple publications is fraught with the potential for bias. Any bias that was introduced in the initial study would be present in all of the other studies, thus weakening their validity. As with many such studies, all of the patients in the cohort suffered from selection bias. Retrospective studies that are based on inpatient records only take into account those patients who required inpatient management. Many minimally displaced angle fractures may have been managed non-surgically and therefore such cases would not be identified. Additionally, the decision on whether to manage an angle fracture non-surgically may well be influenced by the presence of an impacted third molar tooth. The methodology of the four papers was the

same. The Pell and Gregory classification (Pell and Gregory, 1942) was used to classify the position of third molar position after the fracture had occurred. The post-fracture position could be significantly different to the pre-morbid condition making position measurements inaccurate. No system was used to classify the impacted tooth itself i.e. whether or not there was any associated bone resorption, tooth follicle enlargement or apical pathology. In addition, as radiographs are 2-dimensional representations of 3-dimensional objects, no account of bucco-lingual displacement of the tooth. This could be as important a factor for fracture development. In Tevepaugh's study, 105 mandibular fractures were found, 73 fractures were associated with third molars and 32 had no associated third molars. The authors calculated the relative risk of suffering an angle fracture with a third molar present to be 3.8. Their proposed mechanism for this was that the third molar weakened the mandible by reducing the cross-sectional area of bone. No association was found between the position or angulation of the tooth and the presence of the angle fracture.

Lee, et al. (2000) concluded that mandibles with the most deeply impacted third molar teeth had a 50% decrease in angle fracture risk compared to superficially placed third molars. The overall relative risk was calculated as 1.9. The *Halmos* study also compared fracture risk and third molar depth. The adjusted odds ratio was calculated as 2.8 with a 95% confidence interval of 2.3 to 3.4. The authors were unable to find a theory, which fitted their findings. The conclusions of all four studies were similar i.e. patients with third molar teeth present had a significantly increased likelihood of an angle fracture. Additionally, they concluded that the risk for an angle fracture was variable and depended on third molar position.

Two studies were only presented as papers at different conferences and therefore it was not possible to examine their methodology in detail (Milzman, et al., 2013; Weiner, et

al., 2012). However, it is clear from the abstracts that the three presentations referred to exactly the patient population, used the same methodology, produced identical results and had the same conclusions. All studies used electronic chart abstraction by a third party who was blinded to the study hypothesis. Five-hundred and sixty-nine patients were identified of which 34 were excluded due to incomplete data. The authors calculated an odds ratio of 5.6 (although the 95% confidence interval was wide at 2.6 - 13.8), suggesting that the presence of a third molar significantly increased the risk of an angle fracture.

There seems to be almost consensus that an impacted third molar may be associated with an increase in angle fractures, however, the mechanism by which this occurs has not been proven. Safdar, et al. (1995) scored third molar impaction using a system based on measurements from two-dimensional panoramic radiographs (Safdar and Meechan, 1995). The influence of bucco-lingual angulation of the tooth was again not accounted for. Third molars were not differentiated on grounds of pathology. The authors felt that the impacted third molar would “weaken the mandibular angle both quantitatively and qualitatively”. They proposed that there was a linear relationship between the degree of impaction and angle fracture susceptibility. It was assumed that the degree of impaction represented the amount of bony space occupied by the tooth. However, no measurement of the volume occupied by the third molars was made. Therefore, the quantitative weakness theory was not formally proven in their study.

Ugboko, et al. (2000), were lone dissenting voices regarding the effect of the third molar on mandibular fracture. Their study population of 490 patients included mostly fractures resulting from inter-personal violence. Sixteen per cent of patients whose third molars were present had angle fractures as opposed to 13% with fractures who did not have third molars ($p=0.57$). Of the patients whose lower third molars were not erupted, 31%

had angle fractures compared with 16% in whom the lower third molars were erupted (p=0.002). The authors reported a relative risk of an angle fracture with a third molar present as 1.2, suggesting that the presence of the third molar tooth minimally increases the risk of mandibular angle fracture. It was also found that mandibular fracture was more likely in the patient with an un-erupted third molar tooth than in the patient with an erupted third molar.

There was no consensus as to whether the depth of impaction increases or decreases the risk of angle fracture. Naghipur, et al. (2013) found no relationship between position and angulation and mandibular angle fracture whereas Iida, et al. (2003) found that if a third molar was close to the inferior border of the mandible there was a high risk of angle fracture. Meisami, et al. (2002) on the other hand found that deep impactions were not associated with an increased risk for angle fracture. Halmos, et al. (2004) concurred in a later study. Angulation of the tooth (as measured in its post-fracture position) was found to have no influence on mandibular angle fractures by Gaddipati, et al. (2014).

The impacted third molar tooth has also been found to influence fractures of the mandibular condyle. Iida, et al. (2002) found that partially erupted third molars decreased the likelihood of ipsilateral condylar fractures. Duan, et al. (2008) also found that the presence of third molars were protective against mandibular condyle fractures, although no distinction was made between deeply impacted and the degree of partial eruption. These studies have been supported by others (Gaddipati, et al., (2014); Naghipur, et al., (2013); Luria, et al. (2013); Thangavelu, et al., (2010); Choi, et al., (2011); Patil, et al., (2011) and Inaoka, et al., (2009)).

Retrospective studies which attempt to find a causal relationship between third molar presence and angle fractures from patient records will always suffer from some form of

selection bias. In the studies reviewed above, only fractures which required treatment were included. No distinction was made in most studies between the mechanisms of injury. One would expect that magnitude, area of impact and direction of force would affect the likelihood of injuries at the mandibular angle (Ugboko, et al. (2000)). Additionally, most studies assumed that the incidence of third molar presence is the same in all population. This is not necessarily the case. Also impacted third molar teeth as a group are heterogeneous. The tooth itself could be ankylosed or could be associated with cystic change which would reduce the amount of cortical or cancellous bone. One would suppose that it would be the reduction in the cortical bone that would have the most significant effect on bony strength in the region of the angle. The only way to determine the effect of un-erupted or partially erupted teeth on the propensity of the mandible to fracture under loading would be to examine geometrically identical mandibles subjected to identical loading conditions with and without the present of an impacted tooth. Unfortunately, this is not possible clinically.

Figure 2.10 Fracture of the right angle of the mandible. Note the un-erupted third molar tooth with a slightly enlarged follicle around the crown. (Radiograph used with permission of the patient.)

Figure 2.11 Fracture of the right angle of the mandible. Note that the third molar tooth is partially erupted. (Radiograph used with permission of the patient).

Investigators/Year	*Study type*	*Aim or Title*	*Authors' conclusions*
Gaddipati, et al., 2014	Retrospective	*"Impacted mandibular third molars and their influence on mandibular angle and condyle fractures - A retrospective study."*	"The presence of impacted third molar predisposes the angle to fracture and reduces the risk of a concomitant condylar fracture. There is no significant relationship, concerning ramus position and angulation of impacted mandibular third molars with the angle fracture."
Milzman, et al., 2013*Δa)	Retrospective	"To determine if the presence of third molars, specifically impacted teeth, is associated with an increased risk of mandibular fracture compared to patients with an already extracted third molar."	"The presence of a third molar increases the likelihood of a mandible angle fracture following trauma."
Naghipur, et al., 2013Δ	Retrospective	*"The effect of lower third molar presence and position on fracture of the mandibular angle and condyle."*	"The incidence of mandibular angle fracture was significantly higher in both patients and mandible sides with an impacted third molar. The rate of condylar fracture was significantly higher in both patients and mandible sides lacking an impacted third molar. A relationship between the position and angulation of third molar in relation to incidence of angle and condylar fractures could not be demonstrated. We also found that patients with a normally erupted third molar were at increased risk of angle fracture and a decreased risk of condylar fracture, compared to patients with no third molar."
Milzman, et al., 2013Δb)	Retrospective	"To determine if the presence of third molars, specifically impacted teeth, is associated with an increased risk of mandibular fracture compared to patients with an already extracted third molar."	"The presence of a third molar increases the likelihood of a mandible angle fracture following trauma."
Luria and Campbell, 2013Δ	Retrospective	"To assess any correlation between mandibular fracture patterns, specifically in the region of the angle or condyle/ sub-condyle, and the presence or absence of mandibular third molars."	"There is a twofold decrease in the risk of condylar/sub-condylar fracture if a third molar is present on the same side, suggesting that retained third molars may serve a "protective" function against condylar and condylar neck fractures."
Abbasi, et al., 2012	Retrospective	"To assess the frequency of un-erupted mandibular third molar in mandibular angle fractures."	"The presence of un-erupted mandibular third molar is associated with an increased risk for mandibular angle fracture."
Weiner, et al., 2012Δ	Retrospective	"To determine if the presence of third molars, particularly impacted teeth, creates an increased risk for mandible fracture compared to persons with an already extracted third molar."	"The presence of a third molar increases the likelihood of a mandible angle fracture following trauma."
Choi, et al., 2011	Retrospective	"We attempt to characterize the effect of a third molar on the incidence of mandibular angle and condylar fractures."	"The presence and the state of the lower third molar affect the risk of future mandibular angle and condylar fracture."
Patil, 2012		"To assess the influence of the presence and state of impaction of mandibular third molars on the incidence of fractures of the mandibular angle and condyle."	"An incompletely erupted third molar reduces the risk of condylar fractures and increases the risk of fractures of the mandibular angle."

Investigators/Year	*Study type*	*Aim or Title*	*Authors' conclusions*
Bezerra, et al., 2011	Retrospective	"To estimate how is the magnitude of the impact of a mandibular third molar on the mandibular angle stiffness."	"The presence of a third molar may double the risk of an angle fracture of the mandible to occur."
Thangavelu, et al., 2010	Retrospective	*"Impact of impacted mandibular third molars in mandibular angle and condylar fractures."*	"Patients with impacted third molars were three times more likely to develop angle fractures and less likely to develop condylar fractures than those without impacted third molars."
Inaoka, et al., 2009	Retrospective	"To relate the condylar and angle fracture with an un-erupted lower third molar, taking into account the position of the tooth."	"The absence of an impacted third molar may increase the risk of condylar fractures and decrease the prevalence of mandibular angle fractures."
Subhashraj, 2009	Retrospective	*"A Study on the Impact of Mandibular Third Molars on Angle Fractures."*	"There is an increased risk of angle fractures in the presence of a lower third molar, as well as a variable risk for angle fracture, depending on the third molar's position."
Rajkumar, et al., 2009	Retrospective	"To evaluate the presence of mandibular third molars as a risk factor for angle fractures in patients with fractured mandibles."	"The results of this study demonstrate that patients with fractured mandibles and mandibular third molars are nearly 2.2 times more likely to have an angle fracture than patients without mandibular third molars."
Duan and Zhang, 2008	Retrospective	*"Does the presence of mandibular third molars increase the risk of angle fracture and simultaneously decrease the risk of condylar fracture?"*	"Third molars were a dominant factor for developing a mandibular angle fracture and preventing condylar fracture."
Iida, et al., 2003	Retrospective	"To clarify the influence of the eruption status of incompletely erupted mandibular third molars on the incidence of mandibular angle fractures."	"The results of this investigation showed that incompletely erupted mandibular third molars close to the inferior border of the mandible have a high risk of angle fractures."
Halmos, et al., 2004†	Retrospective	"To measure associations between mandibular third molar status/position and risk for angle fracture."	"The presence of third molars was associated with a 2.8-fold increased risk for angle fractures. Third molar position was associated with a variable risk for angle fracture. Deep impactions were not associated with an increased risk for fracture."
Hanson, et al., 2004	Retrospective	"To estimate the relative risk of mandibular angle fractures among people with a lower third molar compared with those without a lower third molar."	"The presence of a lower third molar may double the risk of an angle fracture of the mandible."
Iida, et al., 2004	Retrospective	*"Influence of the incompletely erupted lower third molar on mandibular angle and condylar fractures."*	"The result of this retrospective investigation shows that an incompletely erupted third molar decreases the risk of condylar fractures and increases the risk of mandibular angle fractures."
Fuselier, et al., 2002†	Retrospective	*"Do mandibular third molars alter the risk of angle fracture?"*	"In patients who sustain a mandible fracture, the presence of third molars significantly increases the likelihood of an angle fracture. In addition, the risk for an angle fracture depends on third molar position."
Meisami, et al., 2002	Retrospective	"To assess the influence of the presence, position, and severity of impaction of the mandibular third molars, on the incidence of mandibular angle fractures."	"Patients with retained impacted third molars are significantly more susceptible to angle fracture than those without. The risk for angle fracture, however, does not seem to be influenced by the severity of impaction."
Ma'aita and Alwrikat, 2000	Retrospective	"To evaluate the association of mandibular angle fractures with the presence and state of the eruption of the mandibular third molar."	"The mandibular angle that contains an impacted third molar is more susceptible to fracture when exposed to an impact than an angle without a third molar."

Investigators/Year	*Study type*	*Aim or Title*	*Authors' conclusions*
Meechan, 2000	Opinion	*"The effect of mandibular third molar presence and position on the risk of an angle fracture."*	Three papers reviewed, two non-clinical, one opinion. No original data produced, no clear conclusion drawn.
Lee and Dodson, 2000†	Retrospective	*"The effect of mandibular third molar presence and position on the risk of an angle fracture."*	"Patients with third molar present have an increased risk for angle fractures. The risk for an angle fracture varied depending on third molar position."
Ugboko, et al., 2000.	Retrospective	*"An investigation into the relationship between mandibular third molars and angle fractures in Nigerians."*	"The presence of a lower third molar does not necessarily predispose to fractures of the angle of the mandible. However, angle fractures are more likely to occur in people with un-erupted lower third molars than in those in whom they have erupted."
Yamada, et al., 1998	Retrospective	*"A study of sports-related mandibular angle fracture: relation to the position of the third molars."*	"Mandibular angle fractures are influenced by the presence and characteristics of the third molar in sports-related injuries."
Safdar and Meechan, 1995	Retrospective	"To relate the incidence of fractures at the mandibular angle with the presence and state of eruption of lower third molars."	"Un-erupted third molar teeth weaken the mandibular angle both quantitatively and qualitatively."
Tevepaugh and Dodson, 1995†	Retrospective	"To evaluate mandibular third molars as risk factors for angle fractures in a patient sample with fractured mandibles."	"Patients with fractured mandibles and mandibular third molars are 3.8 times more likely to have an angle fracture than patients without mandibular third molars."

Table 2.15 Summary of clinical papers. The aim or title and authors' conclusions are direct quotations from the associated clinical paper.

****Denotes that the same paper was presented at three different conferences with identical data and results.***
†Denotes four studies that have used entirely or partially the same dataset.
Titles of the paper appear in italics where no specific aim is stated in the paper.
Δ Denotes a poster or conference presentation.

2.4.3.3.2 Conclusion

The effect of the un-erupted third molar tooth on the propensity of the angle of the mandible to fracture remains unclear from the reviewed studies due to the heterogeneity of the third molar group. One of the aims of the 3DFEA studies is to address questions that cannot be fully answered using epidemiological data.

Chapter 3 Methodology

3.1 Introduction

This chapter describes the methodology that will be employed throughout this research.

3.2 Re-statement of research question

The primary purpose of this research is to determine if an anatomically and geometrically accurate finite element model of the mandible can be produced. The computer model should be capable of accurately simulating the biomechanical effects of loading and additionally simulating fractures encountered in experimental mechanical studies, with the potential to extrapolate the findings to clinical situations.

3.3 Research questions

The research objective, general and specific research questions are shown in table 3.1

Research objective	General research question	Specific research question
To develop a finite element model capable of reproducing the biomechanical response of the mandible to physical trauma.	Can a validated mandibular 3DFEA model be produced which is capable of reproducing the biomechanical response of the mandible under load?	What are the effects of the muscles of mastication on the biomechanical response of the mandible under load?
		What is the effect of tooth loss on the mandible under direct loading?
		What are the effects of generalized material property changes on the mandible under load?
	How does the mandible respond to static physiological loading?	What is the effect of load site on the mandible?
		What is the effect of load angulation on the mandible?
	How does the mandible respond to static loading?	Are the patterns of mandibular stress and strain similar under physiological and loading?
	How does the mandible respond to dynamic loading?	What is the effect of deformation rate on mandibular fracture?
	How do localized changes in material properties (i.e. bony lesions) in the mandible change the dynamic response to loading?	What is the effect of cystic lesions at the angle of the mandible on fracture propensity?
		What is the effect of solid at the angle of the mandible (un-erupted third molar teeth) on fracture propensity?

Table 3.1 Research objectives

3.4 Required tools

The most important tool required to fulfil the requirements of this research is a 3DFEA model of the mandible which has been verified and validated where possible. It is understood that true clinical validation will not be possible and therefore the closest form of validation will be employed. At the time of undertaking this research there are no existing models suitable for answering the specific research questions and no models are available that may be easily converted for the purpose. As a result, part of this research will be the production of a 3DFEA model. In order to produce the model and perform the research several other tools will be required. The specifications of these tools are outlined below.

3.4.1 Computational resources

As the aim of this research is to produce a simulation model that has value in the laboratory and the medico-legal office situations, the computational and software resources used must be within the scope of that which would be considered reasonable expense for such situations. At the time of planning this research reasonable expense has been estimated as £1500. This would acquire a well-specified computer capable of running the required software. Although the budget of the hardware will remain the same, it is envisaged that at the end of the research this will acquire a significantly more powerful computer.

3.4.2 Software and file formats

File incompatibilities amongst software packages tend to be common even when standardized export formats are used. Where possible it is intended that open-source software will be used, however, file incompatibilities are even more common in such packages, therefore several software packages and file formats will have to be trialled in

combination before the final software is decided upon. It is anticipated that this will be a time consuming process. Software cost will also be a limiting factor with the best high quality software, costing many thousands of pounds, being out of the range of the research budget. Specialized software will be licenced for the period of the research where possible. This will reduce cost.

3.4.3 Image processing

The standard tools for producing finite element models in the field of engineering are usually computer-aided design packages or the pre-processors of finite element analysis packages. As organic structures have a much more complex form than those of man-made structures, routine CAD/CAM software will be inadequate for producing FE models. The most efficient way of generating organic structures is to utilize the serial images from CT, magnetic resonance, or histological preparations. In this research the CT scans of patients taken for therapeutic reasons will be used with consent, therefore image processing software will be required.

3.4.4 Pre-processing

The pre-processing phase of analysis will involve the setting up of the simulation conditions. This will include the application of boundary conditions, muscle forces and material properties. Many analysis packages have built-in pre-processors, but this is not always the case, therefore, specific pre-processors will be required where they are not available in the analysis software.

3.4.5 Analysis software

The analysis software will require the following capabilities:

- The ability to perform linear and non-linear analyses

- The ability to perform static analyses
- The ability to perform dynamic analyses

3.5 Required data

The data required to answer the research questions will come in the form of calculations designed to measure performance. As mentioned previously, performance may refer to the mechanical efficiency or strength of a specific system. Failure of the system i.e. bony failure will be determined by the use of the von Mises formula.

The von Mises formula was developed to predict yielding of isotropic ductile materials such as metals (see equation 3.1). Under this criterion, failure occurs when the von Mises stress equals the ultimate stress of the material. Cortical bone has been described as ductile in fracture (Nalla, et al., 2003) although Hansen, et al. (2008) noted a ductile-to-brittle transition, which was strain-rate related, in tensile and compressive tests to failure.

Some authors have suggested that this criterion is not very realistic for determining failure in bone (Doblaré, et al., 2004) von Mises stress (also referred to as the equivalent stress) has been used throughout biological literature to predict bony failure. Keyak and Rossi (2000) found that when isotropic material properties were used, von Mises criterion was the most accurate for fracture location prediction in cortical bone. This was even the case when the differences in compressive and tensile stress were accounted for. This same accuracy was not found in cancellous bone (Fenech and Keaveny, 1999). The equation frequently used to determine von Mises stress is found below.

$$\sigma_{vm} = \sqrt{\frac{1}{2}[(\sigma_1 - \sigma_2)^2 + (\sigma_2 - \sigma_3)^2 + (\sigma_3 - \sigma_1)^2]}$$

Equation 3.1 von Mises equivalent stress where σ_1, σ_2, σ_3 are principal stresses such that $\sigma_1 < \sigma_2 < \sigma_3$.

A similar equation has been used to define von Mises strain.

$$\varepsilon_{vm} = \sqrt{\frac{1}{2}[(\varepsilon_1 - \varepsilon_2)^2 + (\varepsilon_2 - \varepsilon_3)^2 + (\varepsilon_3 - \varepsilon_1)^2]}$$

Equation 3.2 von Mises equivalent strain where ε_1, ε_2, ε_3 are principal stresses such that $\varepsilon_1 < \varepsilon_2 < \varepsilon_3$.

This research will use von Mises stress and strain, along with strain rate as determinants of bony failure for two main reasons. Firstly to allow comparison with previous research and secondly as 3DFEA studies of bony fractures in other parts of the body have shown good comparison with clinical findings when these parameters have been used.

3.6 Appropriateness of the research design

This research will follow a type-2 design-based methodology as defined by Richey et al. (2004). This will be supplemented by the use of a modified error tracking system based upon the SAFESA (Safe Structural Analysis) approach developed by Cranfield University for controlling finite-element idealization errors (Morris, 1996; Vignjevic, et al., 1998). The modelling protocols of National Agency for Finite Element Method and Standards (NAFEMS) which are designed to establish the best practice for 3DFEA simulation will be followed as closely as possible.

3.7 Technique of data analysis

Finite element analyses tend to produce large quantities of data, therefore a method of post-processing results will be required that can simplify this in an understandable manner. The choices available to display the results include, colour contour maps (3-

dimensional), vector maps (3-dimensional), and graphical representation of data. It is anticipated that all display options will be used in this research.

3.8 Research structure

The research will have three distinct phases namely:

1. **Phase I** **The development of the finite element model**
    - Ia Model production
    - Ib Model verification
2. **Phase II** **Static analyses**
    - IIa Linear static analyses
    - IIb Non-linear static analyses
3. **Phase III** **Dynamic analyses**
    - IIIa Basic non-linear dynamic analyses
    - IIIb Applied non-linear dynamic analyses

The iterative nature of finite element analysis requires a step-wise progression through the phases, with the results of each phase informing the next. The result will be that some modelling and analysis techniques that are employed in earlier phases will be absent in later phases if they are found to be computationally inefficient or unnecessary.

3.9 Phase Ia: Model production

In the type-2 design research methodology the development process is generally constructed by reference to a number of methods including survey of previous successful modellers within the field, review of models in the literature and the use of an iterative model design process whereby the model is verified by a number of methods. The literature review in chapter 2 has already reviewed the work of the published authors in the field (and where appropriate related modelling techniques) therefore in this phase the model production itself will be addressed.

The aim will be the production of an anatomically and geometrically accurate 3-dimensional model of an adult human mandible. The model will not aim to be a reproduction of the entire biological system under investigation (i.e. the mandible and its supporting tissues) in computer terms. An entirely accurate model would require complete knowledge of the functioning and material properties of the system under investigation, which is unavailable, and the ability to accurately model those properties in computing terms, which is also unavailable. Additionally, the computing power required to solve such a complex model would be significant and beyond the reach of most investigators. Therefore, where information is incomplete, reasonable assumptions will have to be made in order to perform an analysis.

In order to answer all of the research questions three functional models will be required (see table 3.2).

Model	**Purpose**
Dentate adult mandible	Static and dynamic analyses
Edentulous adult mandible	Static and dynamic analyses –comparison studies
Adult fist	Dynamic analyses

Table 3.2 Models required for analyses

3.9.1 Model data source

The literature review revealed that the most anatomically accurate mandibular models could be produced from CT data. It is possible to derive this from three sources, namely, clinical data i.e. that previously obtained from a therapeutic scan of a consenting patient; volunteer data, and cadaveric data. Whilst data derived from volunteers would seem to be acceptable, the non-therapeutic use of ionizing radiation would be unethical. Data should therefore be utilized from either the therapeutic scans of consenting patients or scans derived from cadaveric material (again with consent where applicable).

3.10 Phase Ib: Model verification

The finite element model will require verification. The methods of verification adopted will be those recommended the NAFEMS. This is an independent association for the international engineering community which sets and maintains standards for finite element modelling (NAFEMS mission statement).

Verification will include the following tests:

Pre-analysis checks:	**Convergence checks:**
Mesh inspection	Relative convergence
Boundary condition checks	Error estimates
Material property checks	Visual examination
Model mass checks	

Table 3.3 Verification checks

It will also be necessary to perform model validation. As true validation against a human subject will be impossible in most cases (certainly for the study of mandibular fractures) validation against laboratory mechanical tests, which is currently the standard in forensic biomechanics, will be employed. Data will be obtained from reported studies in the literature.

3.11 Phase IIa: Static linear analysis

As this is the simplest form of finite element analysis this will form the basis of biomechanical deformation studies and prediction of fracture site initiation.

This series of investigations will need to investigate the following effects.

- Effect of muscles
- Effect of modelling teeth
- Effect of load position
- Effect of load angulation
- Effect of material properties

The outcome variables for these investigations will be von Mises stress and strain. In addition to giving information regarding the biomechanics of the mandible, these

analyses will also be used to give an indication of which anatomical features need to be modelled to achieve the desired aim of traumatic fracture simulation. As the least computationally expensive analysis it will also give an indication of the required run time, which should also inform the researcher regarding the utility of this method of analysis in a clinical/scientific situation, when compared to traditional methods of investigation. A “physiological load” will be defined as one which is within the elastic load of the mandibular cortical bone.

3.12 Phase IIb: Static non-linear analysis

Although some studies of the mandible under load have found that linear analyses provide deformation results that show good correlation with mechanical and clinical studies, this is not universal. Whether or not this non-linearity manifests itself in a way that would be significant to a forensic scientist or medico-legal investigator is important therefore non-linear analyses will be required. The main difference between the phase IIa and phase IIb investigations will be the use of a load sufficient to fracture the mandible and the use of non-linear analysis. This will be defined as the “non-physiological load”. Results will be displayed in a similar manner to the static linear results and conclusions from these analyses will be fed into the design of the dynamic analyses.

3.13 Phase IIIa: Basic dynamic non-linear analyses

The first analyses in this series will aim to investigate the effect of two factors that can influence the nature of fracture patterns i.e. the impact kinetic energy and the mandibular strain rate. Additionally, an attempt will be made to model the pattern individual fractures, rather than purely identifying the site of initiation.

The fracture patterns observed will be compared with those discovered in the literature review (section 2.5). It is understood that all fracture patterns are unlikely to be represented, however, common fracture patterns (as opposed to fracture initiation sites) should be found.

As fractures are influenced by impact site, impact kinetic energy and strain rate, the effect of these on fracture pattern will also be investigated.

A dynamic solver will be required for these analyses from which vast quantities of data are generated for each analysis. Simulations will be presented graphically at the last time step of the simulation, which will be 1ms. This limitation is imposed as the general fracture pattern should have manifested itself by this time (as opposed to displacement of fractures). The computation time has been estimated at approximately 48hrs. Videos of the full dynamic simulation will be available on a companion disc.

3.14 Phase IIIb: Applied non-linear dynamic analyses

Phase IIIb will be the culmination of the research. The final analyses will be used to investigate features of a clinical problem related to traumatic mandibular fractures which presents in clinical practice.

In the literature review (section 2.6) current research was reviewed regarding the effect of impacted third molar teeth on mandibular fractures. There was almost consensus amongst the various authors (Ugboko, et al., 2000 dissenting) that the impacted third molar tooth is associated with an increase in mandibular angle fractures and a reduction in ispilateral condylar fractures, although authors could not agree on a mechanism action. This research will attempt to test this commonly held theory, using the research model produced and 3DFEA. Models will be produced that only differ by the presence or absence of un-erupted third molar teeth. An un-erupted third molar tooth is effectively

a local change in material properties of the mandible. The material properties of the un-erupted tooth will be varied to extremes to understand the range of effects.

3.15 Research summary

This research will involve the production of a 3DFEA model produced using the guidelines of NAFEMS. The model will be verified and validated as far as possible within ethical guidelines. Specific research questions (see section 3.3) will be answered using data derived from research phases II and III. The flow diagram for the research methodology is shown in figure 3.1.

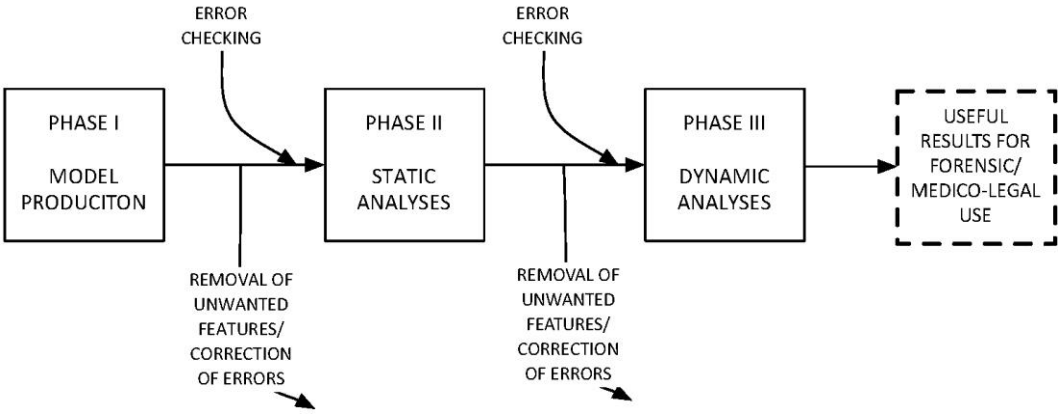

Figure 3.1 Research methodology

Any deviations from the methodology will be reported in the chapter 4 which details the execution of the research.

Chapter 4 Research

4.1 Phase Ia: Model production

4.1.1 Aim

This section describes the completion of Phase I, the production of anatomically and geometrically accurate finite element models and their validation. The stages involved data capture; construction of mandibular geometry, the creation of finite element meshes; mesh quality analysis; material property assignment and the application of boundary conditions.

4.1.2 Method

4.1.2.1 Stage 1: Data capture

Models were developed from an open-source CT data archive. The dataset was obtained from a radiographic archive at the University Hospital Geneva (available at http://www.osirix-viewer.com/datasets) from which the "INCISIX" sample dataset was used. This anonymized public dataset which licensed exclusively for research and teaching. At the time of model production the manager of the archive was contacted, and confirmed that the appropriate consent was obtained from patients who donated their CT data.

The "INCISIX" dataset consisted of contiguous 750µm axial slices obtained as 8-bit images in Digital Imaging and Communications in Medicine (DICOM) format.

4.1.2.2 Stage 2: Data import

4.1.2.2.1 The INCISIX dataset

CT data of the complete skull and upper cervical vertebrae was imported from the INCISIX CT dataset into the Mimics® Innovation Suite (Materialise NV, 2011) as a DICOM image stack of sequentially numbered axial images. Image orientation was performed such that the image slices corresponded to their anatomical position.

4.1.2.3 Stage 3: Construction of mandibular geometry

4.1.2.3.1 Geometry-based model production

A geometry-based approach rather than voxel-based approach was adopted to reproduce the mandibular anatomy. The rationale behind this decision was that as the resolution of the model produced by the voxel-based approach was largely determined by the resolution of the CT scan and the direct conversion of voxels into finite elements was limited to hexahedral elements with the software available at the time. The geometry-based approach involved using the acquired image stack to produce hollow, watertight, three-dimensional objects composed of interconnected polygons. These were then converted into surfaces composed of triangular elements.

4.1.2.3.2 Thresholding

Thresholding is a method of digital image processing that allows subtraction of pixels lying outside a predetermined threshold value. When applied to the radiographic region of interest (ROI) on a CT it results in image segmentation i.e. separation of the ROI from the remaining data. The thresholding value used was determined with reference to the Hounsfield values for enamel, dentine, cancellous and cortical bone. The thresholding algorithm within the Mimics Innovation Suite ® did not directly use Hounsfield Units

(HU) to perform the segmentation; rather it used its own related greyscale of 4094 values (-1023 to 3071). The thresholding range chosen was between -452 and 3071. This produced a segmentation mask consisting of only bone and teeth in each slice of the image stack (see figure 4.1).

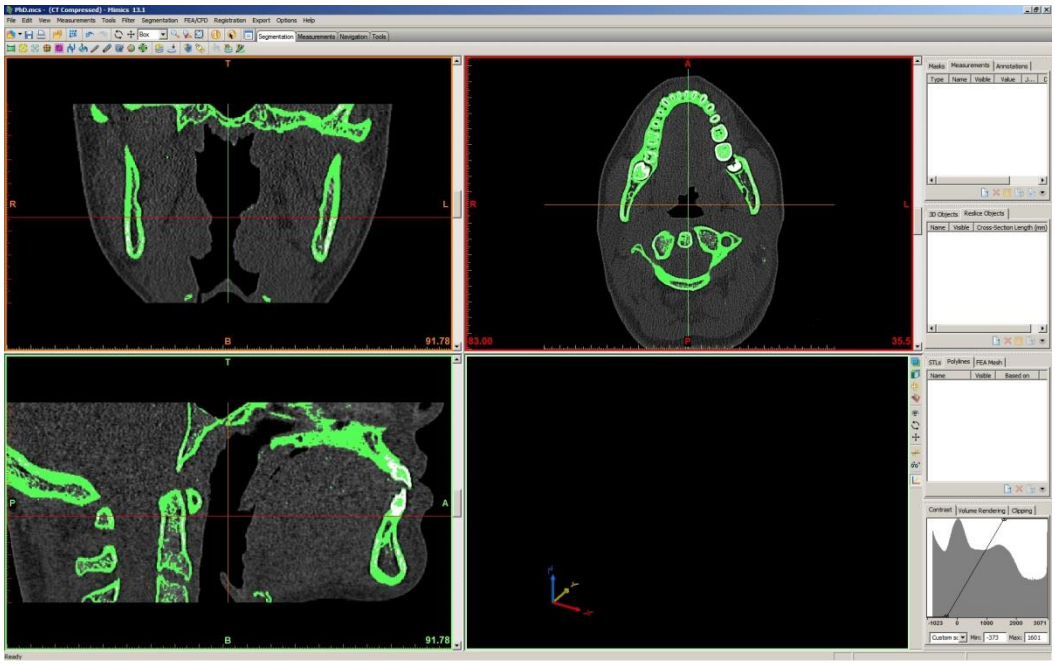

Figure 4.1 The thresholding segmentation process in Mimics 13.1®. Hard tissue (green) was segmented form the surrounding hard tissue

4.1.2.3.3 Mask creation

Once the ROI (i.e. the mandible) had been defined it was necessary to segment out the remaining hard tissues. This could not be performed with standard thresholding as the maxillary bone has a similar greyscale range to the mandibular bone; therefore the Region Grow algorithm within Mimics® was employed. This allowed selection of pixels which had similar greyscale values representing same tissue. The accuracy of the segmentation relied on the homogeneity of the ROI. Cortical bone, dentine and enamel appeared relatively homogeneous and therefore selection was relatively simple (see figure 4.2).

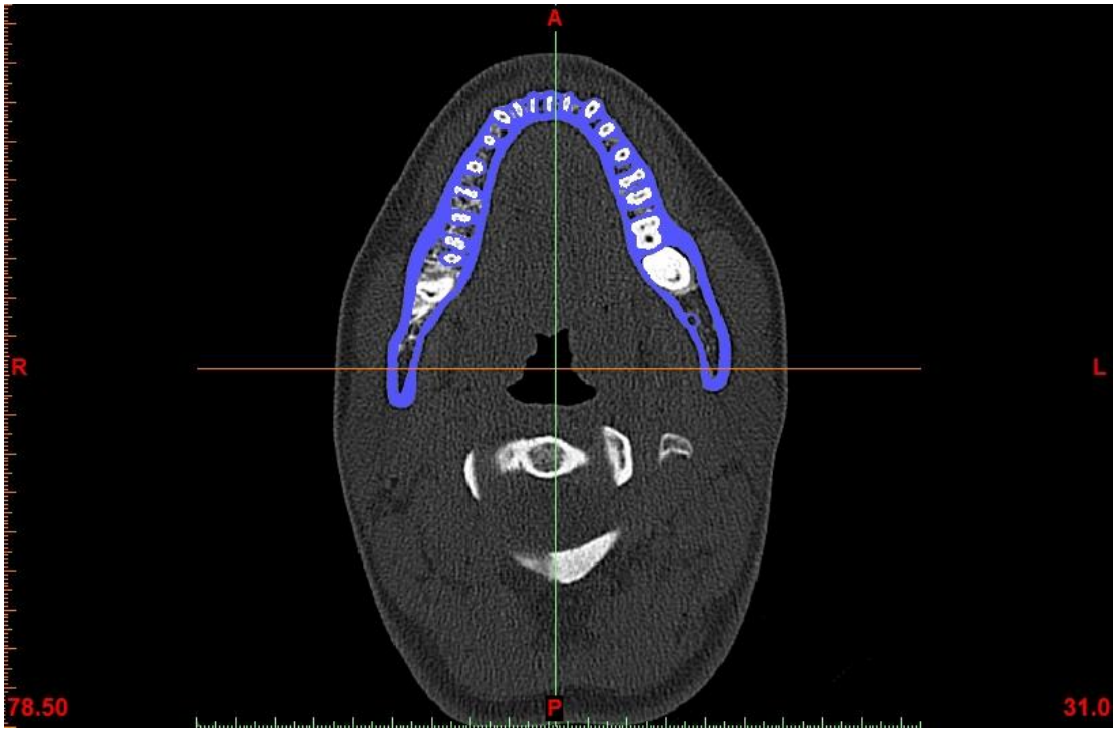

Figure 4.2 Creation of the mandibular mask

Whilst the automated routines performed a rough segmentation, the resulting masks were still inadequate for model production; therefore, further manual adjustment was required. The mandible was manually separated from the maxilla by the deletion of one pixel outside the required segmentation area on each slice of the CT scan. This was performed in the axial, sagittal and coronal planes. Following this, the Region Grow algorithm was re-employed over all of the slices. The resulting segmented regions constituted the mandibular mask. The teeth, cancellous bone and cortical bone were further segmented using Boolean operations on the various masks. At the end of the process there were three different hard tissue masks, namely the mandibular cortex, the cancellous bone and the teeth (see figure 4.3).

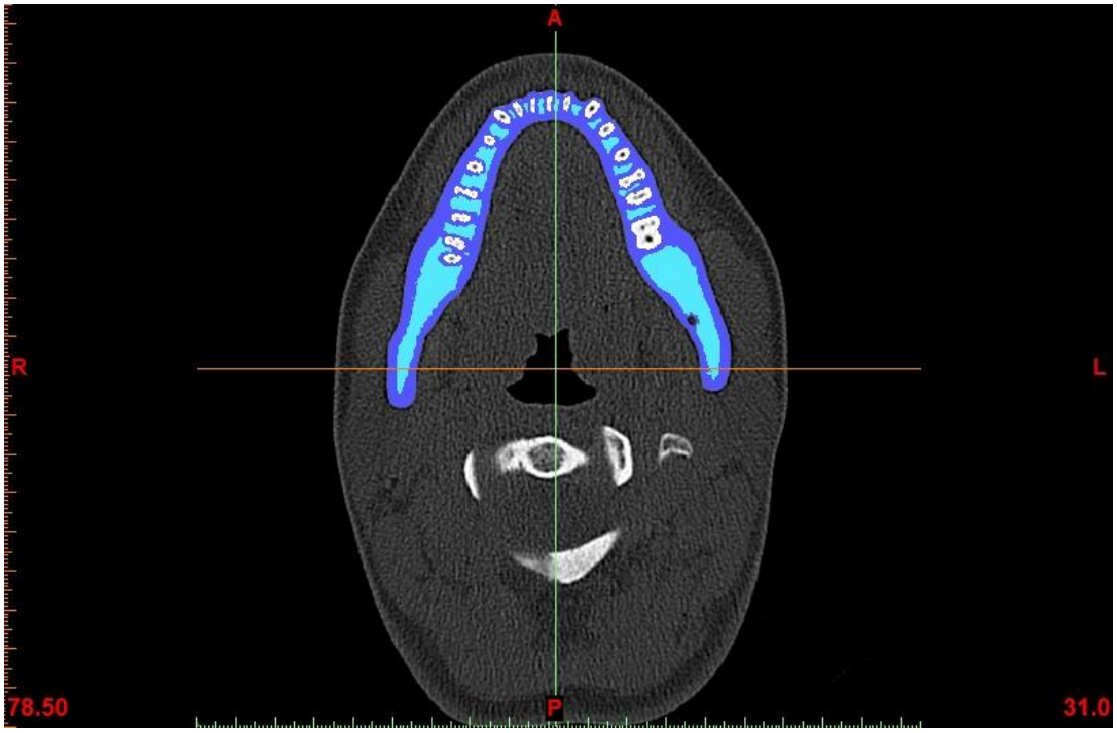

Figure 4.3 Cross-section of segmented mandibular volumes. Mandible with segmented cortical (purple) and cancellous (light blue) bone.

4.1.2.3.4 Model formation

The individual mandibular masks (cortical bone, cancellous bone and teeth) were converted into individual 3-dimensional models using 3-Matic ® (Materialise NV, 2011) and then exported in the Standard Tessellation Language (STL) format.

Model 1:	Mandibular cortex alone
Model 2:	Mandibular cancellous bone alone
Model 3:	Mandibular teeth
Model 4:	Assembled edentulous model (cortical and cancellous bone)
Model 5:	Assembled dentate model (cortical cancellous bone and teeth)
Model 6:	Clenched fist

Table 4.1 3-dimensional models produced.

Of the two STL variations, the binary STL format was used throughout the modelling stage rather than the ASCII version. Five final models were produced as STL surface meshes.

4.1.2.3.5 Additional model

A further model was produced for the analyses using a commercial CAD/CAM surface mesh of a clenched fist under a royalty-free licence (see Appendix 16). This was also converted into STL format and resized to produce a fist of normal proportions.

4.1.2.3.6 Model refinement

The models were refined using a modified protocol for biological 3DFEA (Grosse, et al., 2007), after they were inspected to ensure that they were composed of topologically closed surfaces. This was a requirement of the meshing algorithm within 3-Matic® (Materialise NV, 2011).

4.1.2.3.7 Complexity reduction

The imported STL model files were subjected to a preliminary meshing using 3-Matic®. This produced a surface mesh of reduced complexity in terms of the triangle number. The meshing settings used for this initial procedure are found in Table 4.2. The resulting files were re-saved in the STL format.

Smoothing parameters		**Reduction parameters**	
Smoothing method	Laplacian	Flip threshold angle	15^{o}
Smoothing factor	0.7	Geometric error	0.05
Number of iterations	3	Number of iterations	3

Table 4.2 Smoothing and reduction parameters applied to modes prior to meshing

4.1.2.3.8 Digital shape sampling and processing

The resulting STL files proved inadequate for producing a finite element mesh; therefore, they were imported into Geomagic Studio 11® for manual adjustment. The remaining artefacts were removed and the model re-smoothed. The two procedures were repeated until anatomically acceptable models were produced using the least number of triangles.

At this stage the model co-ordinate system was also aligned so that the yz-plane was aligned parallel with the medial sagittal plane. Finally, the models were 'cleaned', exported from Geomagic Studio 11®as STL files and re-imported into 3-matic® for final meshing.

4.1.2.4 Stage 4. Creating the finite element meshes

4.1.2.4.1 Element choice

Having used a geometry-based method of finite element model production, element choice was not restricted to hexahedral elements. In line with the majority of biological, mandibular finite element models (see chapter 2); tetrahedral elements were used in this study. These elements were chosen for their better ability to conform to the intricate geometry of biological structures without the need to resort to excessively high element resolutions. At the volume meshing stage, 4-noded (linear) tetrahedra were chosen rather than 10-noded (quadratic) tetrahedra as analyses were comparatively less computationally expensive, even though a higher element count was required to achieve the equivalent accuracy in the result. It has been suggested that at element resolutions of less than 252000, (in the analysis of the complete facial skeletons of bats), the difference between 4-noded tetrahedra and 10 noded tetrahedra is approximately 10% (Dumont, et al., 2005).

4.1.2.4.2 Re-meshing protocol

Using a modified protocol originally devised by Dumont, (2009), 3-Matic® was chosen to perform the surface and volume meshing of the model. A shape quality threshold of 0.3 with a maximum geometric error of 0.02 was selected for the initial surface meshing. When surface meshing was successfully completed the mesh was manually checked for errors. The models then underwent a quality preserving triangle reduction and finally volume discretization i.e. the conversion of the surface meshed model into a volume of finite elements. The full meshing protocol is summarized in figure 4.4.

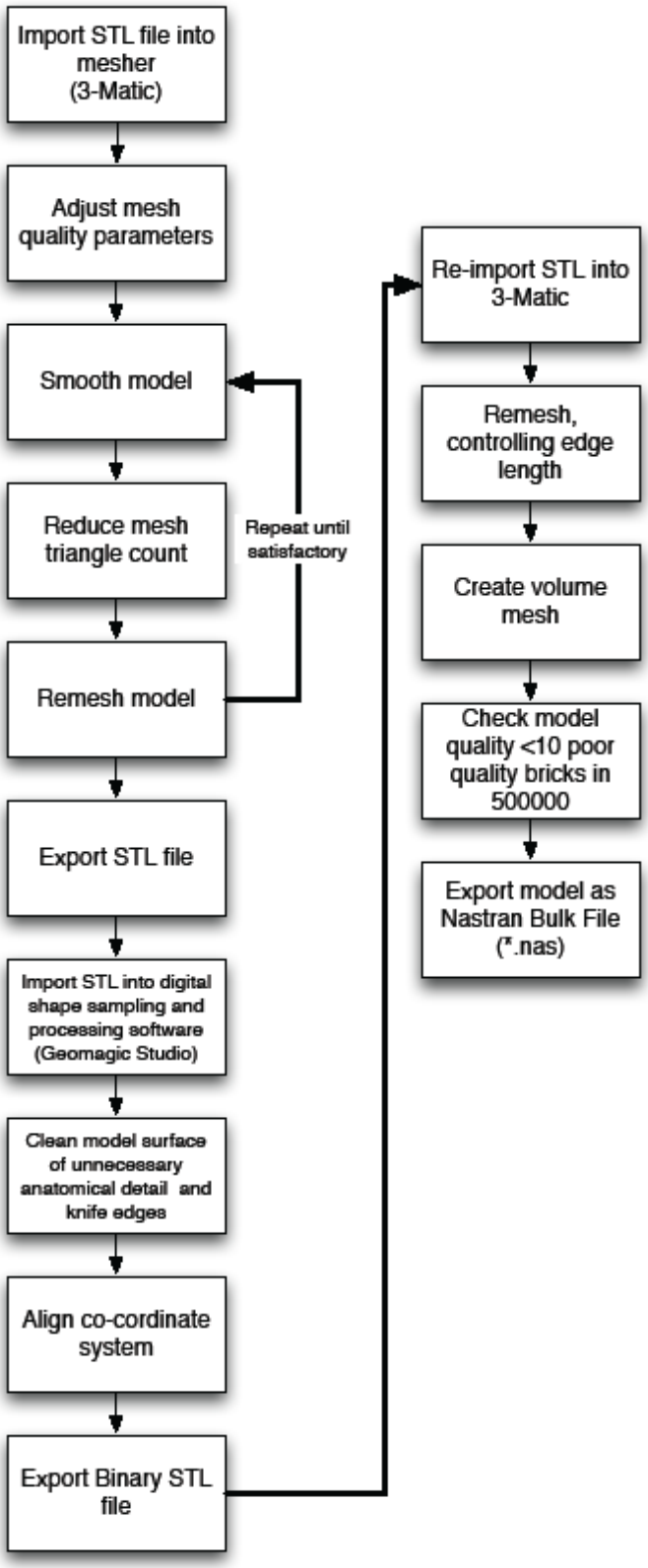

Figure 4.4 Meshing protocol

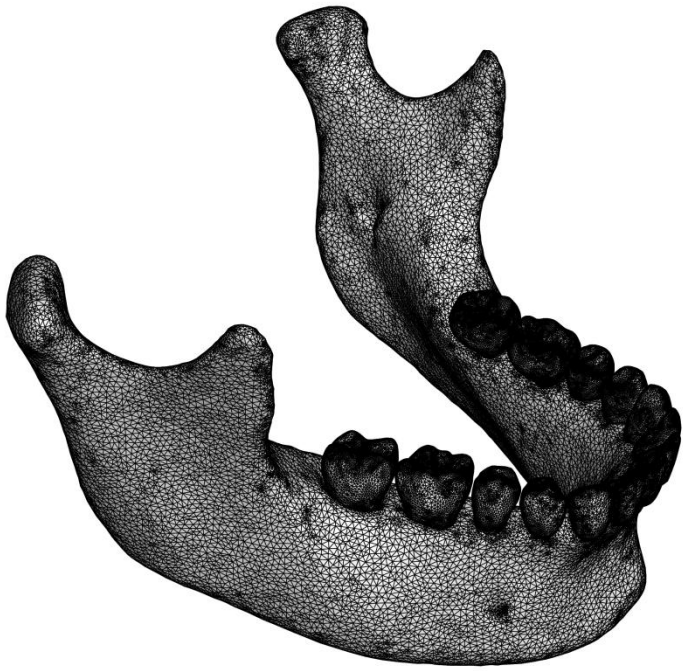

Figure 4.5 The final meshed mandibular model (model 5). All parts of the model are assembled.

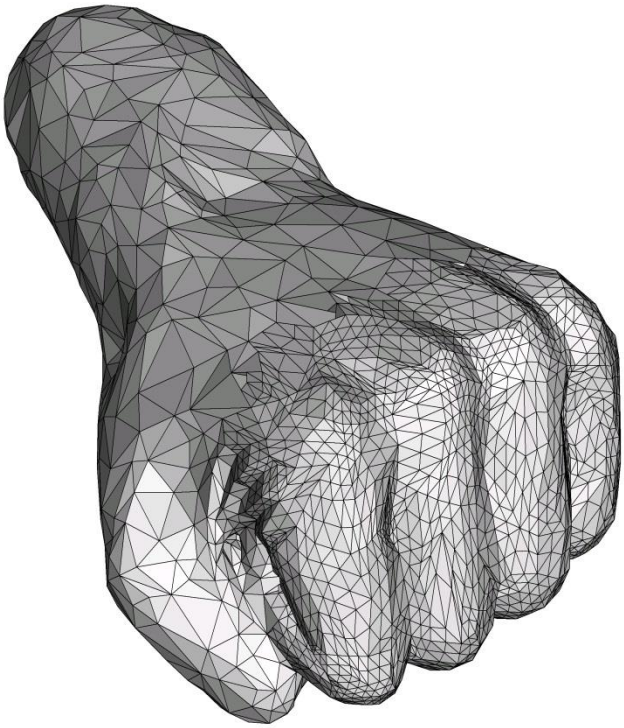

Figure 4.6 The final volume mesh for the clenched fist model used in the dynamic analyses (model 6). This model was composed of 27836 four-noded tetrahedra and 6143 nodes. Note the increased mesh density at the area of contact

4.1.2.5 Stage 5. Mesh quality analysis

In order to confirm the quality of the resulting model mesh and hence the mathematical accuracy, the models underwent mesh quality analyses using the absolute edge ratio (max/min) shape measure as the quality indicator. A shape quality threshold of 10 was chosen. A maximum of 10 in 500000 poor quality elements i.e. those that fell below the shape quality threshold of 10, were allowed for all of the models. These unsatisfactory elements were only allowed if they were not close to each other or the specific area under investigation.

4.1.2.6 Stage 6. Model export

All sets of models were exported as Nastran Bulk Files (Nastran), ready for importing into the finite element analysis packages.

4.1.2.7 Stage 7. Assigning material properties to the model

4.1.2.7.1 Introduction

Several methods of material property assignment were trialled; however, the mask method of assignment was finally used throughout the investigations. This method involved directly assigning material properties to each of the three-dimensional masks which were produced in section 4.1.2.3.4.

4.1.2.7.2 Modelling compromises

Although anatomically the dentinal components of the roots of teeth are covered with a thin covering of cementum (see appendix 4), this was not modelled, rather teeth were modelled as being entirely composed of dentine. The periodontal ligament was also not modelled. The rationale for these modelling simplifications was that neither of them were the object of the investigations and the element resolution required to accurately model these structures would have resulted in a huge increase in processing time with no analysis benefit. The published material properties for the periodontal ligament available during this investigation varied widely, sometimes by two and three orders of magnitude (Dorin Ruse, 2008; Fill, et al., 2012). Failing to model the periodontal ligament has been reported to provide a negligible difference in cortical strains (Goussard, et al., 2010). In order to attach the teeth to the alveolar bone rigid links were used after a method described by Goussard, et al. (2010).

4.1.2.7.3 Isotropism, orthotropism and anisotropism

Accurate modelling of the mandibular bone presented a number of problems. It has been demonstrated that the elastic properties of the mandible vary continuously and significantly in numerical terms, according to region (Schwartz-Dabney and Dechow, 2003). The mandible is also highly anisotropic therefore modelling its exact properties accurately was impractical. Vollmer, et al. (2000) found a high correlation between results predicted using finite element analysis and in vitro biomechanical studies on mandibular specimens even when the mandible was modelled as isotropic. This approach was taken in this study.

4.1.2.8 Stage 8. Application of boundary conditions

The boundary conditions were the mandible, its muscular insertions, its articulation at the temporomandibular joint, and the external forces acting on them. The temporomandibular joints were not directly modelled and were represented by restraints – see figure 4.7.

4.1.2.8.1 Application of restraints

Restraints were placed at the condylar heads, inhibiting translation but allowing rotational movement in all three axes.

	Translational			*Rotational*		
	x	y	z	x	y	z
Left mandibular condyle	●	●	●	○	○	○
Right mandibular condyle	●	●	●	○	○	○

Table 4.3 Fixed and rotational restraints used for the condylar head on the mandibular model. ●=constrained ○=unconstrained

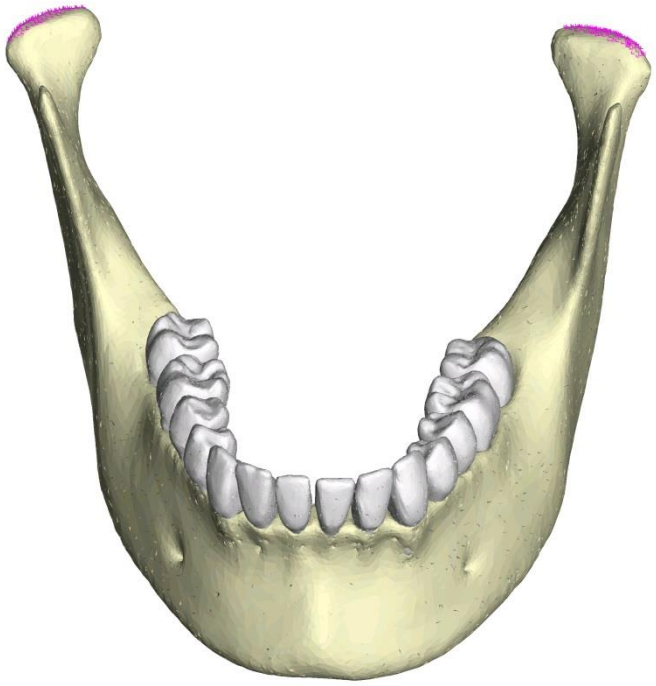

Figure 4.7 Condylar restraints (static analyses). Translational restraints are seen on the condylar heads in pink. Translation was prevented in the global perpendicular x, y and z directions

4.1.2.8.2 Application of muscular forces

In determining the relationship between mandibular morphology and sub-site patterns of mandibular fracture, only the muscles of mastication i.e. those producing the greatest potential load on the mandible were initially modelled.

The muscles were modelled as load vectors applied from the insertion point. They were modelled to provide half of their maximum contraction force in humans. This was considered to be a more natural situation than using values for maximum contraction. Additionally, all muscle groups were considered to be recruited simultaneously rather than in any particular pattern as patterns were considered to be unique to the particular function being performed at the time.

The work of Nelson, (1986) provided the basis for modelling muscle forces. Eight muscle groups were modelled, namely superficial and deep masseters; anterior, middle and posterior temporalis; superior and inferior lateral pterygoid; and medial pterygoid. The insertion sites for each muscle group were determined from the work of Baron and Debussy, (1979).

The muscle forces and vectors were derived from the work of Weijs and Hillen, (1985b) and were calculated using the formula in equation 4.1 where A_m was the cross-sectional area of the muscle in question (cm^2), K was a constant for skeletal muscle (Ncm^{-2}) and CR_m was the ratio of muscle contraction relative to the maximal response. The value of K was estimated as $40Ncm^{-2}$ (Weijs and Hillen, 1985b).

$$F_m = [A_m.K].CR_m$$

Equation 4.1 Calculating muscle forces and vectors. A_m = muscle cross-sectional area, K= skeletal muscle constant, CR_m = muscle contraction ratio. The product of A_m and K is also known as the weighting factor for the given muscle.

Muscle group	Cross-sectional area (cm^2) A_m	Muscle group weight $[A_m.K]$
Deep Masseter	2.04	81.6
Superficial Masseter	4.76	190.4
Medial pterygoid	4.37	174.8
Anterior temporalis	3.95	158.0
Mid temporalis	2.39	95.5
Posterior temporalis	1.89	75.6
Inferior lateral pterygoid	1.67	66.9
Superior lateral pterygoid	0.72	28.7

Table 4.4 Muscle groups and cross-sectional area (Weijs and Hillen, 1984a) (Nelson, 1986).

Muscle orthogonal components						
Muscle group	Maximum opening					
	Right			Left		
	X	Y	Z	X	Y	Z
Deep Masseter	0.10	0.15	0.21	-0.10	0.15	0.21
Superficial Masseter	0.69	0.34	1.44	-0.69	0.34	1.44
Medial pterygoid	-0.53	-0.69	1.12	0.53	-0.69	1.12
Anterior temporalis	-0.01	4.71	3.12	0.01	4.71	3.12
Mid temporalis	0.65	0.30	1.09	-0.65	0.30	1.09
Posterior temporalis	1.13	0.28	0.63	-1.13	0.28	0.63
Inferior lateral pterygoid	-7.60	-6.30	-1.75	7.60	-6.30	-1.75
Superior lateral pterygoid	-3.52	-4.15	0.40	3.52	-4.15	0.40

Table 4.5 Muscle groups and orthogonal components (Nelson, 1986).

Resultant muscle force vectors (F_v) were calculated using the equation 4.2.

$$F_v = F_m.R_c$$

Equation 4.2 Calculating the resultant force vector. F_m = muscle force, R_c = resultant of orthogonal components

The final model (including vectors) appeared as in figure 4.8.

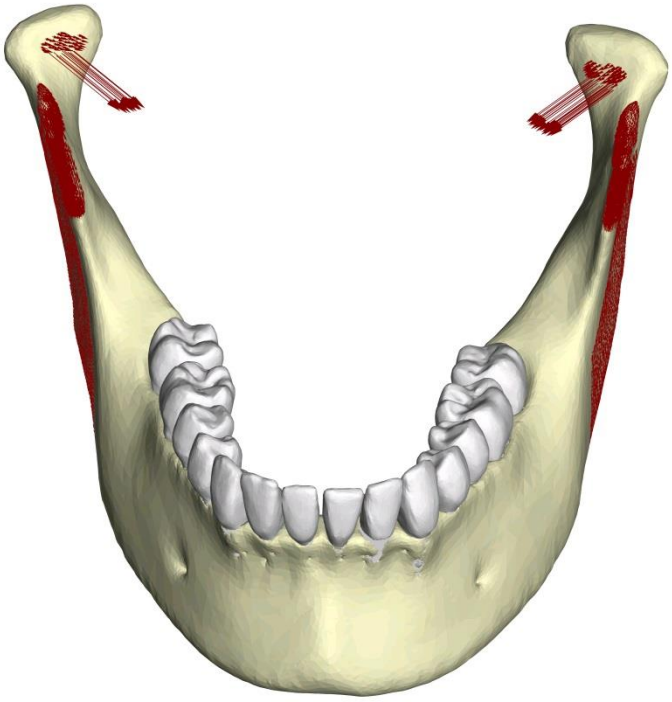

Figure 4.8 Assembled model with muscular forces assigned as vectors (brown).

4.1.2.9 Final model details

The final details of the two models used throughout the study are displayed below.

	Mass (kg)	*Volume (m^3)*	*Brick Count*	*Node count*	*Number of links*	*Material*
Cancellous bone	0.01526095	2.18013e-05	217176	48898	N/A	Isotropic
Cortical bone	0.067639933	3.88735e-05	484837	112273	N/A	Isotropic
Teeth	0.015547444	7.26516e-06	481963	115039	3982	Isotropic
Total	0.0984483	6.794e-5	1183976	276210	3982	

Table 4.6 Details of the assembled mandibular model. All bricks were 4-noded linear tetrahedra.

	Mass (kg)	*Volume (mm^3)*	*Brick Count*	*Node count*	*Number of links*	*Material*
Cortical bone	0.0595968	34251.3	163670	40400	N/A	Isotropic

Table 4.7 Details of the atrophic mandibular model. All bricks were 4-noded linear tetrahedra.

	Mass (kg)	*Volume (mm^3)*	*Brick Count*	*Node count*	*Number of links*	*Material*
Fist	0.479752	275719	27836	6143	N/A	Isotropic

Table 4.8 Details of the fist/forearm. All bricks were 4-noded linear tetrahedra.

4.1.2.10 Cortical node sampling areas for post-processing

As part of the analyses, it was decided that cortical strain and stress would be determined at equivalent points on the model under different loads. A predetermined number of buccal and cortical nodes were selected at approximately the mid-point between the tip of the alveolar crest and the lower border of the mandible in symphyseal, parasymphyseal, body and angle regions and between the anterior and posterior border of the mandible in the region of the ramus. In the region of the condyle, samples were taken at a midpoint on the cortex between the anterior and posterior border of the condylar neck. The positions of the nodes sampled and the sub-site they represented are shown in figures 4.9-4.10 and tables 4.9-4.10.

Lingual nodes	*Approximate anatomical position*
1-7	Right Condyle
8-16	Right Ramus
17-21	Right Angle
22-30	Right Body
31-34	Right Parasymphysis
35-37	Symphysis
38-42	Left Parasymphysis
43-51	Left Body
52-56	Left Angle
57-66	Left Ramus
67-74	Left Condyle

Table 4.9 Lingual node positions.

Figure 4.9 Lingual cortical sampling zones. Nodes are in brown with various positions labelled

Buccal nodes	*Approximate anatomical position*
1-4	Right Condyle
5-10	Right Ramus
11-15	Right Angle
16-18	Right Body
19	Right Incisive foramen
20-23	Right Parasymphysis
24-25	Symphysis
26-30	Left Parasymphysis
31	Left Incisive foramen
32-34	Left Body
35-37	Left Angle
38-44	Left Ramus
45-49	Left Condyle

Table 4.10 Buccal node positions.

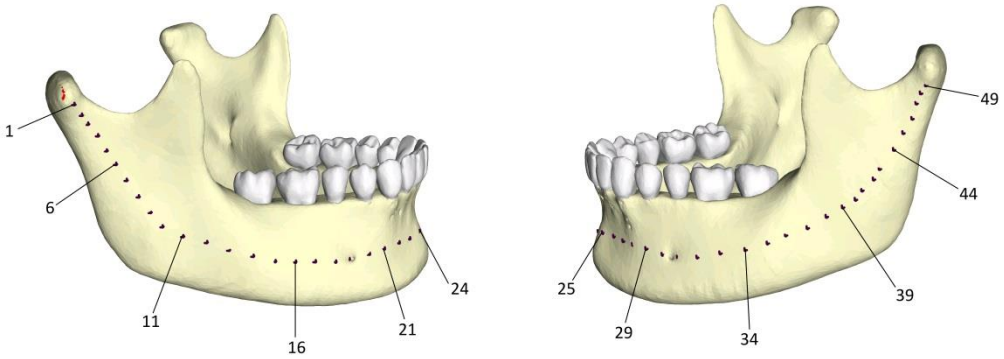

Figure 4.10 Buccal cortical sampling zones. Nodes are in brown with various positions labelled

4.2 Phase Ib: Model verification

4.2.1 Aim

Model verification involved checking the mathematical accuracy of the finite element mesh and was an important step before any analysis was performed. Several steps were taken to verify the mesh accuracy at the resolutions used.

4.2.2 Method

4.2.2.1 Visual examination

Much of this study was based on making a visual assessment of the distribution of areas of high stress or strain therefore this form of verification was appropriate. To perform this assessment models were produced at different element resolutions and subjected to a test load of 100N which was well within the elastic limit of cortical bone. A static linear analysis was performed. When there was no perceptible difference in the distribution of areas of high stress, and convergence was assumed have occurred.

4.2.2.2 Software convergence (relative convergence)

The Strand7® analysis software was capable of giving an automated h-adaptive convergence study with a custom algorithm. The finite element mesh was refined until there was less than 5% error between successive iterations.

4.2.2.3 Increased local element resolution

The element resolution only needed to be high in areas of the mesh where the stresses and strains were high or changed quickly over a small cortical distance therefore, when such areas were encountered, the element resolution was increased by up to eight

times to check that the captured response was correct. A response difference of <5% was considered acceptable.

4.2.2.4 Model validation

In order to perform mechanical validation of the model used in the static linear analysis, the results of loading the model were compared with the experimental results of Vollmer, et al. (2000). In these experiments, explanted, hydrated human mandibles were fixed at the TMJs in specially designed apparatus. Strain guages were applied along the buccal surface. Mastication forces were simulated by the application of forces (130N) at the coronoid processes. Forces were applied to the mandibular body and the resulting strains recorded by a personal computer.

Model 5 was used to mimic the experimental set-up of Vollmer et al. Condylar restraints were placed similarly. Forces of increasing magnitude up to 140N were applied to the body of the mandible and the resultant strain calculated using finite element analysis. The calculated results were compared with the strain results of Vollmer et al. using the Pearson product-moment correlation coefficient (r). This was calculated using Micorsoft Excel® (2010). The analysis time was approximately 14 minutes for each run.

4.3 Phase IIa: Static linear analysis

The methods of the first series of analyses, aimed at investigating the effect of physiological loads on the mandible, are shown below. A physiological load was defined as one within the elastic limit of both cortical and cancellous bone.

4.3.1 Aim

The aims of these analyses were to determine what features of the model would significantly influence mandibular cortical strain and secondly, to use the model to determine the effect of global changes in material properties on the distribution of cortical stress and strain. Finally, to determine the effect of load position and angulation on the distribution of cortical stress and strain.

4.3.2 Method

4.3.2.1 Material properties

Materials were assumed to be homogeneous, linearly elastic and isotropic. The values for Young's Modulus and Poisson's ratio used are shown in table 4.3.

	Elastic Modulus (E) MPa	*Poisson's Ratio (v)*
Cortical bone	13700	0.30
Cancellous bone	7930	0.30
Dentine	18600	0.31

Table 4.3 Material property assumptions used in the finite element model (static analyses only). Material properties for cortical and cancellous bone were obtained from the literature (Carter and Spengler, 1978; Carter, et al., 1980).

4.3.2.2 Load and boundary conditions

A physiological load of 1000Pa was applied at defined points on the mandibular cortex. The boundary conditions were as described in section 4.1.2.8.1. Forces representing the activated muscles were present throughout.

4.3.2.3 Solver

A linear static solver was used for the analyses.

4.3.2.4 Post-processing

Results were displayed using colour contour maps of the entire cortical bone under load. Lingual and buccal mid-cortical node stress and strain were plotted against node position.

4.3.2.5 Analysis

4.3.2.5.1 Analysis 1: The effect of the muscles of mastication on the mandibular cortex

Model 5 (dentate model) was used to examine the effect of the muscles of mastication on the lingual and buccal cortical strain patterns. All muscles were 'activated' simultaneously with the appropriate vector (see table 4.1.2.8.2). It was decided that 50% of the estimated maximal contractile force would be used in this analysis initially. In most cases unexpected loading of the mandible (such as a traumatic insult) would result in less occlusal force. As this was a linear analysis, scaling the response was a simple matter. No additional external load was placed on the model. Bone and dentine material properties were as in table 4.4.

4.3.2.5.2 Analysis 2: The effect of tooth loss on the loaded mandibular cortex

Two models (4 and 5), which represented two clinical states i.e. the early post-extraction state (model 4), and the fully dentate state (model 5), were utilized for this analysis. The muscles of mastication were "inactivated" on all models. Utilizing a local co-ordinate system a static global face pressure of 1000Pa was applied over a buccal cortical area of approximately 1cm^2 in the symphyseal region (see figure 4.11).

Linear static analysis was carried out using Strand 7® finite element analysis system.

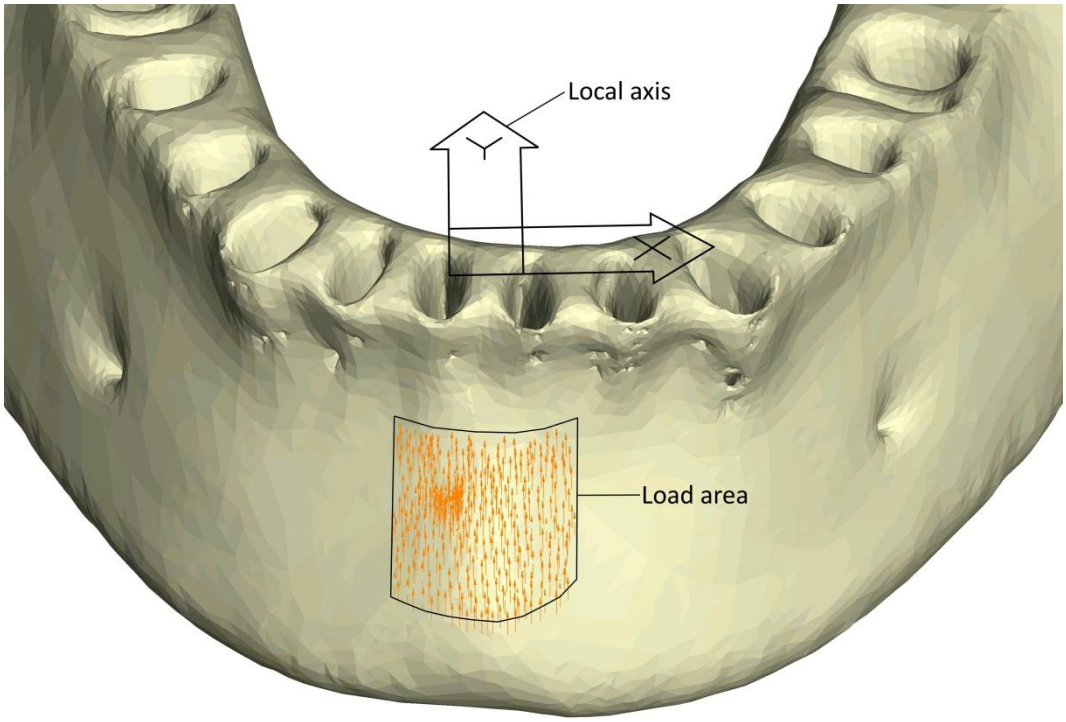

Figure 4.11 The edentulous model of the mandible showing the local axis, load area and applied symphyseal load (orange arrows). The load in this case is applied at 90 degrees to the x-axis in the horizontal plane

4.3.2.5.3 Analysis 3: The effect of load position on the mandibular cortex

Each model was loaded at five individual places (A to E) representing the symphysis, parasymphysis, body, angle and ramus of the mandible. Physiological loads were applied over a cortical element area of approximately 1cm^2 at 90 degrees to the face area, using a local axis in each area (see Figure 4.12). Muscles were activated.

Equation 1	Equation 2	Equation 3
x = (L*cos (θ))/TA y = (L*sin (θ))/TA z = 0	x = 0 y = (L*sin (θ))/TA z = (L*cos (θ))/TA	x = 0 y = (L*sin (θ))/TA z = (L*cos (θ))/TA

Equation 4.3 Equations for determining load path. L= load in Pascals, θ=angulation in degrees at local axis, and TA= total area over which the load was applied.

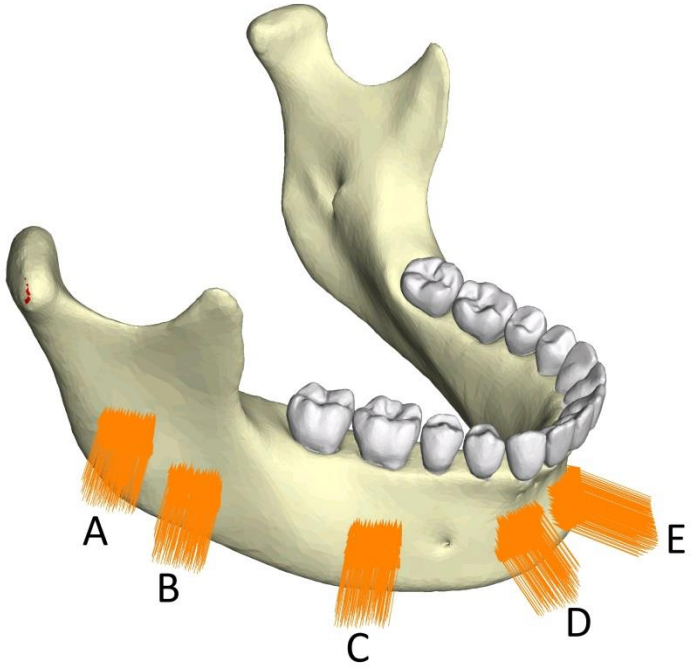

Figure 4.12 Load positions for the static analysis. The anatomical positions of the loads were; A (ramus), B (angle), C (Body), D (parasymphysis) and E (symphysis).

4.3.2.5.4 Analysis 4: The effect of load angulation on the mandibular cortex

Loads at each site were placed at 45, 90 or 135 degrees in the horizontal plane (see figure 4.13). A physiological load was applied over the identical cortical load area as in section 4.3.2.5.1. Muscles were once again activated.

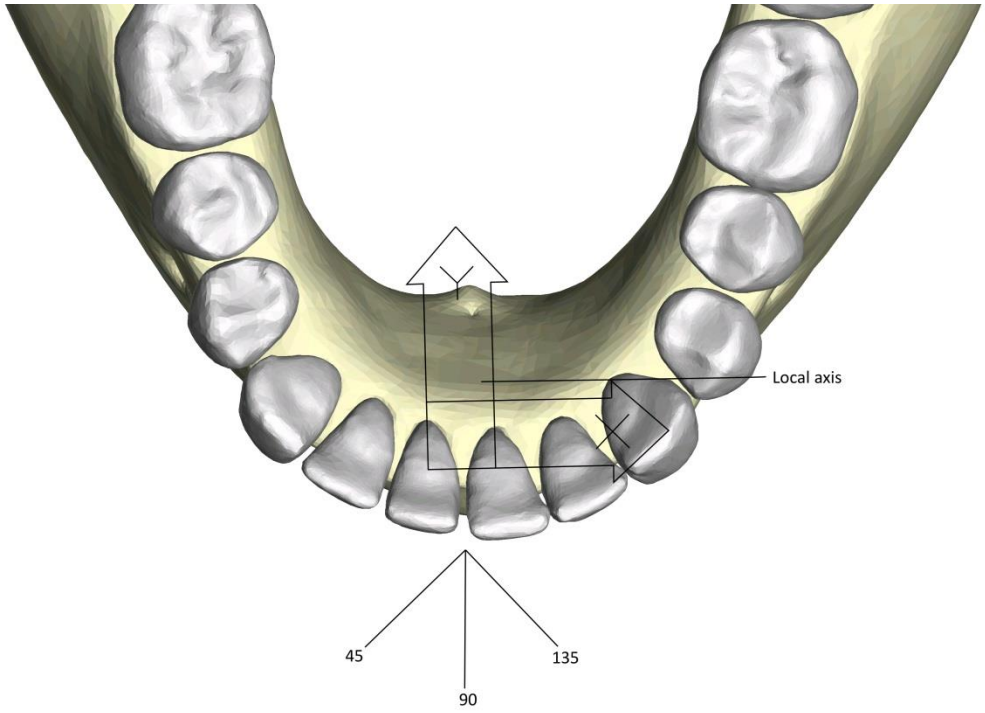

Figure 4.13 Load angle and local axis for a symphyseal load

4.3.2.5.5 Analysis 5: The effect of material properties on stress in the loaded mandible

The material properties of model 5 were adjusted to those of a patient with osteogenesis imperfecta and those of a mandible composed entirely of steel for comparison. The properties used for steel (structural steel AS 4100-1998) were a Young's Modulus of 200GPa and a Poisson's ratio of 0.25. For osteogenesis imperfecta (type III) the material properties were Young's Moduli of 19.7 and 19.2 for cortical and cancellous bone respectively and a Poisson's ratio of 0.3. A physiological load in the area of the symphysis was applied. The results from section 4.3.2.5.3 were used as a comparison.

4.4 Phase IIb: Static non-linear analyses

4.4.1 Aim

The use of linearly elastic material properties placed theoretical limitations, which may have affected the scope of the previous investigations in an adverse manner. Fractures occur in a non-linear fashion and therefore non-linear material properties were employed in the analyses in this section. A failure load of 200MPa was used. This exceeded the elastic limit of the cortical and cancellous bone.

4.4.2 Method

Material non-linearity was introduced into the model using an elastic-plastic material. Model 5 was used for these analyses. The muscles of mastication were activated.

4.4.2.1 Material properties

A stress vs. strain curve of bone was employed to derive the non-linear behaviour of bone. This was obtained from the work of Kemper, et al. (2007). Although this curve referred to human tibial bone, it was considered close enough to mandibular bone to make a generalised comparison. Cortical and cancellous bone material properties were considered as homogeneous and isotropic.

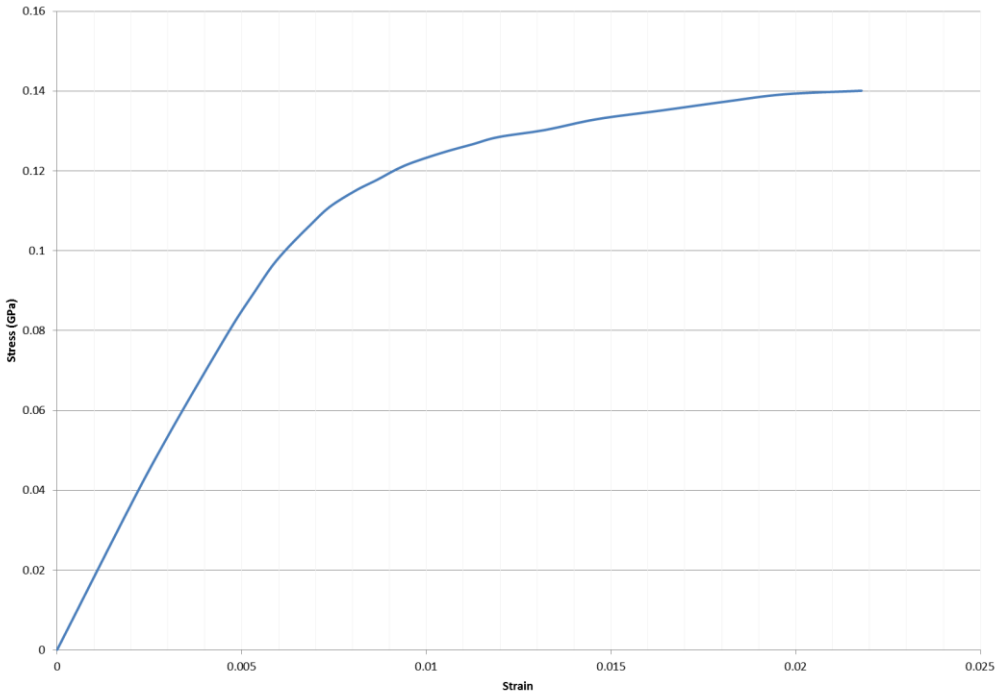

Graph 4.1 Static tensile material properties of human tibial cortical bone taken from the work of Kemper et al., 2007. Specimens were taken from unembalmed, fresh frozen male human cadavers. Both stress and strain refer to the engineering variants.

4.4.2.2 Load and boundary conditions

Models loads were applied in a similar manner to Phase IIa. Both physiological and failure loads were employed for comparison. Muscles were activated.

4.4.2.3 The solver

An incremental-iterative process, (automatic load stepping) was employed. The displacement changes between consecutive iterations were used to indicate convergence of the solution (see figure 4.14). The mean run time for analyses was 28 hours and 14 minutes.

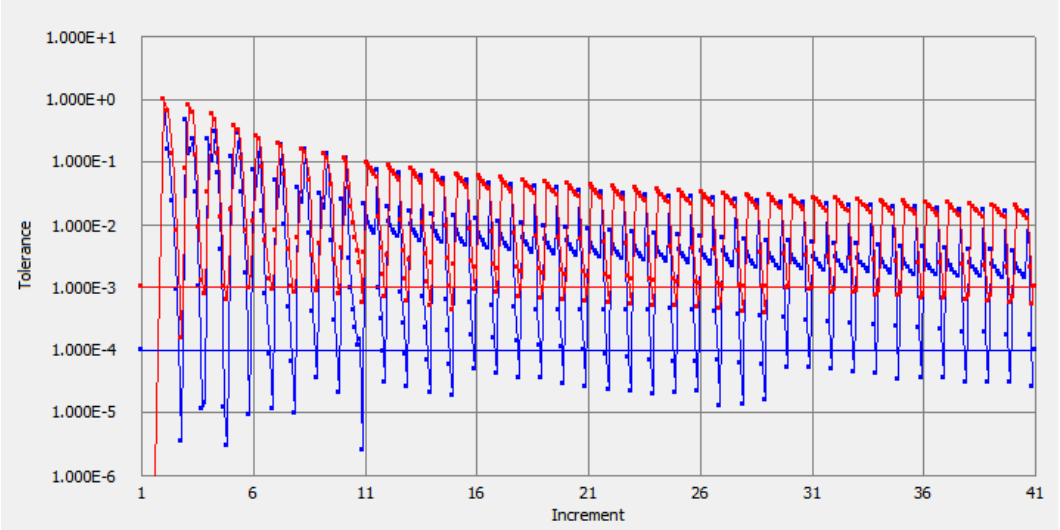

Figure 4.14 Computer display showing the incremental-iterative process. The blue vertical lines represent displacement norm (tolerance $1x10^{-4}$) and the vertical red lines represent force/moment norm (tolerance $1x10^{-3}$). Convergence was achieved when the solution changed minimally, with respect to the defined tolerances, between iterations

4.4.2.4 Post-processing (displaying results)

Von Mises stress and strain were plotted against node cortical position; additionally a stress colour contour map was plotted.

4.4.2.5 Analyses

4.4.2.5.1 Analysis 6: Non-linear analysis with a physiological load

This analysis was a non-linear re-run of analysis 3. This was necessary for comparison as different material properties were used in these analyses. The loading protocols were the same as in section 4.3.2.5.1.

4.4.2.5.2 Analysis 7: Non-linear analysis with a failure load

This analysis was a re-run of analysis 6, the only difference being a change to a failure load was made.

4.5 Phase IIIa: Basic non-linear dynamic analyses

4.5.1 Aim

Phase IIIa describes the series of dynamic of analyses, which aimed at characterizing the effect of a failure load on the mandible. In these analyses, the impact object was a calibrated fist (model 6). This was given various kinetic energies in the simulations. As with the previous static analyses, only direct impacts to the mandible were modelled.

The specific aims in this series of analyses were:

a) To simulate the pattern and anatomical sub-site of mandibular fractures.
b) To determine the temporal arrangement of traumatically induced mandibular fractures.
c) To determine the effect of increased impact kinetic energy on the nature of mandibular fractures.

4.5.2 Method

This series of analyses used model 4 and model 6 to simulate a punch to the mandible. The muscles of mastication were not activated.

4.5.2.1 Material properties

In the dynamic analyses the material properties were slightly altered as was the behaviour of the elements used. An elastic-plastic material capable of taking into account strain-rate effects with a defined stress vs. strain curve was used. The yield point for bone was estimated directly from the stress vs. strain curve (graph 4.2). Failure based on a pre-determined plastic strain was selected.

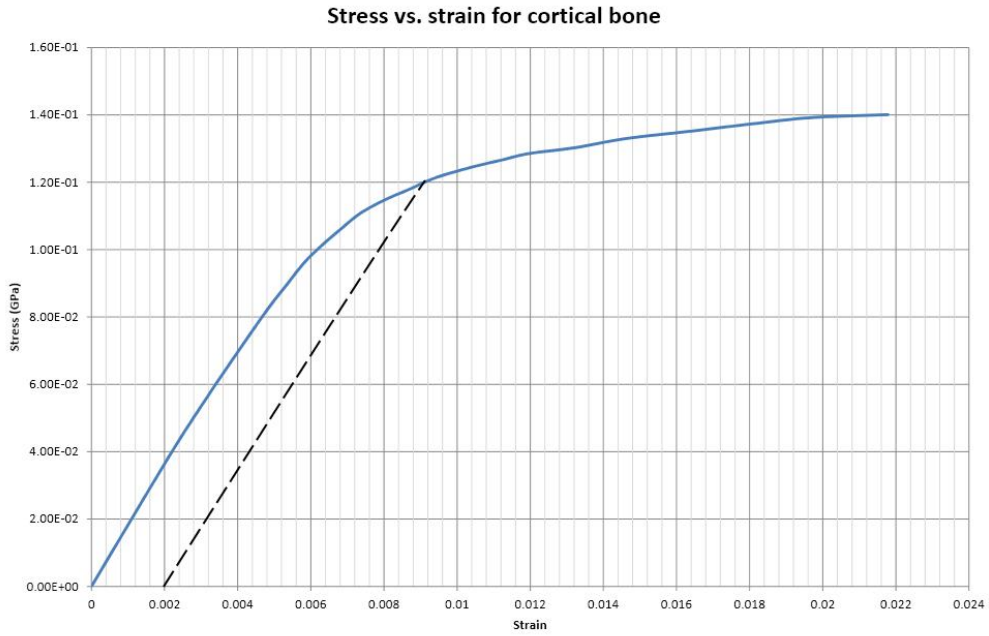

Graph 4.2 Stress vs. strain curve for bone. The dashed black line parallel to the linear portion of the curve (blue) intersects at the assumed yield point (0.2% proof stress). Data taken from the work of Kemper, et al., 2007.

4.5.2.2 Load and boundary conditions

As this series of analyses was dynamic the load was applied to the mandible via a modelled fist of differing kinetic energies. The condylar restraints were changed to encompass the entire condylar head. These changes were made to simulate the set up of mechanical cadaveric studies in the literature, allowing comparison of results. This change was also closer to the anatomical arrangement. Muscles were inactivated.

4.5.2.3 Failure criteria and strain rate

The ultimate strain value used was 0.02, at a mean strain rate of $2.2s^{-1}$ (see Kemper, et al., 2007). A yield stress of 120MPa was used as the value for cortical bone in tension (graph 4.2). Strain rate effects were accounted for using two methods initially. Firstly, a table of curves was defined for three different strain rates. Effective plastic strain vs. yield stress curves for mean strain rates of $0.046s^{-1}$, $0.584s^{-1}$ and $6.027s^{-1}$ were input into

the analysis software (data obtained from the work of Kemper, et al. (2007)). The yield stress was then determined by the software interpolation (Livermore Software Technology Corporation (LSTC), February 2013). This method was eventually abandoned as strain rate data was only available for cortical bone, as opposed to cancellous bone, at the time. Therefore yield stress was calculated using the Cowper and Symonds model (Cowper and Symonds, 1957). Using this model, the initial yield stress (σ_y^0) was scaled as in equation 4.1, where $\dot{\varepsilon}$ was the strain rate and the constants for the particular material were C and p.

$$\sigma_y = \sigma_y^0 \left(1 + \left(\frac{\dot{\varepsilon}}{C}\right)^{1/p}\right)$$

Equation 4.1 Equation for calculating the yield stress using the Cowper and Symonds model (Livermore Software Technology Corporation (LSTC), February 2013).The initial yield stress is denoted by σ_y^0.

$$\dot{\varepsilon} = \sqrt{\dot{\varepsilon}_{ij}\dot{\varepsilon}_{ij}}$$

Equation 4.2 The definition of strain rate ($\dot{\varepsilon}$).

4.5.2.4 Post-processing (displaying results)

Post-processing was performed using LS-pre-post. Colour contour maps of von Mises stress, strain and strain rate were produced. A deletion algorithm was employed whereby elements were removed from the calculation when the strain reached at predetermined value. Analyses focussed on the lingual aspect of the mandible as failure commonly occurs on the side of tension, (Reilly and Burstein, 1975).

4.5.2.5 Analyses

4.5.2.5.1 Analysis 8: The relationship of impact site with fracture distribution

This series of analyses used models 4 and 6. Two impact sites were used, the ramus, and the symphysis. These represented anterior and posterior impacts in the horizontal plane. In order to model a scenario involving a punch, a number of modelling assumptions were made.

Assumption 1

An amateur pugilist would be able to engage 3-5% of their body weight when punching (Gorman, 2009). Assuming the weight of the average man to be approximately 70kg this would mean that the mass engaged during the punch would be 2.8kg (assuming 4% engagement).

Assumption 2

A professional pugilist would be able to maximally engage 10% of their body weight (i.e. using shoulder, arm and fist) whilst punching (Gorman, 2009). Again, assuming the weight of the average man was approximately 70kg this would mean that the mass engaged during the punch would be 7kg (assuming 10% engagement).

Assumption 3

An amateur pugilist would be able to generate a punch with an impact speed of $5ms^{-1}$ (Gorman, 2009).

Assumption 4

A professional pugilist would be able to generate a punch with an impact speed of approximately $10ms^{-1}$(Gorman, 2009).

Utilizing the assumptions above the energy delivered by non-professional (low energy) and professional (high energy) punches was calculated as shown below. Higher punch velocities have been recorded in karate experts (Gorman, 2009).

Kinetic energy for low energy punch = ½ mv^2

$=0.5 \times 2.8 \times (5)^2$

$=35J$

Kinetic energy for high energy punch = ½ mv^2

$=0.5 \times 7.0 \times (10)^2$

$=350J$

The fist model initial kinetic energies (E_i) were therefore scaled between 35J and 400J.

The actual kinetic energies were:

Low kinetic energy punch (amateur)	35J
High kinetic energy punch (professional)	188J
Very high kinetic energy punch (karate expert).	384J

Table 4.4 Calculated initial kinetic energies (E_i) for the fist model.

4.5.2.5.2 Analysis 9: The relationship of impact KE with fracture pattern

In these simulations, two sites were investigated, the symphysis and ramus. Impacts were varied from low kinetic energy to high kinetic energy, noting the change in predicted injuries.

The change in kinetic energy of the fist model was equal to the net work done on the fist model by the mandible. This enabled the calculation of mean force delivered, kinetic energy absorbed by the mandible.

The energy absorbed (ΔE_{kf}) was calculated as the difference in the initial kinetic energy of the fist (E_i) and final kinetic energy (E_f). This was calculated as shown in equation 4.3 where m was the mass of the fist, v_i the initial velocity of the fist and v_f the final velocity.

$$\Delta E_{kf} = E_i - E_f = \frac{1}{2}m(v_i^2 - v_f^2)$$

Equation 4.3 Energy absorbed.

The percentage energy absorbed was calculated as:

$$\Delta E_{kf}(\%) = \frac{E_i - E_f}{E_i} \times 100 = \frac{v_i^2 - v_f^2}{v_i^2} \times 100$$

Equation 4.4 Percentage energy absorbed.

The energy absorbed was $\Delta E_{kf,}$ and the time was t. The time for each punch was 1ms.

The work required to reduce the fist kinetic energy was equal to:

$$F_{avg}d = -\Delta E_{kf}$$

Equation 4.5 Calculating the average impact force (F_{avg}) where d is the distance travelled by the fist at 1ms.

4.5.2.5.3 Analysis 10: The relationship between strain rate and fracture sub-site

The biomechanical properties of bone have generally been evaluated at relatively low strain rates; however, traumatic fractures may occur at relatively high strain rates. Hansen, et al. (2008) reported that there was a simple linear relationship between yield properties and strain rate in human cortical bone, with stress and strain decreased for strain rates greater than $1s^{-1}$ in tension and compression. The aim of this analysis was to compare symphyseal impacts at two strain rates. The Cowper-Symonds equation was

used with two sets of strain rate parameters to scale the yield stress (see equation 4.1). Strain rate parameters for human bone have been variously reported as being between C=2.5, p=7 (Li, et al., 2010), in reference to rib cortical and cancellous bone, and C=360.7, p=4.605 (Iwamoto, et al., 2005) when referring to all bones in the lower leg. Models 4 and 6 were used to determine the effect of strain rate changes on fracture characteristics of a symphyseal impact. The two sets of strain rate parameters chosen for this study were C=40 and p=5 (for high strain rate) and C=2.5 and p=7 (for low strain rate).

4.6 Phase IIIb: Applied non-linear dynamic analyses

4.6.1 Aim

The aim of these analyses was to apply the model to a clinical problem. The problems were deliberately chosen to test the properties of the mandible. These scenarios would not normally involve maxillary teeth. The two problems were:

a) What is the effect of impacted third molar teeth on the susceptibility of the mandible to fracture?
b) What is the effect of cystic lesions in the jaw on the susceptibility of the mandible to fracture?

4.6.2 Method

The material properties, boundary conditions, failure criteria and post-processing were the same as in section 4.5.2.

4.6.2.4 Analyses

4.6.2.4.1 Analysis 11: Influence of localized changes in material properties on mandibular angle fractures- 1

Model 4 was used for this simulation however; an area of cancellous bone with the same volume and shape and position as an un-erupted third molar tooth had its material properties changed to those of enamel, to simulate an un-erupted third molar tooth. The tooth was assumed to have no associated periodontal ligament and no cystic change associated with the crown. The modelling technique more closely approximated an ankylosed tooth. The tooth was also entirely enclosed in cancellous bone and the thickness of the surrounding cortical bone was unaffected. High kinetic energy symphyseal impacts were modelled. Cortical stress was recorded over the posterior surface of the condylar neck from lateral to medial along the path shown in figure 4.17 symphyseal impacts and on the medial aspect of the condylar neck from posterior to anterior for angle impacts. Cortical stress on the lingual aspect of the third molar region on the right was measured from posterior to anterior for both impacts.

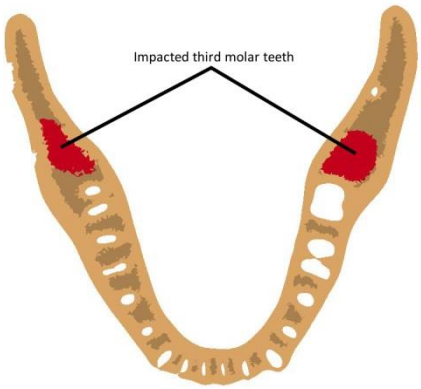

Figure 4.15 An illustration of a cross-section of the mandibular model showing the position of the impacted mandibular molar teeth in red. Note that the teeth were completely contained within the cancellous bone and the cortical thickness was not reduced in this case.

Figure 4.16 Diagram showing the relationship of the lingual angle-sampling zone (in black) to the third molar area

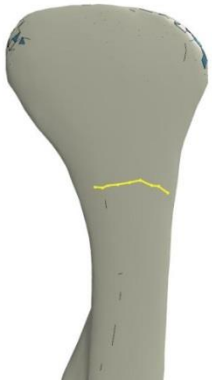

Figure 4.17 Sampling zone for posterior condylar neck stress (in yellow). Measurements were taken from lateral to medial.

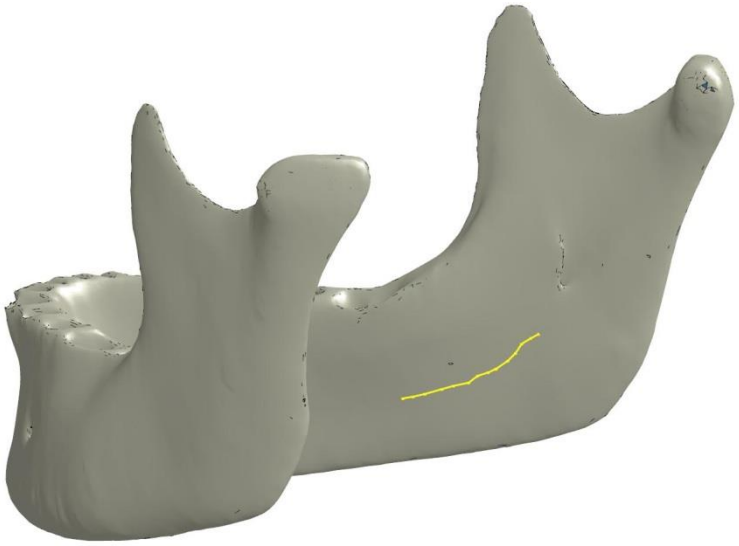

Figure 4.18 Sampling zone for lingual angle cortical stress (in yellow). Measurements were taken from posterior to anterior.

4.6.2.4.2 Analysis 12: Influence of localized changes in material properties on mandibular angle fractures- 2

Model 4 was used for this analysis. In this case an area of cancellous bone was deleted from the model. The area was the same as that occupied by the un-erupted third molar tooth in analysis 11. There was no change in the cortical bone thickness. Analyses were performed with respect to strain energy density and effective stress.

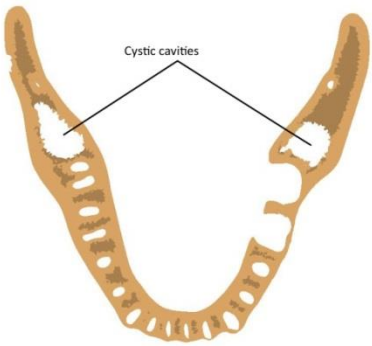

Figure 4.19 An illustration of a cross-section of the mandibular model showing cystic cavities completely contained within the cancellous bone. The cortical thickness was not reduced in this case

Chapter 5 Findings and conclusions

5.1 Findings. Phase Ib: model verification

5.1.1 Mesh quality analysis results

The results of the model mesh quality analysis process are shown below. The threshold value was 0.3 (min/max aspect ratio). Figure 5.1 shows that very few of the elements failed to achieve this value and that the main problem areas were around the mental foramen, however, these were acceptable. Overall the mesh quality reached the standard for analysis.

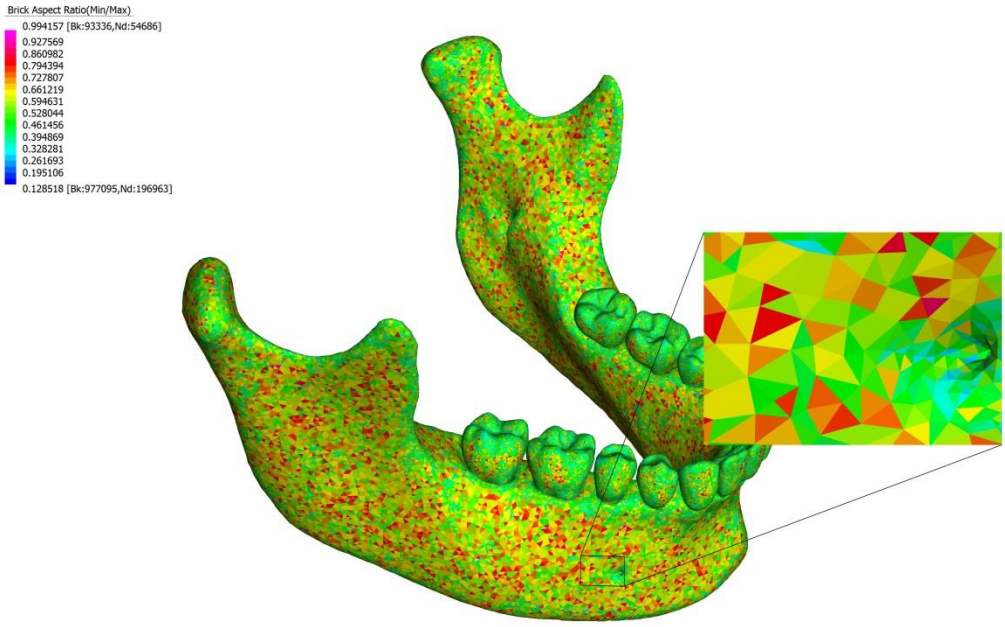

Figure 5.1 Graphical representation of mesh quality. The chosen index was the minimum/maximum edge length ratio.

5.1.2 Model verification and validation

The results of the model verification and validation process are given below.

5.1.2.1 Visual verification

The two models in figures 5.2 and 5.3 show element resolutions of 350000 and 458000 respectively. As can be seen, the distributions of high strain (red areas) on the two models were almost identical suggesting that the model had almost converged. The white areas on the condylar heads and the in the canine region represent the point restraints for this particular analysis.

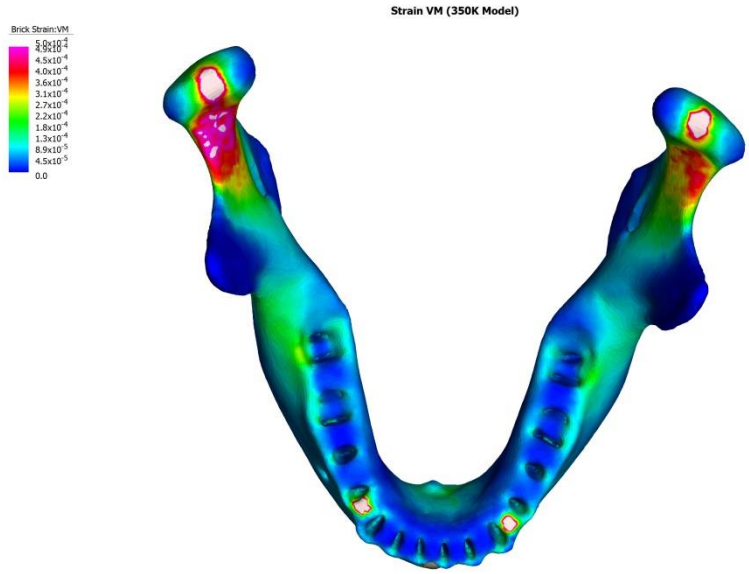

Figure 5.2 A model with an element resolution of 350000 tetrahedral elements. Compare the strain contour with the higher element resolution figure 5.3.

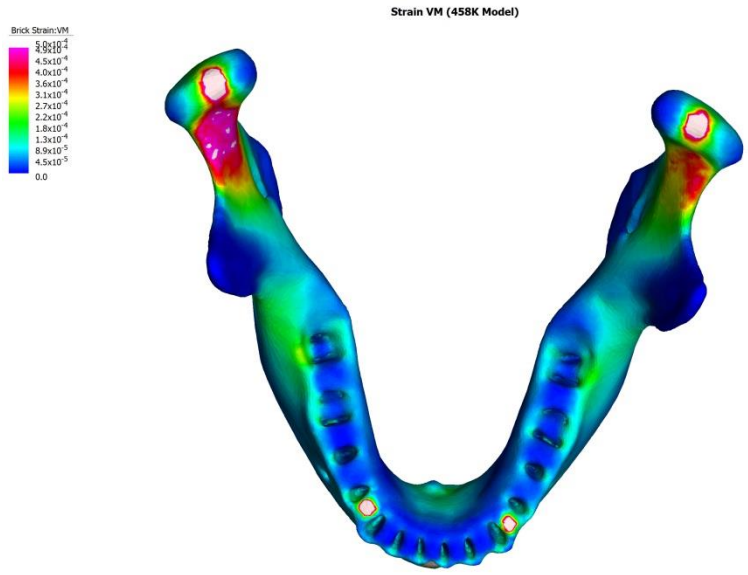

Figure 5.3 A model with a higher element resolution of 458000. Note the minimal difference in strain contour.

5.1.2.2 Software convergence and increased local element resolution

Whilst the analysis software was able to perform h-adaptive convergence, the element resolution only needed to be high in areas of the mesh where the stresses and strains were high or changed quickly over a small cortical distance. When such areas were encountered, the element resolution was increased by up to eight times to check that the captured response was correct. Figure 5.4 shows the model with increased resolution in the right condylar region. In all cases, increased local element resolution showed that an acceptable response had been recorded, usually with a response difference of <5%.

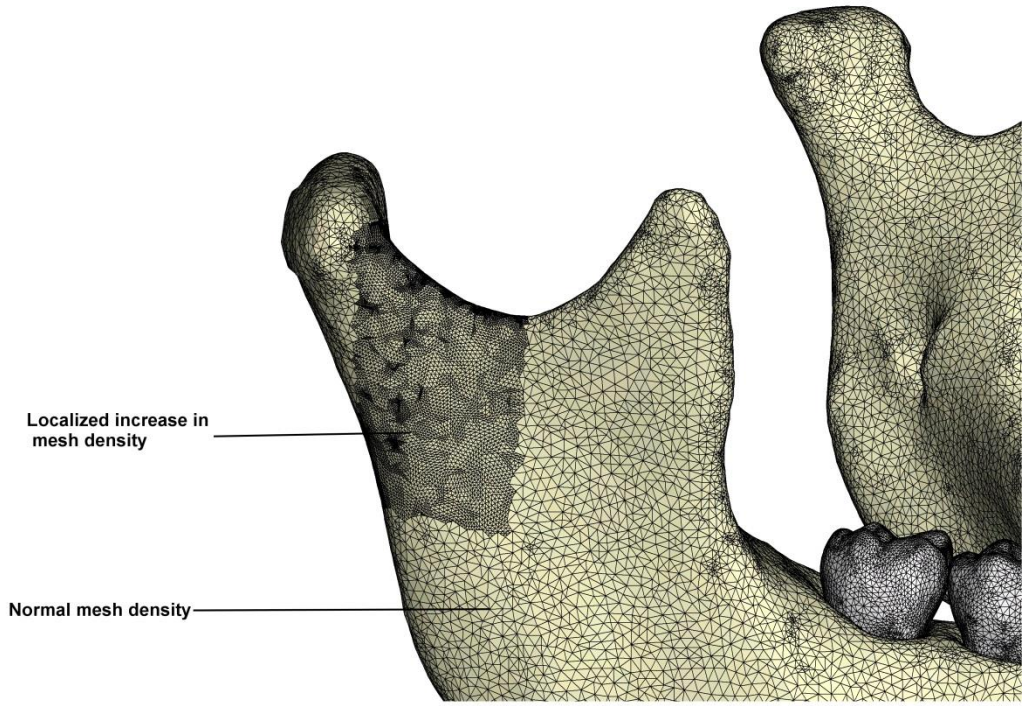

Figure 5.4 The analysis model with increased resolution in the condylar region to verify the response.

5.1.2.3 Model validation

Graph 5.1 shows a Pearson product-moment correlation curve comparing the experimental results of Vollmer et al. (1992) and the phase Ib 3DFEA results. As can be seen, there was good correlation (0.9998) between the experimental mechanical results of Vollmer et al. (in blue) and the calculated 3DFEA results (in red). As laboratory cadaveric experiments are the current gold standard for the determination of fracture thresholds in humans, this result suggests that the 3DFEA model was at least as accurate as the cadaveric biomechanical experiments, within the elastic limit of bone.

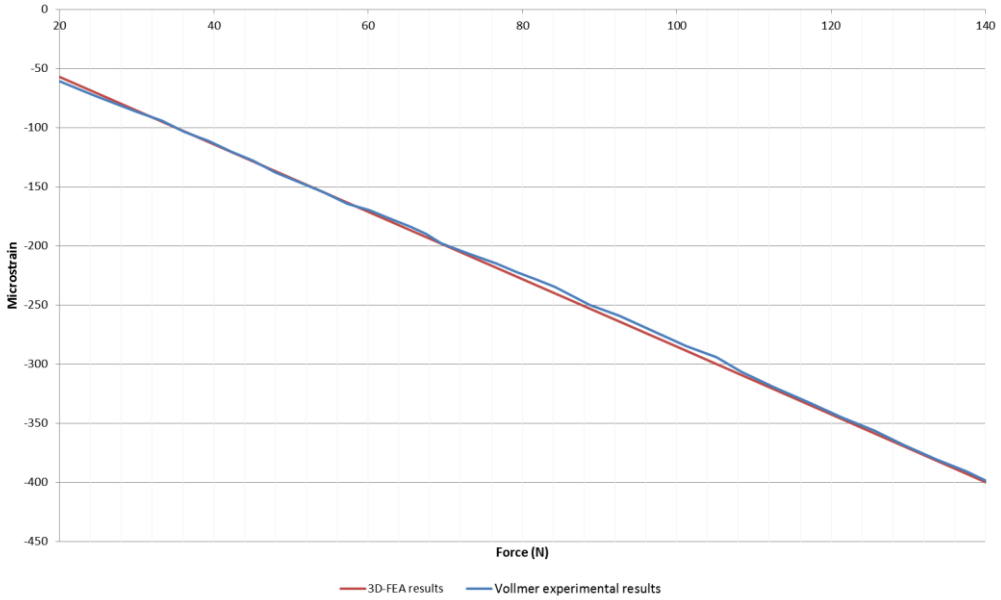

Graph 5.1 A comparison of experimental and 3DFEA results

5.2 Phase I conclusions

The aim of phase Ib was to verify the 3DFEA model produced in phase Ia as far as possible, within the parameters set out in the methodology. The mesh quality analysis showed that the final model would be sufficient to capture the stresses of interest. Whilst the 3DFEA results were found to be comparable with those of Vollmer et al., it is understood that cadaveric mechanical results themselves are not an accurate representation of the natural situation. Cadaveric material has different material properties to live bodily tissue. Normal muscular tone is lost in cadaveric experiments. This results in a change in the forces acting on the mandible. Whether or not these forces play a significant role in the initiation of fractures has been debated in the literature. The model produced has an additional feature in the ability to replicate the site of action of muscular forces and to some degree the magnitude. This gives the 3DFEA model an advantage over the cadaveric models that have been used in the past to provide data on fracture thresholds and mandibular deformation. Additionally, the 3DFEA model can calculate stress and strain in any area non-invasively without affecting the derived results.

5.3 Findings. Phase IIa: Static linear analyses

5.3.1 Results 1: The effect of musculature on mandibular cortical stress and strain

Von Mises stress and strain (hereafter referred to as stress and strain respectively) were calculated. The superior surface of the condylar heads showed the highest stress and strain (see figure 5.5). These were constrained areas of the model representing the glenoid fossa at the base of the skull. Stress was increased in the areas with the smallest cross-sectional area, namely the condylar necks anteriorly. Examination of graphs 5.2 and 5.3 show that the magnitude of strain was over 15 times greater at the condylar neck compared to the mandibular symphysis (see appendix 10 for the tabulated data). A similar pattern was noted on examination of the cortical stress graphs.

In terms of the magnitude, even with the abnormal situation of simultaneous, synchronous muscular contraction, the values of cortical stress and strain were extremely low.

The stress required to cause bony fracture has been calculated at 140MPa in tension. The values of stress estimated in this study were orders of magnitude lower.

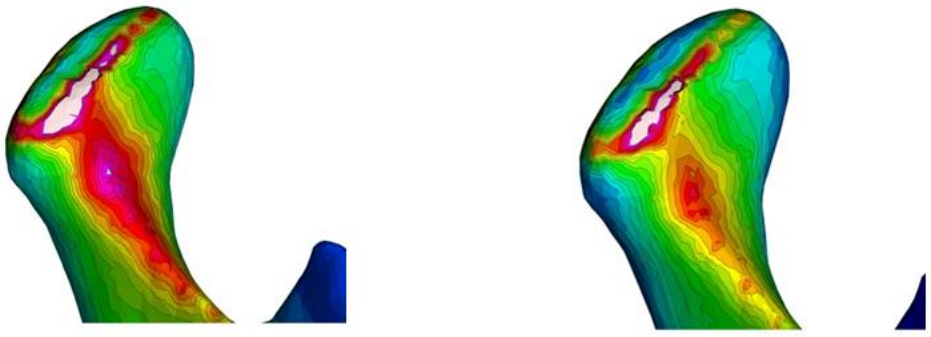

Figure 5.5 Colour contour maps of the right mandibular condyle. Strain is mapped on the left and stress on the right.

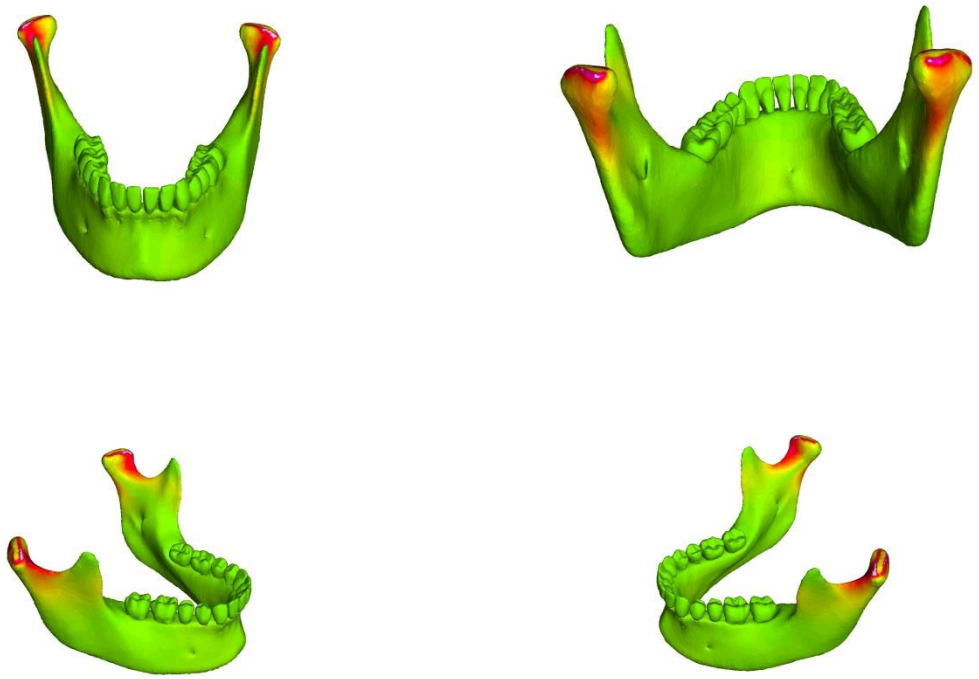

Figure 5.6 Colour contour map showing von Mises stress variation over the cortex. High strain is red.

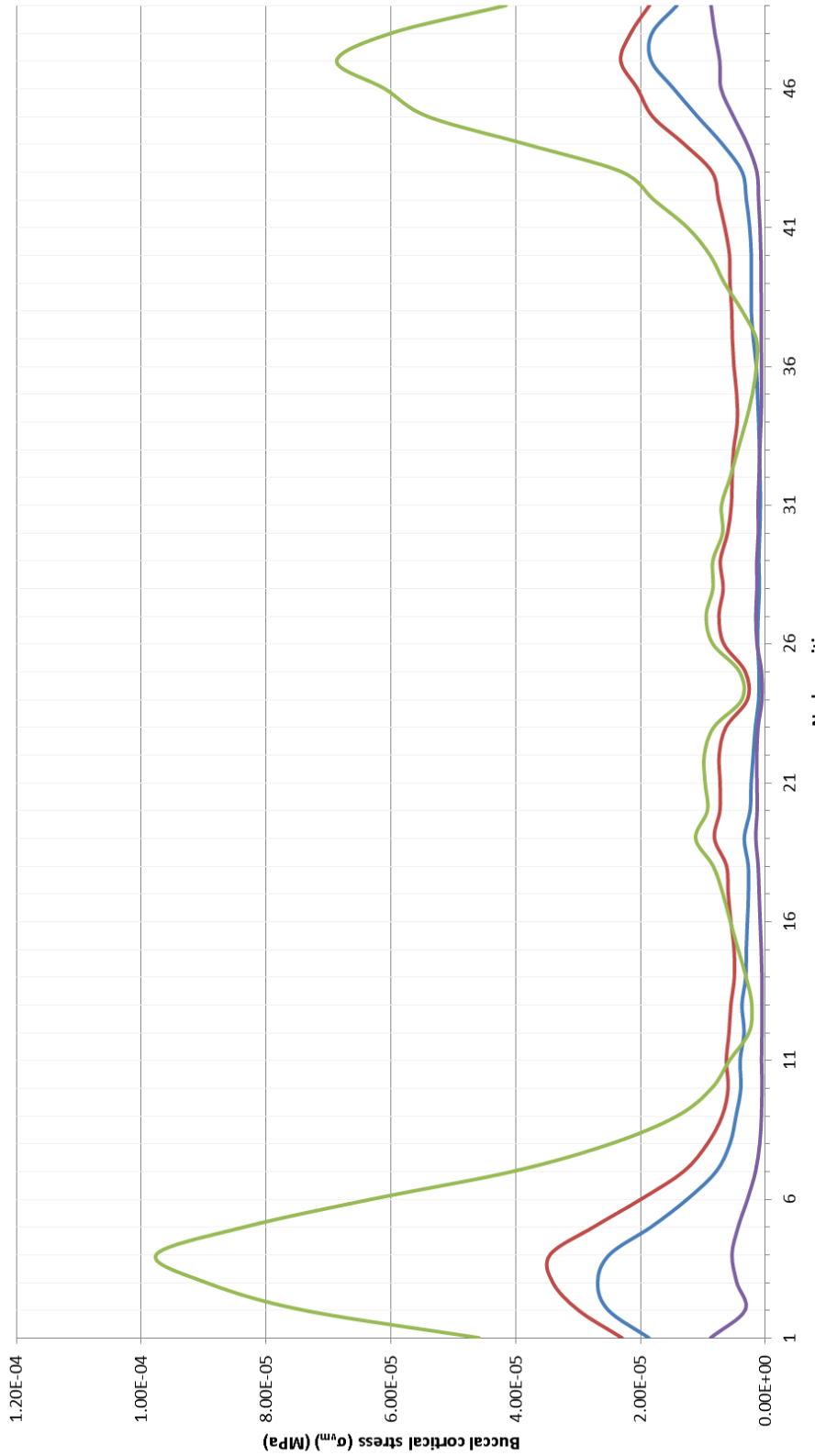

Graph 5.2 The effect of muscular contraction on buccal cortical von Mises stress (σ_{vm}). Stress at each node position is noted.

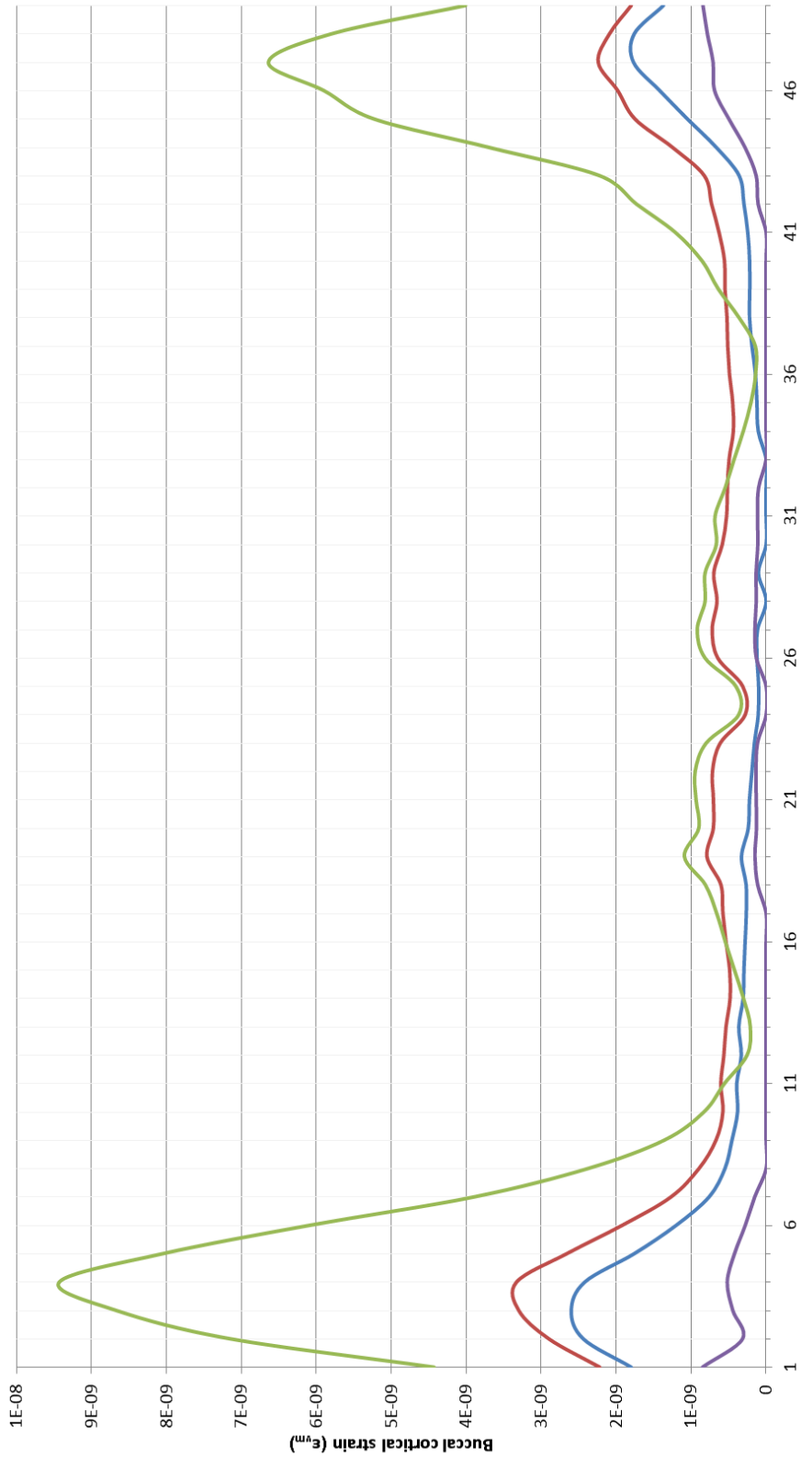

Graph 5.3 The effect of muscular contraction on buccal cortical strain (ε_{vm}). Stress at each node position is noted.

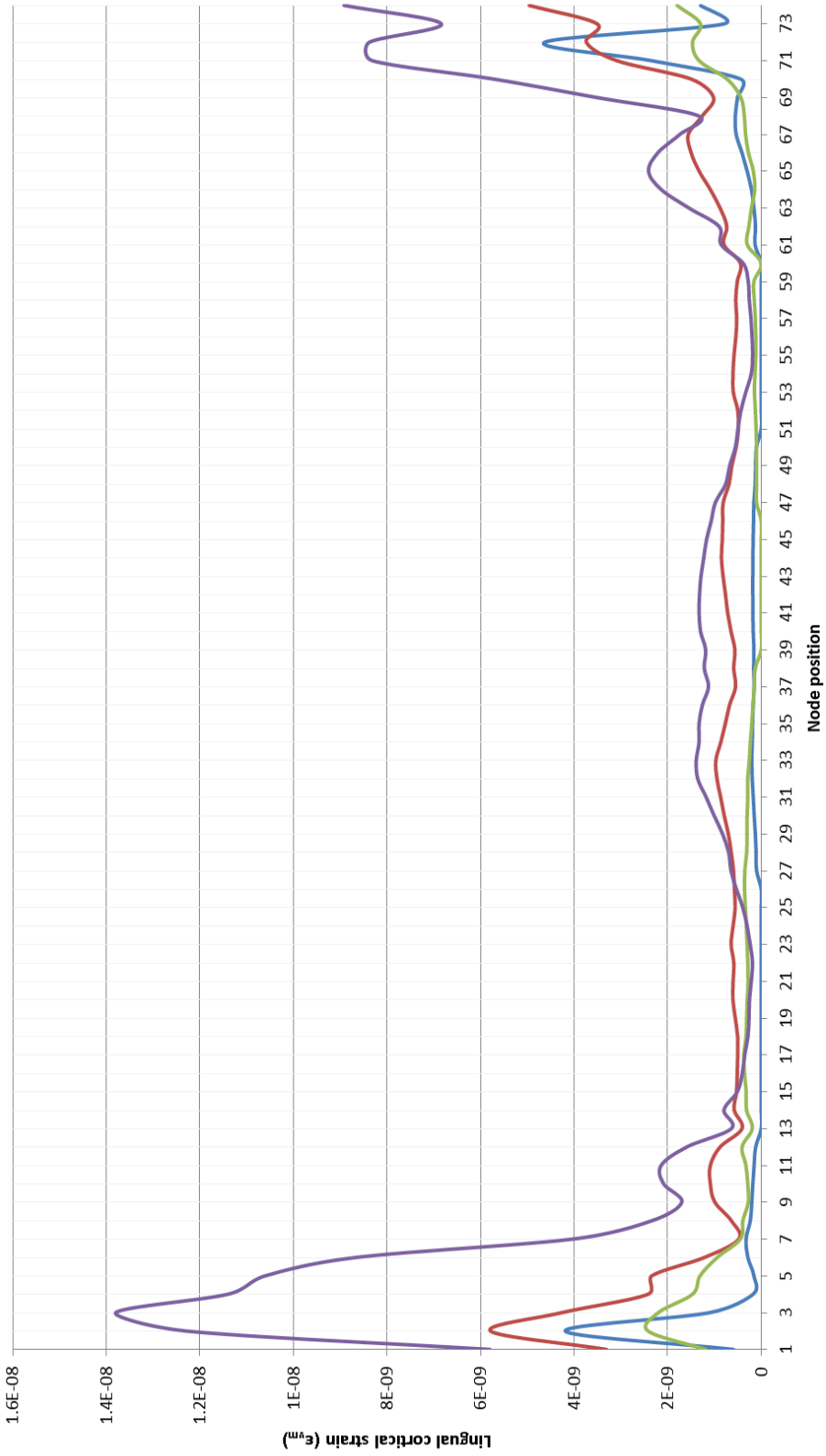

Graph 5.4 The effect of muscular contraction on lingual cortical von Mises strain (ϵ_{vm}). Strain at each node position is noted.

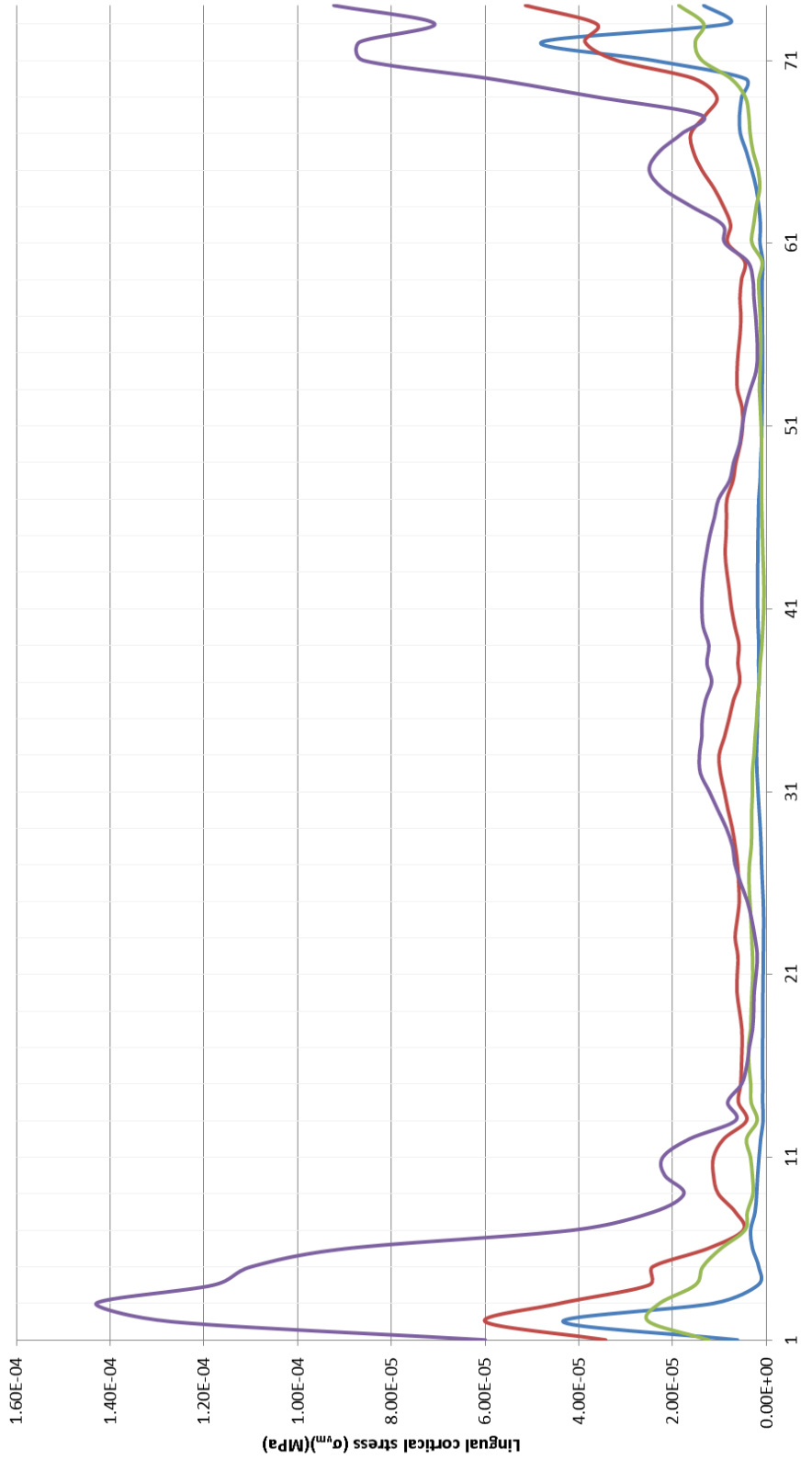

Graph 5.5 The effect of muscular contraction on lingual cortical stress (σ_{vm}). Stress at each node position is noted.

5.3.2 Results 2: The effect of tooth loss on the loaded mandibular cortex

5.3.2.1 The dentate and edentulous mandible

Examination of the colour contour plots for models 4 and 5 following loading of the mandibular body (figures 5.8 and 5.9) show that the cortical strain was increased at the loading site on the right buccal aspect, the ipsilateral condylar neck buccally and on the condylar heads bilaterally (although these were also constrained sites). The cortical stress and strain signatures mirrored each other.

The graphs of buccal and lingual cortical strain for the edentulous and dentate mandibles showed little variation between each other in terms of the cortical signature, i.e. the pattern of peaks and troughs on cortical strain graphs, were similar. The calculated Pearson product-moment correlation coefficients for the lingual and buccal samples and were found to be 0.9988 and 0.9998 respectively, indicating strong relationships. This suggests that there were no significant local effects, at the sample level, on tooth removal. In terms of magnitude of strain on loading, the maximum difference was approximately 100με and in most cases much less. This was much less than the estimated yield strain of cortical bone.

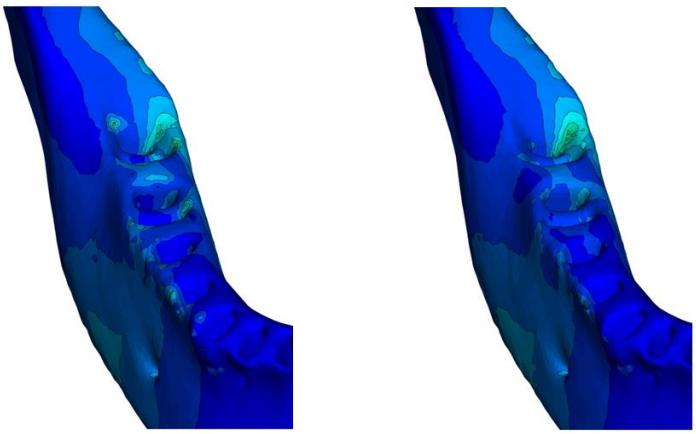

Figure 5.7 Alveolar strain comparison between the dentate and edentulous mandible. The edentulous mandible is on the right and the dentate mandible on the left (teeth removed to demonstrate the alveolar bone). The same contour scale is used for both.

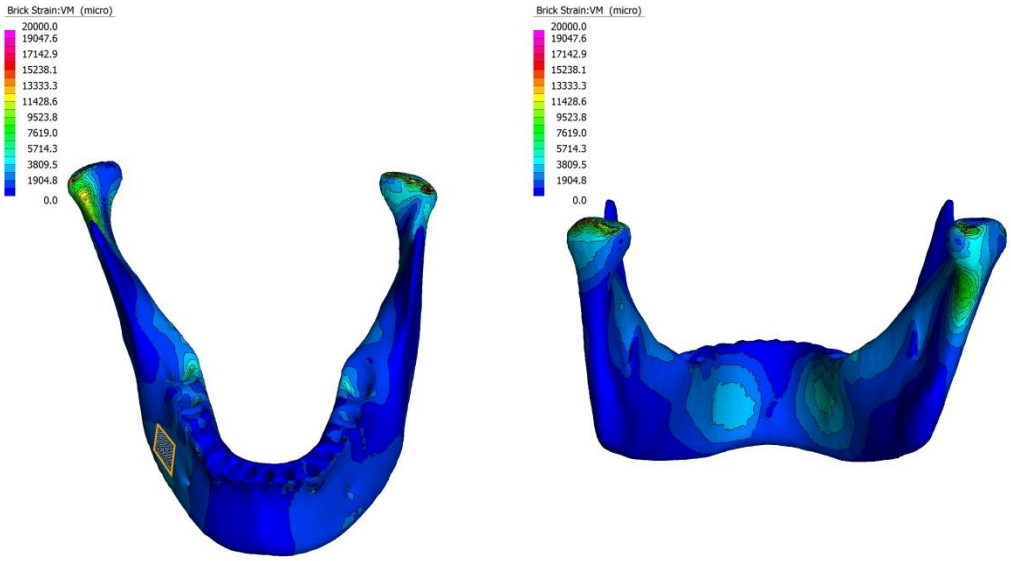

Figure 5.8 Colour contour maps of von Mises strain showing the buccal and lingual aspects of cortex of model 4. Area of load is contained within the orange rectangle. Displacements are exaggerated by 10%.

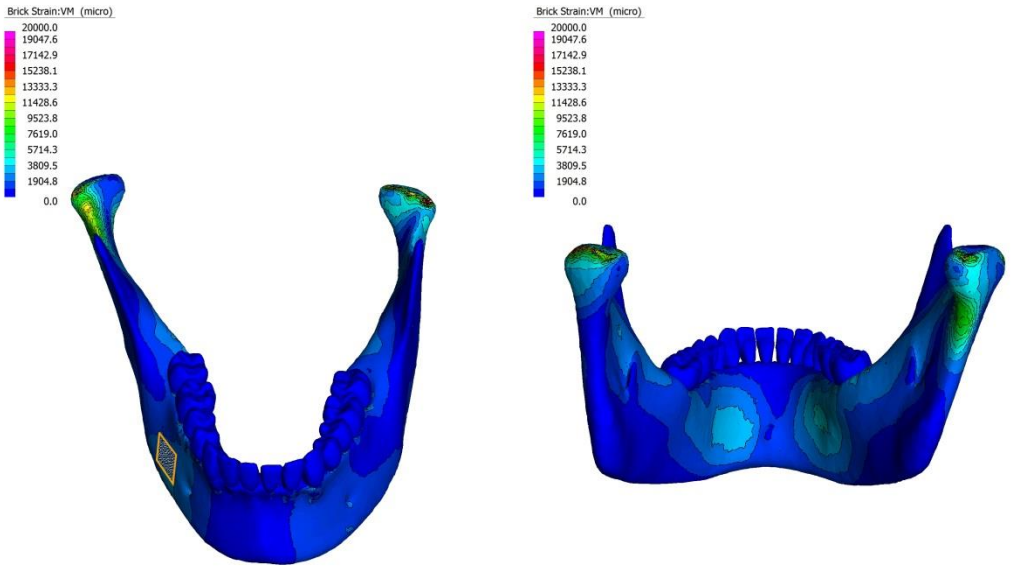

Figure 5.9 Colour contour maps of von Mises strain showing the buccal and lingual aspects of cortex of model 5. Area of load is contained within the orange rectangle. Displacements are exaggerated by 10%.

The most significant changes in cortical stress and strain were noted at the alveolar crest. This would be expected as this is an area with a small cross-sectional. The overall effect was minimal.

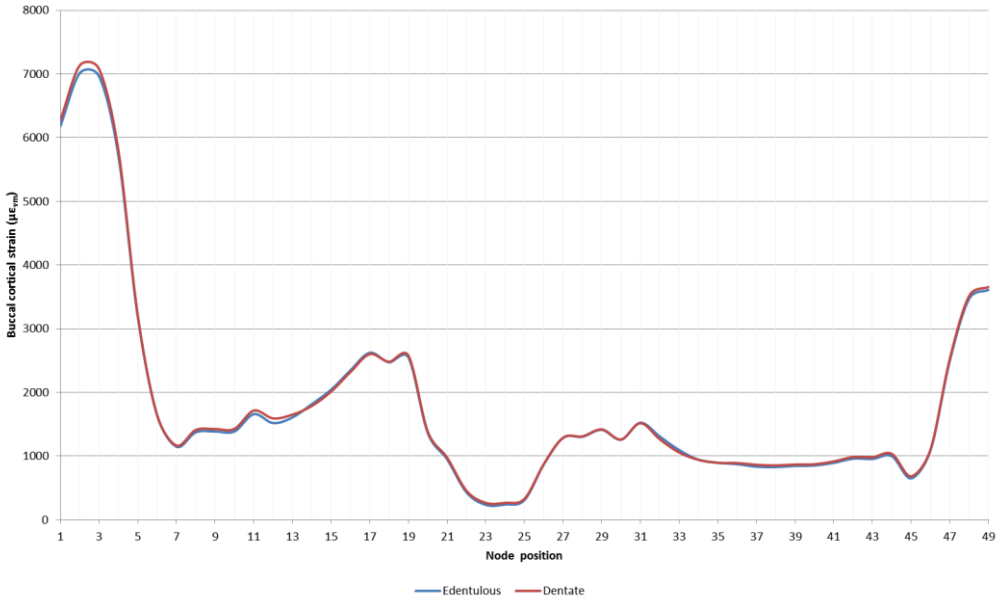

Graph 5.6 A comparison of buccal cortical strain in the edentulous and dentate state.

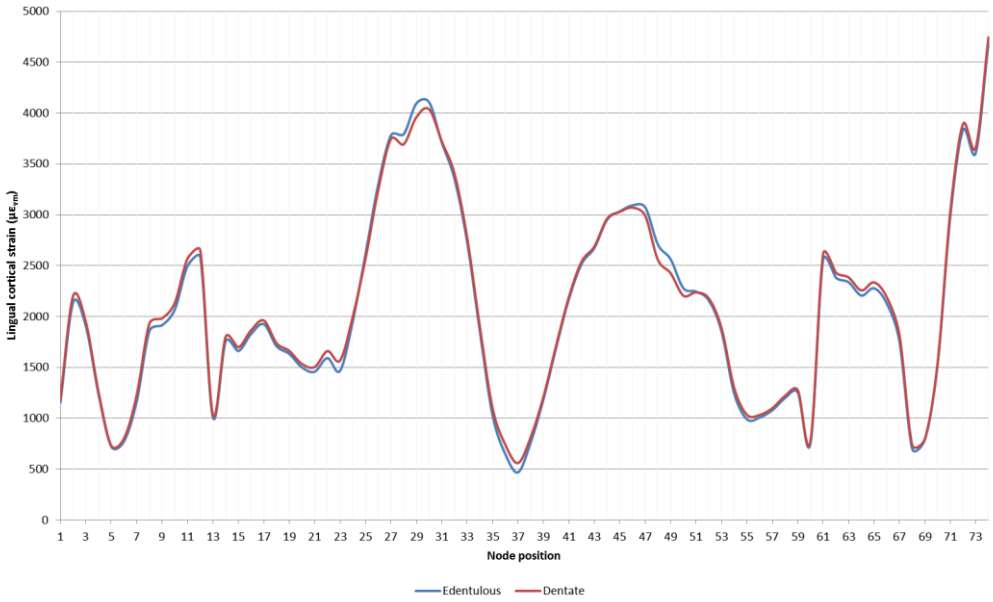

Graph 5.7 A comparision of lingual cortical strain in the edentulous and dentate state.

5.3.3 Results 3: The effect of load position on the mandibular cortex

5.3.3.1 The symphyseal load

Symphyseal loading resulted in increased strain and stress at the condylar head and neck both lingual and buccally. There was also increased stress and strain on the lingual aspect of the mandible in the midline, although this was to a much lesser extent. The midline, although being the loading site, registered a lesser change in the cortical stress and strain which was most likely due increased cortical bone width in that region. Lateral to this bridge the strain was significantly increased.

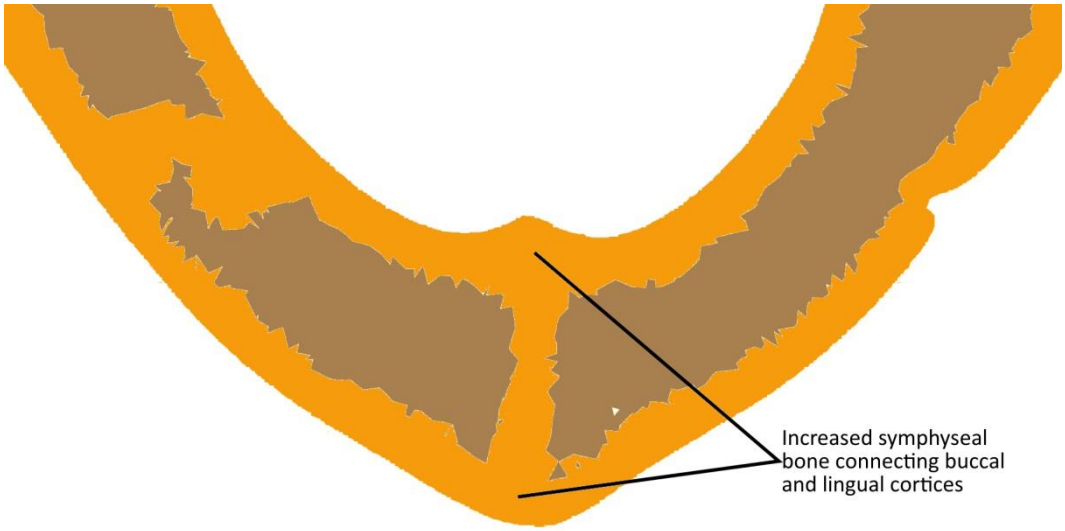

Figure 5.10 A cross section of the mandibular cortex showing a bridge of bone between the buccal and lingual cortices at the symphysis.

The cancellous bone which was sandwiched between the buccal and lingual cortices was capable of undergoing considerably more strain than the cortical bone.

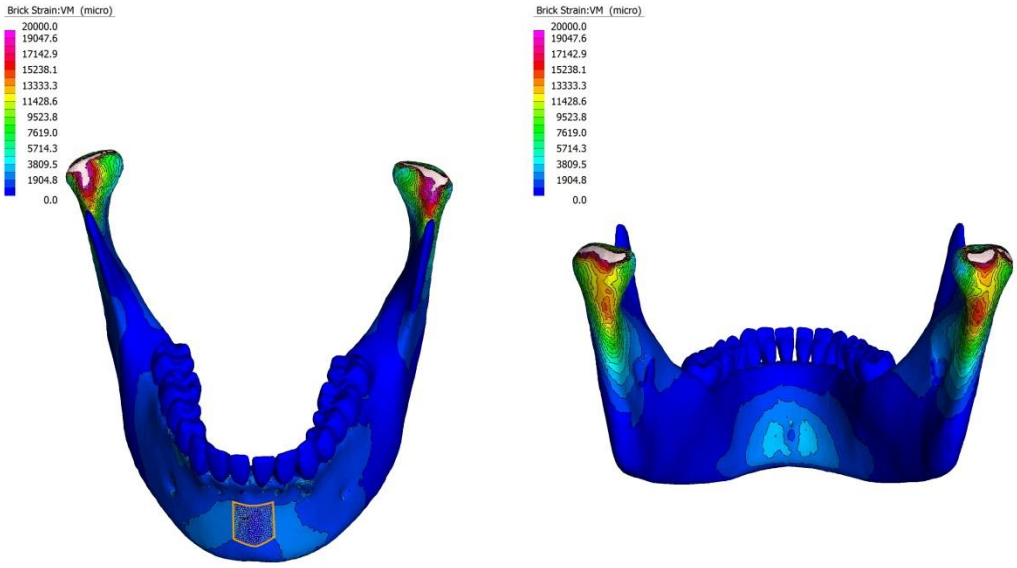

Figure 5.11 Colour contour maps of von Mises strain showing the buccal and lingual aspects of cortex of model 5. Area of load is contained within the orange rectangle. The global face load was 1000Pa along the y-axis of the local axis in the symphyseal region. Displacements are exaggerated by 10%.

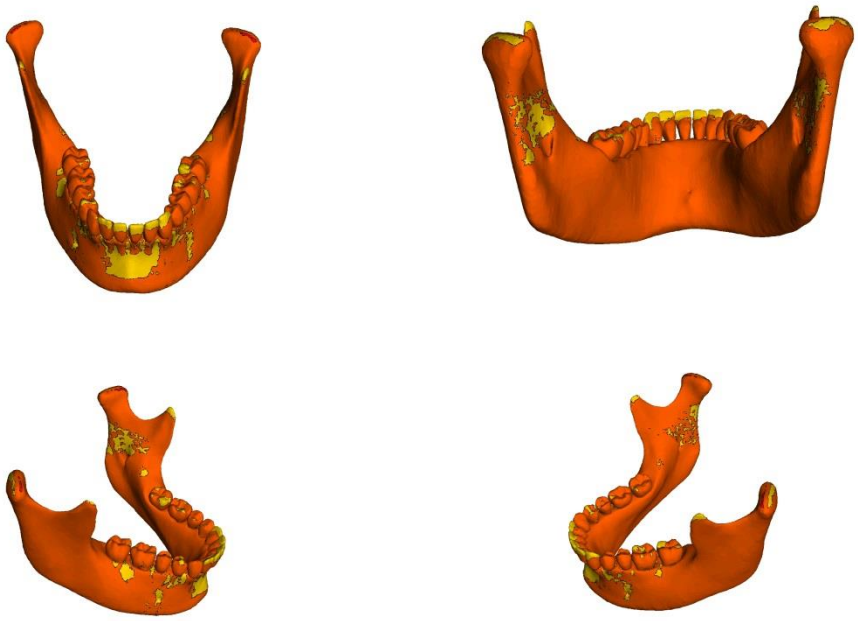

Figure 5.12 Mandibular map showing areas of tensile stress (red) and compressive (yellow) stress, following symphyseal loading.

5.3.3.2 The parasymphyseal load

Parasymphyseal loading resulted in increased stress and strain at the ipsilateral and contralateral condylar head and neck, with the ipsilateral side being greater. Increased stress and strain occurred at the loading site, although, values were considerably less than those encountered at the condyles. The cortical strain signature showed peaks at nodes 3, 19 and 49 (right condyle, left condyle and right incisive foramen respectively). Node 19 was of interest as it was not on the direct load path; however, it did represent an anatomical feature, a bony foramen, which would be prone to high stress on loading. Figure 5.14 shows the compressive and tensile stress map for the same analysis.

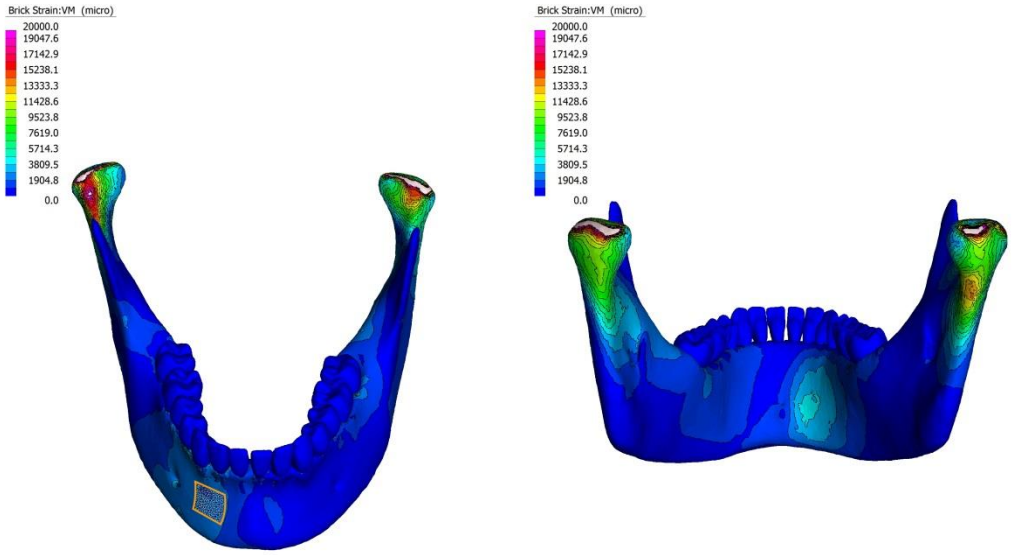

Figure 5.13 Colour contour maps of von Mises strain showing the buccal and lingual aspects of cortex of model 5. Area of load is contained within the orange rectangle. The global face load was 1000Pa along the y-axis of the local axis in the parasymphyseal region. Displacements are exaggerated by 10%.

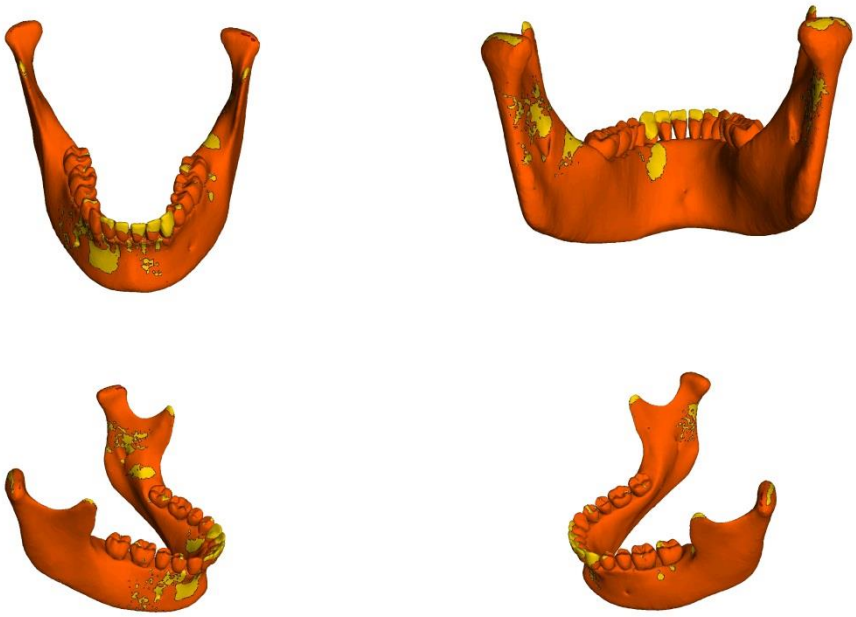

Figure 5.14 Mandibular map showing areas of tensile stress (red) and compressive (yellow) stress, following parasymphyseal loading.

5.3.3.3 The body load

Body loading resulted in increased buccal cortical strain in the right condylar neck, the left condylar neck, the right body (loading site) and the right parasymphyseal regions, in decreasing order of magnitude. On the lingual aspect, the greatest tensile strain occurred in the region of the right body/right parasymphysis. A second lingual peak in tensile strain occurred between nodes 37 and 53 on the left, peaking at node 44 in the left body of the mandible. The lingual cortical strain signature showed that, at mid-cortical level, the greatest strain was no longer at mandibular condyles, but at the loading area.

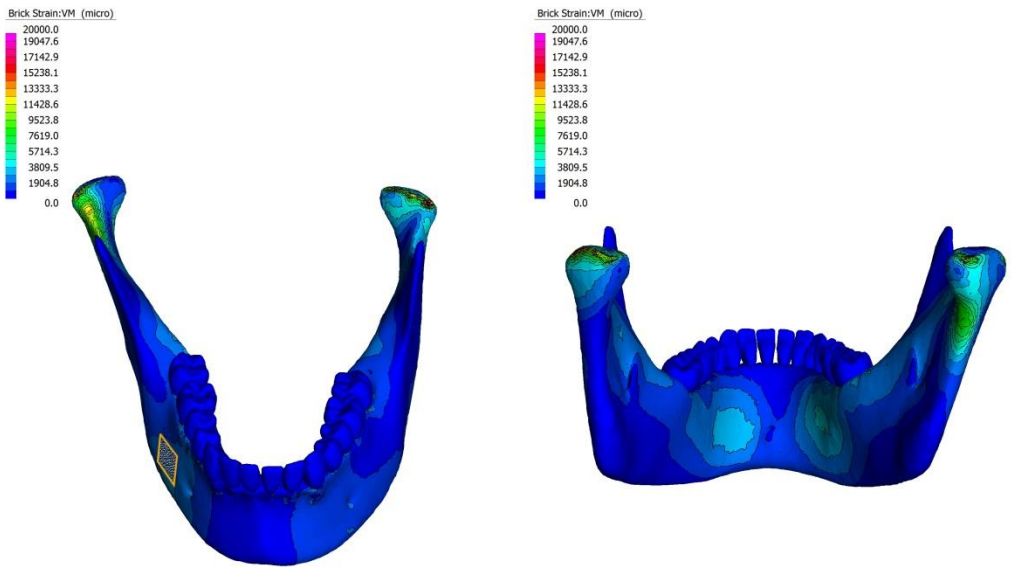

Figure 5.15 Colour contour maps of von Mises strain showing the buccal and lingual aspects of cortex of model 5. Area of load is contained within the orange rectangle. The global face load was 1000Pa along the y-axis of the local axis in the body region. Displacements are exaggerated by 10%.

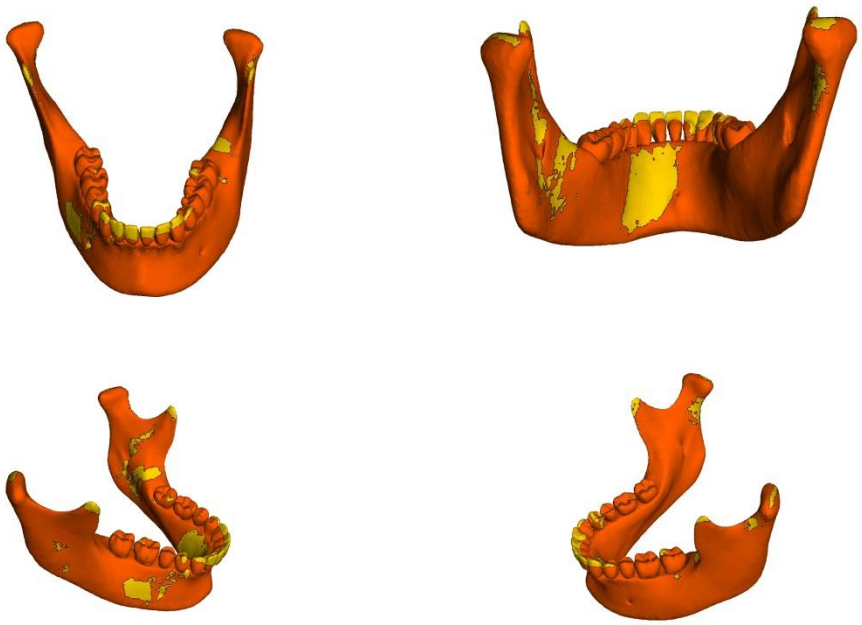

Figure 5.16 Mandibular map showing areas of tensile stress (red) and compressive (yellow) stress, following body loading.

5.3.3.4 The angle load

Right angle loading resulted in increased strain at the ipsilateral condyle neck and the contralateral parasymphysis buccally and lingually. The buccal cortical strain signature showed peaks at nodes 2, 8, 19, 27 and 48. The lingual cortical strain signature only showed one significant peak, other than the condylar peaks. This was at node 12. Compressive stress was mainly found at the left parasymphyseal region lingually (see figures 5.17 and 5.18).

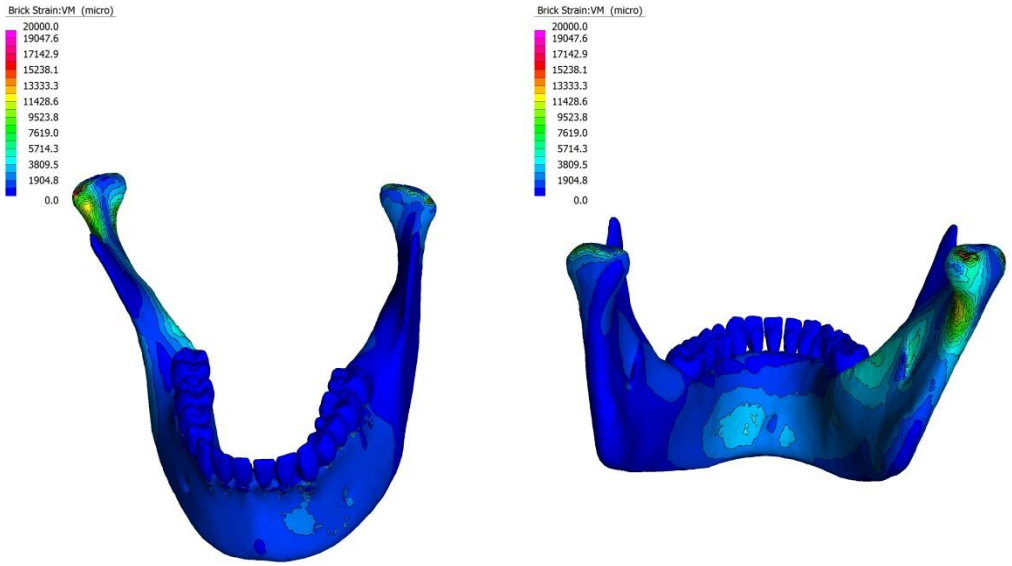

Figure 5.17 Colour contour maps of von Mises strain showing the buccal and lingual aspects of cortex of model 5. The global face load was 1000Pa along the y-axis of the local axis in the angle region. Displacements are exaggerated by 10%.

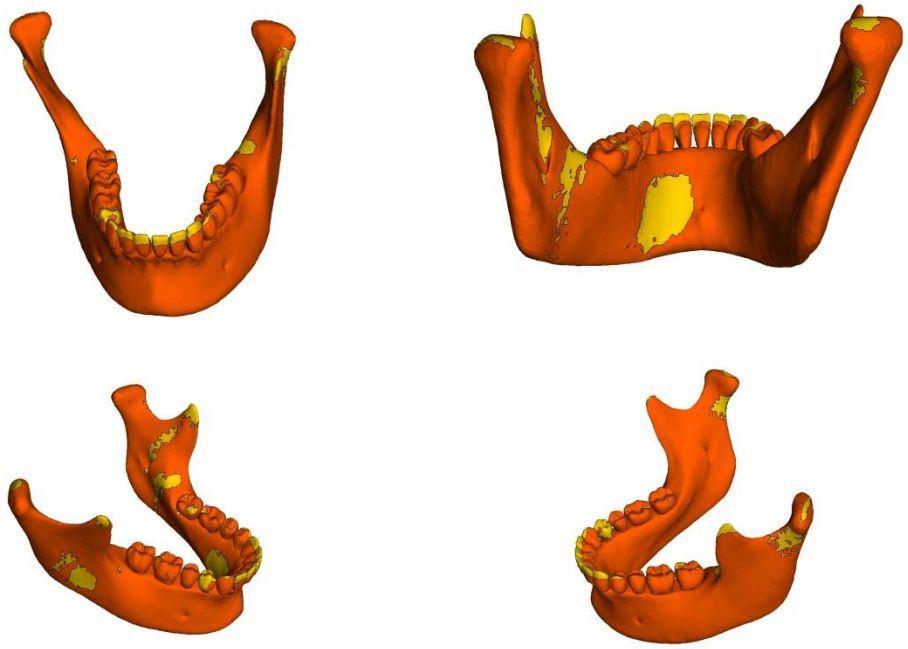

Figure 5.18 Mandibular map showing areas of tensile stress (red) and compressive (yellow) stress, following angle loading.

5.3.3.5 The ramus load

Loading the ramus of the mandible resulted in main peaks at nodes 2, 8 and 48. These were similar to those on loading the angle of the mandible. This would be expected as the ramus load was in approximately the same antero-posterior position as the angle but varied in the supero-inferior position. There was significant compressive strain in the parasymphyseal region lingually; the loading area, the condylar neck and the retromolar area on the contralateral side (see figure 5.20).

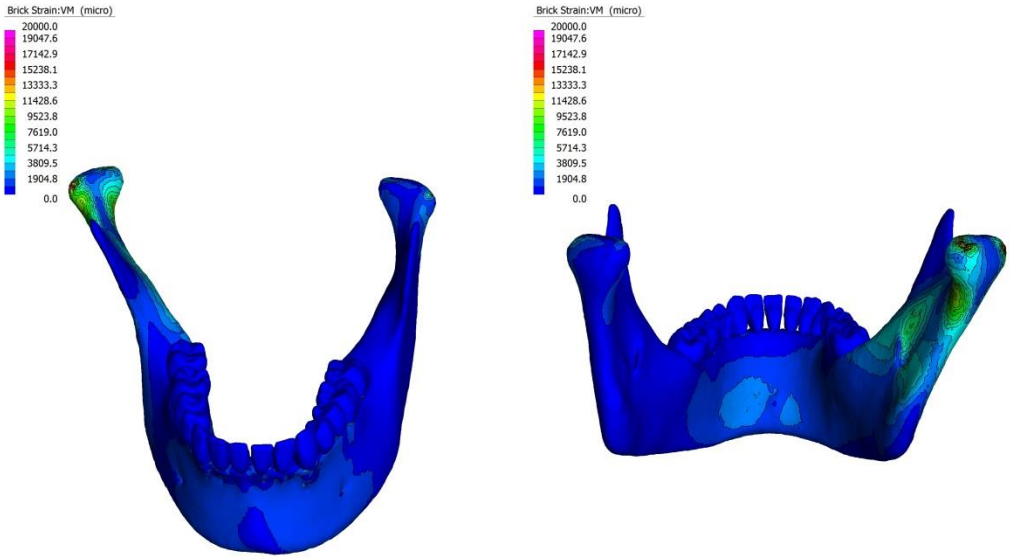

Figure 5.19 Colour contour maps of von Mises strain showing the buccal and lingual aspects of cortex of model 5. The global face load was 1000Pa along the y-axis of the local axis in the ramus region. Displacements are exaggerated by 10%.

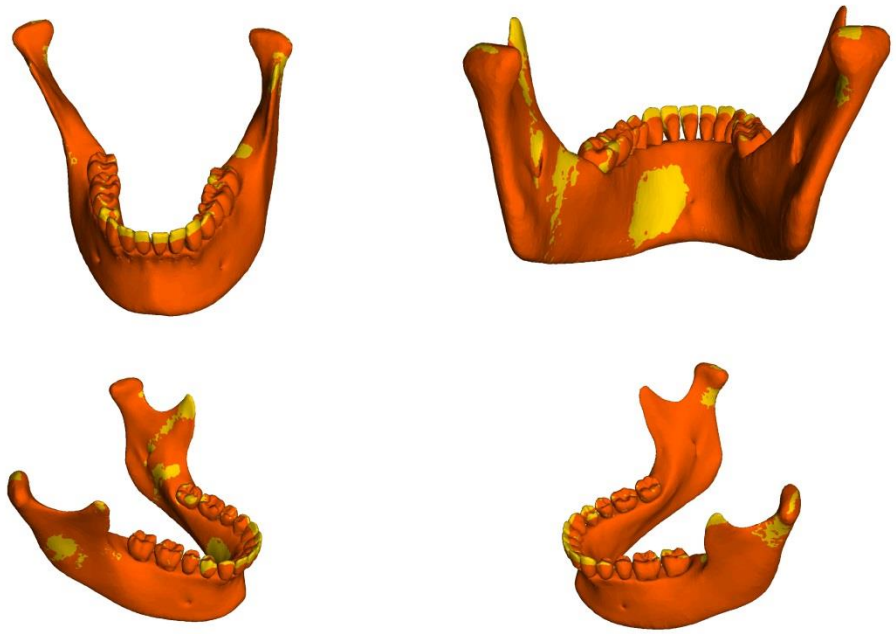

Figure 5.20 Mandibular map showing areas of tensile stress (red) and compressive (yellow) stress, following ramus loading..

The combined cortical signatures for the ramus, angle, body, parasymphysis and symphyseal loading are shown in graphs 5.9 and 5.10. As fractures are more likely to occur in an area of bone under tension rather than an area of compression, the lingual surface was of most interest. In general, as the load area moved from the anterior region (symphysis) to the posterior region (ramus) the stress on the condylar region reduced contralaterally. The ipsilateral parasymphyseal and body regions also experienced a reduction in stress. There was then a rise sharply at the angle and body.

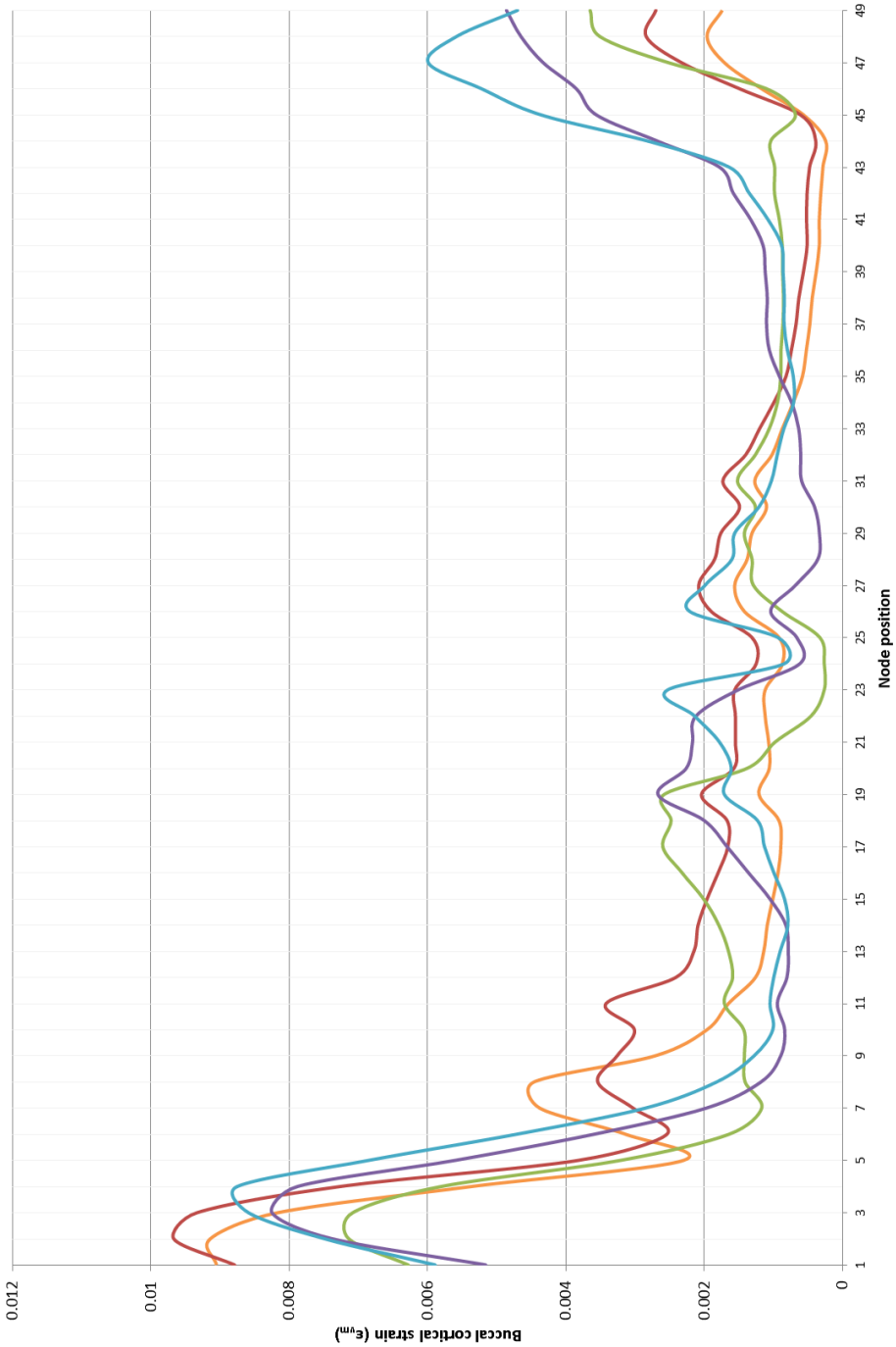

Graph 5.8 The effect of load position on buccal cortical strain (ε_{vm}). Buccal cortical strain (ε_{vm}) plotted against node position for an impact at 90o at different mandibular sub-sites

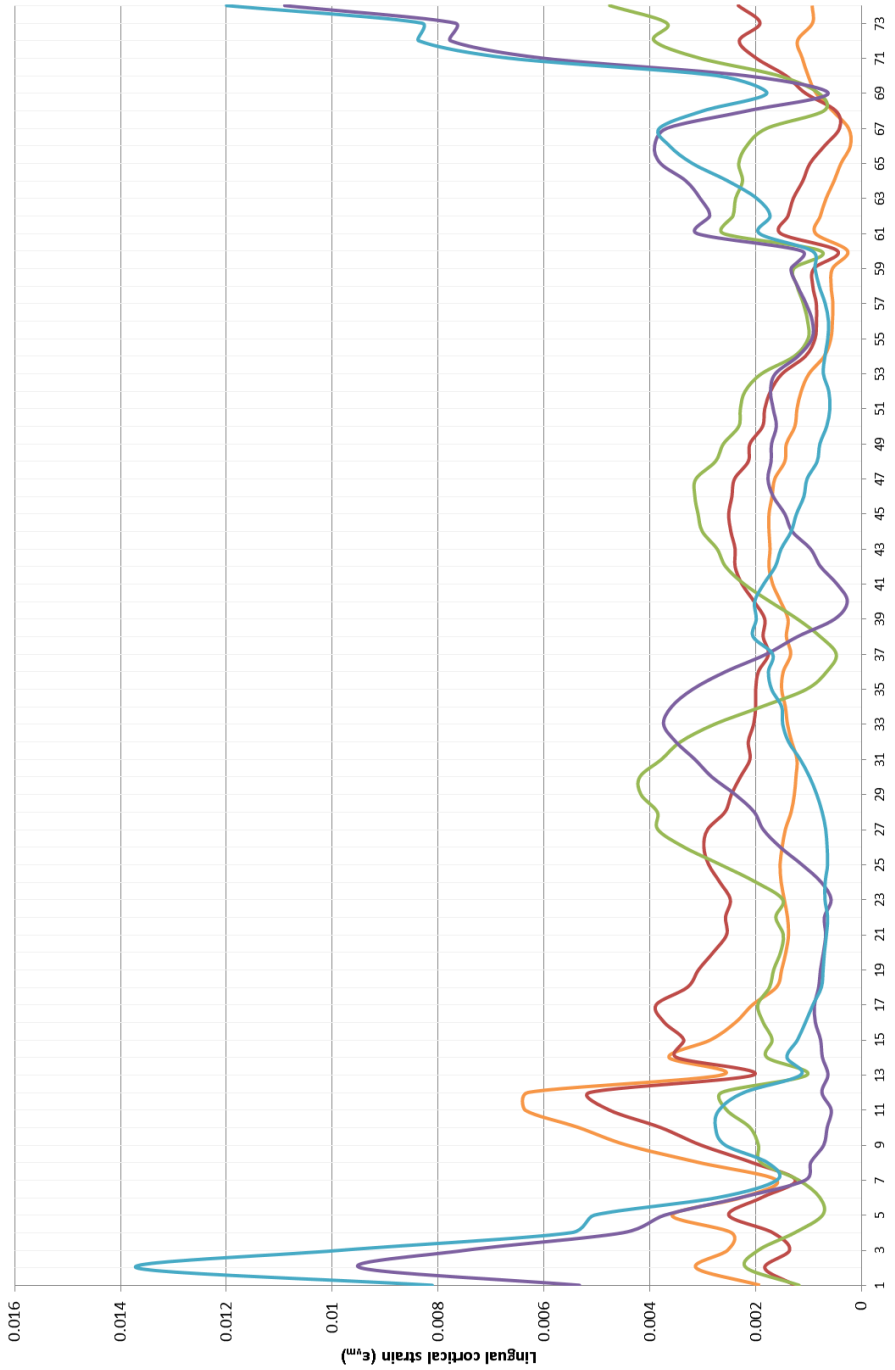

Graph 5.9 Graph of the effect of load position on lingual cortical strain (ε_{vm}). Lingual cortical strain (ε_{vm}) plotted against node position for an impact at 90° at different mandibular sub-sites.

Areas of increased stress are likely to be the site where fractures initiate. Whether they propagate cannot be determined from these analyses. Propagation may result in a fracture which eventually enters a different anatomical sub-site, resulting in it being classified as a fracture of the new sub-site. As such, the areas identified in these analyses may differ from clinical fracture patterns.

5.3.4 Results 4: The effect of load angulation on the mandibular cortex

5.3.4.1 Symphyseal loading

On symphyseal loading, the change in the angulation of the load resulted in a change in the magnitude of buccal strain. Peaks in strain at nodes 4, 47, 23 and 27 on the 90 degree buccal cortical signature were also present on the 135 degree and 45 degree signatures, however, the magnitude of the peaks changed (see graph 5.10). Loading at 45 degrees increased the strain on the left side of the mandible and diminished those on the right. Loading at 135 degrees had the opposite effect i.e. shifting the main loading peak to the right and diminishing strain values on the left.

Lingually, the effect of change in angulation on calculated strain was more significant, shifting the symphyseal peak of the lingual cortical signature to the right of the graph on loading at 45 degrees and to the left on loading at 135 degrees. Lingual symphyseal strain peaks were also increased in magnitude on angulation. Loading at 45 degrees increased the strain magnitude on the left and loading at 135 degrees increased it on the right. Strain in the condylar region was decreased at any angulation less than 90 degrees in the horizontal plane.

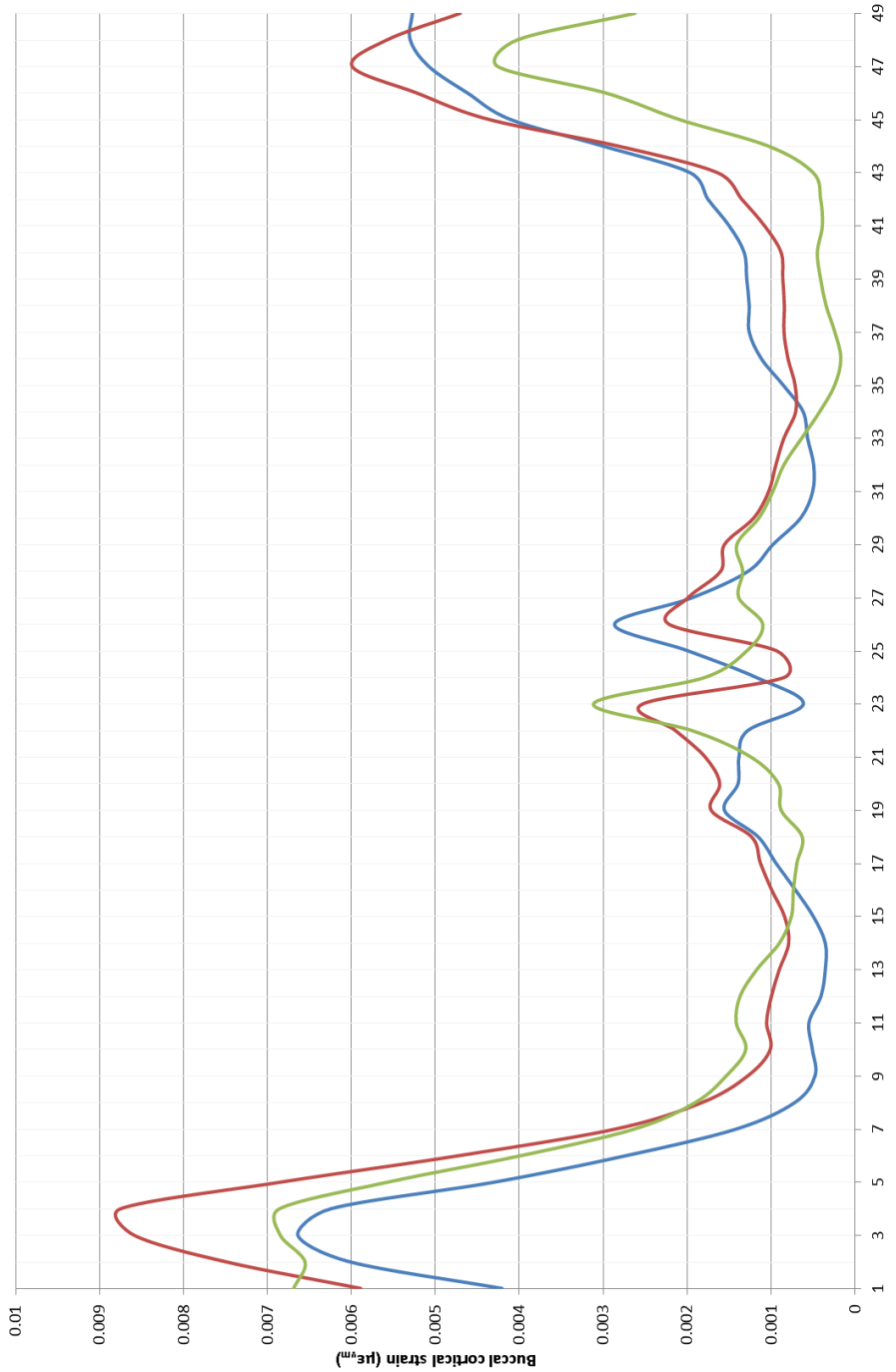

Graph 5.10 Graph showing buccal cortical strain ($\mu\varepsilon_{vm}$) plotted against node position for different impact angles at the symphysis of the mandible.

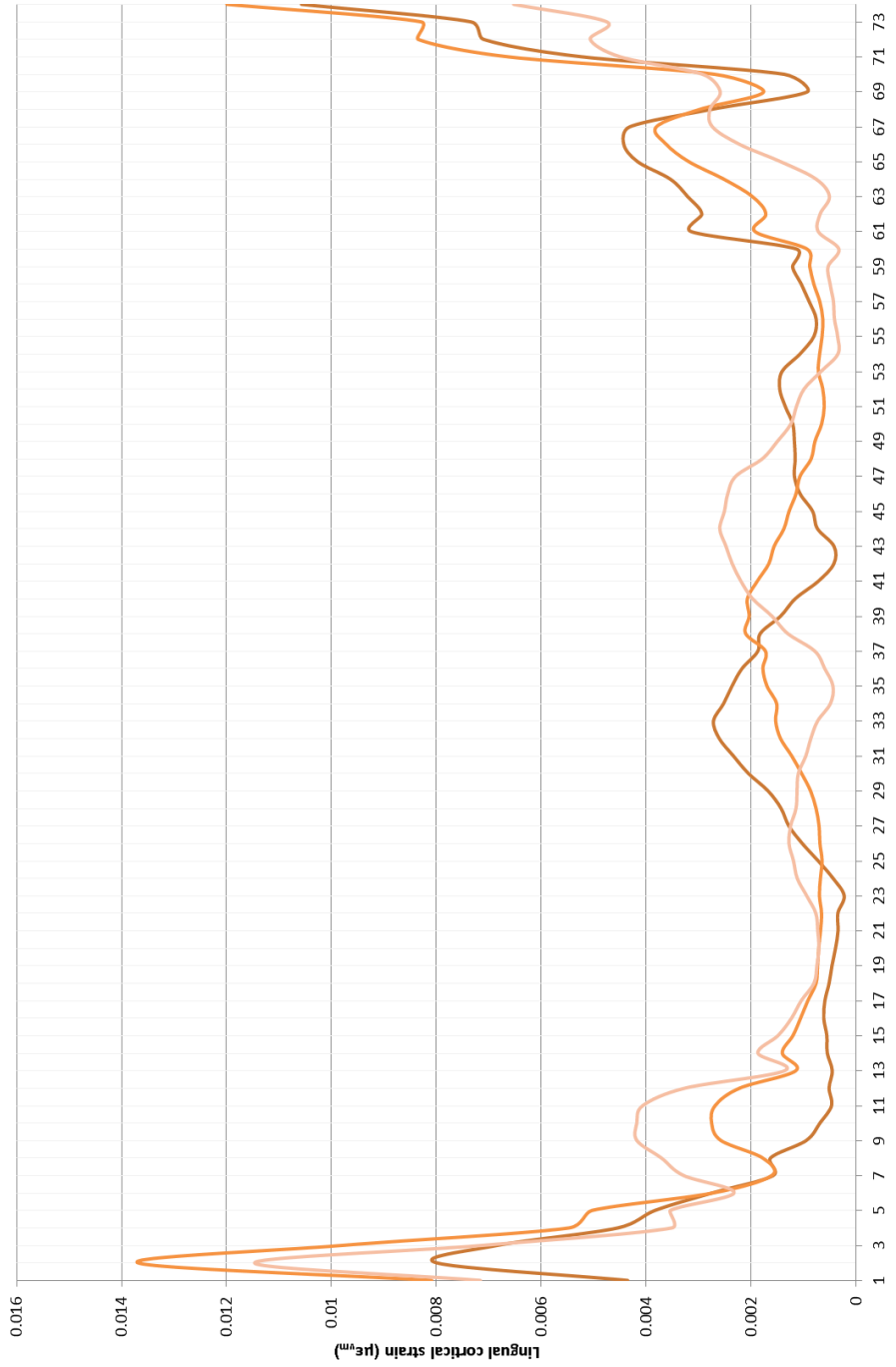

Graph 5.11 Graph showing lingual cortical strain ($\mu\varepsilon_{vm}$) plotted against node position for different impact angles at the symphysis of the mandible

5.3.4.2 Body loading

Graph 5.13 shows the variation in load angulation and cortical strain at various node positions following body loading of the buccal cortex. On the buccal aspect increasing the load angulation to 135 degrees increased the right condylar strain significantly. The strain at the buccal load site was also increased (by approximately 43% compared to 90 degree loading), although this was not as significant as in the condylar region. The strain in the left parasymphyseal region was minimally changed. On the lingual aspect peaks in strain remained in approximately the same position. With a load at 135 degrees the right lingual parasymphyseal remained at approximately the same magnitude, however, the left lingual parasymphyseal strain was reduced by approximately 50%. The reverse patten occurred on loading at 45 degrees.

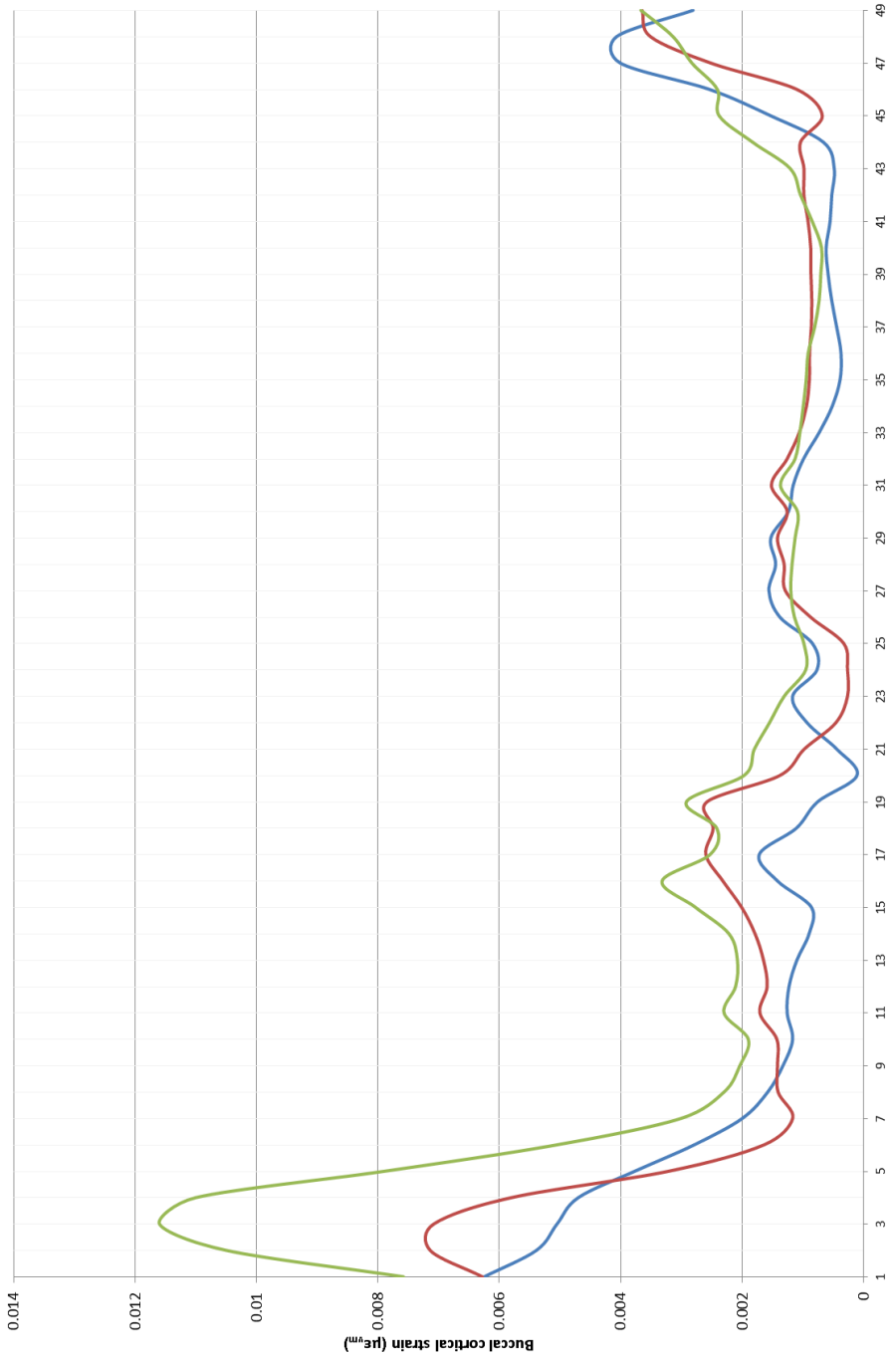

Graph 5.12 showing buccal cortical strain ($\mu\varepsilon_{um}$) plotted against node position for different impact angles at the body of the mandible. All loads are in the y-x (horizontal) plane.

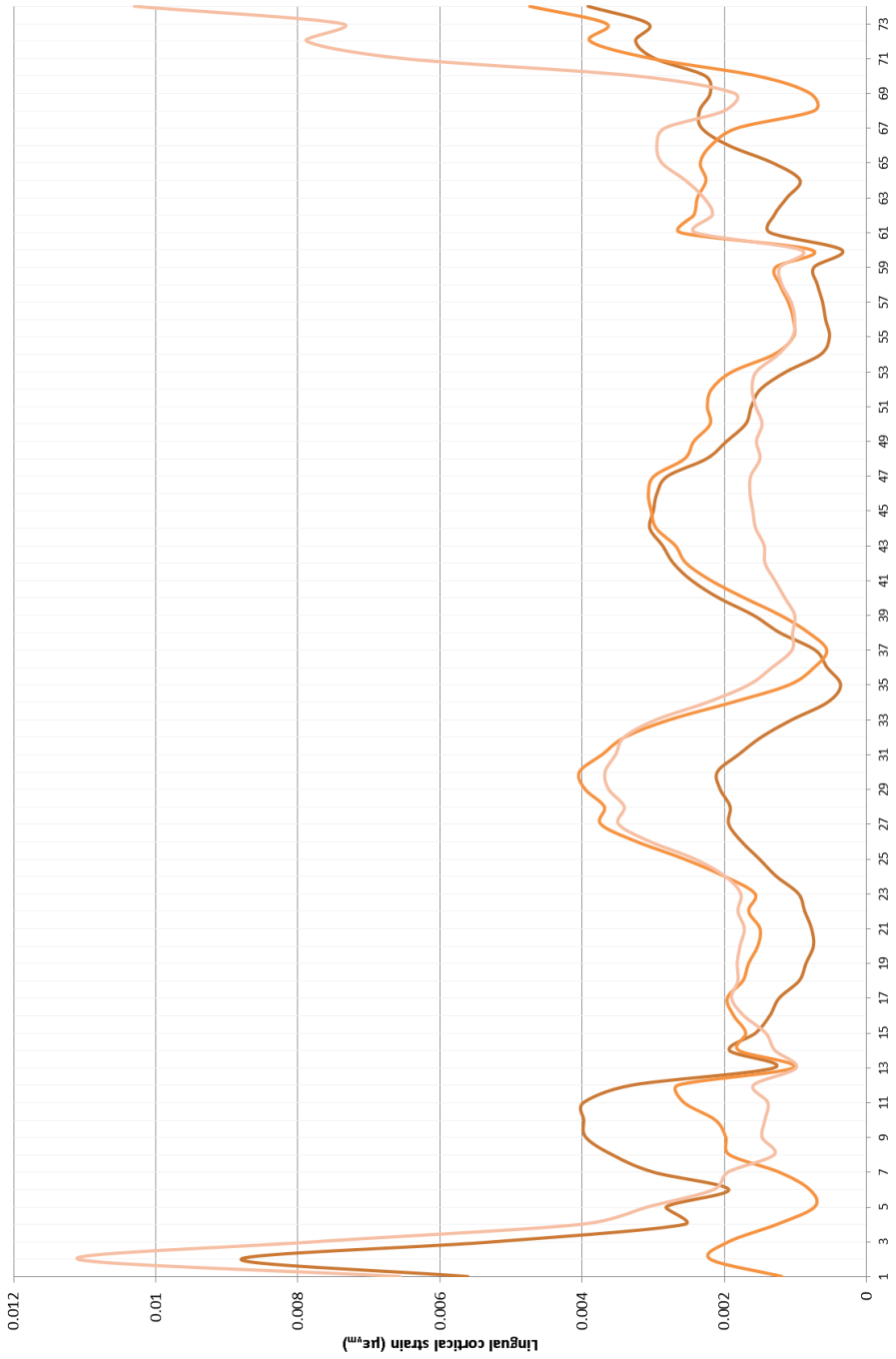

Graph 5.13 showing lingual cortical strain ($\mu\varepsilon_{vm}$) plotted against node position for different impact angles at the body of the mandible. All loads are in the y-x (horizontal) plane.

5.3.5 Results 5: The effect of material properties on stress in the loaded mandible

On loading it can be seen that despite the significant change in material properties, the cortical signatures of the two loading scenarios show significant similarity in form. The condylar peaks, (nodes 4 and 5 and 47) appear in the same position in graphs 5.14, 5.15 and 5.16 although the ratio of the maximal buccal condylar stress to maximal buccal symphyseal stress was greater for the steel model than the bone model. This may be explained by the fact that the steel model was modelled as a solid object with no cancellous bone substitute. The calculated correlation coefficient for the steel and bone in graphs 5.14 and 5.15 was 0.997 showing that the curves were strongly related.

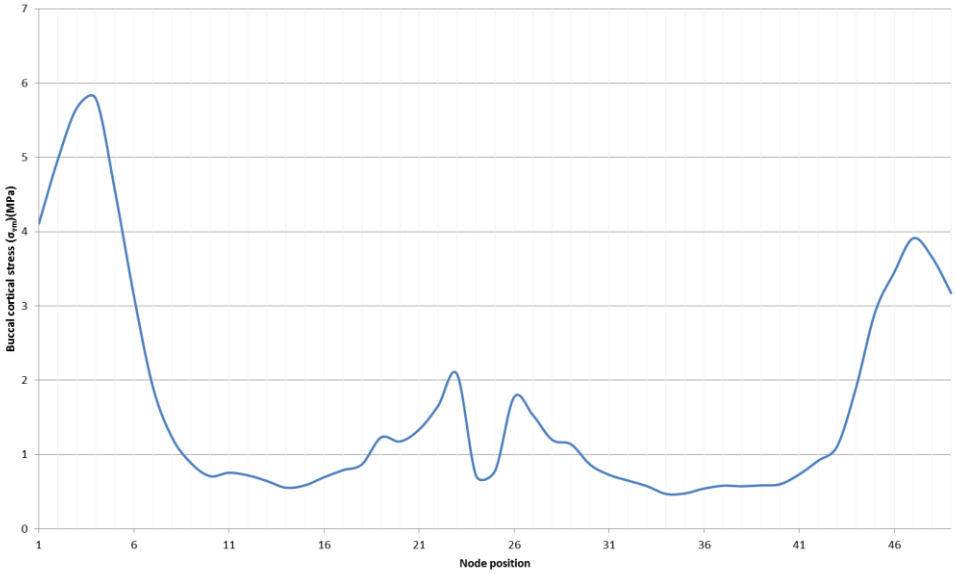

Graph 5.14 showing buccal cortical stress plotted against node position for a symphyseal impact on model 5. Material properties are those of normal cortical bone.

These results reinforce the findings of previous analyses that areas of mandibular susceptibility are predominantly determined by geometry rather than material properties, assuming that there is no significant local material property difference in the structure.

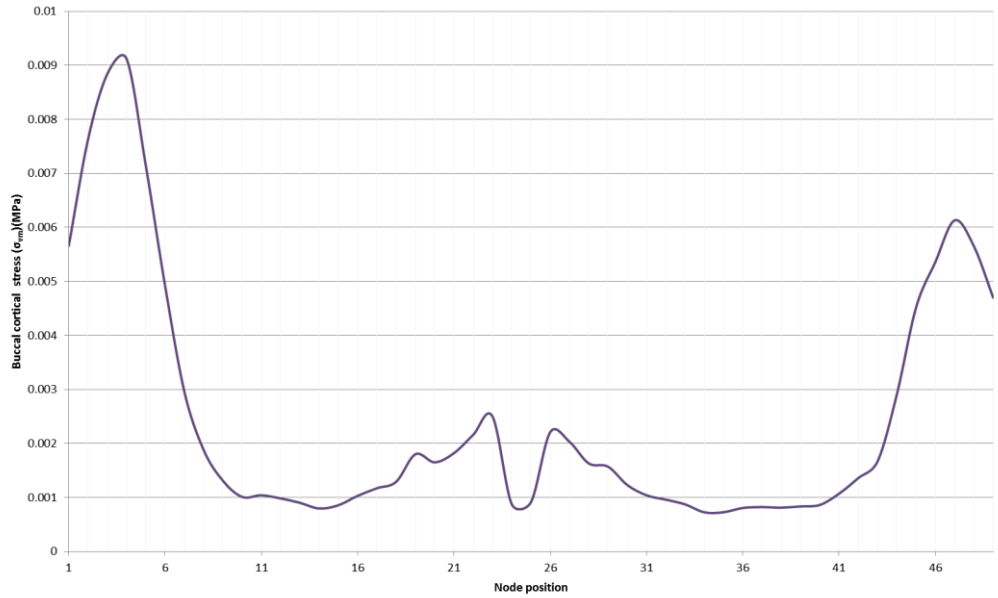

Graph 5.15 showing buccal cortical stress plotted against node position for a symphyseal impact on model 5. Material properties are those of a patient with osteogenesis imperfecta.

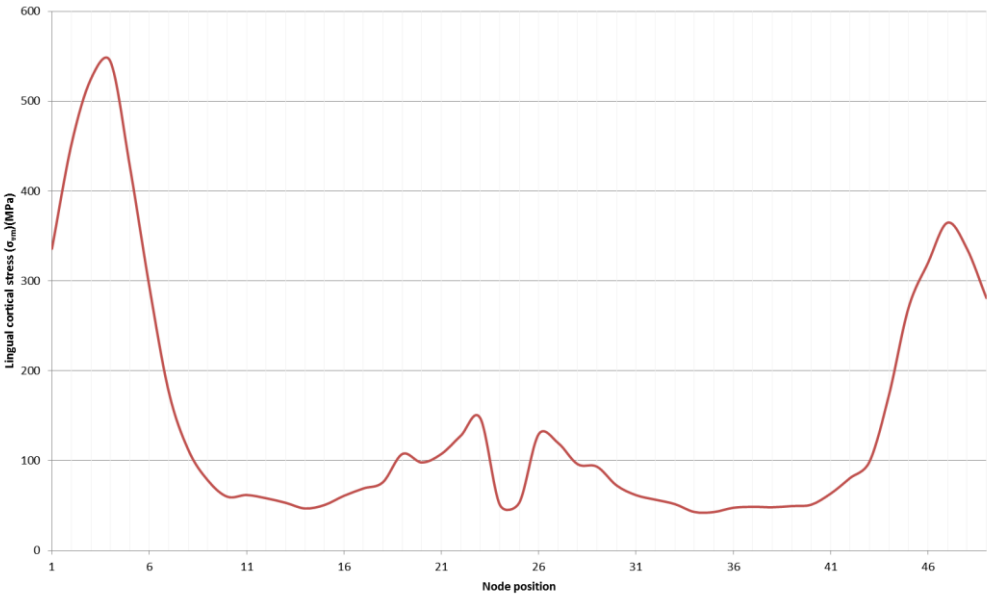

Graph 5.16 showing buccal cortical stress plotted against node position for a symphyseal impact on model 5. Material properties are those of steel.

5.4 Findings. Phase IIb: Static non-linear analyses

5.4.1 Results 6: Non-linear analysis with a physiological load

With the physiological load one would have expected the cortical strain signatures to be similar, and this was the case. However, there were differences in the magnitude of the peaks within each signature. The largest buccal peak in the linear analysis occurred at the right condyle on angle loading whereas this was only the third highest peak in the non-linear analysis. Body loading resulted in the lowest overall stress and strain magnitudes of all the cortical signatures.

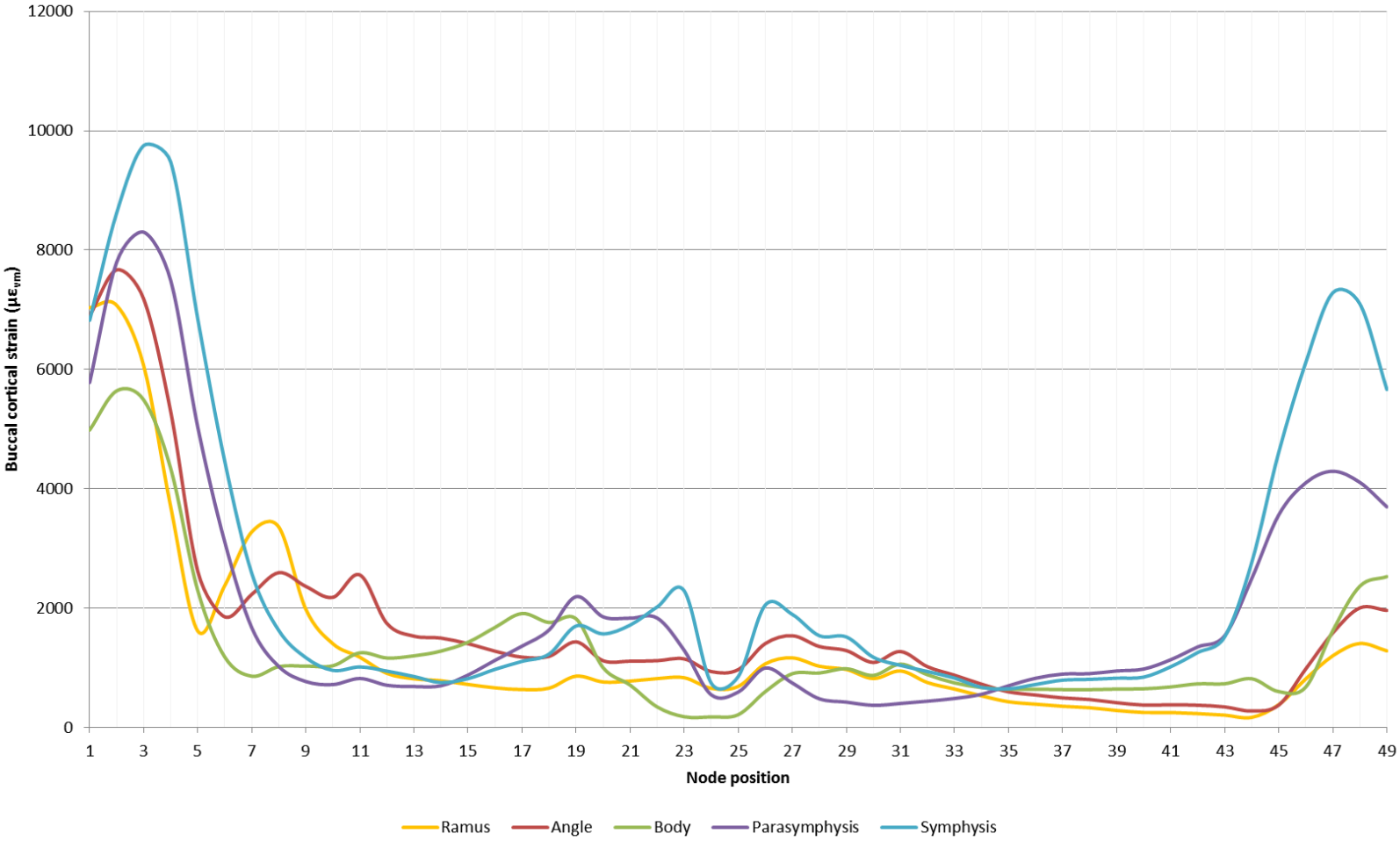

Graph 5.17 Graph of buccal cortical strain ($\mu\varepsilon_{vm}$) plotted against node position for a physiological load at 90^0 at different mandibular sub-sites. Strain at each position was indicated by node position.

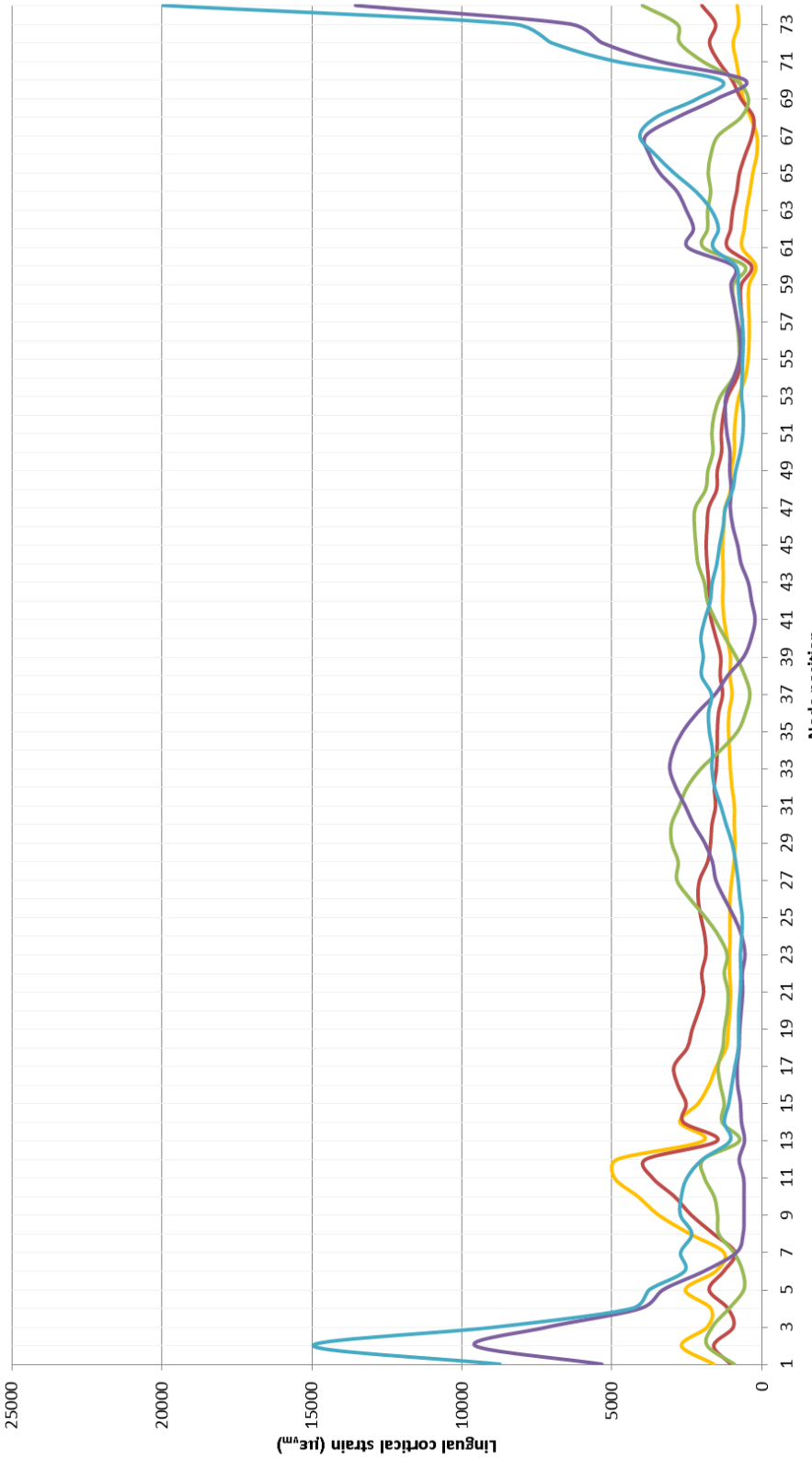

Graph 5.18 Lingual cortical strain ($\mu\varepsilon_{vm}$) plotted against node position for a physiological load at 90° at different mandibular sub-sites. Strain at each position was indicated by node position.

5.4.2 Results 7: Non-linear analysis with a failure load

5.4.2.1 Symphyseal loading

Symphyseal loading resulted in increased stress in three areas, the loading site, and the left and right condylar regions. The stress at the right condylar region was greater than the left. Examination of the cortical signature graphs (see graphs 5.19 and 5.20) showed similar patterns to the linear analyses, with increased stress and strain in the condylar and symphyseal regions on the buccal and lingual aspects. The magnitudes of stress and strain were obviously different due to the different load employed and the difference in material properties; however, they still mirrored each other with respect to regions of increased stress.

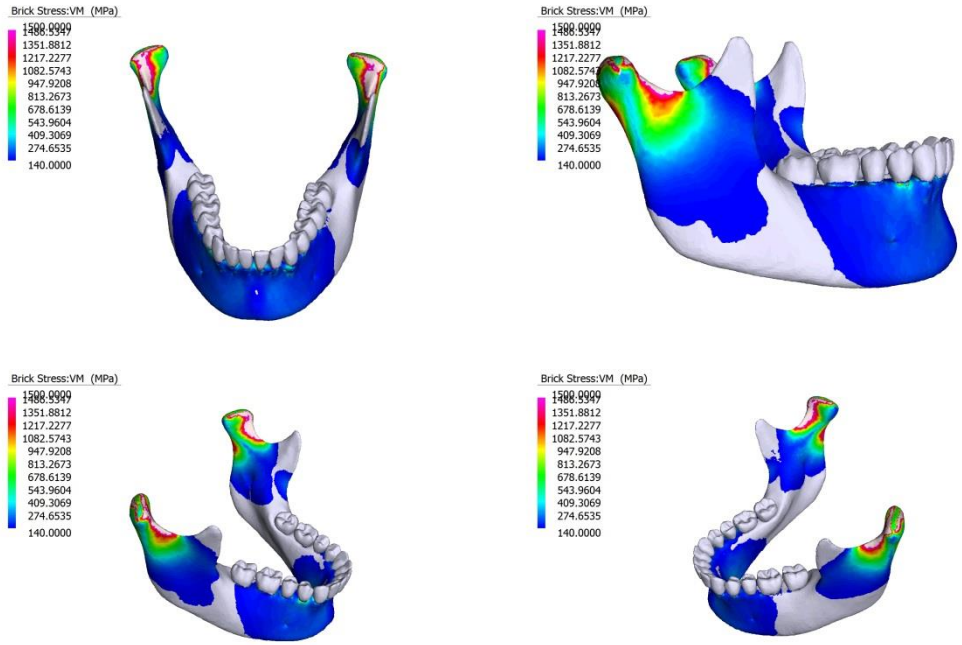

Figure 5.21 Stress colour contour map of the mandible in response to a failure load of 200MPa at the mandibular symphysis. Only elements that show stress greater than 140MPa are coloured (other than grey). High stress areas are in red.

5.4.2.2 Parasymphyseal loading

Parasymphyseal loading resulted in increased stress in three areas, namely the impact site and the left and right condylar regions. The stress at the left condylar region was greater than the right. There was no significant difference noted between the linear and non-linear sub-sites showing high stress on loading (see figure 5.22).

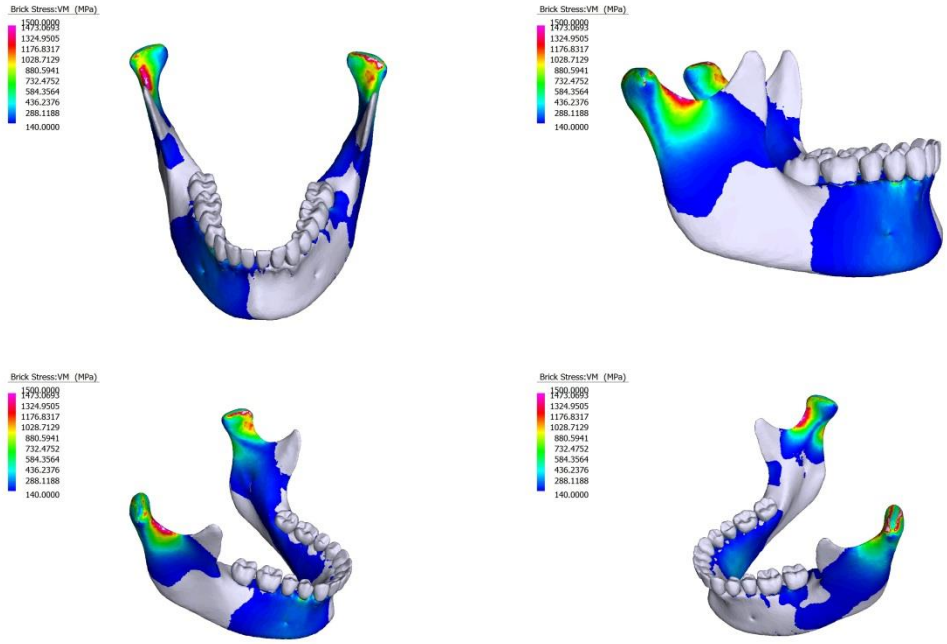

Figure 5.22 Stress colour contour map of the mandible in response to a failure load of 200MPa at the mandibular parasymphysis. Only elements that show stress greater than 140MPa are coloured (other than grey). High stress areas are in red.

5.4.2.3 Body loading

Body loading resulted in increased stress in four areas, namely the loading site, and the left and right condylar regions, with the stress at the right condylar region being greater than the left. There was also increased stress over a significant area at the ipsilateral parasymphyseal area (see figure 5.23).

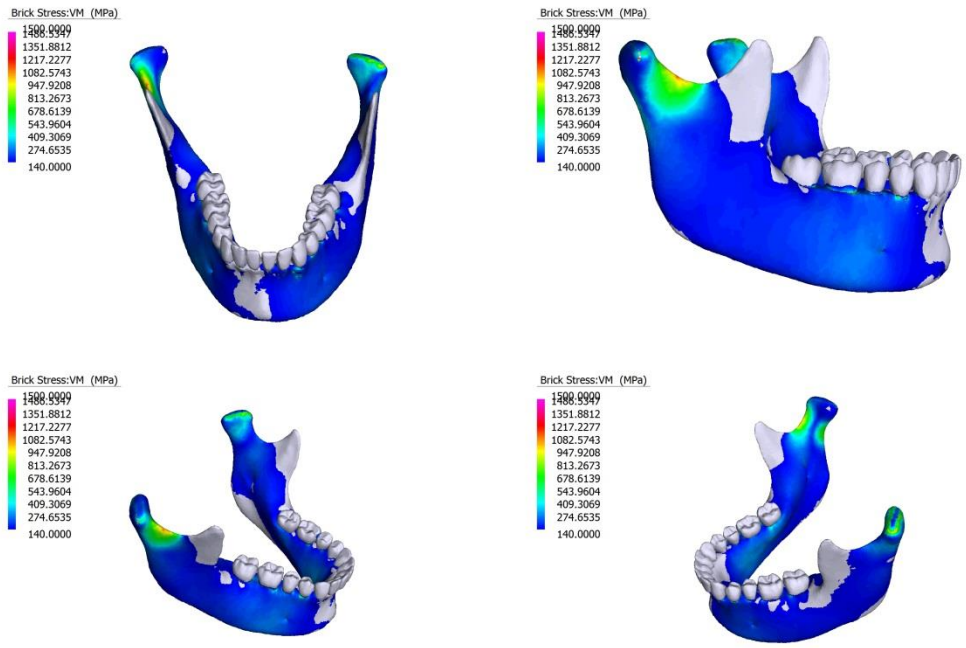

Figure 5.23 Stress colour contour map of the mandible in response to a failure load of 200MPa at the mandibular body. Only elements that show stress greater than 140MPa are coloured (other than grey). High stress areas are in red.

5.4.2.4 Ramus loading

Ramus loading resulted in increased stress in four areas, namely, the loading area, the left and right condylar regions, and increased stress over a significant area at the contralateral parasymphyseal area.

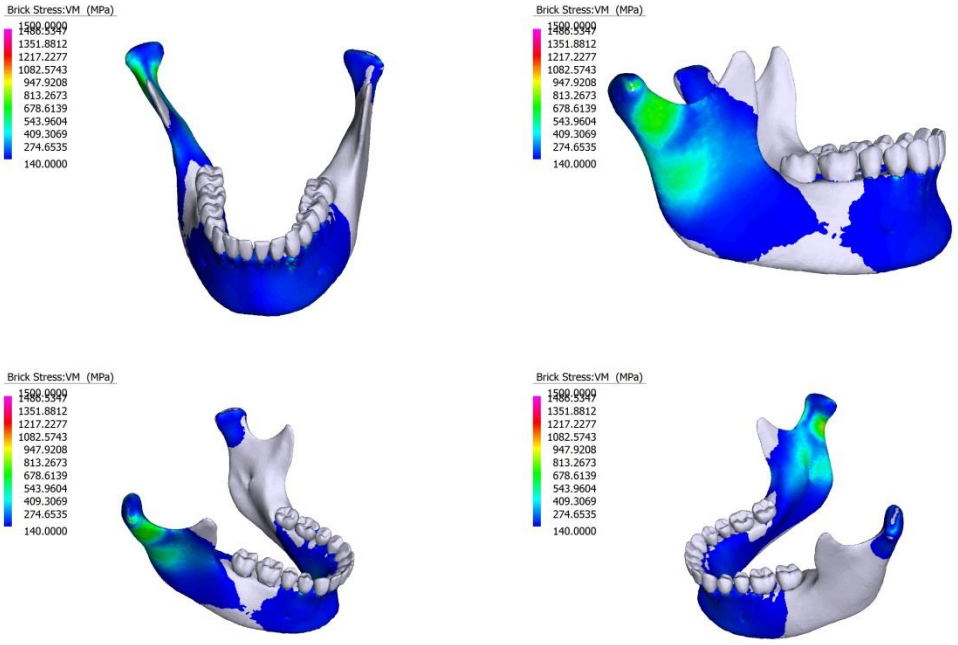

Figure 5.24 Stress colour contour map of the mandible in response to a failure load of 200MPa at the mandibular ramus. Only elements that show stress greater than 140MPa are coloured (other than grey). High stress areas are in red.

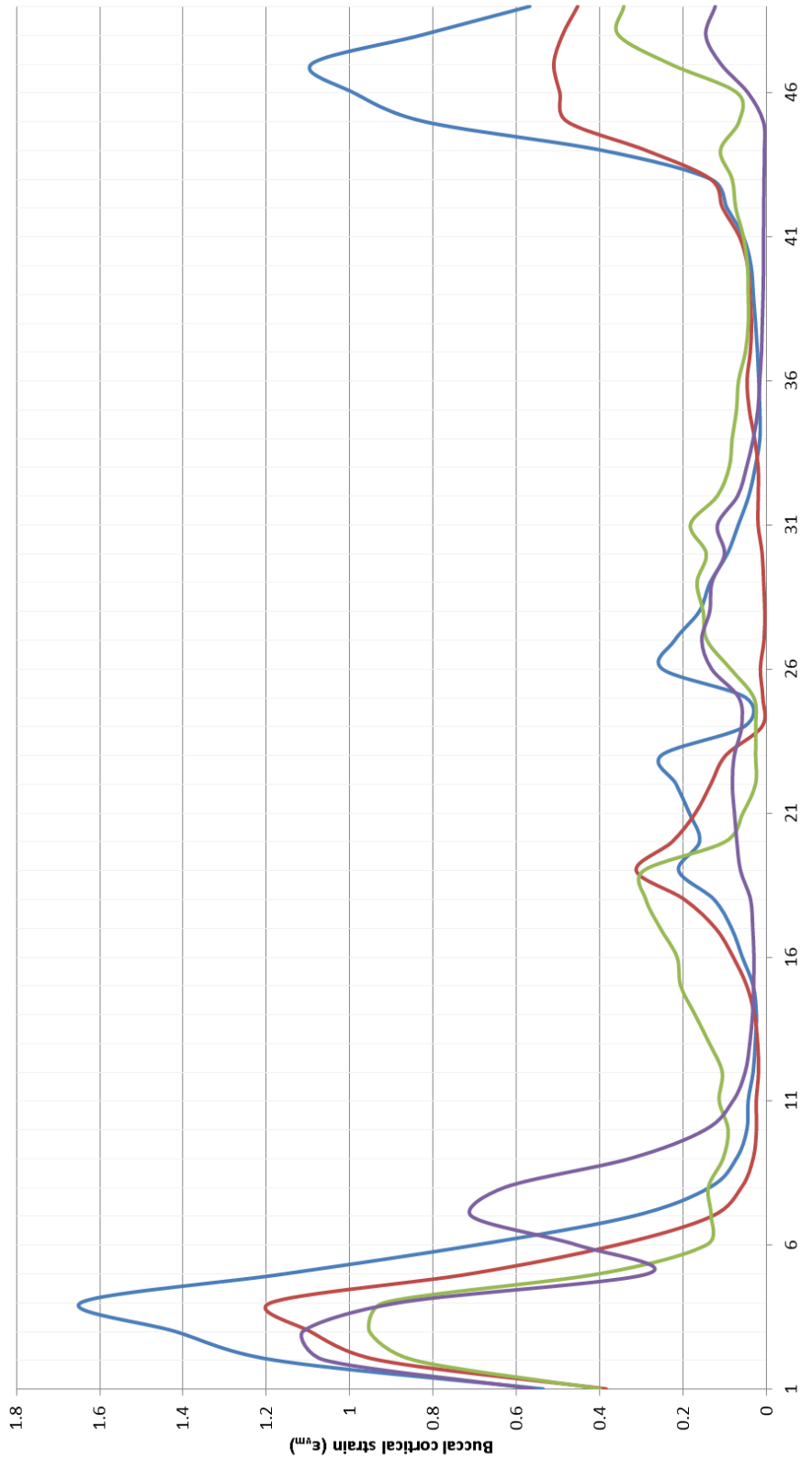

Graph 5.19 The combined buccal cortical strains (ε_{vm}) plotted against node position for failure loads (200MPa) at 90° to each mandibular sub-site.

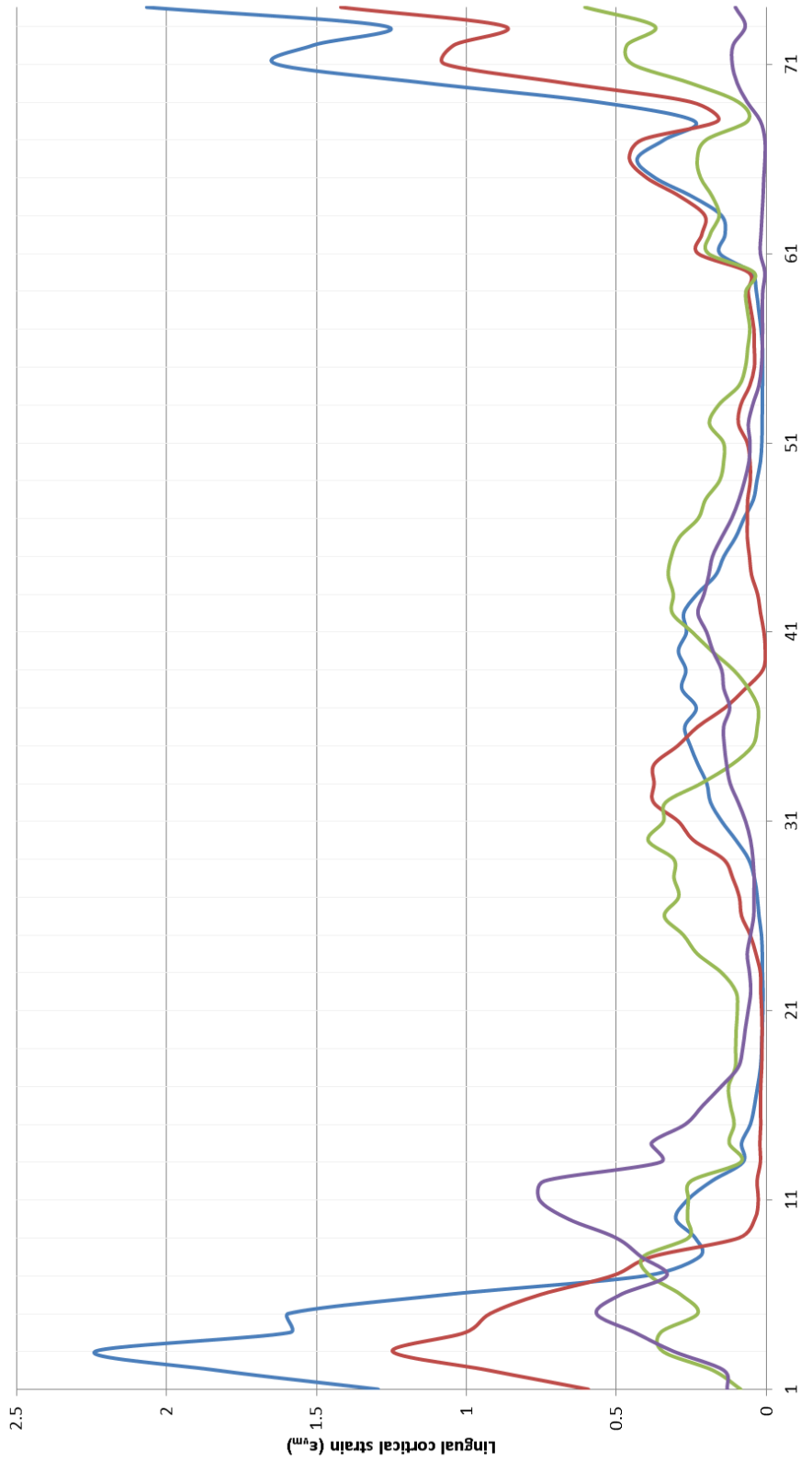

Graph 5.20 The combined lingual cortical strains (ε_{vm}) plotted against node position for failure loads (200MPa) at 90^0 to each mandibular sub-site.

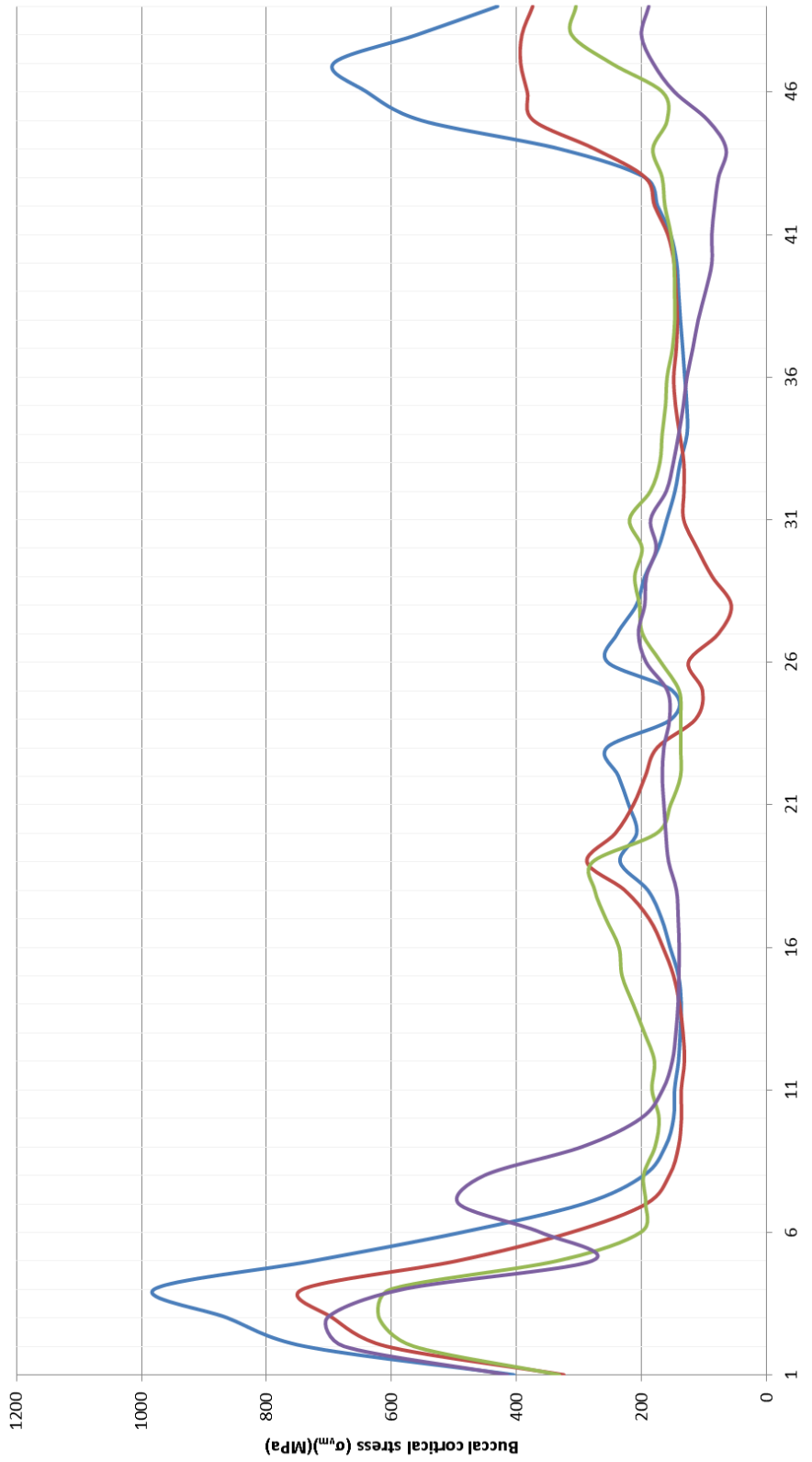

Graph 5.21 The combined buccal cortical stress (σ_{vm}) (MPa) plotted against node position for failure loads (200MPa) at 90° to each mandibular sub-site.

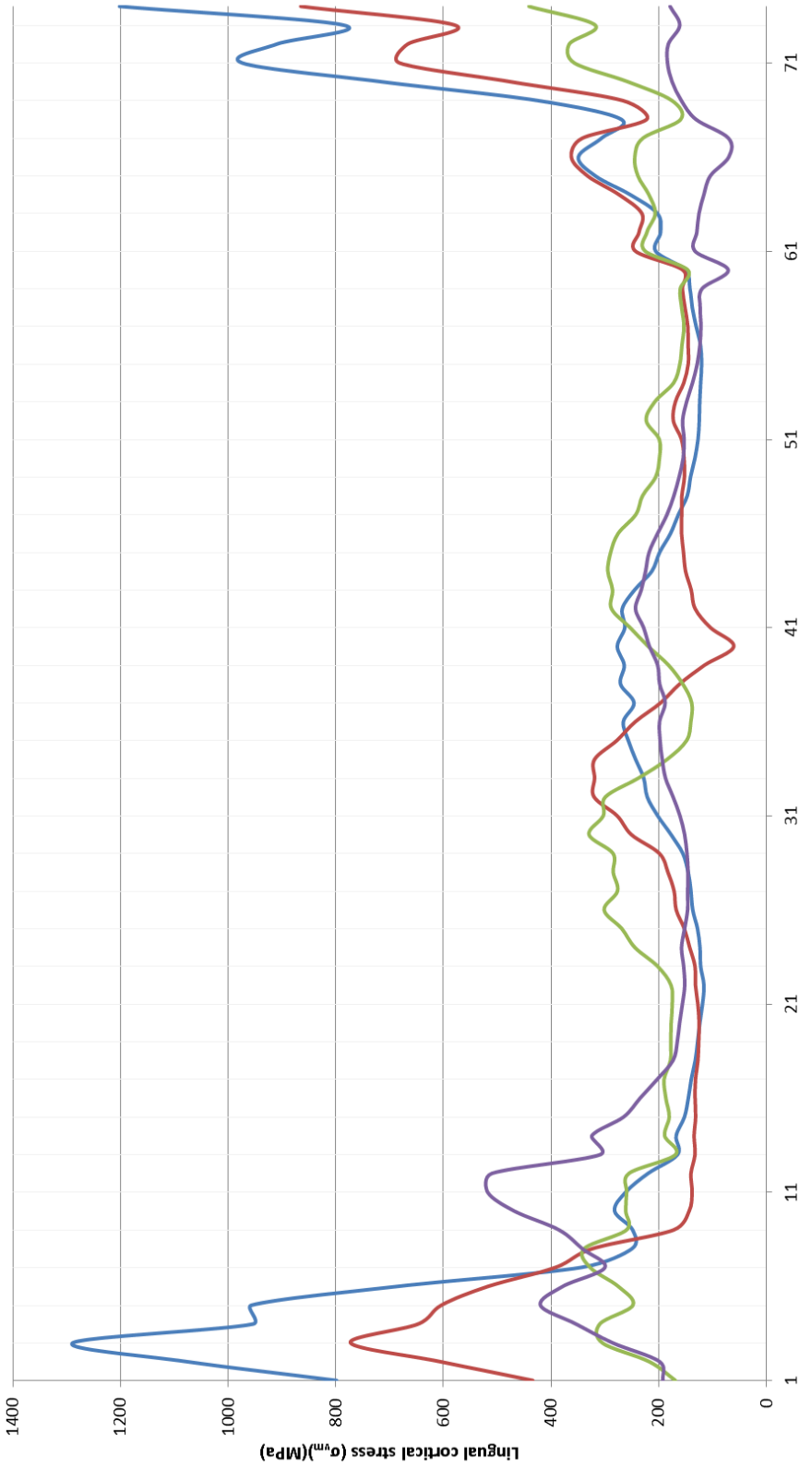

Graph 5.22 The combined lingual cortical stress (σ_{vm}) (MPa) plotted against node position for failure loads (200MPa) at 90° to each mandibular sub-site.

5.5 Phase II conclusions

A number of important conclusions may be drawn from the phase II results. The investigation of the effect of the muscles of mastication on the cortical stress and strain suggests that muscular contraction plays a minimal part in mandibular deformation or initiation of fractures. As movers of the mandible, this is clearly the most desirable outcome. The unusual muscular contraction pattern modelled in these investigations (i.e. bilateral synchronous contraction of all muscles groups) would likely represent a greater net contractile force (in the form of mandibular elevation) than would be encountered in the normal situation. As direct muscular contraction is unlikely to provide sufficient force to fracture the mandible, therefore, in a fracture scenario muscular contraction need not be modelled for direct impacts. In clinical situations where the mandible has been fractured during an epileptic seizure (Costa et al. 2011; Aragon and Burneo, 2007; Nakken and Lossius, 1993) it is rarely the direct effect of muscular contraction that caused the fracture. The most likely cause is the indirect effect of the maxillary teeth, objects within the oral cavity or direct trauma from an external force resulting in areas of localized high stress in. In rare cases, where muscle is inserted into a very small cross-sectional area, such as the coronoid process, very high stresses may cause avulsion fractures.

Tooth loss does not significantly waeken the mandible when the mandibular height is not significantly reduced. There was minimal effect on the cortical signature at the sampled level. This should be true as long as the alveolar sockets themselves were modelled and the teeth were not loaded. Smith, (1983) suggested that failure to incorporate, or account for teeth and the associated periodontal ligament in primate models could lead to significant errors in stress and strain distributions throughout the model. Whilst some researchers have included the periodontal ligament in craniofacial

finite element studies (Gröning, et al., 2011; Kupczik, et al., 2007; Panagiotopoulou, et al., 2011) many studies have not done so due to either difficulty in obtaining scan data of sufficient resolution or due to the very large increase in element resolution required to accurately model the ligament. As it was not the purpose of the analyses to understand the stress and strain patterns in the alveolar process, accurate modelling of the tooth and periodontal ligament was deemed unnecessary. Rigidly linked teeth were used in the analyses, resulting in over-stiffening of the alveolus (Daegling, et al., 2008). However, as may be concluded from the comparison with the edentulous mandible, the difference between a rigidly linked tooth and an absent tooth on the alveolar crest was minimal when the mandibular cortex was loaded directly in the horizontal plane. This is consistent with findings obtained by Wood, et al. (2011) who performed finite element modelling analyses. Panagiotopoulou, et al. (2011) combined their computational analyses with ex-vivo bending tests and measured strain using digital speckled pattern interferometry on models of primate jaws, and found that the differences in modelling the periodontal ligament and modelling the teeth continuously with the bone were minimal. The effect on the global stress and strain patterns across mandibular cortex can therefore be considered minimal in relation to deformation. The results presented here are inconsistent with the results of Gröning, et al. (2011) who examined the effect of the periodontal ligament on the stiffness of the mandible and found significant differences in the magnitude of stress and strain over mandibular body depending on when the ligament was either present or absent. The effect of rigidly linked teeth (as in this study) must therefore only be local. This would be in agreement with the work of Marinescu, et al. (2005) and Grosse, et al. (2012) who hypothesized that the contradictory findings of Gröning, et al. (2011) and Panagiotopoulou, et al. (2011) might be explained by ‘the size of the tooth roots relative the height of the mandible could make [the] effect significant on a global level.’ The clinical relevance of these finding is

that the extraction of teeth should not make the mandible significantly weaker or more prone to fracture than normal as long as the alveolar height remains the same i.e. in the immediate post-extraction phase. Of course, the natural response of the body is resorption of bone in areas that are not under load and therefore in time the mandible will become increasingly prone to fracture in this area.

As far as predicting fracture, sub-sites are concerned; the sites of high stress and strain identified on static analysis do not necessarily identify the whole fracture area, only areas where fractures could initiate. A fracture line starting in one sub-site may travel in to another.

The results of the loading analyses lead to important conclusions. Each loading site resulted in a unique cortical signature. From this it was possible to identify sites prone to fracture. Unfortunately, due to the limitations of static analyses it was not possible to identify more than primary fracture initiation site i.e. the site with the highest stress under load. Static analyses rely on the assumption that the load path remains constant throughout the analysis. This would not be the case once the load had caused the mandible to fail. Therefore, other high stress sites present on static analysis may not exist dynamically.

In the normal anatomical condition, an articular disc lies between the mandibular condyle and the glenoid fossa, reducing the stress at the condylar head. The maxillary teeth limit the rotation and superior displacement of the mandible. The condylar restraints will have artificially increased the stress at the condylar heads on loading, however, according to St. Venant's principle this should have little influence on stress at the condylar neck. The analyses suggest that condylar fractures are most likely on anterior impact, whereas lateral impacts, cause significant strain in the contralateral parasymphyseal region and ipsilateral condylar neck.

Impact angulation did not change the fracture prone areas of the mandible significantly, however, the magnitude of stress at each weak area varied, again suggesting that a static analysis is sufficient to determine potentially weak areas but insufficient to determine fracture pattern.

The final conclusion in this section relates to the effect of generalized material properties on the weak areas of the mandible. The results show that even when the material properties were varied widely the areas of high stress remained identical when load sites remained the same. The magnitude of the stress varied according to the material suggesting that fractures would be initiated at differing levels of force. Clinically one would not expect an osteoporotic mandible to fracture at different sites unless there was a change in the geometry.

The findings of phase II are summarized below.

a. The effect of the muscles of mastication in vivo may not be as pronounced as the model suggested as the synchronous muscle group recruitment was employed was non-physiological.
b. The cortical stress and strain effects of the muscles of mastication were found to be minimal when compared to the magnitudes required to cause bony fracture, therefore muscular contraction is unlikely to be a major cause of mandibular fracture in the normal mandible.
c. The muscles of mastication may reasonable be excluded from future analyses which aim at determining the site of fracture initiation. Their role is more likely to be in fracture displacement.
d. The removal of the teeth from the finite element model had minimal effect on the buccal and lingual cortical signatures in the sample zone therefore it is reasonable to remove the teeth from the model in future analyses in involving

direct bone loading. The clinical relevance of this is that the mandible is unlikely to be significantly weakened in the immediate post-extraction state.

e. The full cortical response is unique for each load. The signatures within the sample zone differed enough to enable identification of the load position in the horizontal plane. Load angulation appeared to primarily change the magnitude of the stress response rather than significantly changing the pattern.

f. The gross geometry of the mandible appeared to be the main determinant of the pattern of cortical stress and strain, whereas the effect of generalized material properties was minimal.

g. The cortical signatures for the static non-linear and linear analyses did differ in magnitude from each other; however, this did not seem to translate into a significant difference in the disposition of areas of high stress or strain. The effect of material non-linearity, however, may have been hampered by the use of static analyses.

5.6 Findings. Phase IIIa: Basic dynamic non-linear analyses

5.6.1 Results 8: The relationship of impact site with fracture distribution

High kinetic-energy impacts were modelled at three sites, the ramus, parasymphysis and symphysis. The impact simulation at 1ms is shown in figure 5.25 first, followed by graphical examination of lingual cortical stress and strain energy density.

5.6.1.1 Impact at ramus (Element deletion algorithm).

Impact with high kinetic energy fist

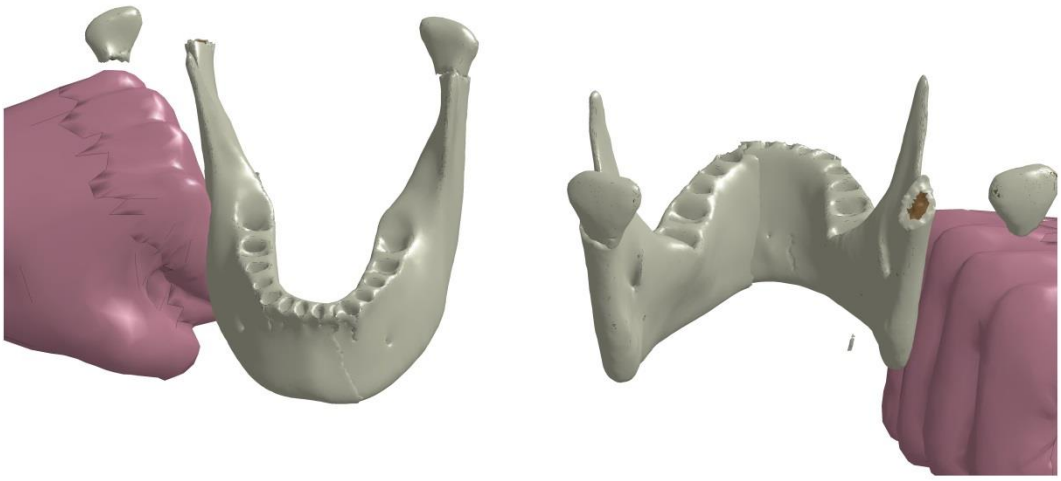

Figure 5.25 The figure shows the results of the computer simulation of a high kinetic energy punch to the right mandibular ramus. An element deletion algorithm was used to simulate the fracture. The impact time was 1ms.

Figure 5.25 shows that the analysis predicted fractures at both condylar necks. The right condylar neck was significantly displaced, whereas the left condylar head was minimally displaced. The reduction in inter-condylar distance (as measured between the necks of the condyle) resulted in an increase in stress and strain at the left parasymphysis. Eventually failure occurred resulting in a third predicted fracture. A small breach of the

lingual cortex was also visible at the left parasymphysis. This did not extend to the buccal cortex.

Graph 5.24 confirms the pictorial impression. Stress was raised rapidly in the nodes sampled at the right condylar neck. There was an associated slow rise in the left parasymphyseal region. The right condylar neck was predicted to fracture at approximately 0.16ms. The calculated nodal stress did not return to zero as values from adjacent elements were included. Later, at about approximately 0.49ms, the stress in the right parasymphysis dropped rapidly as the associated element was deleted. The final fracture occurred at 0.62ms in the left condylar neck. The change in strain energy density mirrored the change in von Mises stress.

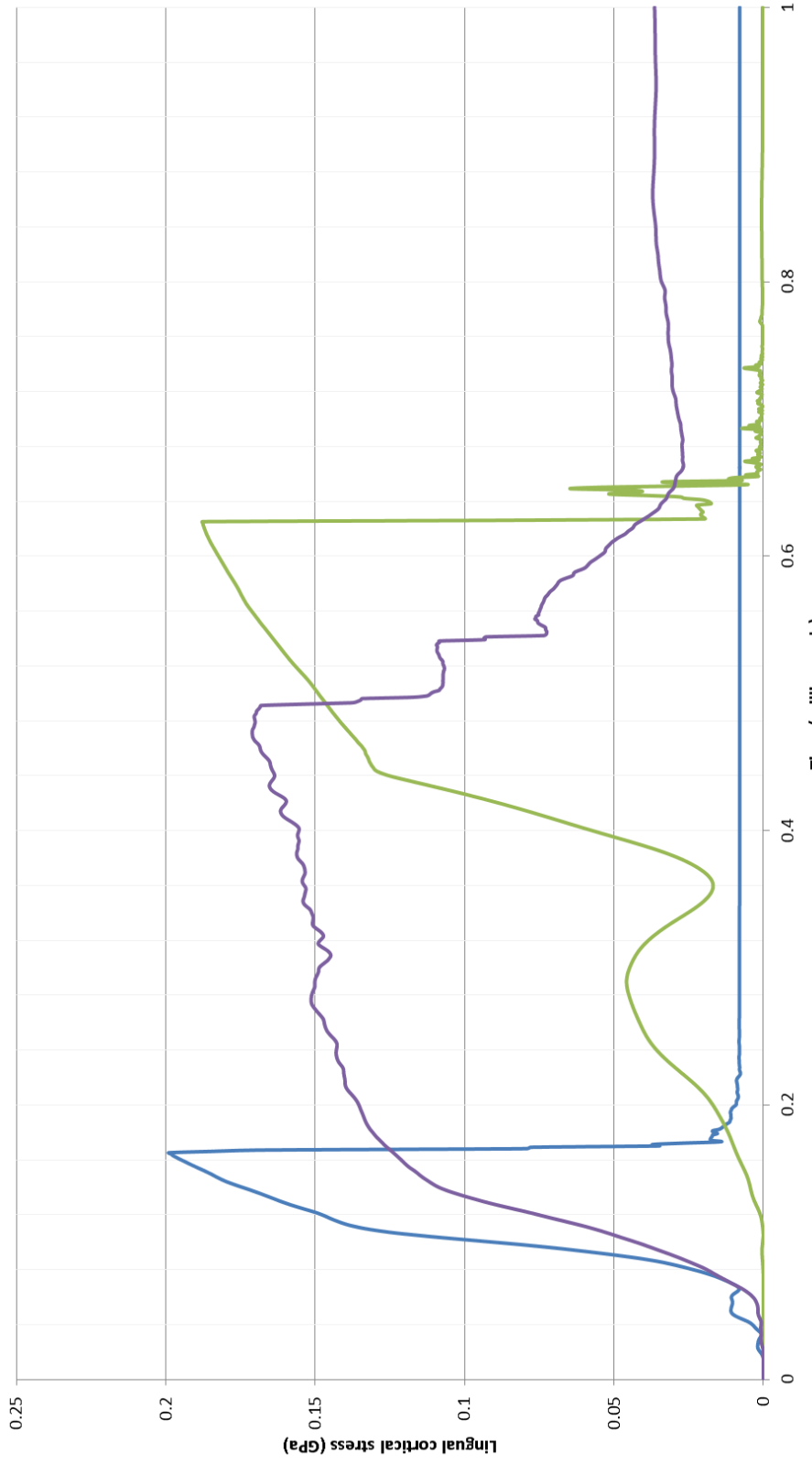

Graph 5.23 The variation of lingual cortical stress (σ_{vm}) with time for the first deleted node at each mandibular sub-site (one at the right condylar neck and one at the left parasymphysis) following impact at the right ramus of the mandible.

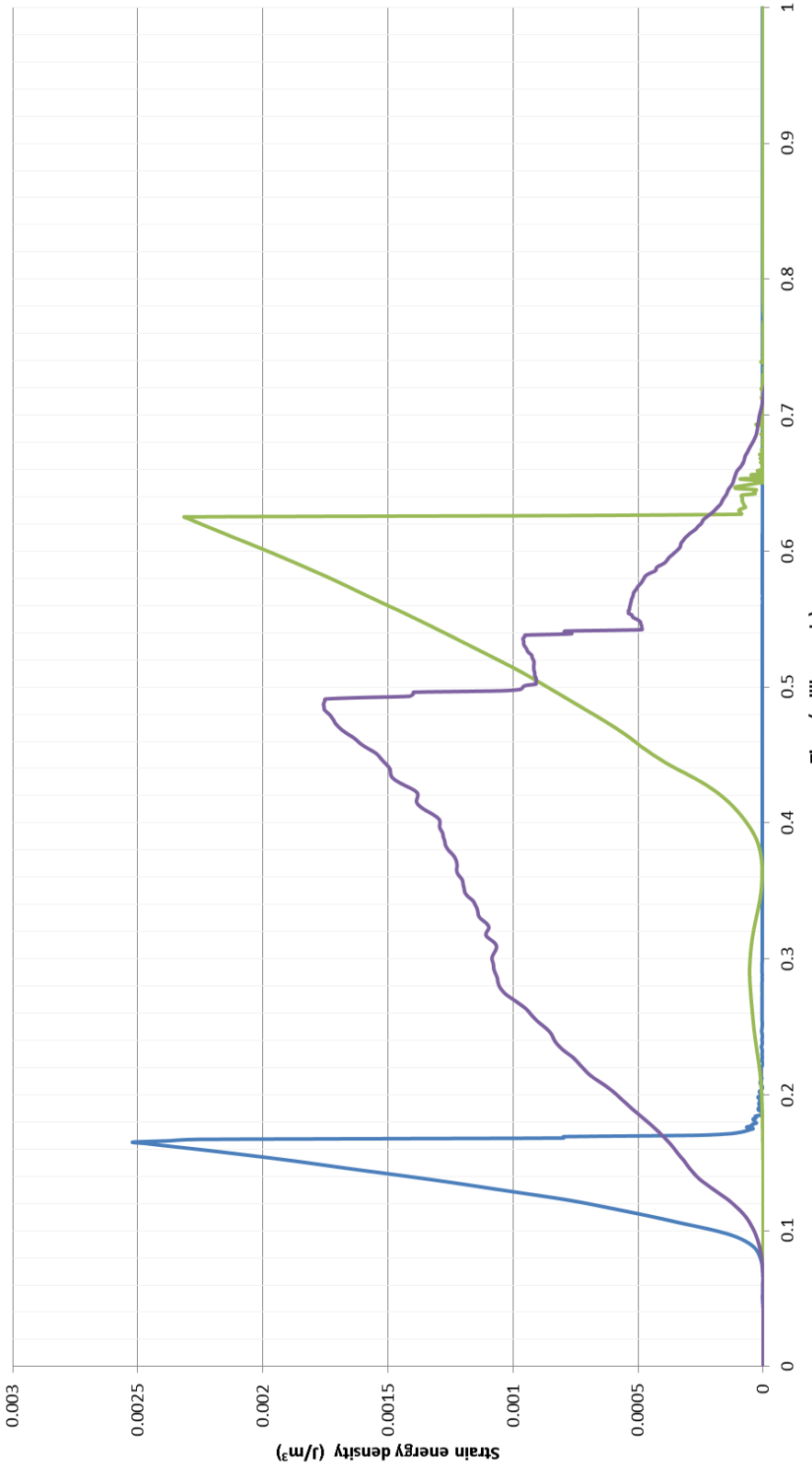

Graph 5.24 The variation of strain energy density with time for the first deleted node at each mandibular sub-site (one at the right condylar neck and one at the left parasymphysis) following impact at the right ramus of the mandible

5.6.1.2 Impact at parasymphysis (Element deletion algorithm)

Impact with high kinetic energy fist

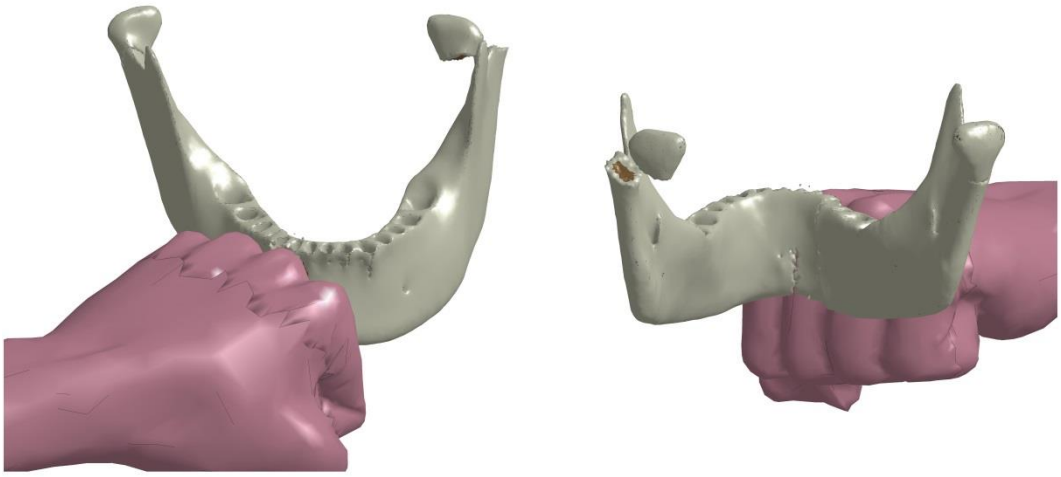

Figure 5.26 The figure shows the result of the computer simulation of a high energy punch to the right mandibular parasymphysis. An element deletion algorithm was used to simulate the fracture. The impact time was 1ms.

Figure 5.26 shows the computer prediction following a modelled impact at the right parasymphyseal region. Fractures were predicted at the impact site with a minimally displaced right condylar neck fracture and a significantly displaced left condylar neck fracture. The fractures of the left and right mandibular condyles and the impact zone occurred at 0.39ms, 0.68ms and 0.56ms respectively. Again the change strain energy density mirrored the change in von Mises stress.

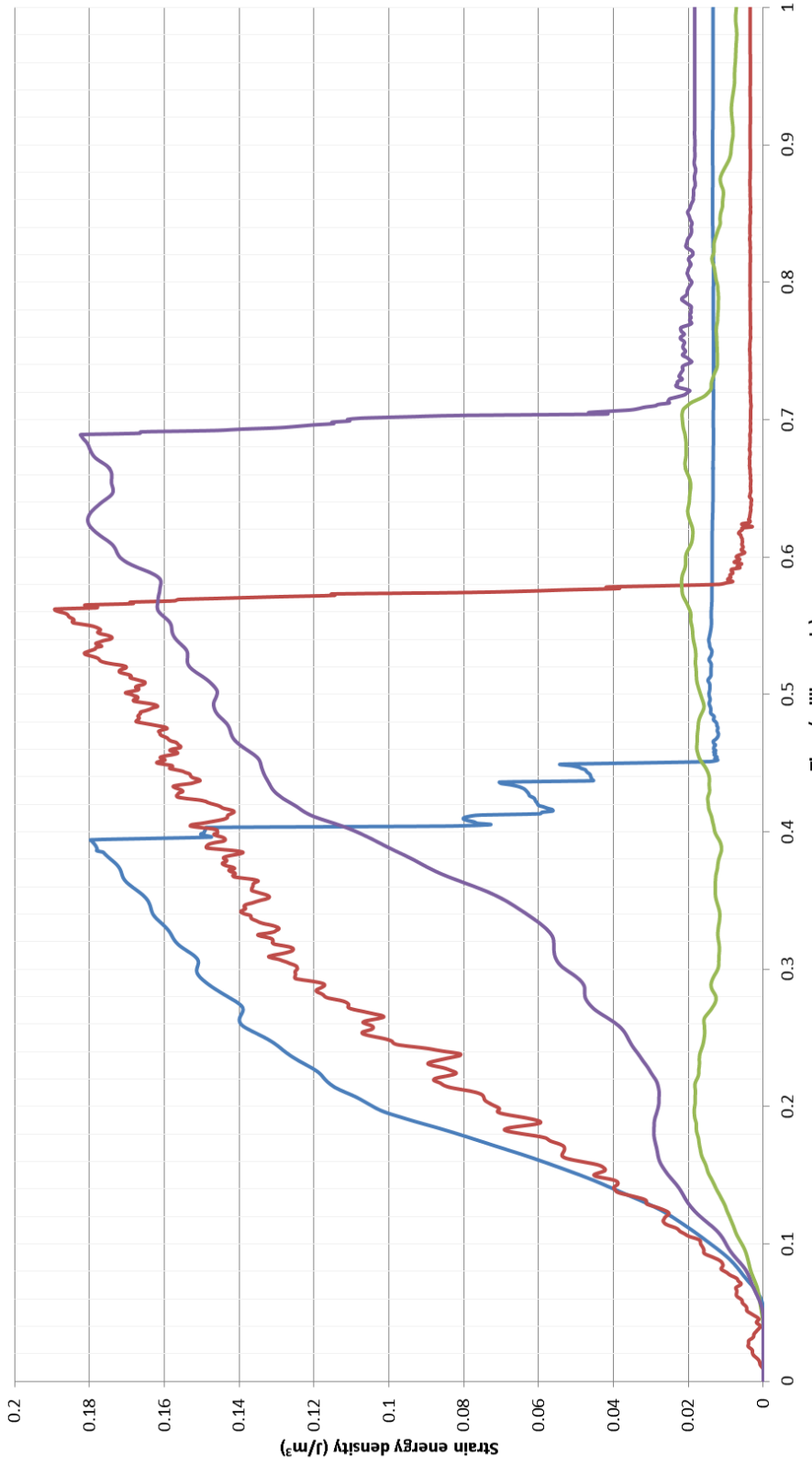

Graph 5.25 The variation of lingual cortical stress (σ_{vm})(GPa) with time for the first deleted node at each mandibular sub-site (one at the right condylar neck and one at the right parasymphysis) following impact at the right parasymphysis of the mandible.

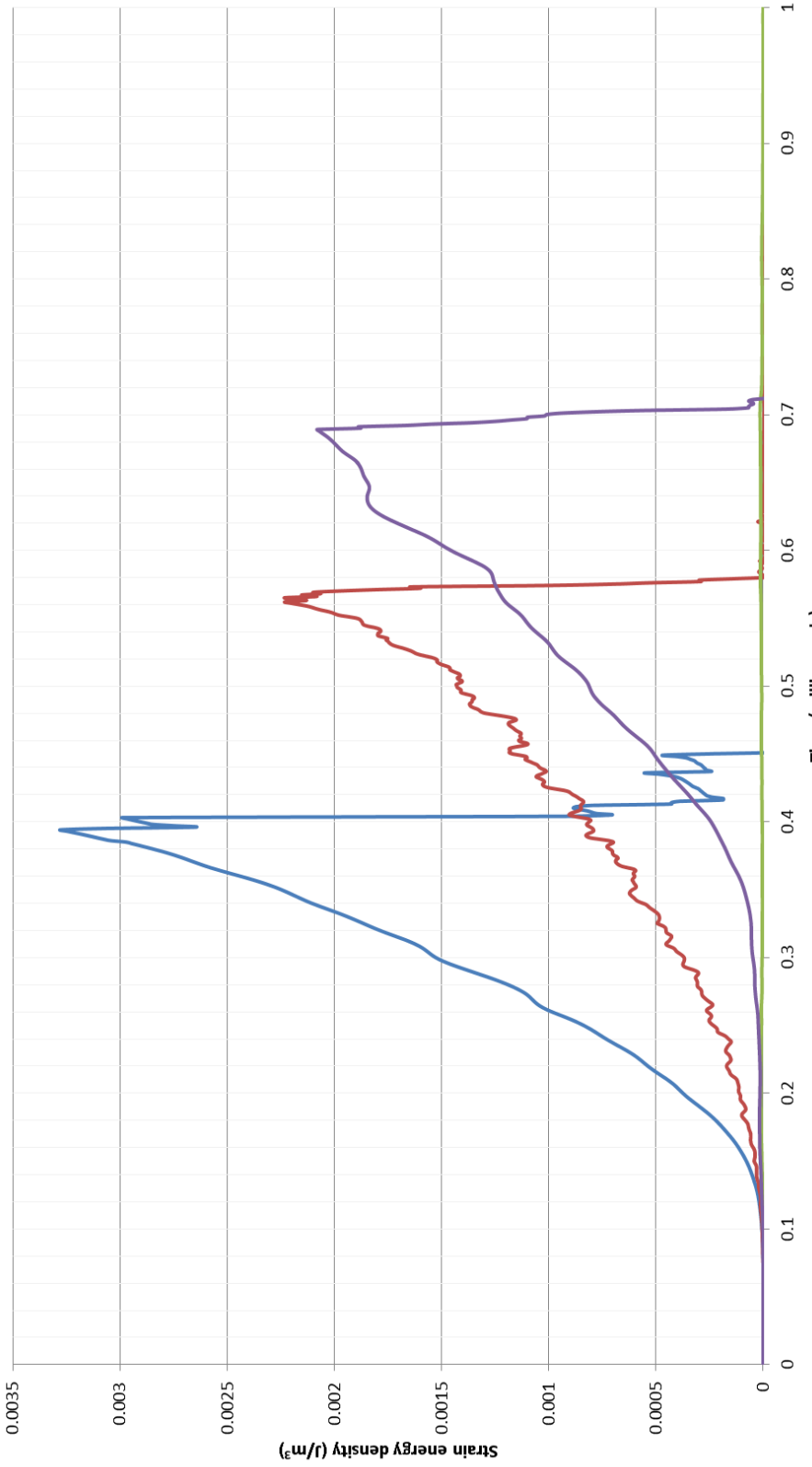

Graph 5.26 The variation of strain energy density with time for the first deleted node at each mandibular sub-site (one at the right condyle and one at the right parasymphysis) following impact at the right parasymphysis of the mandible.

5.6.1.3 Impact at symphysis (Element deletion algorithm)

The simulated impact of the fist at the mandibular symphysis is shown pictorially in figure 5.27. Three fractures were predicted. Right and left condylar necks were fractured along with the mandibular symphysis. Impact at the symphysis resulted in bilateral displacement of the angles of the mandible initially.

Impact with high kinetic energy fist

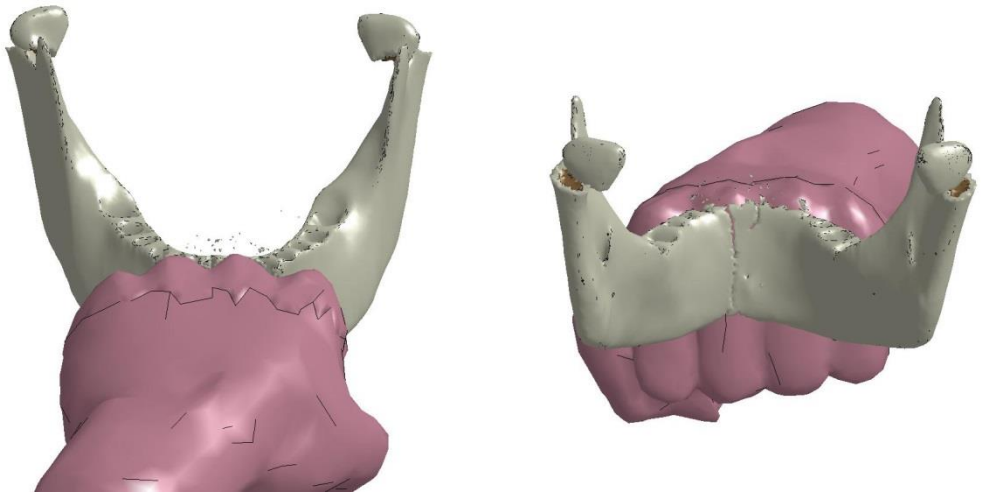

Figure 5.27 The figure shows the results of the computer simulation of a high energy punch to the right mandibular body. An element deletion algorithm was used to simulate the fracture. The impact time was 1ms.

The lingual cortical stress (graph 5.26) and strain energy density (graph 5.27) suggest that the right condylar neck failed at approximately 0.48ms, followed by the left condyle at 0.5ms. Stress at the mandibular symphysis began to fall at 0.72ms, and by 0.8ms the element had been completely deleted indicating fracture. The right condyle may have failed first due to either the non-central impact site, the angulation of the impact or asymmetry of the mandible itself. However, if the mandible was symmetrical, and the impact in the midline, one would expect the condyles to simultaneously fracture.

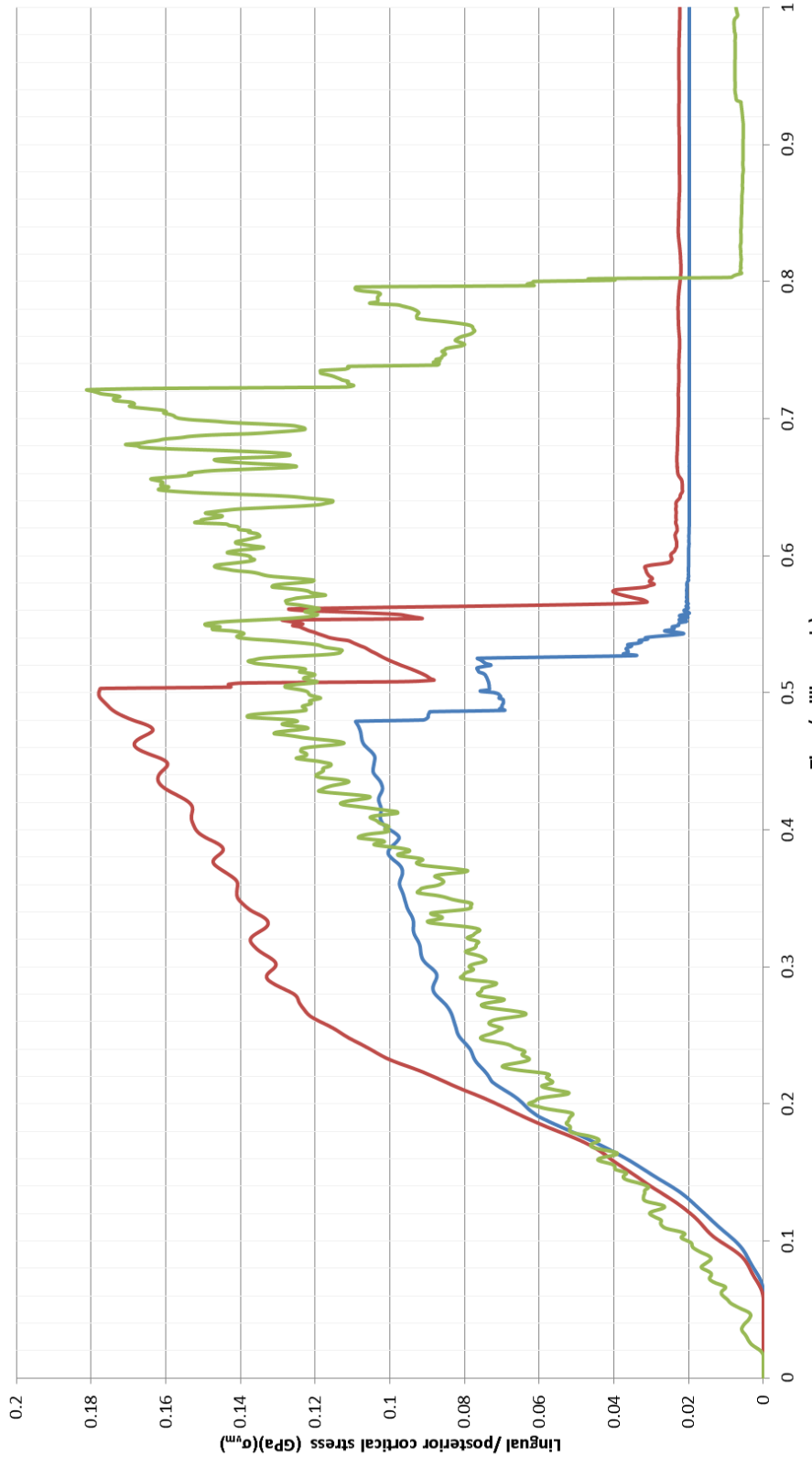

Graph 5.27 The variation of lingual/posterior cortical stress (σ_{vm}) (GPa) with time for the first deleted node at each mandibular sub-site (one at the right posterior condyle, one at the left posterior condyle and one at the lingual symphysis) following impact at the symphysis the mandible.

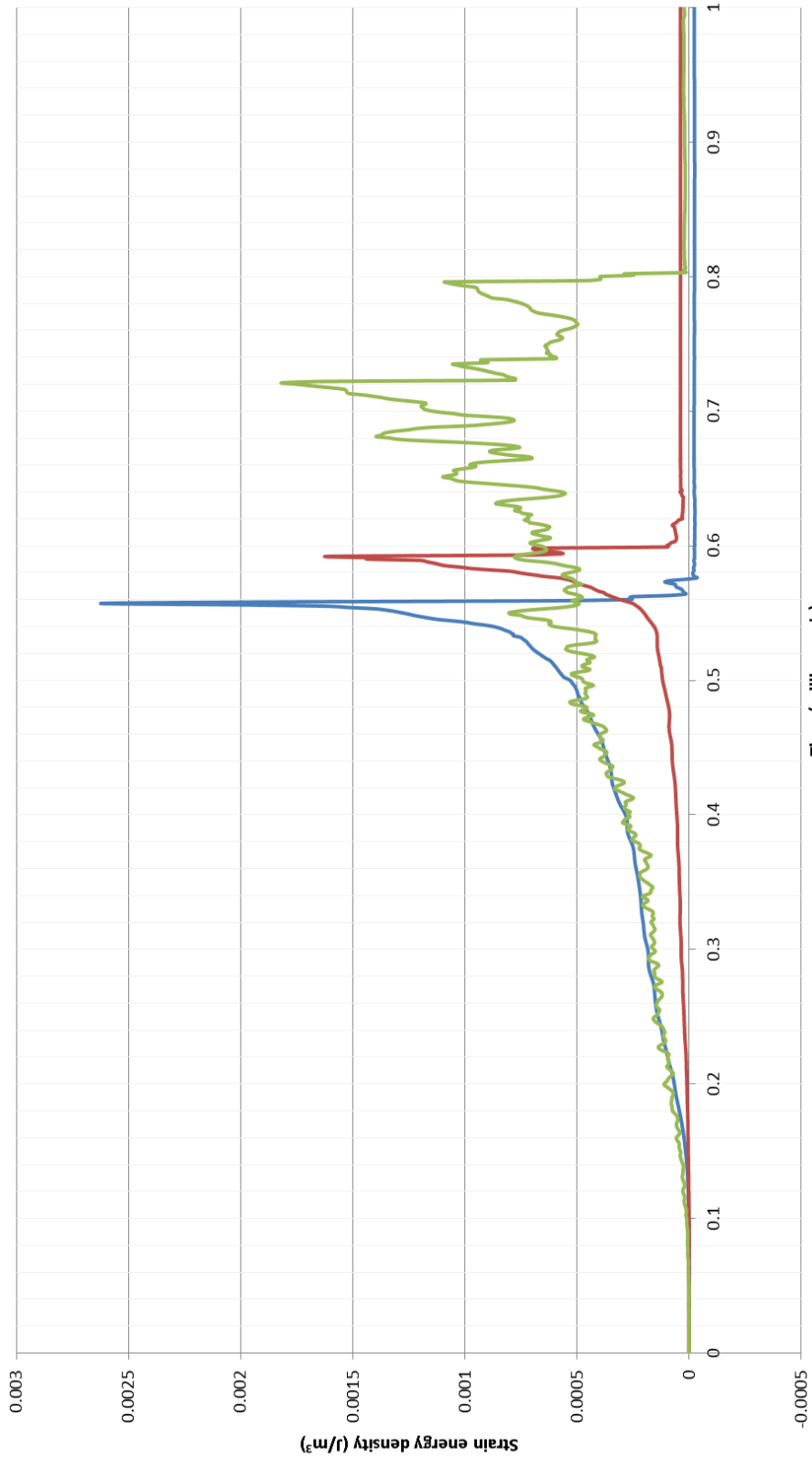

Graph 5.28 The variation of strain energy density with time for the first deleted node at each mandibular sub-site (one at the right condyle, one at the left condyle and one at the symphysis) on the lingual aspect of the mandible following impact at the symphysis the mandible.

5.6.2 Results 9: The relationship of impact KE with fracture pattern

The simulation suggested that increasing the kinetic energy of the impact resulted in increased damage to the mandible. Furthermore, when the fist kinetic energy was very high, increased fragmentation appeared at the impact site. In terms of weak areas of the mandible, the simulation was in agreement with the clinical impression that an impact in the symphyseal region is likely to result in bilateral fractures of the condylar neck and occasionally the symphysis itself.

5.6.2.1 Symphyseal impact

Pictorial results

Picture A

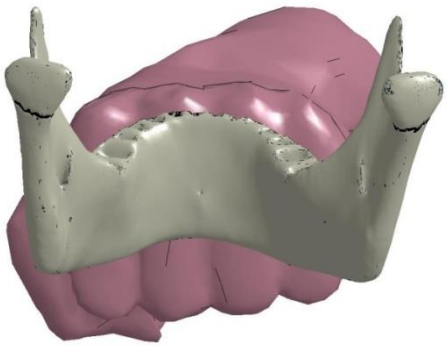

Picture B

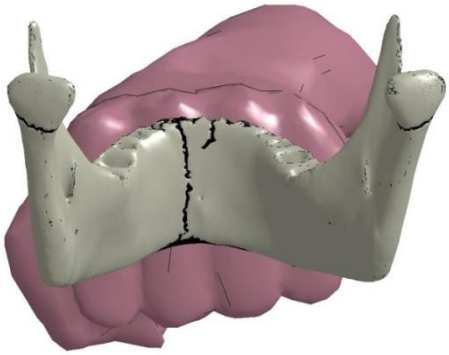

Picture C

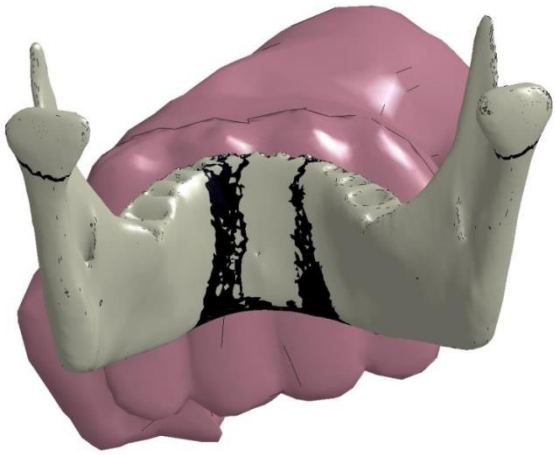

Figure 5.28 Impacts at the mandibular symphysis energy from punches with kinetic energies of 35J (Picture A), 188J (Picture B) and 384J (Picture B). Impact at 1ms is shown. The deleted elements are shown.

	E_i(J)	E_f(J)	ΔE_{kf}(J)	ΔE_{kf} (%)	d (m)/ ms	F (N)
Low kinetic energy	35	19	16	45	0.009 (0.8)	1778
High kinetic energy	138	85	53	38	0.0109 (0.47)	4862
Very high kinetic energy (karate)	384	266	118	31	0.0018 (0.3)	10000

Table 5.1 Values of energy absorbed (ΔE_{kf}(J)) by the mandible following fist impact at 1ms at the symphysis. ΔE_{kf}(J) represents the percentage energy absorbed. Note that values have been rounded to the nearest whole number. The fracture time (ms) is in brackets under the distance the fist had travelled.

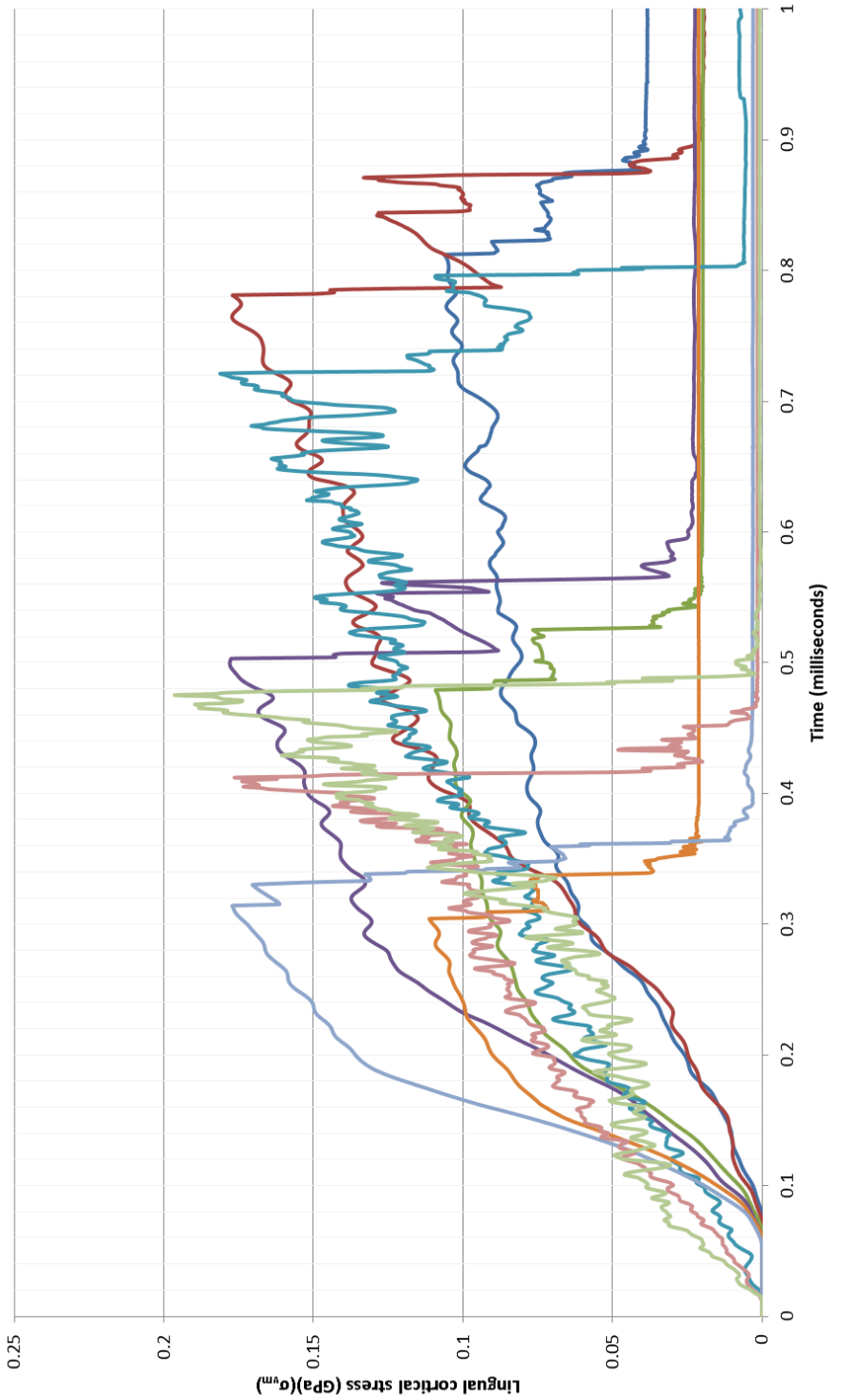

Graph 5.29 The variation of lingual/posterior cortical stress with time for nine nodes (the first deleted node at each mandibular sub-site in each case) on the lingual aspect of the mandibular symphysis and posterior condylar neck following impact at the symphysis of the mandible by a punch of varying

5.6.2.2 Ramus impact

Pictorial results

Pictures A and B

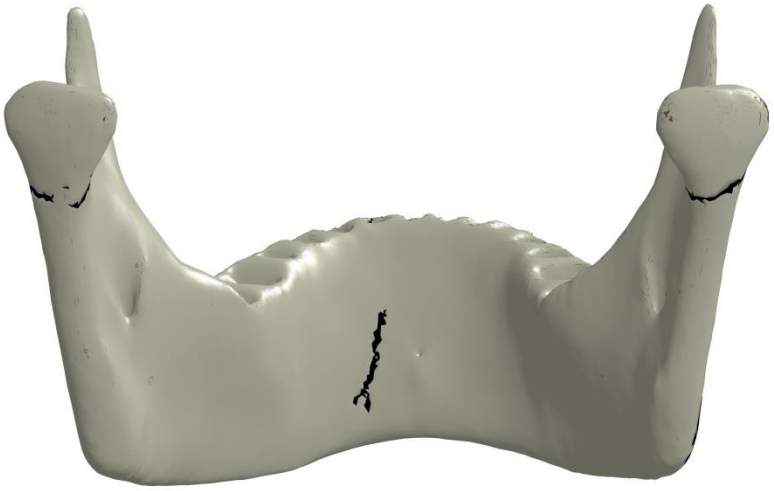

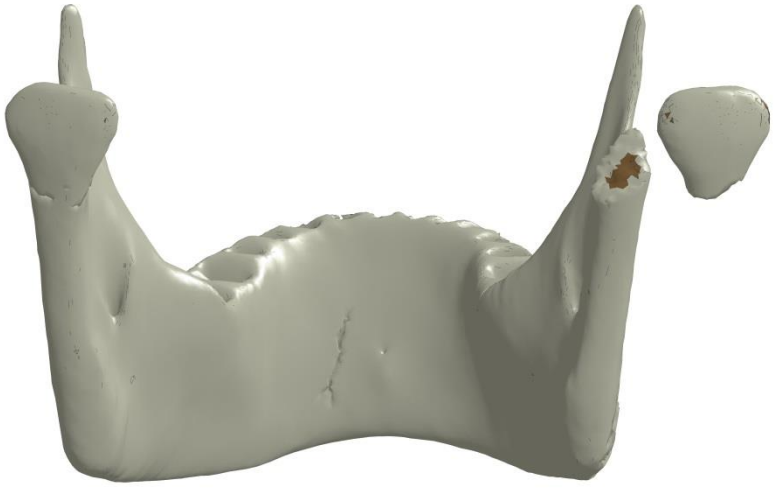

Picture C

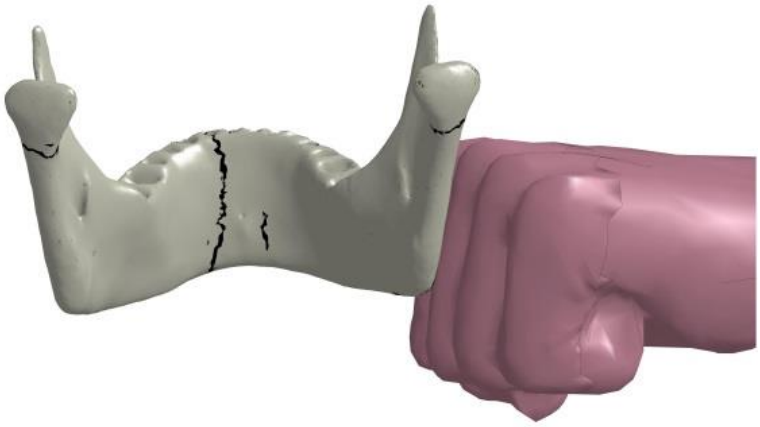

Picture D

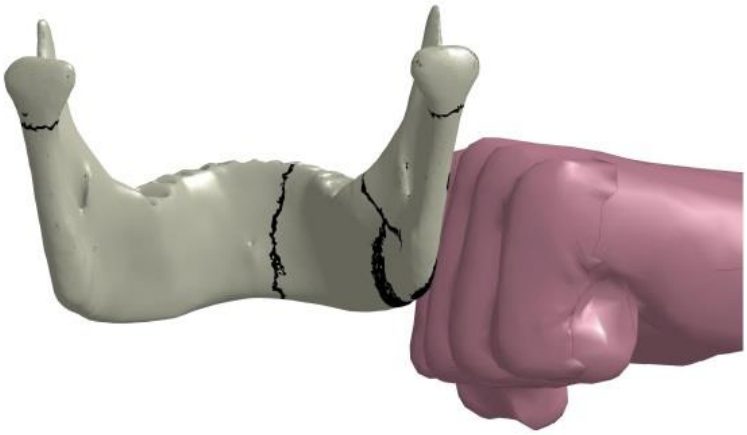

Figure 5.29 Impacts at the right mandibular ramus energy from punches with kinetic energies of 35J (Pictures A and B), 188J (Picture C) and 384J (Picture D). Picture b shows the displacement view. Impact at 1ms was shown. The deleted elements are shown.

Impacts at the ramus of the mandible showed a similar pattern to the impacts at the symphysis i.e. increased impact kinetic energy resulted in an increase in the number of

predicted fractures in the mandible as a whole, in addition to fragmentation at the impact site. Fractures occurred in the right condylar region at low fist kinetic energy. There was also damage to the left condyle but this was not sufficient to cause a displaced fracture (compare pictures A and B which show the simulation with deleted elements and displaced fractures respectively). A fracture such as the simulated left condyle viewed using plain radiography might not be visible.

At high fist kinetic energy, in addition to right and left condylar neck, fractures occurred at the left parasymphysis with some damage at the lingual aspect of the right parasymphysis. The fracture pattern was different at very high impact kinetic energy when a comminuted fracture occurred at the right angle in addition to the condylar necks. The parasymphyseal fracture in this case occurred at the right parasymphysis.

Graph 5.29 suggests that in all cases the mandibular condyle would fracture first on loading. When the impact area is very small one would expect that local damage would occur first as when the cross-sectional area is very small the local stress will be high.

	E_i(J)	E_f(J)	ΔE_{kf}(J)	ΔE_{kf} (%)	d(m) ms	F (N)
Low kinetic energy	35	25	10	29	0.0101 (0.23)	990
High kinetic energy	138	109	29	21	0.0221 (0.16)	1312
Very high kinetic energy (karate)	384	327	57	15	0.0377 (0.14)	1511

Table 5.2 Values of energy absorbed (ΔE_{kf}(J)) by the mandible following fist impact at 1ms at the right ramus. ΔE_{kf}(J) represents the percentage energy absorbed. Note that values have been rounded to the nearest whole number. The fracture time (ms) is in brackets under the distance the fist had travelled.

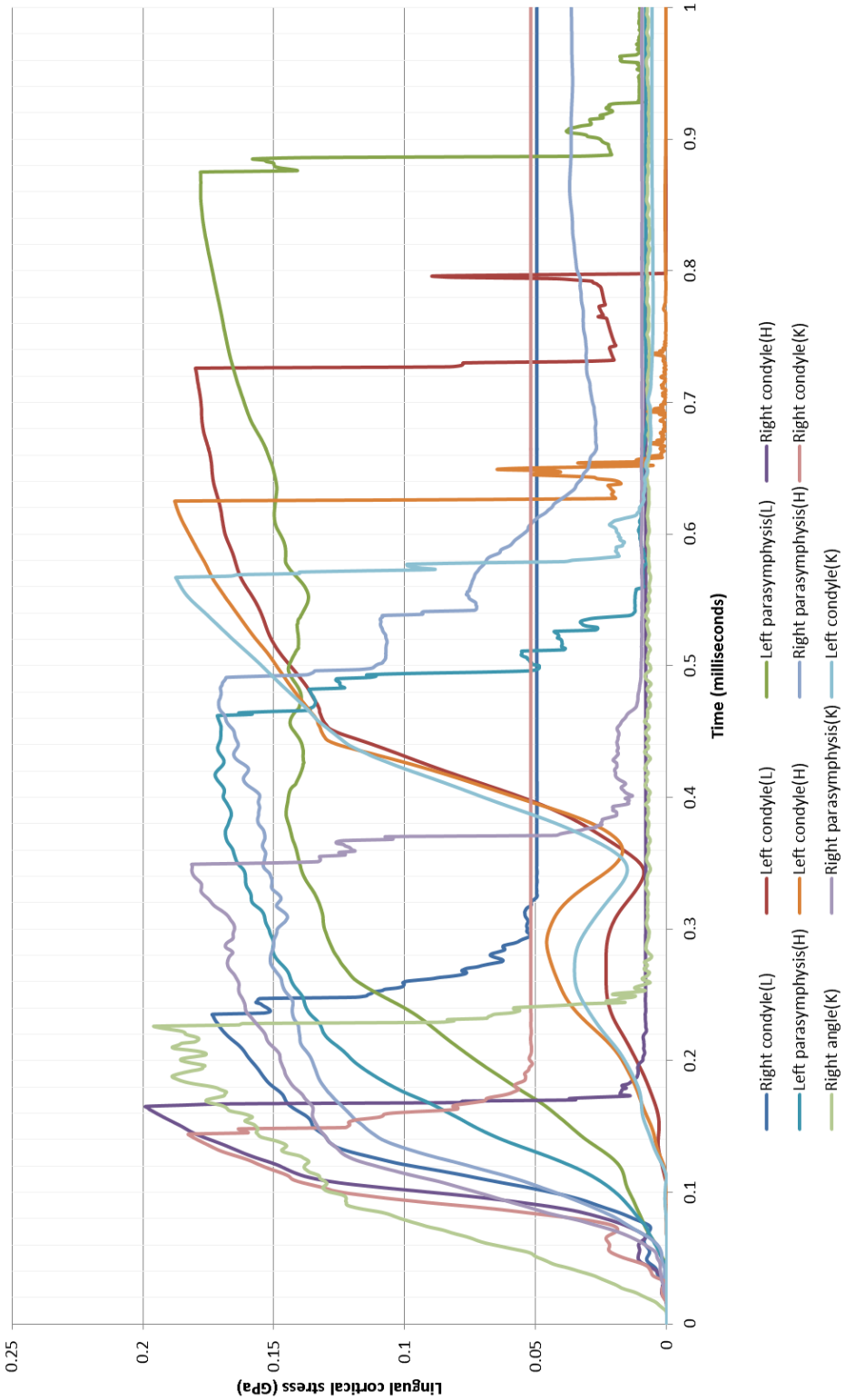

Graph 5.30 The variation of lingual cortical stress with time for eleven nodes (the first deleted node at each mandibular sub-site in each case) on the lingual aspect of the mandible following impact at the right ramus of the mandible by a punch of varying kinetic energies. K denotes a karate high kinetic energy punch (384J), H denotes a high kinetic energy punch (138J), L denotes a low kinetic energy punch (35J).

5.6.3 Results 10: The relationship between strain rate and fracture sub-site

Figure 5.30 shows sequential snap shots of a colour contour map of the mandible where strain rate is displayed following a symphyseal punch. Observing the lingual aspect, at 0.1ms, strain waves were observed radiating from the lingual aspect of the symphysis, along the mandibular body to the ramus of the mandible. On reaching the condylar head they were reflected down the neck of the condyle bilaterally. The areas of highest strain rate (coloured red) coincided with the appearance of fractures on the lingual aspect of the mandible or posterior condyle.

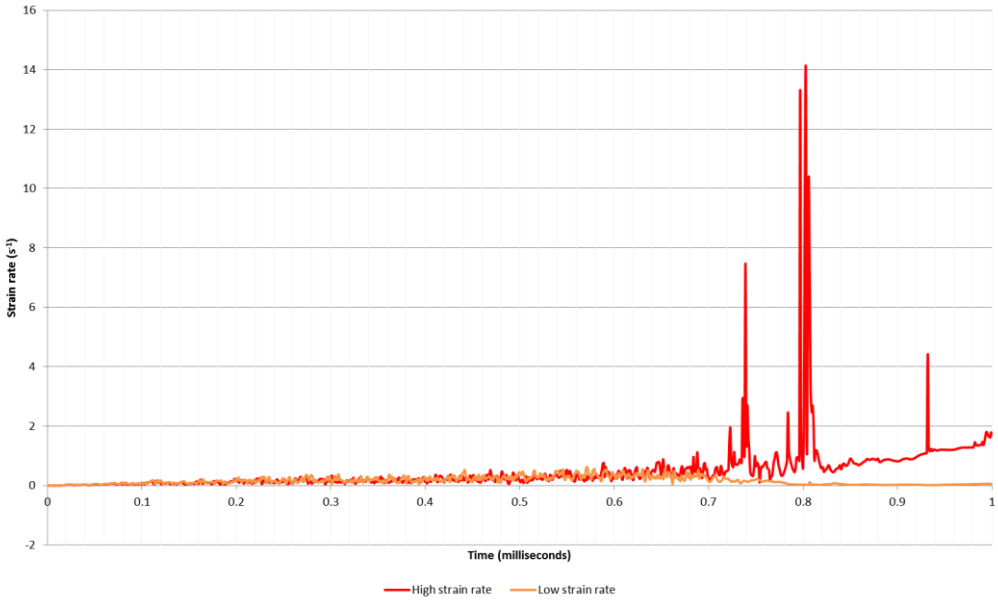

Graph 5.31 The figure shows the variation of lingual strain rate with time for the first deleted node at the symphysis of the mandible

Graph 5.30 shows the strain rate plotted against time for both low and high strain rate models sampled at the fracture site on the lingual aspect of the symphysis. Reviewing graph 5.28, the predicted fracture occured at about 0.8ms. Graph 5.30 shows that the strain rate reached just over $14s^{-1}$ in the high strain rate model (red).

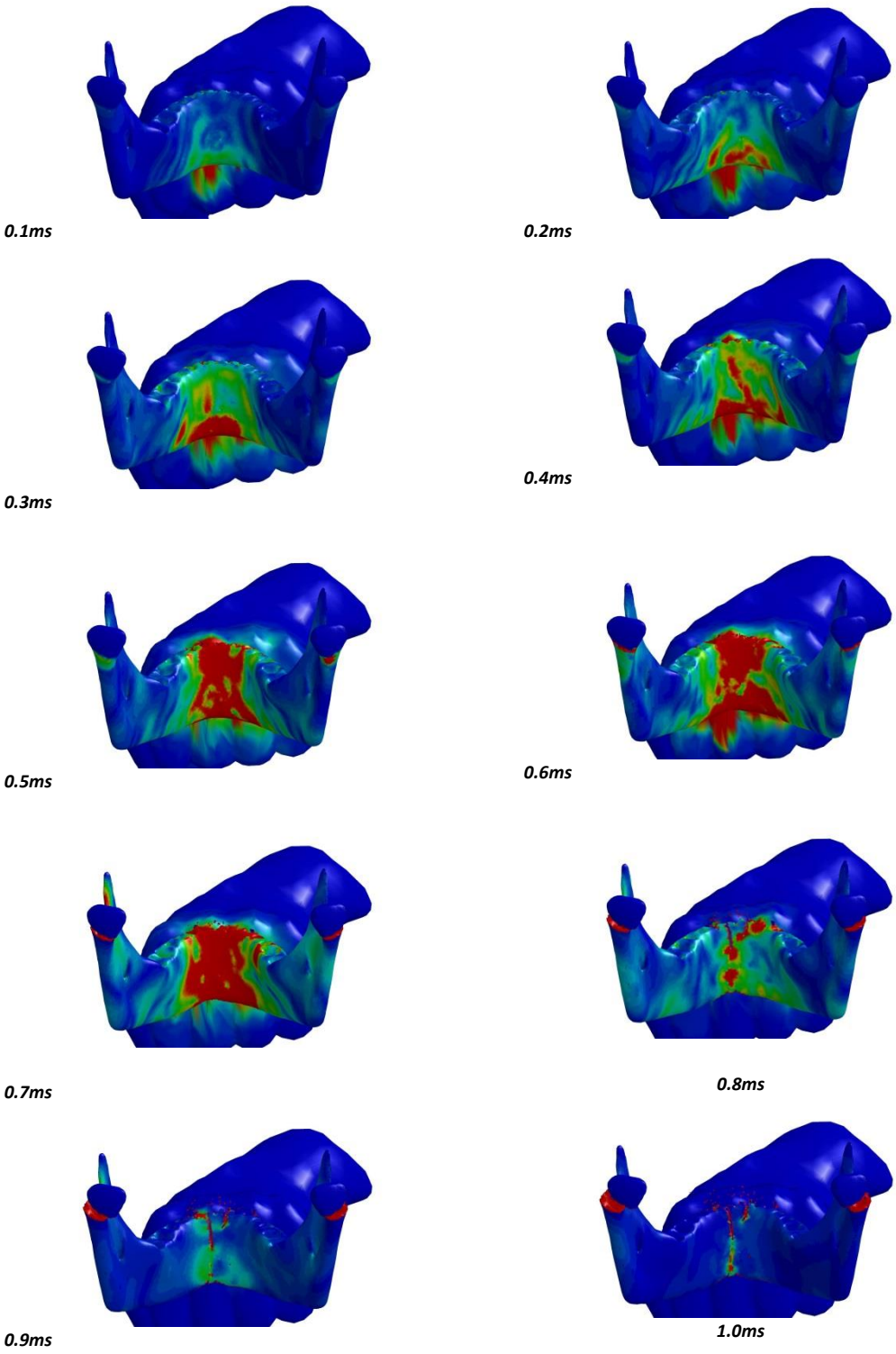

Figure 5.30 Change in strain rate over time on symphyseal impact. Red areas indicate the highest strain rate and blue the lowest. The strain rate parameters were C=40 and p=5.

In the low strain rate model (orange), the strain rate never rose above $1s^{-1}$ and the element was not deleted, suggesting no fracture occurred in that area. With the different strain rate model the pattern of symphyseal fractures differed. With the low strain rate model the fracture began on the right of the genial tubercles superiorly and only reached half way down the lingualaspect over the analysis time. In the high strain rate model the lingual fracture occurred to the left of the genial tubercles and traversed the cortical surface superiorly to inferiorly (compare figures 5.31 and 5.32).

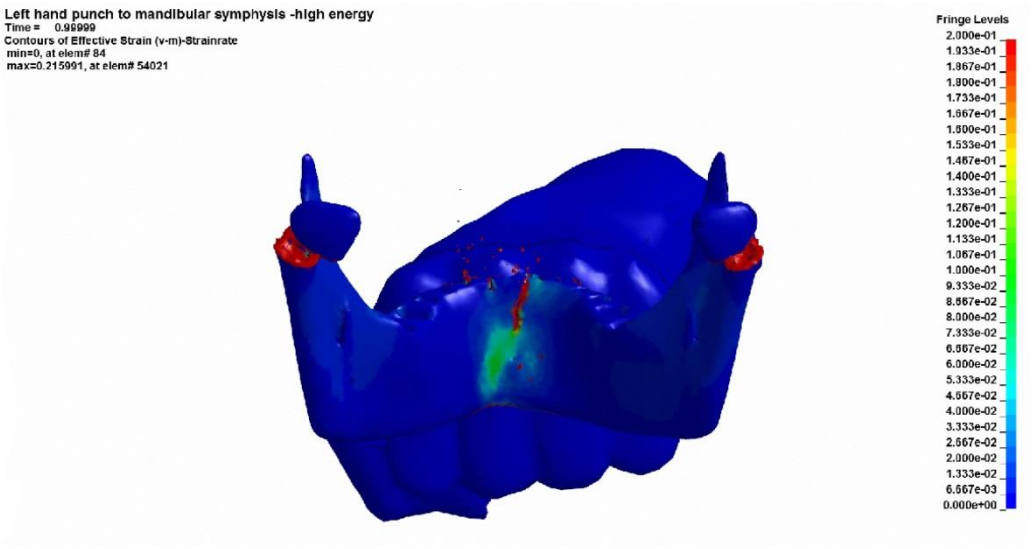

Figure 5.31 Colour contour map of the mandible following a symphyseal impact. Here the lower scaled strain rate model is used.

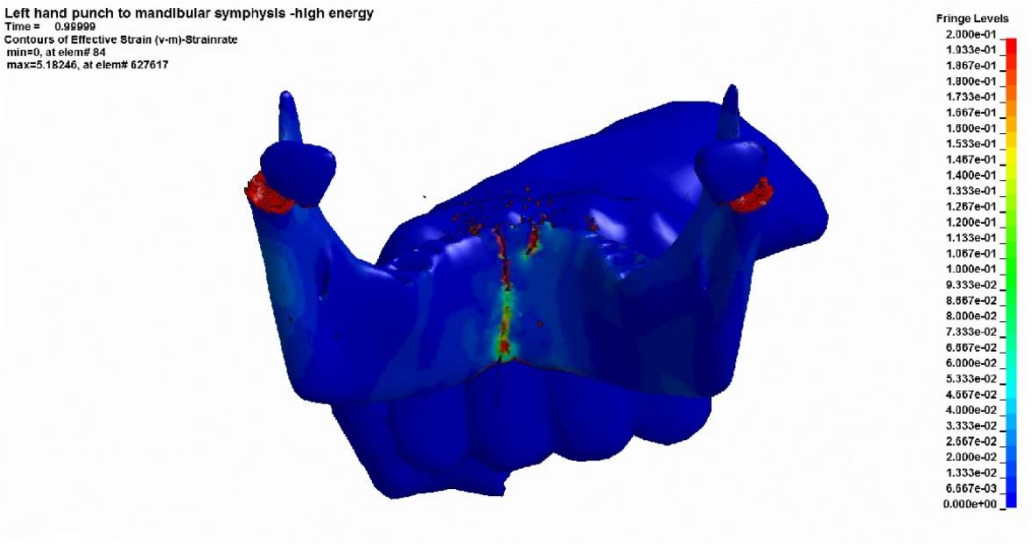

Figure 5.32 Colour contour map of the mandible following a symphyseal impact. Here the higher scaled strain rate model is used.

5.7 Findings. Phase IIIb: Applied non-linear dynamic analyses

5.7.1 Results 11: Influence of localized changes in material properties on mandibular angle fractures- 1

Figure 5.33 shows the effect of a simulated punch to the right angle of the mandible. The element deletion algorithm was used and the predicted displacement of fragments is as shown. There were fractures at the right condylar neck, the left parasymphysis with a minimally displaced fracture at the left condylar head. No fracture was seen at the lingual aspect of the impact zone at the right angle of the mandible. The dispacements shown are unlikely to be any more than indications of the direction of movement of fragments due to the 1ms run time and the lack of muscular action. The results for symphyseal impacts are similar to those of the angle impact and are found in the found in appendix 18.

No lesion, no impacted third molar tooth right angle of mandible

Picture A

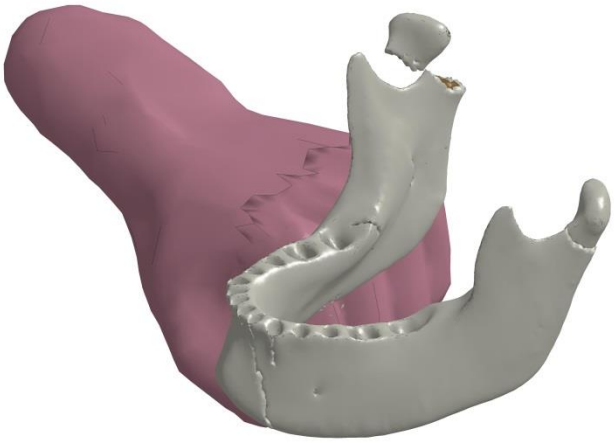

Picture B

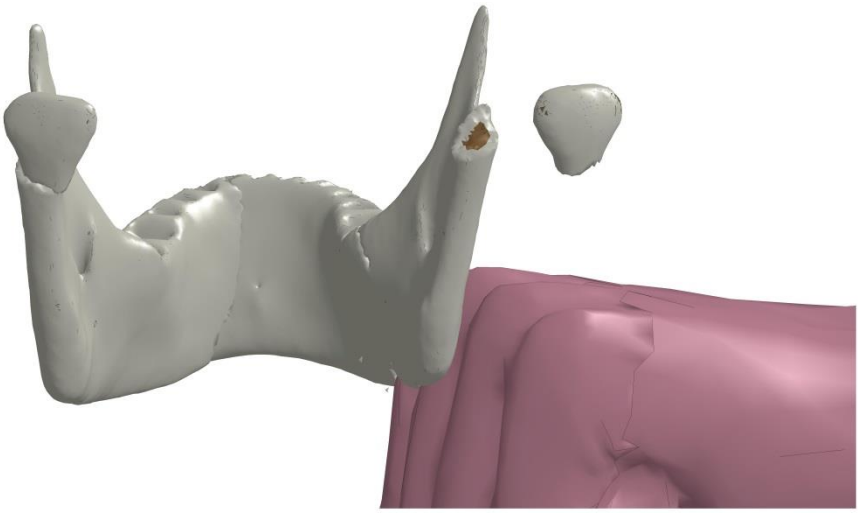

Picture C

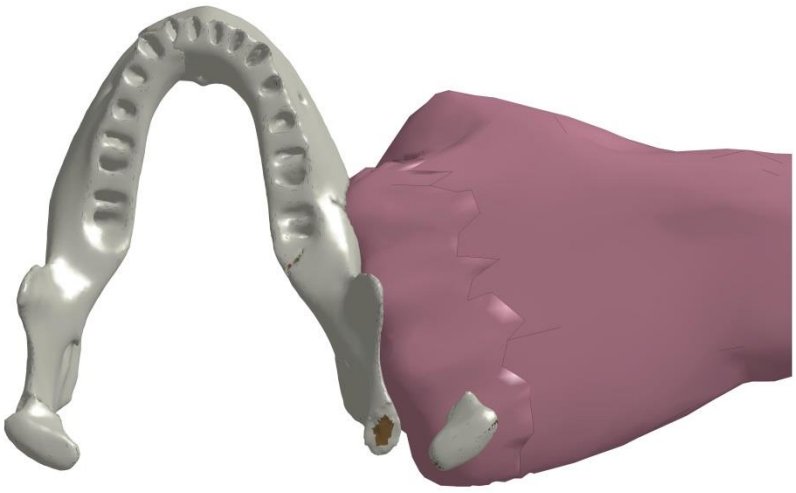

Figure 5.33 Sequence of pictures showing the computer simulation of a punch to the right angle of the mandible in a mandible with no impacted tooth in the third molar region. The kinetic energy of the fist was 188J

Un-erupted third molar tooth

Examination of the simulation sequence (see figure 5.34), which included an un-erupted third molar tooth, showed a predicted fracture of the right condylar neck, a minimally displaced left condylar neck, a fracture of the right parasymphysis and a fracture of the left lingual plate in the parasymphyseal region.

Figure 5.34 seems to suggest that the presence of a deeply impacted third molar tooth does not necessarily make a fracture more likely at the angle of the mandible. The increased stiffness in the area may have increased the likelihood of a fracture in the region of the right parasymphysis.

Picture A

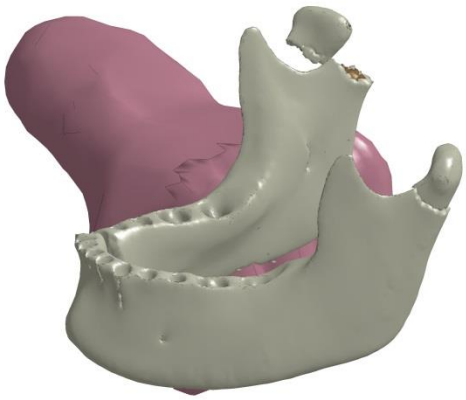

Picture B

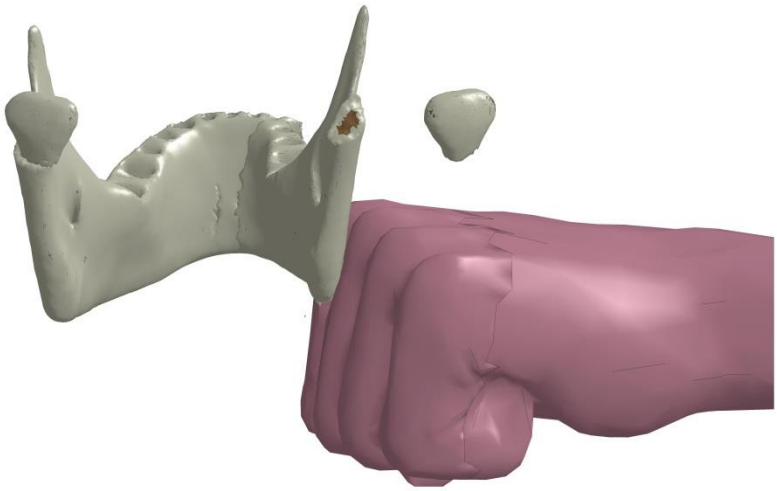

Picture C

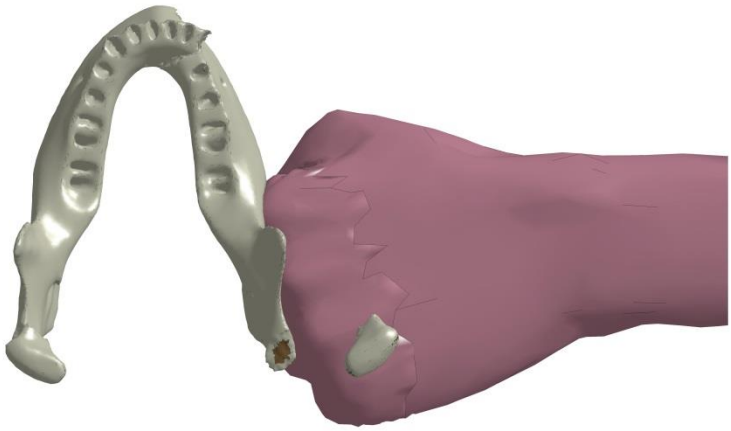

Figure 5.34 Sequence of pictures showing the computer simulation of a punch to the right angle of the mandible in a mandible with impacted the third molar teeth. The kinetic energy of the fist was 188J.

5.7.2 Results 12: Influence of localized changes in material properties on mandibular angle fractures- 2

The result of an impact in a mandible with a cystic lesion at the angle of showed a clear weakness in that region. The impact was in exactly the same position as in section 5.7.1 and the fist had the same kinetic energy. The difference in damage was significant. There were predicted fractures at the right and left condylar necks, (with the left being relatively undisplaced), the right angle of the mandible, the left parasymphysis. The right condylar neck was significantly displaced.

Sequence showing impact with cystic lesion at right angle of the mandible

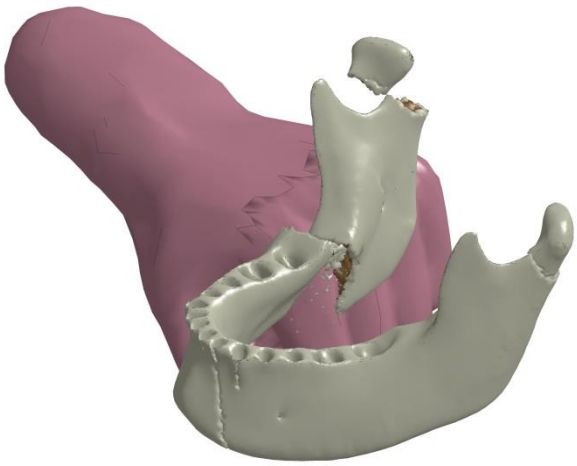

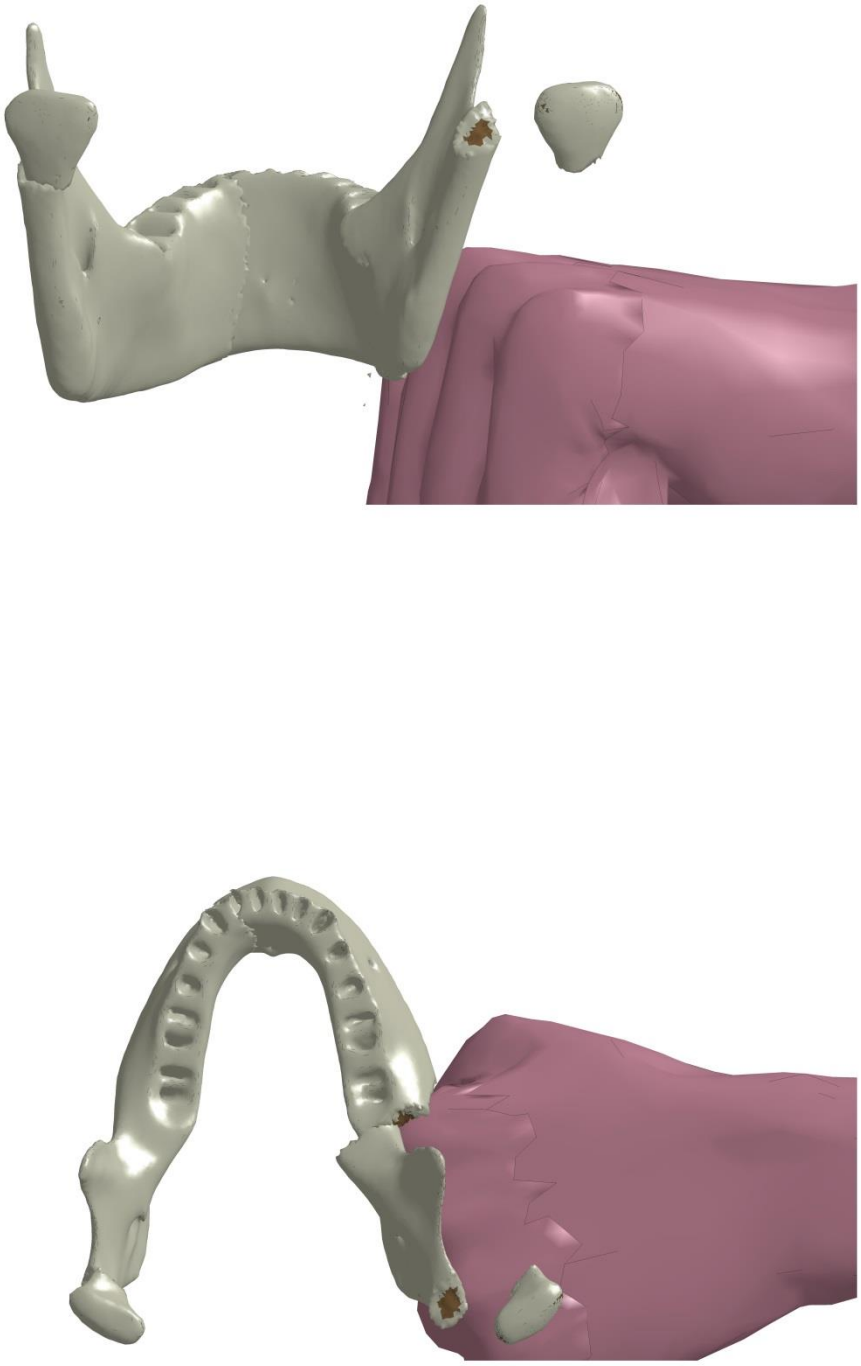

Figure 5.35 Sequence of pictures showing the computer simulation of a punch to the right angle of the mandible in a mandible with a cystic lesion in the third molar region. The kinetic energy of the fist was 188J.

As may be seen from table 5.9, similar energy is absorbed by the mandible when the impacted third molar is in situ as with no un-erupted tooth. Less kinetic energy was lost from the fist when there was an intra-bony cystic lesion at the impact site and proportionally less energy was absorbed by the mandible. Examining the cortical stress at the lingual aspect of the impact site showed that with an un-erupted third molar tooth less stress occurred compared to the tooth-free state. The stress on the lingual cortex when there was a cystic lesion present initially rose as in the normal case, dropped slightly, then rose again rapidly until the lingual cortex failed

	$E_i(J)$	$E_f(J)$	$\Delta E_{kf}(J)$	$\Delta E_{kf}(\%)$
Un-erupted third molar	188	151	37	20
No un-erupted tooth	188	151	37	20
Cystic lesion at angle	188	155	33	18

Table 5.3 Values of energy absorbed ($\Delta E_{kf}(J)$) by the mandible following fist impact at 1ms at the right ramus. $\Delta E_{kf}(J)$ represents the percentage energy absorbed. Note that values have been rounded to the nearest whole number.

Graphs 5.32 shows the effect of angle impacts on medial condylar neck cortical stress. It can be seen that at the right condyle (which was predicted to fracture at about 0.25ms) the medial cortical stress was always significantly lower for the un-erupted tooth, and slightly lower for the cystic lesion, when compared to the model without un-erupted teeth. The cystic lesion and the un-erupted tooth had exactly the same volume and position. The suggestion is that the un-erupted third molar tooth, as modelled, did not increase the risk of fracture at the angle on impact.

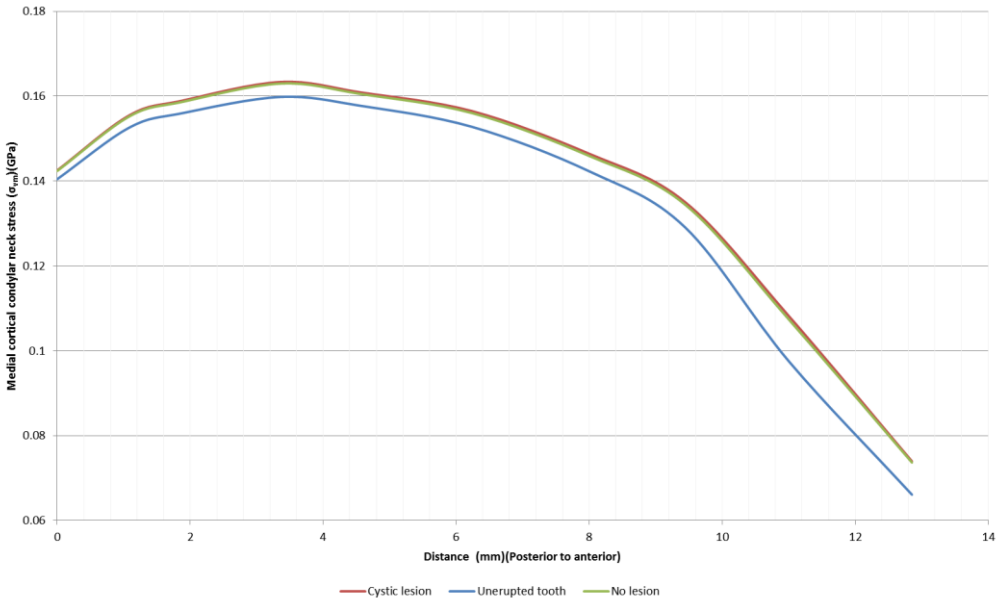

Graph 5.32 The variation of right medial condylar cortical stress (σ_{vm})(GPa) for the node set following impact at the angle of the mandible. Three cases are considered, as shown. The sample takes place at 0.23ms (i.e. just before the condylar neck fractures).

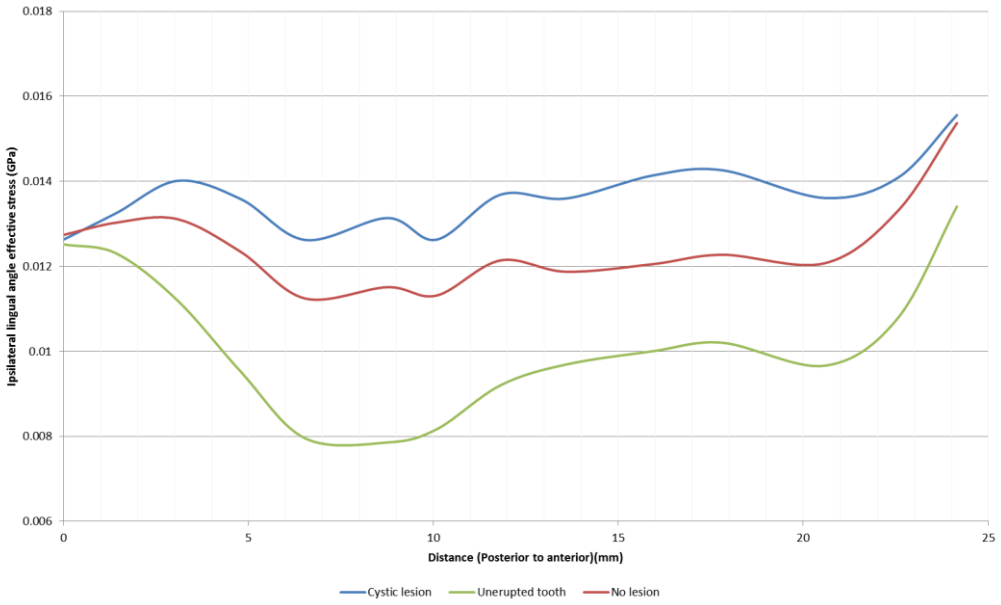

Graph 5.33 The figure shows the variation of right lingual angle cortical stress (σ_{vm})(GPa) for the node set following impact at the symphysis of the mandible. Three cases are considered, as shown. The same sample set is used in each case. The sample takes place at 0.2ms (i.e. just before the condylar neck fractures).

5.8 Phase III conclusions

Fracture patterns

The basic dynamic non-linear analyses and associated simulations seemed to predict fractures (as a result of direct impact to the mandible) in patterns similar to those that are encountered in laboratory cadaveric studies and selected clinical situations. Rather than merely the fracture initiation sites, which were predicted in the static analyses, the actual form and direction of fractures were simulated using an element deletion algorithm. This algorithm is an imperfect method of fracture simulation. The main problem is that the algorithm deletes elements when the stress or strain reaches a predefined value. This alters the mass of the model and thus affects the remaining calculations. In a real fracture, tissue is not simply lost. One would hope that the small number of elements deleted would not significantly affect the results. Despite the problems mentioned, the non-linear dynamic analyses offered an improvement over both the static analyses in terms of simulation.

The calculated fracture forces (see tables 5.8) were slightly lower than those derived from reported mechanical testing. Huelke and Compton, (1983) experimentally measured the fracture threshold to be 2442N. It has been shown that the facial soft tissues can absorb significant energy from the impact resulting in less energy to produce mandibular fracture. In such cases, the mandible may fracture at significantly greater load. Nahum, (1975) found that single condylar factures could be experimentally induced with forces of between 2383N and 2443N whereas bilateral condylar fractures with the symphysis would require 3816N to 4120N. The values calculated in the simulation represent a force at which the mandible would fracture when impacted over the surface area of the simulated fist. These forces are not fracture threshold values and differ due to the different impacted objects used in the mechanical experiments above.

Once the effect of impact surface area (i.e.stress is calculated) is eliminated, the results are similar. Another reason for the difference in values most likely lies in the definition a fracture. In this dynamic study a fracture was deemed to have occurred once the first element on the posterior surface of the condylar neck had been deleted. This would equate with a crack on the cortex under tension. A crack does not always propage and produce a fracture and thus this artificial threshold is likely to occur before mechanical failure and may not have a detectable experimental mechanical equivalent.

Impact kinetic energy

Increased kinetic energy seemed to be related to the degree of bony fragmentation at the impact site when assessed qualitatively. Additionally, the number of fractures increased, although the fractures still occurred in the same susceptible sites when the energy increase was moderate. At very high energies, there was increased fragmentation at the impact site in addition to linear fractures at other sites. These results agree with the clinical finding that high-energy injuries are associated with greater degrees of soft and hard tissue trauma.

Impact kinetic energy alone would not be a suitable method for the determination of fracture threshold in a real patient. As the work of Schneider and Nahum (1974) suggested, significant impact energy may be absorbed by soft tissues, thus reducing the likelihood of fracture. This means that the modelled fractures were calculated at a lower threshold than the cadaveric exxperiments of Schneider and Nahum.

Strain rate

The mechanical behaviour of bone is strain rate dependant. Physiological strain rates in humans have been reported to be between $0.004s^{-1}$ and $0.05s^{-1}$ (Lanyon, et al., 1975; Burr, et al., 1996). Hansen, et al. (2008) reported that in traumatic events, such as falls from a significant height and road traffic accidents, the strain rate of cortical bone may reach $25s^{-1}$. It would seem that the results obtained here are comparable to a relatively low energy injury. Bone becomes stiffer and is able to sustain a higher load before failure as the strain rate increases, however, there is a corresponding reduction in fracture toughness (Zimmermann, et al., 2014). The modelling techniques used to capture the shift in yield stress with strain rate did not seem to have any significant effect on the results qualitatively. There seemed to be only an effect on a few elements at the initial impact site. This would be in line with the work of Mukherjee, et al. (2011) who reported similar results on investigation the mechanical properties of human shoulder bone at the strain rates associated with automotive impacts. The strain rate encountered in the automotive impact scenario would be significantly greater than those encountered in interpersonal violence.

Localized changes in material properties (lesions at the angle of the mandible)

As previously mentioned in section 2.6, all of the clinical studies investigating the effect of third molar teeth on angle fracture susceptibility, have treated third molar teeth as a homogeneous group. Pathological conditions such as cystic change in the follicle of the crown, which is common, were ignored, as were ankylosed teeth. This made it difficult to determine whether it was the presence of the tooth itself or a pathological un-erupted tooth that suggested the increased fracture susceptibility. The conclusions of Gaddipati, et al. (2014) and, Inaoka, et al. (2009), seem to be partially supported by the results presented here; however, their conclusions appear incomplete. The results

suggest that the nature of the impacted tooth itself is the primary determinant in whether or not the angle is more susceptible to fracture. The point of impact is a secondary factor. As the nature of the impacted tooth changes from the ankylosed state (which appears to be protective for fracture at the angle of the mandible) to the cystic state, through pathological change, the susceptibility to fracture increases. The fate of the normal un-erupted third molar remains in question for many reasons. Firstly, many patients tend to present when they have problems with third molar teeth. Others present when the surrounding follicle has undergone spontaneous pathological change. The width of the normal periodontal ligament is said to be approximately 0.2mm and the normal dental follicle has been measured as being between 0.0mm and 4.0mm (de Oliveira, et al., 2008). Normal cortical bone can undergo 2% strain before failure and cancellous bone can undergo 70% strain. Therefore, if the width of the angle of the mandible is approximately 10mm and the cortical bone is not reduced in thickness, then the angle of the mandible should not be more susceptible to fracture on symphyseal impact and condyle should be unaffected on angle impact (see cyst angle results). These findings suggest that when the periodontal ligament and dental follicle are at the lowest range of normality (in terms of width) then the un-erupted tooth should behave as modelled in this investigation and present no increased risk of fracture at the angle or condyle.

The findings here are incompatible with those of Weiner, et al. (2012), Milzman, et al. (2013) whose conclusions were too broad. The presence of the third molar does not always increase the risk of angle fracture, especially when the site of impact is unspecified. The conclusions of Safdar and Meechan, (1995) were also not fully supported by these results. An ankylosed third molar tooth, whilst changing the amount of bone at the angle quantitatively, will not weaken the angle of the mandible in the same way that a dense bone island in a similar place would not weaken the angle. In

conclusion, the results of this 3DFEA simulation suggest that the consensus view that an un-erupted third molar tooth weakens the mandible is incomplete without qualification i.e. the pathological nature of the tooth.

5.9 Research summary

In concluding this research, we return to the initial research aims (table 5.10) to determine if these have been satisfied. The basic research objective was to develop a three-dimensional finite element model capable of reproducing the biomechanical response of the mandible to loading. This research produced an anatomically and dimensionally accurate model, the final iteration of which allowed meaningful, clinically relevant problems to be analysed. There are currently no reported mandibular models capable of fulfilling these aims.

The research model exceeds the specifications of the only other model designed for a similar purpose (Gallas Torreira and Fernandez, 2004) in the following ways:

- The research model is capable of studying the effect of any impacting object. A model fist was used in the dynamic analyses; however, any model was possible.
- An attempt has been made at model validation. The research model has been validated against experimental mechanical data for deformation within the elastic limit. Calculated forces sufficient to cause various patterns of mandibular fracture have been found to be within the general range of those of many authors' experimental mechanical data. No in vivo data for cortical stress and strain during mandibular fractures is available in the literature and is unlikely to be in future; therefore the most accurate forms of validation have been performed. Additionally, fracture patterns obtained experimentally agree with clinical patterns found in similar loading situations.

Research objective	General research question	Specific research question
To develop a three-dimensional finite element model capable of reproducing the biomechanical response of the mandible to physical trauma.	Can a validated mandibular 3DFEA model be produced which is capable of reproducing the biomechanical response of the mandible under load?	What are the effects of the muscles of mastication on the biomechanical response of the mandible under load?
		What is the effect of tooth loss on the mandible under direct loading?
		What are the effects of generalized material property changes on the mandible under load?
	How does the mandible respond to static physiological loading?	What is the effect of load site on the mandible?
		What is the effect of load angulation on the mandible?
	How does the mandible respond to static loading?	Are the patterns of mandibular stress and strain similar under physiological and loading?
	How does the mandible respond to dynamic loading?	What is the effect of deformation rate on mandibular fracture?
	How do localized changes in material properties (i.e. bony lesions) in the mandible change the dynamic response to loading?	What is the effect of cystic lesions at the angle of the mandible on fracture propensity?
		What is the effect of lesions at the angle of the mandible (un-erupted third molar teeth) on fracture propensity?

Table 5.4 Intial research aims.

- More than two impact scenarios have been modelled. The model produced, is capable of modelling any impact site or angle that could occur in real life.

- The model is capable of estimating strain rate effects, which have been shown to be related to the genesis of fractures.
- The model has been used to study other anatomical features (such as impacted teeth) that may be related to mandibular fractures and has been able improve understanding and extend existing theories of fracture.

Additionally, a sound modelling methodology for 3DFEA was developed. This should be applicable to any biological structure.

The research has produced results that shed light on several often quoted (but unproven) theories of mandibular fracture. Analyses suggested that the mandible is unlikely to be fractured by any normal, co-ordinated muscular contraction, assuming that there are no global changes in material properties. Even the uncontrolled muscular activity of epileptic seizures is unlikely to result in direct mandibular fracture. This is contrary to many former beliefs.

Whilst an increase in fracture propensity might be expected to result from mandibular atrophy following tooth extraction, the immediate post extraction mandible does not appear to be at any significantly increased risk of fracture when compared to the immediate pre-extraction state.

Impact kinetic energy has been shown to be a factor in the pattern on mandibular fracture, with fragmentation occurring at high energy. However, this is an unreliable method of predicting the exact pattern of fractures as there the amount of kinetic energy converted to strain energy available to cause bony fracture is dependent on how much energy has been absorbed by the surrounding tissues.

In Phase IIIb the practical application of the technique was considered. The problem to be solved was whether a change in material properties significantly increased the

propensity of the mandible to fracture under load. Questions of this nature would be of interest to those trying to determine whether a particular purported mechanism of injury was more or less than likely when determining accident from intention in traumatic injuries.

The computer imparts the ability to study cases, which vary by a single variable. This is not possible using mechanical laboratory experimentation without very large numbers of studies and even then, these are fraught with potential errors. As such, computer simulation of mandibular fractures using 3DFEA fills an important investigatory void.

Returning to the research application scenarios presented in chapter 1, it is necessary to determine whether the completed research would be of use to medico-legal practitioners or forensic scientists.

a) A dentist extracted a right molar tooth in a young man. Apparently, the procedure was routine and completed without complication. A week later, the patient complained of a pain in the contralateral parasymphysis of the mandible. After radiographic examination of the area, it was found that there was an ectopic tooth with a minimally enlarged follicle in the area of the fracture. The patient decided to take legal action and an expert witness was asked to provide information on whether the dentist had used excessive force or improper technique during the extraction or whether the ectopic tooth had made the mandible susceptible to fracture.

Whilst there are studies related to the effect of impacted third molar teeth on the propensity of the mandible to fracture there are none related to ectopic teeth and mandibular fractures, as these are rarer and each case will be unique. The expert witness would have to extrapolate the finding from studies on impacted third molar

teeth in order to give an opinion. This would make the opinion more speculative. 3DFEA could aid in answering this question. In this case, one would need to determine the force required to fracture a mandible by applying force in the region of the extraction, and the range of forces required to fracture a mandible with the ectopic tooth. In order to use the research model to analyse this, a radiograph of the injury would be required in order to determine the position and size of the third molar tooth. These would be part of the normal clinical radiographs. Two models would be analysed, one with the ectopic tooth in the radiographic position and another without the tooth. Dynamic analyses would be performed which would determine whether forces applied in this area were likely to cause this pattern of mandibular fracture and the relative difference in forces required in the two modelled scenarios. It may be the case that the analysis suggested that the fracture pattern is incorrect for forces applied in that area, and that some other incident had occurred in the intervening week before presentation, fracturing the mandible. Alternatively, it may be found that the position of the ectopic tooth was such that there was little difference in the strength of the mandible at that point. The range of forces required to remove teeth is available in the literature. The expert witness could therefore use the 3DFEA data as supporting evidence for his opinion on whether the dentist's actions were likely to have caused the fracture or whether another injury was more likely. Relative fracture risk could easily be determined by examination of the ratio cortical stress $_{\text{ectopic tooth}}$: cortical stress$_{\text{normal mandible}}$.

b) Forensic science deals with the relationship between medicine and law, and whilst much of the work is performed post mortem (Gordon and Shapiro, 1975) the ability to demonstrate the correlation between an assault weapon and injury in live patients is often the requirement of an expert witness. At their best, an expert can only suggest a possible cause of an injury and differentiating

between assaults with a foot, a fist, an elbow, a forehead or indeed any other blunt or sharp weapon resulting in a mandibular fracture may be difficult. Any additional supporting evidence would strengthen an opinion.

In this second scenario, the research 3DFEA model could be of significant benefit in providing supporting information. The model is capable of providing information on mandibular impacts using any object, from any position and any angle. Multiple scenarios could be tested, using 3DFEA as a method not necessarily identifying the possible assault weapon, but to exclude weapons and scenarios related to purported mechanisms of injury. As with all expert testimony, the more supporting evidence that may be presented the better.

At the conclusion of this research, it can be said that the research aims have been achieved. This research begins to fill a void in understanding between laboratory cadaveric experimentation and clinical findings. Having produced a 3DFEA model through an iterative process, the final model is capable of answering both basic and applied biomechanical questions related to mandibular fracture that may be of real benefit to those working in medico-legal or forensic fields.

Chapter 6 Limitations and future research

The research limitations associated with the modelling and analysis phases of the research are detailed below.

6.1 General project limitations

Three of the main limitations of any academic research include the availability of resources, specifically finances and time. This research was no exception. As biological 3DFEA was a research area which was relatively new to the university at the time of the research, the learning curve was steep, especially the production of a suitable 3DFEA model. As no standard modelling technique exists, much time was spent on this aspect of research, trying software and hardware combinations. In many commercial research-establishments, this stage is performed by a third-party. The model production aspect of the research (Phase I) occupied almost 12 months, including finding suitable open source data, software packages and learning their use. Had sufficient funding been available the author could have attended advanced training courses to increase learning speed and productivity. However, with the modelling knowledge gained and the protocols derived from this research, future models would take a fraction of the time to produce.

Financial constraints were mentioned previously. As this research is heavily dependent on computing power, with increased power more detailed modelling could have been undertaken and more complex analyses undertaken. The number of analyses that could be performed would have been increased as analyses could have been performed quicker. Computation time was a serious limitation, with the initial computing power resulting in analyses which took up to 10 days to run.

6.2 Research limitations

Much research using 3DFEA is undertaken in industry where custom software and advanced proprietary algorithms are available for use. There may be better material models to describe bone, rather than the generalized elastic-plastic material model used for this research. Most analysis software has many available add-on modules, which increase functionality and simplify tasks. Unfortunately, only the basic software was available for this research, limiting functionality.

Although much literature on 3DFEA is in English, research is published in many languages and the author was on occasions limited in the ability to extract technical details from them. Time could have been saved, reducing technical errors, or detailing more efficient ways to achieve results, if some of the literature had been made available in English.

The literature review in chapter two showed that at the time of the research there was only a single paper published that could be described as being of a similar nature to the research undertaken here. Studying the work of others in the field can only help to expedite research progress, however, with such little published data the research may be considered evolutionary rather than revolutionary.

6.2.1 Modelling limitations.

6.2.1.1 Data

3DFEA begins with the acquisition of data. The facial CT data of a 17-year-old male was selected for this research. This was an open-source clinical scan and as such was insufficient to capture all of the mandibular structures, such as the complete structure of the tooth and its surrounding ligament. Additionally, the actual trabeculation of the

cancellous bone was not captured, meaning that this important structure was modelled as a homogeneous mass.

Many biological 3DFEA studies on extinct organisms have used micro CT scans. These extremely high-resolution scans provide very high radiation dosages, which are inappropriate for clinical use, providing practical and ethical limitations. On reflection, such a scan could have been performed on a cadaveric skull; however, neither the opportunity to obtain cadaveric material or the facility for undertaking micro CT scans was available at the time of the research. The voxel-based modelling approach could have been used to increase model production speed. Importing CT scans into software, which employs voxel transformation, would have seemed a more streamlined process. This was attempted, however, several problems were encountered. The surface quality of the model was relatively poor, being entirely determined by the resolution of the clinical scan. As voxels were directly converted into finite elements, any artifacts contained in the original scan were also converted into finite elements. The direct conversion of voxels into finite elements limited elements to the hexahedral type. These were found to be less useful for complex shapes unless the element resolution was very high.

6.2.1.2 Model complexity

Initially a very high-resolution model was produced similar in form to that of Castaño, et al. (2002). It included individual components for the cortical bone and the cancellous bone. Teeth were modelled individually and contained enamel, dentine, cementum and pulp components as well as individual periodontal ligaments. A modelled hemi-mandible was produced which was then mirrored to produce a complete symmetrical mandible. The final model had an element resolution well in excess of 10 million tetrahedra. Unfortunately, this was well above the level that could be used to perform calculations

with the software and computing resources that existed at the time. It was also realized that many of the structures represented were not directly under investigation and therefore did not require modelling; however, this limitation reduced the number of useful “incidental” findings that research may sometimes reveal.

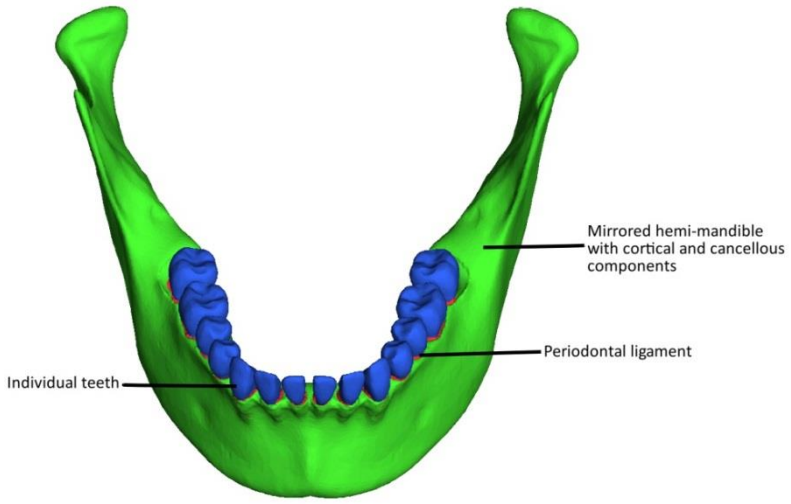

A mandibular model produced with all mandibular structures including cortical bone, cancellous bone, individual teeth and individual supporting periodontal ligaments.

The acquisition of other forms of required data also presented limitations to the research. Bone is one of the most complex mandibular structures to model. It is known that both cortical and cancellous bone have anisotropic, non-linear material properties, yet no model to date has succeeded in the application of such properties to mandibular bone in a finite-element model. The reasons are two-fold. Firstly, there is simply a lack of data available and secondly, the application of such properties to finite elements would be extremely difficult. Orthotropic bone properties have been substituted by many authors to approximate to anisotropic properties. In this research, a model based on orthotropic properties was produced. The mandible was divided into sections and local axes were assigned to each section (after Lovald, et al., 2009). Unlike the *Lovald* study, different material properties were applied lingually and buccally. When the

analyses were run, artificial boundaries were found where the material properties suddenly changed from one value to another. This made the interpretation of the results very difficult. The resulting models produced very little difference in results compared to the isotropic models for a much greater processing overhead.

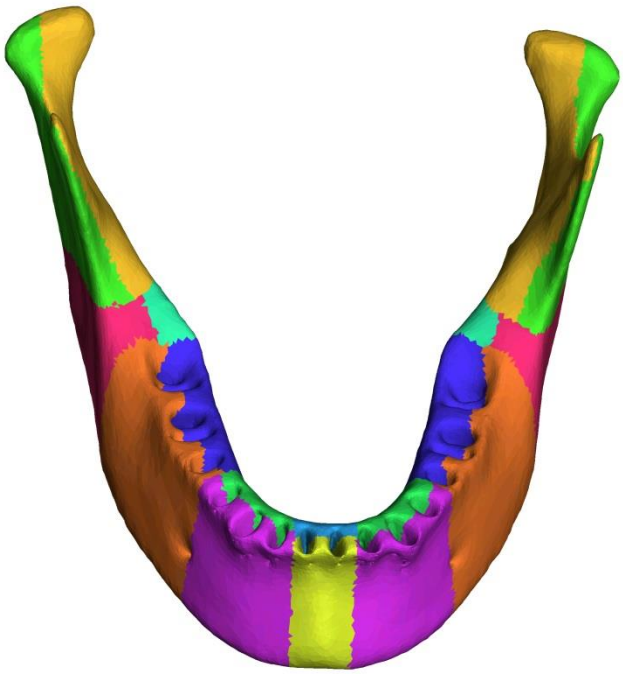

The mandibular model with regionally orthotropic material properties. The various colours represented areas where the mean Young's Modulus differed and a different local axis was assigned. Cancellous bone was still modelled as isotropic in this model. This was an improvement on the model of Lovald, et al. (2009), in that individual regional buccal and lingual orthotropic properties were assigned to the model.

Eventually the model was abandoned due to unnecessary complexity and little increase in accuracy (and possibly a reduction) in deformation studies.

Other modelling compromises that may have influenced the results were the lack of facial soft tissues, especially the muscles attached to the mandible. It was decided that the model would only include the muscles of mastication, as these are the most powerful movers of the mandible. The depressor muscles and the other facial soft-tissues were not considered. The combined effect of these on the cortical stress may

have been significant, especially in terms of the absorbing impact energy and shielding the mandible. Thus, the calculated forces required to fracture the mandible would relate only to explanted cadaveric dried specimen, rather than the real life situation. This does not negate the value of the research, as the modelling of such structures is merely a limitation that could be resolved with greater computing power. The principle of the calculations may be applied to any future model with soft-tissues.

6.2.1.3 Muscles

The finite element model employed an ad hoc traction modelling method whereby the effect of muscle forces was provided by the direct application of resultant muscle force vectors to the model over the area of muscle insertion. This method assumed that in the natural situation, muscle fibres were all of the same contractile power and were distributed evenly over the site of insertion. This is not the case in real life. The modelling method only took into account the resultant force vector, which is again non-physiological. This modelling limitation tended to over-estimate the effect of the muscles. This tended to be insignificant with respect to bony fracture, however, as mentioned earlier not all muscles were modelled.

An improved technique, other than modelling the muscles themselves, would be to employ a muscle-wrapping technique (or the tangential-plus-normal-traction model, Grosse et al. 2007) to take into account tangential and normal effects of muscles on cortical bone. Modelling the muscles themselves, would have to be validated against in vivo strain gauge measurements, which would be both unethical and impractical, presenting a limitation, which is unlikely to be overcome until a non-invasive method of determining strain in vivo is developed.

The muscles were applied at muscular insertion sites on the mandible according to standard anatomical texts. This simplification ignores the fact that all muscle insertions are individual and related to skeletal form and function. The mandibular muscles may provide an additional bracing effect on the surrounding bones, which could provide additional protection against fracture due to lateral forces.

The analyses on the effect of musculature on the mandibular cortex provided useful information on the likelihood of direct fracture. The model was limited in that no particular muscle recruitment pattern was modelled. This may mean that the simultaneous contraction of all muscle groups may have work antagonistically to reduce the total load on the mandible. The lack of a co-ordinated muscle action meant that bony displacement could not be studied. The muscle action would have been minimal in real life in the first 1ms of fracture formation.

6.2.1.4 Ligaments

Several ligaments that are important clinically, including the lateral temporomandibular and sphenomandibular, were not modelled. This band of fibrous tissue tightens when the mandible moves from its rest position, stabilising the joint. The degree of restraint provided by these ligaments directly influences the propensity of the condylar neck to fracture, or dislocate. As the temporomandibular joint was only modelled as an ankylosis, only one part of the range of joint movements was modelled, meaning that the model, whilst providing an accurate replication of the cadaveric experimental laboratory validation studies, was insufficient to fully replicate clinical scenarios.

The lack of maxillary teeth in the model had an effect on the fractures modelled. When teeth are in occlusion, no strain is placed on the TMJ when the mandible receives an upward impact, reducing the incidence of condylar head and neck damage. This meant

that in the research model, there were a higher number of impacts resulting in condylar injuries than might normally occur.

It would have been possible to model the effect of teeth by placing a point restraint on the crowns of the affected teeth to mimic the occlusion. However, modelling the potential contacts of 32 teeth realistically could have been problematic.

6.2.1.5 Biomechanical parameters

In an attempt to study the effect of variations in strain rate on mandibular fracture, the Cowper-Symonds scaling equation was used to provide an estimate of the yield stress. The strain rate parameters are individual for each material. These were obtained from the literature. These varied widely, and none were available for mandibular bone. This made calculations inaccurate for providing anything other than the derivation of a trend. As the equation provides an estimation of yield stress it is not as accurate as determining the yield stress of samples of fresh cadaveric human mandibular bone. The use of biological tissue, which would involve ethical approval, would involve the acquisition of human material, testing facilities and an increase in research time.

6.2.1.6 Validation

True quantitative validation of the research model was not possible for ethical reasons. This would require mandibular strain data to be obtained from human beings before, during and after mandibular fracture. It would be equally unethical to perform such tests on animals. Clearly, any lack of validation is a serious limitation on the model's use in medico-legal or forensic situations in any form other than as supporting evidence for a purported theory of mechanism of injury. That being said, no other mandibular trauma model, mechanical or otherwise has been validated against human data.

6.2.2 Limitations of the analyses

6.2.2.1 Load position and angulation

This reduced the number of fracture patterns seen in the results. As these limitations were purely due to constraints of the stated in the research scope there should be no reason that these could not be studied given more time.

6.2.2.2 Material properties

The effects of changes in global or local material properties were studied rather crudely. The properties for the clinical condition of osteogenesis imperfecta (type III) were for a single sample of bone and did not take into consideration the changes in Young's modulus associated with the other forms of the disease. Where local changes in properties, such as un-erupted third molar teeth and the associated periodontal ligament and dental follicle, were modelled they relatively poor approximations of clinical conditions. It would have been useful to study the effect size of third molar tooth, depth of impaction, angulation and follicle size on the propensity of the mandible to fracture. This would have enabled a more comprehensive conclusion to be drawn. However, the three extreme lesions studied i.e. a cystic lesion, no lesion and an ankylosed un-erupted third molar tooth (all of the same position and volume) allowed a derivation of the general trend rather than exact calculation of associated risk. The cystic lesion itself only represented the unilocular variant.

6.2.2.3 Non-linear analyses

There are many forms on non-linearity e.g. material non-linearity, boundary non-linearity and geometric non-linearity. Only material non-linearity was considered in the

analyses. When changes in geometry have a significant effect on the stiffness of the structure geometric non-linearity is important. It was assumed that this would not be the case; however, this was not formally tested.

6.2.2.4 Impacting objects

Fracture patterns may be influenced by the nature of the impacting object. The dynamic analyses included a single impacting object i.e. a model fist. Other objects of different surface area would result in different areas of high stress on impact, changing the temporal occurrence of multifocal fractures and the fracture combinations. The model produced is capable of analysing impacts with any object that may be modelled, limited only by time and available computing power.

6.2.3 Limitations on forensic and medico-legal use

Despite the useful advances made in this research, the 3DFEA model is not ready for everyday forensic or medico-legal work. This particular model has been designed to answer specific questions and therefore the model set-up (especially the details modelled and the arrangement of the temporomandibular joint) would not be applicable to other situations. The whole modelling process takes an extremely long time (although not as long as laboratory cadaveric experiments) and this is not something that the end-user would want to be involved in. As a result of this, if this were to be available to scientists and clinicians, the modelling would have to be performed by a third party which was aware of the research question. The end-user would then presented with an analysis model upon which a limited number of parameters such as the material properties and impact object and angulation could be changed. Output variables would also have to be limited so as to reduce the processing overhead. The end-user would have to specify these output variables beforehand. The

current model cannot determine the true displacement of fragments due to the lack of muscle modelling, however, this would not be necessary, as the clinical picture would show these details. Currently, only direct impacts to the mandible may be modelled and this tends to limit the medico-legal use more than the forensic.

6.3 Future work

Future work the 3DFEA study of traumatic mandibular fractures will be based around two areas, namely the improvement of the model and the development of the model to a complete clinical problem-solving environment.

Improving the model

Many of the limitations of the current research were imposed by the availability of computing power at an affordable price. Since the start of this research, the £1500 allocated for computing equipment could purchase a significantly more powerful, multiprocessor machine, which would allow analysis of a much larger more complex model.

In terms of features that could be usefully improved would be expansion of the model to include the whole craniofacial skeleton. There are many models available in the literature that study individual parts of the facial skeleton including the zygomatic complex, the individual bones of the cranium, the orbits and the maxilla. As such, the traumatic injuries studies in each of these regions appear to occur in isolation. This is clearly not the case in real life. Each injury affects the surrounding tissues to a greater of lesser extent. Knowledge of this is of particular interest in the detection of injuries. A good example would be the research model where the temporomandibular joints were modelled using restraints. A whole craniofacial skeleton would not only allow the study of the whole range of mandibular fractures but also the effect of mandibular fractures

on other parts of the head, such as the brain. The study of brain injuries was one of the first uses for 3DFEA. These studies were related to brain injury from cranial impacts; however, with the recent focus on sport-related brain injury, especially boxing, it might be pertinent to study the effect of recurrent mandibular impacts on cranial base and brain injuries.

As the mandible was modelled in isolation, many mandibular structures were not modelled, such as the periodontal ligament, the cementum, enamel and pulp of the tooth. The modelling of tooth structures was restricted by the scan resolution of clinical data, however, in future, as any model produced would be generic, micro CT scan data from cadaveric material would solve this problem. Modeling teeth with the accompanying periodontal ligaments may also be important in studying injuries to other regions such as the brain. The loss of teeth during an impact to the mandible may have a protective effect on the brain in a similar manner to fracture at the condylar neck. Whether or not this is true has not been formally tested. This would only require a small extension to the current model i.e. the inclusion of the maxilla and cranial base.

Cancellous bone was modelled as a single homogeneous structure, and given isotropic properties. Modelling cortical bone as an anisotropic material will continue to present a problem as sufficient data to perform this is unavailable. Cancellous bone presents an even greater problem. Solving these problems in the short-term is unlikely to be possible.

The soft-tissue were largely ignored in the analyses, however, they lay a significant role in the absorption of impact energy. Firstly, muscles could be more effectively modelled rather than being represented as force vectors. Multibody dynamics analysis has been combined with finite element analysis to calculate loading conditions and joint reaction forces of muscles groups (Curtis, et al., 2008). Calculating the forces produced by

muscles will allow the study of the displacement of fracture fragments, which themselves cause injury.

Eventually, the research model will require the application of all facial soft tissues. Before this can be performed, more details on the material properties will be required. The decision will then be whether to model the tissues as a homogeneous mass or model each layer. This will depend on the application to which the model is being put. It is likely that a homogeneous mass would be satisfactory for a trauma simulation, but this might not be the case for forensic cases where soft tissue injuries are also important.

This research largely concentrated on the use of the 3DFEA model to solve some clinically related problems that may arise in forensic or medico-legal practice. A full craniofacial 3DFEA model would have great potential as an academic tool to understand the effect of injuries three-dimensionally i.e. what injuries to expect following a traumatic impact, especially those that are remote from the impact site, how such injuries occur and how the craniofacial skeleton can be protected to avoid them. Such a tool could improve trauma understanding, teaching, and perhaps treatment, in the same way in which three-dimensional computer models have improved anatomy understanding and radiographic interpretation.

Bibliography

Abbasi, M.M., Abbas, I., Khan, N., Shah, S.M., Hameed, H., Shad, S. and Zulfiqar, K. (2012) 'Frequency of un-erupted mandibular third molar in mandibular angle fractures', Journal of Ayub Medical College Abbottabad, vol. 24, no. 1, pp. 30-32.

Abdullah, W.A., Al-Mutairi, K., Al-Ali, Y., Al-Soghier, A. and Al-Shnwani, A. (2013) 'Patterns and etiology of maxillofacial fractures in Riyadh City, Saudi Arabia', Saudi Dental Journal, vol. 25, no. 1, Jan, pp. 33-38.

Adebayo, E.T., Ajike, O.S. and Adekeye, E.O. (2003) 'Analysis of the pattern of maxillofacial fractures in Kaduna, Nigeria', British Journal of Oral and Maxillofacial Surgery, vol. 41, no. 6, Dec, pp. 396-400.

Adams, V.A. (2008) A Designer's Guide to Simulation with Finite Element Analysis, NAFEMS.

Adekeye, E.O. (1980) 'Pediatric fractures of the facial skeleton: a survey of 85 cases from Kaduna, Nigeria', Journal of Oral Surgery, vol. 38, no. 5, May, pp. 355-358.

Adekeye, E.O. (1980) 'The pattern of fractures of the facial skeleton in Kaduna, Nigeria. A survey of 1,447 cases', Oral Surgery Oral Medicine and Oral Pathology, vol. 49, no. 6, Jun, pp. 491-495.

Adi, M., Ogden, G.R. and Chisholm, D.M. (1990) 'An analysis of mandibular fractures in Dundee, Scotland (1977 to 1985)', British Journal of Oral and Maxillofacial Surgery, vol. 28, no. 3, Jun, pp. 194-199.

Ajagbe, H.A., Daramola, J.O. and Oluwasanmi, J.O. (1977) 'Civilian type facial injuries - a retrospective study of cases seen at the University College Hospital, Ibadan', Nigerian Medical Journal, vol. 4, pp. 432-437.

Aksoy, E., Unlü, E. and Sensöz, O. (2002) 'A retrospective study on epidemiology and treatment of maxillofacial fractures', Journal of Craniofacial Surgery, vol. 13, no. 6, Nov, pp. 772-775.

Al Ahmed, H.E., Jaber, M.A., Abu Fanas, S.H. and Karas, M. (2004) 'The pattern of maxillofacial fractures in Sharjah, United Arab Emirates: a review of 230 cases', Oral Surgery Oral Medicine Oral Pathology Oral Radiology and Endodontics, vol. 98, no. 2, Aug, pp. 166-170.

Al-Aboosi, K. and Perriman, A. (1976) 'One hundred cases of mandibular fractures in children in Iraq', International Journal of Oral Surgery, vol. 5, no. 1, Feb, pp. 8-12.

Al-Khateeb, T. and Abdullah, F.M. (2007) 'Craniomaxillofacial injuries in the United Arab Emirates: a retrospective study', Journal of Oral and Maxillofacial Surgery, vol. 65, no. 6, Jun, pp. 1094-1101.

Alonso, M.B., Costa, P.P., Issa, J.P., Monteiro, S.A., Tiossi, R. and Watanabe, P.C. (2011) 'Radiographical evaluation of bone quality after extraction of mandibular impacted and semi-impacted third molars', Minerva Stomatologica, vol. 60, no. 7-8, pp. 359-364.

Ammar, H.H., Ngan, P., Crout, R.J., Mucino, V.H. and Mukdadi, O.M. (2011) 'Three-dimensional modeling and finite element analysis in treatment planning for orthodontic tooth movement', American Journal of Orthodontics and Dentofacial Orthopedics, vol. 139, no. 1, Jan, pp. e59-e71.

Anderson, P.J. (1995) 'Fractures of the facial skeleton in children', Injury, vol. 26, no. 1, Jan, pp. 47-50.

Andersson, L., Hultin, M., Nordenram, A. and Ramström, G. (1984) 'Jaw fractures in the county of Stockholm (1978-1980) (I). General survey', International Journal of Oral Surgery, vol. 13, no. 3, Jun, pp. 194-199.

Anker, A.H. (1996) 'What is the future of third molar removal? A critical review of the need for the removal of third molars', Annals of the Royal Australasian College of Dental Surgeons, vol. 13, pp. 154-157.

Ansari, M.H. (2004) 'Maxillofacial fractures in Hamedan province, Iran: a retrospective study (1987-2001)', Journal of cranio-maxillo-facial surgery : official publication of the European Association for Cranio-Maxillo-Facial Surgery, vol. 32, no. 1, Feb, pp. 28-34.

Antoun, J.S. and Lee, K.H. (2008) 'Sports-related maxillofacial fractures over an 11-year period', Journal of Oral and Maxillofacial Surgery, vol. 66, no. 3, Mar, pp. 504-508

Anyanechi, C.E. and Saheeb, B.D. (2011) 'Mandibular sites prone to fracture: analysis of 174 cases in a Nigerian tertiary hospital', Ghana Medical Journal, vol. 45, no. 3, Sep, pp. 111-114.

Arbag, H., Korkmaz, H.H., Ozturk, K. and Uyar, Y. (2008) 'Comparative evaluation of different miniplates for internal fixation of mandible fractures using finite element analysis', Journal of Oral and Maxillofacial Surgery, vol. 66, no. 6, Jun, pp. 1225-1232.

Arosarena, O., Ducic, Y. and Tollefson, T. (2012) 'Mandible Fractures. Discussion and Debate', Facial Plastic Surgery Clinics of North America, vol. 20, no. 3, pp. 347-363.

Arrigoni J. and Lambrecht J.T. (2004) 'Complications during and after third molar extraction', Schweiz Monatsschr Zahnmed, vol. 114, no. 12, pp. 1271-1286.

Arvind, R.J., Narendar, R., Kumar, P.D., Venkataraman, S. and Gokulanathan (2013) 'Maxillofacial trauma in Tamil Nadu children and adolescents: A retrospective study', Journal of Pharmacy and Bioallied Sciences, vol. 5, no. Suppl 1, pp. S33-S35.

Ashman, R.B., Cowin, S.C., Van Buskirk, W.C. and Rice, J.C. (1984) 'A continuous wave technique for the measurement of the elastic properties of cortical bone', Journal of Biomechanics, vol. 17, no. 5, Jan, pp. 349-361.

Ashman, R.B. and Van Buskirk, W.C. (1987) 'The elastic properties of a human mandible', Advances in Dental Research, vol. 1, no. 1, Oct, pp. 64-67.

Ashman, R.B., Van Buskirk, W.C., Cowin, S.C., Sandborn, P.M., Wells, M.K. and Rice, J.C. (1985) 'The mechanical properties of immature osteopetrotic bone', Calcified Tissue International, vol. 37, no. 1, Jan, pp. 73-76.

Atanasov, D.T. and Vuvakis, V.M. (2000) 'Mandibular fracture complications associated with the third molar lying in the fracture line', Folia Medica, vol. 42, no. 1, pp. 41-46.

Bamjee, Y., Lownie, J.F., Cleaton-Jones, P.E. and Lownie, M.A. (1996) 'Maxillofacial injuries in a group of South Africans under 18 years of age', British Journal of Oral and Maxillofacial Surgery, vol. 34, pp. 298-302.

Banks, P. and Brown, A. (2003) Fractures of the facial skeleton, 1st edition, Edinburgh, London, New York, Oxford, Philadelphia, St Louis, Sydney, Toronto: Butterworth-Heinemann.

Barabas, J., Sandor, G.K., Bujtar, P. and Szucs, A. (2010) 'Finite element analysis of the human mandible to assess the effect of removing an impacted third molar', Journal of the Canadian Dental Association, vol. 76, p. a72.

Baron, P. and Debussy, T. (1979) 'A biomechanical functional analysis of the masticatory muscles in man', Archives of Oral Biology, vol. 24, pp. 547-553.

Bataineh, A.B. (1998) 'Etiology and incidence of maxillofacial fractures in the north of Jordan', Oral Surgery Oral Medicine Oral Pathology Oral Radiology and Endodontics, vol. 86, pp. 31-35.

Begg, C.B. and Mazumdar, M. (1994) 'Operating characteristics of a rank correlation test for publication bias', Biometrics, vol. 50, pp. 1088-1101.

Bezerra, T.P., Studart-Soares, E.-C., Pita-Neto, I.-C., Costa, F.-W.-G. and Batista, S.-H.-B. (2011) 'Do third molars weaken the mandibular angle?', Medicina Oral, Patologia Oral y Cirugia Bucal, vol. 16, no. 5, pp. e657-e663.

Bither, S., Mahindra, U., Halli, R. and Kini, Y. (2008) 'Incidence and pattern of mandibular fractures in rural population: a review of 324 patients at a tertiary hospital in Loni, Maharashtra, India', Dental Traumatology, vol. 24, no. 4, Aug, pp. 468-470.

Boccaccio, A., Cozzani, M. and Pappalettere, C. (2011) 'Analysis of the performance of different orthodontic devices for mandibular symphyseal distraction osteogenesis', European Journal of Orthodontics, vol. 33, no. 2, Apr, pp. 113-120.

Boccaccio, A., Pappalettere, C. and Kelly, D.J. (2007) 'The influence of expansion rates on mandibular distraction osteogenesis: a computational analysis', Annals of Biomedical Engineering, vol. 35, no. 11, pp. 1940-1960.

Boffano, P., Ferretti, F., Giunta, G. and Gallesio, C. (2012) 'Surgical removal of a third molar at risk for mandibular pathologic fracture: Case report and clinical considerations', Oral Surgery, Oral Medicine, Oral Pathology and Oral Radiology, vol. 114, no. 6, pp. e1-e4.

Bonfield, W. and Li, C.H. (1968) 'The temperature-dependence of the deformation of bone', Journal of Biomechanics, vol. 1, pp. 323-329.

Bonfield, W. and Tully, A.E. (1982) 'Ultrasonic analysis of the Young's modulus of cortical bone', Journal of Biomedical Engineering, vol. 4, pp. 23-27.

Boole, J.R., Holtel, M., Amoroso, P. and Yore, M. (2001) '5196 mandible fractures among 4381 active duty army soldiers, 1980 to 1998', The Laryngoscope, vol. 111, pp. 1691-1696.

Borenstein, M., Hedges, L.V., Higgins, J.P.T. and Rothstein, H.R. (2009) Introduction to meta-analysis, Chichester, West Sussex: John Wiley and Sons, Ltd.

Bormann, K.-H., Wild, S., Gellrich, N.-C., Kokemüller, H., Stühmer, C., Schmelzeisen, R. and Schön, R. (2009) 'Five-year retrospective study of mandibular fractures in Freiburg, Germany: incidence, etiology, treatment, and complications', Journal Of Oral And Maxillofacial Surgery, vol. 67, no. 6, Jun, pp. 1251-1255.

Brasileiro, B.F. and Passeri, L.A. (2006) 'Epidemiological analysis of maxillofacial fractures in Brazil: a 5-year prospective study', Oral Surgery Oral Medicine Oral Pathology Oral Radiology and Endodontics, vol. 102, no. 1, Jul, pp. 28-34.

Breeze, J., Gibbons, A.J., Hunt, N.C., Monaghan, A.M., Gibb, I., Hepper, A. and Midwinter, M. (2011) 'Mandibular fractures in British military personnel secondary to blast trauma sustained in Iraq and Afghanistan', British Journal of Oral and Maxillofacial Surgery, vol. 49, no. 8, pp. 607-611.

Buitrago-Tellez, C.H., Audige, L., Strong, B., Gawelin, P., Hirsch, J., Ehrenfeld, M., Ruddermann, R., Louis, P., Lindqvist, C., Kunz, C., Cornelius, P., Shumrick, K., Kellman, R.M., Sugar, A., Alpert, B., Prein, J. and Frodel (2008) 'A comprehensive classification of mandibular fractures: a preliminary agreement validation study', International Journal of Oral and Maxillofacial Surgery, vol. 37, pp. 1080-1088.

Burr, D.B., Milgrom, C., Fyhrie, D., Forwood, M., Nyska, M., Finestone, A., Hoshaw, S., Saiag, E. and Simkin, A. (1996) 'In vivo measurement of human tibial strains during vigorous activity', Bone, vol. 18, pp. 405-410.

Cankaya, A., Erdem, M., Cakarer, S., Cifter, M. and Oral, C. (2011) 'Iatrogenic mandibular fracture associated with third molar removal', International Journal of Medical Sciences, vol. 8, no. 7, pp. 547-553.

Carter, D.R. (1984) 'Mechanical loading histories and cortical bone remodeling', Calcified Tissue International, vol. 36, pp. 519-524.

Carter, D.R., Harris, W.H., Vasu, R. and Caler, E. (1981) 'The mechanical and biological response of cortical bone to in vivo strain histories', American Society of Mechanical Engineers, vol. 45, p. 81.

Carter, D.R., Hayes, W.C. and Schurman, D.J. (1976) 'Fatigue life of compact bone -II. Effects of microstructure and density', Journal of Biomechanics, vol. 9, pp. 211-218.

Casey, D.M. and Emrich, L.J. (1988) 'Changes in the mandibular angle in the edentulous state', Journal of Prosthetic Dentistry, vol. 59, no. 3, pp. 373-380.

Castaño, M.C., Zapata, U., Pedroza, A., Jaramillo, J.D. and Roldán (2002) 'Creation of a Three-dimensional Model of the Mandible and the TMJ by means of the Finite Element Method ', International Journal of Computerized dentistry, vol. 5, pp. 87-99.

Chamay, A. (1970) 'Mechanical and morphological aspects of experimental overload and fatigue in bone', Journal of Biomechanics, vol. 3, pp. 263-270.

Chambers, I.G. and Scully, C. (1987) 'Mandibular fractures in India during the Second World War (1944 and 1945): analysis of the Snawdon series', British Journal of Oral and Maxillofacial Surgery, vol. 25, no. 5, Oct, pp. 357-369.

Chen, Y., Miao, Y., Xu, C., Zhang, G., Lei, T. and Tan, Y. (2010) 'Wound ballistics of the pig mandibular angle: a preliminary finite element analysis and experimental study', Journal of Biomechanics, vol. 43, pp. 1131-1137.

Choi, B.-H., Huh, J.-Y., Suh, C.-H. and Kim, K.-N. (2005) 'An in vitro evaluation of miniplate fixation techniques for fractures of the atrophic edentulous mandible', International Journal of Oral and Maxillofacial Surgery, vol. 34, no. 2, Mar, pp. 174-177.

Choi, J.-P., Baek, S.-H. and Choi, J.-Y. (2010) 'Evaluation of stress distribution in resorbable screw fixation system: three-dimensional finite element analysis of mandibular setback surgery with bilateral sagittal split ramus osteotomy', The Journal of Craniofacial Surgery, vol. 21, no. 4, Jul, pp. 1104-1109.

Chole, R.H., Patil, R.N., Chole, S.B., Gondivkar, S., Gadbail, A.R. and Yuwanati, M.B. (2013) 'Association of mandible anatomy with age, gender, and dental status: a radiographic study', ISRN Radiology, vol. 2013, pp. 1-4.

Chrcanovic, B.R. and Custodio, A.L.N. (2010) 'Considerations of mandibular angle fractures during and after surgery for removal of third molars: A review of the literature', Oral and Maxillofacial Surgery, vol. 14, no. 2, pp. 71-80.

Christiaens, I. and Reychler, H. (2002) 'Complications after third molar extractions: retrospective analysis of 1,213 teeth', Revue De Stomatologie Et De Chirurgie Maxillo-Faciale, vol. 103, no. 5, pp. 269-274.

Colton, C.K.S., Schatzker, J. and Trafton, P. (2014) AO Surgery Reference. Online reference in clinical life, [Online], Available: https://www2.aofoundation.org/wps /portal/surgery [1 April 2014].

Copcu, E., Sisman, N. and Oztan, Y. (2004) 'Trauma and fracture of the mandible', European Journal of Trauma, vol. 2, pp. 110-115.

Courant, R. (1943) 'Variational methods for the solution of problems of equilibrium and vibrations', Bulletin of the American Mathematical Society, vol. 49, pp. 1-23.

Cowper, G. and Symonds, P. (1957) 'Strain hardening and strain-rate effects in the impact loading of cantilever beams', Technical report (Brown University, Division of Applied Mathematics), vol. 28, p. c11.

Cox, T., Kohn, M.W. and Impelluso, T. (2003) 'Computerized analysis of resorbable polymer plates and screws for the rigid fixation of mandibular angle fractures', Journal of Oral and Maxillofacial Surgery, vol. 61, no. 4, Apr, pp. 481-87.

Craig, R.G., Peyton, F.A. and Johnson, D.W. (1961) 'Compressive properties of enamel, dental cements and gold', Journal of Dental Research, vol. 40, no. 5, pp. 936-945.

Curtis, N., Kupczik, K., O'Higgins, P., Moazen, M. and Fagan, M. (2008) 'Predicting Skull Loading: Applying Multibody Dynamics Analysis to a Macaque Skull', The Anatomical Record, vol. 291, pp. 491-501.

Daegling, D.J., Hotzman, J.L. and Rapoff, A.J. (2008) 'Effects of Dental Alveoli on the Biomechanical Behavior of the Mandibular Corpus', in Primate Craniofacial Function and Biology, Springer US.

de Matos, F.P., Arnez, M.F.M., Sverzut, C.E. and Trivellato, A.E. (2010) 'A retrospective study of mandibular fracture in a 40-month period', International Journal of Oral and Maxillofacial Surgery, vol. 39, no. 1, Jan, pp. 10-15.

de Oliveira, D.M., Andrade, E.S., da Silveira, M.M.F. and Carmargo, I.B. (2008) 'Correlation of the Radiographic and Morphological Features of the Dental Follicle of Third Molars with Incomplete Root formation', International Journal of Medical Sciences, vol. 5, no. 1, pp. 36-40.

Dingman, R.O. and Natvig, P. (1964) Surgery of Facial Fractures, Philadelphia: WB Saunders.

Doblaré, M., García, J.M. and Gómez, M.J. (2004) 'Modelling bone tissue fracture and healing: a review', Engineering Fracture Mechanics, vol. 71, pp. 1809-1840.

Dodson, T.B. (1996) 'Impacted third molar and mandibular angle fractures', Oral Surgery Oral Medicine Oral Pathology Oral Radiology and Endodontics, vol. 81, no. 3, pp. 264-265.

Dongas, P. and Hall, G.M. (2002) 'Mandibular fracture patterns in Tasmania, Australia', Australian Dental Journal, vol. 47, no. 2, Jun, pp. 131-137.

Dorin Ruse, N. (2008) 'Propagation of erroneous data for the modulus of elasticity of the periodontal ligament and gutta perch in FEM/FEA papers: A story of broken links', Dental Materials, vol. 24, pp. 1717-1719.

Duan, D.H. and Zhang, Y. (2008) 'Does the presence of mandibular third molars increase the risk of angle fracture and simultaneously decrease the risk of condylar fracture?', International Journal of Oral and Maxillofacial Surgery, vol. 37, no. 1, pp. 25-28.

Duarte, B., Assis, D., Ribeiro-Junior, P. and Gonçales, E. (2012) 'Does the relationship between retained mandibular third molar and mandibular angle fracture exist? An assessment of three possible causes', Craniomaxillofacial trauma and reconstruction, vol. 5, no. 3, pp. 127-136.

Dumont, E.R., Picrririllo, J. and Grosse, I.R. (2005) 'Finite-element analysis of biting behaviour and bone stress in the facial skeletons of bats', The Anatomical Record Part A: Discoveries in Molecular, Cellular, and Evolutionary Biology, vol. 283A, no. 2, pp. 319-330.

Duncanson, M.G. and Korostoff, E. (1975) 'Compressive viscoelastic properties of human dentin: 1. Stress-relaxation behaviour', Journal of Dental Research, vol. 54, pp. 1207-1212.

Eggensperger Wymann, N.M., Holzle, A., Zachariou, Z. and Iizuka, T. (2008) 'Pediatric craniofacial trauma', Journal of Oral and Maxillofacial Surgery, vol. 66, no. 1, pp. 58-64.

Egger, M. (1997) 'Bias in meta-analysis detected by a simple, graphical test', British Medical Journal, vol. 315, pp. 629-634.

Elgehani, R.-A. and Orafi, M.-I. (2009) 'Incidence of mandibular fractures in Eastern part of Libya', Med Oral Patol Oral Cir Bucal, vol. 14, no. 10, pp. e529-532.

Ellis 3rd, E., Moos, K.F. and el-Attar, A. (1985) 'Ten years of mandibular fractures: an analysis of 2,137 cases', Oral Surgery Oral Medicine and Oral Pathology, vol. 59, no. 2, Feb, pp. 120-129.

Emshoff, R., Schöning, H., Röthler, G. and Waldhart, E. (1997) 'Trends in the incidence and cause of sport-related mandibular fractures: a retrospective analysis', Journal of Oral and Maxillofacial Surgery, vol. 55, no. 6, Jun, pp. 585-92.

Ericson, S. and Bjerklin, K. (2001) 'The dental follicle in normally and ectopically erupting maxillary canines: a computed tomography study', Angle Orthodontist, vol. 71, no. 5, pp. 333-342.

Ertem, S.Y., Uckan, S. and Ozden, U.A. (2013) 'The comparison of angular and curvilinear marginal mandibulectomy on force distribution with three dimensional finite element analysis', Journal of cranio-maxillo-facial surgery : official publication of the European Association for Cranio-Maxillo-Facial Surgery, vol. 41, no. 3, Apr, pp. e54-8.

Eskitaşcıoğlu, T., Ozyazgan, I., Coruh, A., Günay, G.K., Yontar, Y. and Altıparmak, M. (2013) 'Fractures of the mandible: a 20-year retrospective analysis of 753 patients', Turkish Journal of Trauma and Emergency Surgery, vol. 19, no. 4, Jul, pp. 348-56.

Eskitaşcıoğlu, T., Ozyazgan, I., Coruh, A., Gunay, G.K. and Yuksel, E. (2009) 'Retrospective analysis of two hundred thirty-five pediatric mandibular fracture cases', Annals of Plastic Surgery, vol. 63, no. 5, Nov, pp. 522-30.

Ethunandan, M., Shanahan, D. and Patel, M. (2012) 'Iatrogenic mandibular fractures following removal of impacted third molars: An analysis of 130 cases', British Dental Journal, vol. 212, no. 4, pp. 179-184.

Fan, Z. and Rho, J.Y. (2003) 'The effects of viscoelasticity and time-dependent plasticity to nanoindentation measurement of a human cortical bone', Journal of Biomedical Materials Research Part A, vol. 67A, pp. 208-214.

Fasola, A.O., Nyako, E.A., Obiechina, A.E. and Arotiba, J.T. (2003) 'Trends in the characteristics of maxillofacial fractures in Nigeria', Journal of Oral and Maxillofacial Surgery, vol. 61, no. 10, Oct, pp. 1140-1143.

Fasola, A.O., Obiechina, A.E. and Arotiba, J.T. (2001) 'Fractures of the mandible in children', East African Medical Journal, vol. 78, no. 11, Nov, pp. 616-618.

Fasola, A.O., Obiechina, A.E. and Arotiba, J.T. (2003) 'Incidence and pattern of maxillofacial fractures in the elderly', International Journal of Oral and Maxillofacial Surgery, vol. 32, no. 2, Apr, pp. 206-208.

Fenech, C.M. and Keaveny, T.M. (1999) 'A cellular solid criterion for predicting the axial-shear failure properties of bovine trabecular bone', Journal of Biomechanical Engineering, vol. 121, pp. 414-422.

Fernández, J.R., Gallas, M., Burguera, M. and Viaño, J.M. (2003) 'A three-dimensional numerical simulation of mandible fracture reduction with screwed miniplates', Journal of Biomechanics, vol. 36, no. 3, Mar, pp. 329-337.

Ferreira, P.C., Amarante, J.M., Silva, A.C., Pereira, J.M., Cardoso, M.A. and Rodrigues, J.M. (2004) 'Etiology and patterns of pediatric mandibular fractures in Portugal: a retrospective study of 10 years', Journal of Craniofacial Surgery, vol. 15, no. 3, May, pp. 384-391.

Fill, T.S., Toogood, R.W., Major, P.W. and Carey, J.P. (2012) 'Analytically determined mechanical properties of, and models for the periodontal ligament: Critical review of literature', Journal of Biomechanics, vol. 45, pp. 9-16.

Fridrich, K., Pena-Velasco, G. and Olson, R. (1992) 'Changing trends with mandibular fractures: a review of 1067 cases', Journal of Oral and Maxillofacial Surgery, vol. 50, pp. 586-589.

Fuselier, J.C., Ellis III, E.E. and Dodson, T.B. (2002) 'Do mandibular third molars alter the risk of angle fracture?', Journal of Maxillofacial and Oral Surgery, vol. 60, no. 5, pp. 514-518.

Gaball, C., Lovald, S., Baack, B. and Olson, G. (2011) 'Minimally invasive bioabsorbable bone plates for rigid internal fixation of mandible fractures', Archives of Facial Plastic Surgery, vol. 13, no. 1, pp. 31-35.

Gaddipati, R., Ramisetty, S., Vura, N., Kanduri, R.R. and Gunda, V.K. (2014 (epub ahead of print)) 'Impacted mandibular third molars and their influence on mandibular angle and condyle fractures - A retrospective study', Journal of cranio-maxillo-facial surgery: official publication of the European Association for Cranio-Maxillo-Facial Surgery, Jan.

Gallas Torreira, M. and Fernandez, J.R. (2004) 'A three-dimensional computer model of the human mandible in two simulated standard trauma situations', Journal of cranio-maxillo-facial surgery : official publication of the European Association for Cranio-Maxillo-Facial Surgery, vol. 32, no. 5, Oct, pp. 303-307.

Gandhi, S., Ranganathan, L.K., Solanki, M., Mathew, G.C., Singh, I. and Bither, S. (2011) 'Pattern of maxillofacial fractures at a tertiary hospital in northern India: a 4-year retrospective study of 718 patients', Dental Traumatology, vol. 27, no. 4, Aug, pp. 257-262.

Ghodke, M.H., Subhash, C.B. and Seemit, V.S. (2013) 'Prevalence of mandibular fractures reported at C.S.M.S.S. Dental College, Aurangabad from February 2008 to September 2009', Journal of International Society of Preventative and Community Dentistry, vol. 3, no. 2, pp. 51-58.

Glazer, M., Joshua, B.Z., Woldenberg, Y. and Bodner, L. (2011) 'Mandibular fractures in children: analysis of 61 cases and review of the literature', International Journal of Pediatric Otorhinolaryngology, vol. 75, no. 1, Jan, pp. 62-64.

Goldberg, M.H. (2000) 'Mandibular fracture after third molar removal', Journal of Oral and Maxillofacial Surgery, vol. 58, no. 10, p. 1112

Goldberg, M.G. and Williams, A.C. (1969) 'The location and occurrence of mandibular fractures. An analysis of 202 cases', Oral Surgery, Oral Medicine and Oral Pathology, vol. 28, no. 3, Sep, pp. 336-341.

Gordon, I. and Shapiro, H.A. (1975) Forensic Medicine- A Guide to Principles, Edinburgh: Churchill-Livingstone.

Gorman, R. H. (2009) 'The Physics of a Karate Punch', [Online], Available at: http://www.thebrotherhoodofveteranwarriors.com/articles/Karate Punch Physics.html, [Accessed 14 2 2014].

Goussard, F., Damien Germain, D., Delmer, C. and Morenod, K. (2010) 'Finite element analysis: A promising tool for the reconstruction of extinct vertebrate graviportal taxa. A

preliminary study based on the metacarpal arrangement of Elephas maximus', Comptes Rendus Palevol, vol. 9, pp. 455–461.

Gröning, F., Fagan, M.J. and O'Higgins, P. (2011) 'The effects of the periodontal ligament on mandibular stiffness: a study combining finite element analysis and geometric morphometrics', Journal of Biomechanics, vol. 44, pp. 1304–1312.

Grosse, I., Dumont, E.R., Coletta, C. and Tolleson, A. (2007) 'Techniques for modelling muscle-induced forces in finite element models of skeletal structures', The Anatomical Record, vol. 290, pp. 1069-1088.

Hall, R.K. (1972) 'Injuries of the face and jaws in children', International Journal of Oral Surgery, vol. 1, no. 2, pp. 65-75.

Hall, S.C. and Ofodile, F.A. (1991) 'Mandibular fractures in an American inner city: the Harlem Hospital Center experience', Journal of the National Medical Association, vol. 83, no. 5, May, pp. 421-423.

Hallmer, F., Anderud, J., Sunzel, B., Güner, N. and Andersson, G. (2010) 'Jaw fractures diagnosed and treated at Malmö University Hospital: a comparison of three decades', International Journal of Oral Maxillofacial Surgery, vol. 39, pp. 446-451.

Halmos, D.R., Ellis III, E. and Dodson, T.B. (2004) 'Mandibular third molars and angle fractures', Journal of Oral and Maxillofacial Surgery, vol. 62, no. 9, pp. 1076-1081.

Hansen, U., Zioupos, P., Simpson, R., Currey, J.D. and Hynd, D. (2008) 'The effect of strain rate on the mechanical properties of human cortical bone', Journal of Biomechanical Engineering, vol. 130, no. 1, pp. 011011(1-8).

Hanson, B.P., Cummings, P., Rivara, F.P. and John, M.T. (2004) 'The association of third molars with mandibular angle fractures: a meta-analysis', Journal of the Canadian Dental Association, vol. 70, no. 1, pp. 39-43.

Harbord, R.M., Egger, M. and Sterne, J.A.C. (2006) 'A modified test for small-study effects in meta-analyses of controlled trials with binary endpoints', Statistics in Medicine, vol. 25, no. 20, pp. 3443-3457.

Haug, R.H., Prather, J. and Indresano, A.T. (1990) 'An epidemiologic survey of facial fractures and concomitant injuries', Journal of Oral and Maxillofacial Surgery, vol. 48, no. 9, Sep, pp. 926-932.

Hayes, W.C. and Bouxsein, M.L. (1997) 'Biomechanics of cortical and trabecular bone: Implications for assessment of fracture risk', in Mow, V.C. and Hayes, W.C. (ed.) Basic Orthopaedic Biomechanics, Philadelphia: Lippincott-Raven.

Higgins, J.P.T. and Thompson, S.G. (2002) 'Quantifying heterogeneity in a meta-analysis', Statistics in Medicine, vol. 21, pp. 1539-1558.

Higgins, J.P.T., Thompson, S.G., Deeks, J.J. and Altman, D.G. (2003) 'Measuring inconsistency in meta-analyses', British Medical Journal, vol. 327, pp. 557-560.

Hill, C.M., Crosher, R.F., Carroll, M.J. and Mason, D.A. (1984) 'Facial fractures-the results of a prospective four-year-study', Journal of Maxillofacial Surgery, vol. 12, no. 6, Dec, pp. 267-270.

Hogg, N.J.V. and Horswell, B.B. (2006) 'Hard tissue pediatric facial trauma: a review', Journal of the Canadian Dental Association, vol. 72, no. 6, pp. 555-558.

Huelke, D.F. and Compton, C.P. (1983) 'Facial injuries in automobile crashes', Journal of Oral and Maxillofacial Surgery, vol. 41, p. 2414.

Hung, Y.C., Montazem, A. and Costello, M.l.A. (2004) 'The correlation between mandible fractures and loss of consciousness', Journal of Oral and Maxillofacial Surgery, vol. 62, no. 8, Aug, pp. 938-942.

Huston, R.L. (2013) Fundamentals of Biomechanics, Florida: CRC Press Taylorand Francis Group.

Iida, S., Hassfeld, S., Reuther, T., Nomura, K. and Muhling, J. (2005) 'Relationship between the risk of mandibular angle fractures and the status of incompletely erupted mandibular third molar', Journal of Cranio-Maxillofacial Surgery, vol. 33, no. 3, pp. 158-163.

Iida, S., Hassfeld, S., Reuther, T., Schweigert, H.-G., Haag, C., Klein, J. and Mühling, J. (2003) 'Maxillofacial fractures resulting from falls', Journal of cranio-maxillo-facial surgery : official publication of the European Association for Cranio-Maxillo-Facial Surgery, vol. 31, no. 5, Oct, pp. 278-283.

Iida, S., Kogo, M., Sugiura, T., Mima, T. and Matsuya, T. (2001) 'Retrospective analysis of 1502 patients with facial fractures', International Journal of Oral and Maxillofacial Surgery, vol. 30, no. 4, Aug, pp. 286-290.

Iida, S., Nomura, K., Okura, M. and Kogo, M. (2004) 'Influence of the incompletely erupted lower third molar on mandibular angle and condylar fractures', The Journal of Trauma: Injury, Infection, and Critical Care, vol. 57, no. 3, pp. 613-617.

Iizuka, T., Tanne, R.S. and Berthold, H. (1997) 'Mandibular fractures following third molar extraction. A retrospective clinical and radiological study', International Journal of Oral and Maxillofacial Surgery, vol. 26, no. 5, pp. 338-343.

Imahara, S.D., Hopper, R.A., Wang, J., Rivara, F.P. and Klein, M.B. (2008) 'Patterns and outcomes of pediatric facial fractures in the United States: a survey of the National Trauma Data Bank', Journal Of The American College Of Surgeons, vol. 207, no. 5, Nov, pp. 710-716.

Inaoka, S.-D., Carneiro, S.-C.-D.A.-S., Vasconcelos, B.-C.-D.E., Leal, J. and Porto, G.-G. (2009) 'Relationship between mandibular fracture and impacted lower third molar', Medicina Oral, Patologia Oral y Cirugia Bucal, vol. 14, no. 7, pp. e349-e354.

Infante Cossio, P., Espin Galvez, F., Gutierrez Perez, J.L., Garcia-Perla, A. and Hernandez Guisado, J.M. (1994) 'Mandibular fractures in children. A retrospective study of 99 fractures in 59 patients', International Journal of Oral and Maxillofacial Surgery, vol. 23, no. 6 Pt. 1, Dec, pp. 329-331.

Iwamoto, M., Miki, K. and Tanaka, E. (2005) 'Ankle skeletal injury prediction using anisotropic inelastic constitutive model of cortical bone taking into account damage evolution', Stapp Car Crash Journal, vol. 49, pp. 133-156.

Janssen, M., Zuidema, J. and Wanhill, R.J.H. (2004) Fracture Mechanics, 2nd edition, London, New York: Taylor and Francis e-Library.

Ji, B., Wang, C., Liu, L., Long, J., Tian, W. and Wang, H. (2010) 'A biomechanical analysis of titanium miniplates used for treatment of mandibular symphyseal fractures with the finite element method', Oral Surgery, Oral Medicine, Oral Pathology, Oral Radiology, and Endodontics, vol. 109, no. 3, Mar, pp. e21-e27.

Ji, B., Wang, C., Song, F., Chen, M. and Wang, H. (2012) 'A new biomechanical model for evaluation of fixation systems of maxillofacial fractures', Journal of cranio-maxillo-facial surgery : official publication of the European Association for Cranio-Maxillo-Facial Surgery, vol. 40, no. 5, Jul, pp. 405-408.

Joshi, S.R., Saluja, H., Pendyala, G.S., Chaudhari, S., Mahindra, U. and Kini, Y. (2013) 'Pattern and prevalence of maxillofacial fractures in rural children of central Maharashtra, India. A retrospective study', Journal of Maxillofacial and Oral Surgery, vol. 12, no. 3, Sep, pp. 307-311.

Kadkhodaie, M.H. (2006) 'Three-year review of facial fractures at a teaching hospital in northern Iran', British Journal of Oral and Maxillofacial Surgery, vol. 44, no. 3, Jun, pp. 229-331.

Kasamatsu, A., Watanabe, T. and Kanazawa, H. (2003) 'Presence of the third molar as a risk factor in mandibular angle fractures', Asian Journal of Oral and Maxillofacial Surgery, vol. 15, no. 3, pp. 176-180.

Kavanagh, E.P., Frawley, C., Kearns, G., Wallis, F., McGloughlin, T. and Jarvis, J. (2008) 'Use of finite element analysis in presurgical planning: treatment of mandibular fractures', Irish Journal of Medical Science, vol. 177, no. 4, Dec, pp. 325-331.

Kazanjian, V.H. and Converse, J. (1974) Surgical Treatment of Facial Injuries, Baltimore, MD: Williams and Wilkins.

Kelly, D. and Harrigan, W. (1975) 'A survey of facial fractures: Bellevue Hospital 1948-1974', Journal of Oral Surgery, vol. 33, pp. 145-149.

Kemper, A., McNally, C., Kennedy, E., Manoogian, S. and Duma, S. (2007) ' The material properties of human tibia cortical bone in tension and compression: Implications for the tibia index', Proceedings of the 20th Enhanced Safety of Vehicles Conference, Lyon, France, pp. 07-0470.

Keyak, J.H. (2000) 'Nonlinear finite element modeling to evaluate the failure load of the proximal femur', Journal of orthopaedic research: official publication of the Orthopaedic Research Society, vol. 18, no. 2, Mar, p. 337.

Keyak, J.H. (2000) 'Relationships between femoral fracture loads for two load configurations', Journal of Biomechanics, vol. 33, no. 4, Apr, pp. 499-502.

Keyak, J.H. (2001) 'Improved prediction of proximal femoral fracture load using nonlinear finite element models', Medical Engineering and Physics, vol. 23, no. 3, Apr, pp. 165-173.

Keyak, J.H., Lee, I.Y., Nath, D.S. and Skinner, H.B. (1996) 'Postfailure compressive behavior of tibial trabecular bone in three anatomic directions', Journal of Biomedical Materials Research, vol. 31, no. 3, Jul, pp. 373-378.

Keyak, J.H., Lee, I.Y. and Skinner, H.B. (1994) 'Correlations between orthogonal mechanical properties and density of trabecular bone: use of different densitometric measures', Journal of Biomedical Materials Research, vol. 28, no. 11, Nov, pp. 1329-1336.

Keyak, J.H., Meagher, J.M., Skinner, H.B. and Mote Jr, C.D. (1990) 'Automated three-dimensional finite element modelling of bone, a new method', Journal of Biomedical Engineering, vol. 12, pp. 389-397.

Keyak, J.H. and Rossi, S.A. (2000) 'Prediction of femoral fracture load using finite element models: an examination of stress- and strain-based failure theories', Journal of Biomechanics, vol. 33, no. 2, Feb, pp. 209-214.

Keyak, J.H., Rossi, S.A., Jones, K.A., Les, C.M. and Skinner, H.B. (2001) 'Prediction of fracture location in the proximal femur using finite element models', Medical Engineering and Physics, vol. 23, no. 9, Nov, pp. 657-664.

Keyak, J.H., Rossi, S.A., Jones, K.A. and Skinner, H.B. (1998) 'Prediction of femoral fracture load using automated finite element modeling', Journal of Biomechanics, vol. 31, no. 2, Feb, pp. 125-133.

Keyak, J.H. and Skinner, H.B. (1992) 'Three-dimensional finite element modelling of bone: effects of element size', Journal of Biomedical Engineering, vol. 14, no. 6, Nov, pp. 483-489.

Keyak, J.H. and Skinner, H.B. (1995) 'Comment on: The use of strain energy as a convergence criterion in the finite element modelling of bone and the effect of model

geometry on stress convergence', Medical Engineering and Physics, vol. 17, no. 4, Jun, p. 320.

Keyak, J.H., Skinner, H.B. and Fleming, J.A. (2001) 'Effect of force direction on femoral fracture load for two types of loading conditions', Journal of orthopaedic research : official publication of the Orthopaedic Research Society, vol. 19, no. 4, Jul, pp. 539-544.

Kimsal, J., Baack, B., Candelaria, L., Khraishi, T. and Lovald, S. (2011) 'Biomechanical analysis of mandibular angle fractures', Journal of Oral and Maxillofacial Surgery, vol. 69, no. 12, Dec, pp. 3010-3014.

King, R.E., Scianna, J.M. and Petruzzelli, G.J. (2004) 'Mandible fracture patterns: a suburban trauma center experience', American Journal of Otolaryngology, vol. 25, pp. 301-307.

Kiong, T.K., Mustafa, W.M.W. and Sockalingam, G. (2007) 'Paediatric facial fractures: one-year survey of 23 government hospitals in Malaysia', Asian Journal of Oral and Maxillofacial Surgery, vol. 19, pp. 30-33.

Knoll, W.-D., Gaida, A. and Maurer, P. (2006) 'Analysis of mechanical stress in reconstruction plates for bridging mandibular angle defects', Journal of cranio-maxillo-facial surgery : official publication of the European Association for Cranio-Maxillo-Facial Surgery, vol. 34, no. 4, Jun, pp. 201-209.

Korkmaz, H.H. (2007) 'Evaluation of different miniplates in fixation of fractured human mandible with the finite element method', Oral Surgery Oral Medicine Oral Pathology Oral Radiology and Endodontics, vol. 103, no. 6, Jun, pp. e1-13.

Korostoff, E., Pollack, S.R. and Duncanson, M.G. (1975) 'Viscoelastic properties of human dentin', Journal of Biomedical Materials Research, vol. 9, pp. 661-674.

Kromka, M. and Milewski, G. (2007) 'Experimental and numerical approach to chosen types of mandibular fractures cured by means of miniplate osteosynthesis', Acta of Bioengineering and Biomechanics, vol. 9, no. 2, pp. 49-54.

Kupczik, K., Dobson, C.A., Fagan, M.J., Crompton, R.H., Oxnard, C.E. and O'Higgins, P. (2007) 'Assessing mechanical function of the zygomatic region in macaques: validation and sensitivity testing of finite element models', Journal of Anatomy, vol. 210, pp. 41-53.

Kyrgidis, A., Koloutsos, G., Kommata, A., Lazarides, N. and Antoniades, K. (2013) 'Incidence, aetiology, treatment outcome and complications of maxillofacial fractures. A retrospective study from Northern Greece', Journal of cranio-maxillo-facial surgery : official publication of the European Association for Cranio-Maxillo-Facial Surgery, vol. 41, no. 7, Oct, pp. 637-643.

Lanyon, L.E., Hampson, W.G.J., Goodship, A.E. and Shah, J.S. (1975) 'Bone deformation recorded in vivo from strain gauges attached to the human tibial shaft', Acta Orthopaedica Scandinavica, vol. 46, pp. 256-268.

Le, B.T., Dierks, E.J., Ueeck, B.A., Homer, L.D. and Potter, B.F. (2001) 'Maxillofacial injuries associated with domestic violence', Journal of Oral and Maxillofacial Surgery, vol. 59, no. 11, Nov, pp. 1277-83; discussion 1283-4.

Lee, K.H. (2008) 'Epidemiology of mandibular fractures in a tertiary trauma centre', Emergency Medicine Journal, vol. 25, no. 9, Sep, pp. 565-568.

Lee, K.H. (2009) 'Interpersonal violence and facial fractures', Journal of Oral and Maxillofacial Surgery, vol. 67, no. 9, pp. 1878-1883.

Lee, J.H., Cho, B.K. and Park, W.J. (2010) 'A 4-year retrospective study of facial fractures on Jeju, Korea', Journal of Cranio-Maxillo-Facial Surgery, vol. 38, pp. 192-196.

Lee, H.L. and Chou, H.-J. (2010) 'Facial fractures in work-related injuries', Asian Journal of Oral and Maxillofacial Surgery, vol. 22, pp. 138-142.

Lee, J. and Dodson, T. (2000) 'The effect of mandibular third molar presence and position on the risk of an angle fracture', Journal of Oral and Maxillofacial Surgery, vol. 58, no. 4, pp. 394-399.

Lei, T., Xie, L., Tu, W., Chen, Y., Tang, Z. and Tan, Y. (2012) 'Blast injuries to the human mandible: development of a finite element model and a preliminary finite element analysis', Injury, vol. 43, no. 11, Nov, pp. 1850-1855.

Liberati, A., Altman, D.G., Tetzlaff, J., Mulrow, C., Gøtzsche, P.C., Ioannidis, J.P.A., Clark, M., Devereaux, P.J., Kleijnen, J. and Moher, D. (2009) 'The PRISMA Statement for Reporting Systematic Reviews and Meta-Analyses of Studies That Evaluate Health Care Interventions: Explanation and Elaboration', PLoS Medicine, vol. 6, no. 7, p. e1000100.

Li, Z., Kindig, M.W., Kerrigan, J.R., Untaroiu, C.D., Subit, D., Crandall, J.R. and Kent, R.W. (2010) 'Rib fractures under anterior-posterior dynamic loads: Experimental and finite-element study', Journal of Biomechanics, vol. 43, pp. 228-234.

Lindahl, L. (1977) 'Condylar fractures of the mandible. I. Classification and relation to age, occlusion, and concomitant injuries of teeth-supporting structures, and fractures of the mandibular body', International Journal of Oral Surgery, vol. 12-21, p. 6.

Lindqvist, C., Sorsa, S., Hyrkäs, T. and Santavirta, S. (1986) 'Maxillofacial fractures sustained in bicycle accidents', International Journal of Oral and Maxillofacial Surgery, vol. 15, no. 1, Feb, pp. 12-18.

Linn, E.W., Vrijhoef, M.M., de Wijn, J.R., Coops, R.P., Cliteur, B.F. and Meerloo, R. (1986) 'Facial injuries sustained during sports and games', Journal of Maxillofacial Surgery, vol. 14, no. 2, Apr, pp. 83-88.

Li, P., Tang, Y., Li, J., Shen, L., Tian, W. and Tang, W. (2013) 'Establishment of sequential software processing for a biomechanical model of mandibular reconstruction with custom-made plate', Computer Methods and Programs in Biomedicine, vol. 111, no. 3, pp. 642-649.

Livermore Software Technology Corporation (LSTC) (February 2013) LS-DYNA KEYWORD USER'S MANUAL. VOLUME II. Material Models, 70th edition, California: Livermore Software Technology Corporation.

Lopes, P (2009) 'Material assignment method', in Mimics 13.0 reference guide, Leuven, Belgium: Materialise.

Lorensen, W.E. and Cline, H.E. (1987) 'Marching Cubes: A High Resolution 3D Surface Construction Algorithm', Computer Graphics, vol. 21, no. 3, pp. 163-169.

Lotz, J.C., Cheal, E.J. and Hayes, W.C. (1991) 'Fracture prediction for the proximal femur using finite element models: Part II- Nonlinear analysis', Journal of Biomechanical Engineering, vol. 113, pp. 361-365.

Loukota, R.A., Eckelt, U., De Bont, L. and Rasse, M. (2005) 'Subclassification of fractures of the condylar process of the mandible', British Journal of Oral and Maxillofacial Surgery, vol. 43, pp. 72-73.

Lovald, S.T., Khraishi, T., Wagner, J. and Baack, B. (2009) 'Mechanical design optimization of bioabsorbable fixation devices for bone fractures', Journal of Craniofacial Surgery, vol. 20, no. 2, Mar, pp. 389-398.

Lovald, S.T., Wagner, J.D. and Baack, B. (2009) 'Biomechanical optimization of bone plates used in rigid fixation of mandibular fractures', Journal of Oral and Maxillofacial Surgery, vol. 67, no. 5, May, pp. 973-985.

Luria, J.S. and Campbell, J.H. (2013) 'Fracture patterns associated with the presence of mandibular third molars', Journal of Oral and Maxillofacial Surgery, vol. 71, no. 9 SUPPL. 1, p. e100.

Ma'aita, J. and Alwrikat, A. (2000) 'Is the mandibular third molar a risk factor for mandibular angle fracture?', Oral Surgery Oral Medicine Oral Pathology Oral Radiology And Endodontics, vol. 89, no. 2, pp. 143-146.

MacLennan, W.D. (1952) 'Consideration of 180 cases of typical fractures of the mandibular condylar process', British Journal of Plastic Surgery, vol. 5, pp. 122-128.

Madhi, A.G.M. and Ali, I.A.A. (2013) 'A retrospective analytic study of mandibular fracture patterns in two different periods in Baghdad', Journal of Oral and Maxillofacial Surgery, Medicine, and Pathology, vol. 25, no. 3, pp. 205-209.

Marinescu, R., Daegling, D.J. and Rapoff, A.J. (2005) 'Finite element modeling of the anthropoid mandible: the effects of altered boundary conditions', The Anatomical Record Part A: Discoveries in Molecular, Cellular, and Evolutionary Biology, vol. 283, no. 3, pp. 300-309.

Marker, P., Eckerdal, A. and Smith-Sivertsen, C. (1994) 'Incompletely erupted third molars in the line of mandibular fractures. A retrospective analysis of 57 cases', Oral Surgery, Oral Medicine and Oral Pathology, vol. 78, no. 4, pp. 426-431.

Martins, M.M., Homsi, N., Pereira, C.C., Jardim, E.C. and Garcia, I.R.J. (2011) 'Epidemiologic evaluation of mandibular fractures in the Rio de Janeiro high-complexity hospital', Journal of Craniofacial Surgery, vol. 22, no. 6, pp. 2026-2030.

McMinn, R.M.H. (1994) Last's Anatomy. Regional and Applied, 9th edition, Edinburgh, London, Madrid, Melbourne, New York and Tokyo: Churchill Livingstone.

McMinn, R.M.H., Hutchings, R.T., Pegington, J. and Abrahams, P.H. (1993) A Colour Atlas of Human Anatomy, 3rd edition, Hong Kong: Mosby-Wolfe.

Meechan, J.G. (2000) 'The effect of mandibular third molar presence and position on the risk of an angle fracture', Journal of Oral and Maxillofacial Surgery, vol. 58, no. 4, p. 399.

Meisami, T., Sojat, A., Sandor, G.K., Lawrence, H.P. and Clokie, C.M. (2002) 'Impacted third molars and risk of angle fracture', International Journal of Oral and Maxillofacial Surgery, vol. 31, no. 2, pp. 140-144.

Mesnard, M., Ramos, A., Ballu, A., Morlier, J., Cid, M. and Simoes, J.A. (2011) 'Biomechanical analysis comparing natural and alloplastic temporomandibular joint replacement using a finite element model', Journal of Oral and Maxillofacial Surgery, vol. 69, no. 4, Apr, pp. 1008-1017.

Mijiti, A., Ling, W., Tuerdi, M., Maimaiti, A., Tuerxun, J., Tao, Y.-Z., Saimaiti, A. and Moming, A. (2014) 'Epidemiological analysis of maxillofacial fractures treated at a university hospital, Xinjiang, China: A 5-year retrospective study', Journal of cranio-maxillo-facial surgery : official publication of the European Association for Cranio-Maxillo-Facial Surgery, vol. 42, no. 3, Apr, pp. 227-233.

Milzman, D., Weiner, D. and Murray, R. (2013) 'Presence of third molars predicts increased mandible fractures', Journal of Investigative Medicine, vol. 61, no. 3, pp. 662-663.

Milzman, D., Weiner, D., Napoli, A. and Smith, M. (2013) 'Presence of third molars predicts increased mandible fractures in blunt facial trauma', Academic Emergency Medicine, vol. 20, no. 5 SUPPL. 1, p. S168.

Ming-Yih, L., Chun-Li, L., Wen-Da, T. and Lun-Jou, L. (2010) 'Biomechanical stability analysis of rigid intraoral fixation for bilateral sagittal split osteotomy', Journal of Plastic, Reconstructive and Aesthetic Surgery, vol. 63, no. 3, Mar, pp. 451-455.

Moore, J.R. (1976) Principles of Oral Surgery, 2nd edition, Manchester: Manchester University Press.

Moroi, H.H., Okimoto, K., Moroi, R. and Terada, Y. (1993) 'Numeric approach to the biomechanical analysis of thermal effects in coated implants', International Journal Of Prosthodontics, vol. 6, pp. 564-572.

Morris, A.J. (1996) 'The qualification of safety critical structures by finite element analytical methods', Journal of Aerospace Engineering, vol. 210, pp. 203-208.

Mukherjee, S., Chawla, A., Borouah, S., Sahoo, D. and Arun, W.J.A. (2011) 'Dynamic properties of the shoulder complex bones', The 22nd International Technical Conference on the Enhanced Safety of Vehicles (ESV), 13 June.

Müller, W. (1969) '[The luxation fracture of the condylar process of the mandible with dislocation towards the back]', Deutsche Zahn-, Mund-, und Kieferheilkunde mit Zentralblatt für die Gesamte Zahn-, Mund-, und Kieferheilkunde, vol. 53, no. 9, Dec, pp. 348-357.

Muñante-Cárdenas, J.L., Asprino, L., De Moraes, M., Albergaria-Barbosa, J.R. and Moreira, R.W.F. (2010) 'Mandibular fractures in a group of Brazilian subjects under 18 years of age: A epidemiological analysis', International Journal of Pediatric Otorhinolaryngology, vol. 74, no. 11, Nov, pp. 1276-1280.

Murakami, K., Sugiura, T., Yamamoto, K., Kawakami, M., Kang, Y.-B., Tsutsumi, S. and Kirita, T. (2011) 'Biomechanical analysis of the strength of the mandible after marginal resection', Journal of Oral and Maxillofacial Surgery, vol. 69, no. 6, Jun, pp. 1798-1806.

Murakami, K., Yamamoto, K., Sugiura, T., Kawakami, M., Kang, Y.-B., Tsutsumi, S. and Kirita, T. (2013) 'Effect of clenching on biomechanical response of human mandible and temporomandibular joint to traumatic force analyzed by finite element method', Med Oral Patol Oral Cir Bucal, vol. 18, no. 3, May, pp. e473-e478.

Mwaniki, D.L. and Guthua, S.W. (1990) 'Occurrence and characteristics of mandibular fractures in Nairobi, Kenya', British Journal of Oral and Maxillofacial Surgery, vol. 28, no. 3, Jun, pp. 200-202.

Mwaniki, D.L. and Guthua, S.W. (1991) 'Mandibular fractures: an appraisal of the weak regions', East African Medical Journal, vol. 68, no. 4, Apr, pp. 255-260.

Naghipur, S., Shah, A.A. and Elgazzar, R.F. (2013) 'The effect of lower third molar presence and position on fracture of the mandibular angle and condyle', Journal of Oral and Maxillofacial Surgery, vol. 71, no. 9 SUPPL. 1, pp. e95-e96.

Nahum, A.M. (1975) 'The biomechanics of facial bone fracture', Laryngoscope, vol. 85, no. 1, pp. 140-156.

Nahum, A.M. (1975) 'The biomechanics of maxillofacial trauma', Clinics in Plastic Surgery, vol. 2, no. 1, Jan, pp. 59-64.

Nalla, R.K., Kinney, J.H. and Ritchie, R.O. (2003) 'Mechanistic failure criteria for the failure of human cortical bone', Nature Materials, vol. 2, pp. 164-168.

Narra, N., Valášek, J., Hannula, M., Marcián, P., Sándor, G.K., Hyttinen, J. and Wolff, J. (2014) 'Finite element analysis of customized reconstruction plates for mandibular continuity defect therapy', Journal of Biomechanics, vol. 47, no. 1, Jan, pp. 264-268.

National Institute for Health and Care Excellence, (2000) 'Guidance on the Extraction of Wisdom Teeth', Available: guidance.nice.org.uk/ta1

Natu, S.S., Pradhan, H., Gupta, H., Alam, S., Gupta, S., Pradhan, R., Mohammad, S., Kohli, M., Sinha, V.P., Shankar, R. and Agarwal, A. (2012) 'An epidemiological study on pattern and incidence of mandibular fractures', Plastic Surgery International, vol. 2012, pp. 1-7.

Nelson, G.J. (1986) Three dimensional computer modelling of human mandibular biomechanics. MSc thesis, Vancouver: The University of British Columbia.

Ogundare, B.O., Bonnick, A. and Bayley, N. (2003) 'Pattern of mandibular fractures in an urban major trauma center', Journal of Oral and Maxillofacial Surgery, vol. 61, no. 6, Jun, pp. 713-718.

Oikarinen, K., Ignatius, E., Kauppi, H. and Silvennoinen, U. (1993) 'Mandibular fractures in northern Finland in the 1980s-a 10-year study', British Journal of Oral and Maxillofacial Surgery, vol. 31, no. 1, Feb, pp. 23-27.

Oji, C. (1998) 'Fractures of the facial skeleton in children: a survey of patients under the age of 11 years', Journal of cranio-maxillo-facial surgery : official publication of the European Association for Cranio-Maxillo-Facial Surgery, vol. 26, no. 5, Oct, pp. 322-325.

Oji, C. (1999) 'Jaw fractures in Enugu, Nigeria, 1985-95', British Journal of Oral and Maxillofacial Surgery, vol. 37, no. 2, Apr, pp. 106-109.

Ólafsson, S.H. (1984) 'Fractures of the facial skeleton in Reykjavik, Iceland, 1970-1979. (I) Mandibular fracture in 238 hospitalized patients, 1970-79', International Journal of Oral Surgery, vol. 13, no. 6, Dec, pp. 495-505.

Olasoji, H.O., Tahir, A. and Bukar, A. (2002) 'Jaw fractures in Nigerian children: an analysis of 102 cases', Central African Journal of Medicine, vol. 48, no. 9-10, pp. 109-112.

Olson, R., Fonseca, R., Zeitler, D. and Osbon, D. (1982) 'Fractures of the mandible: a review of 580 cases', Journal of Oral and Maxillofacial Surgery, vol. 40, pp. 23-28.

Ortakoğlu, K., Günaydin, Y., Aydintuğ, Y.S. and Bayar, G.R. (2004) 'An analysis of maxillofacial fractures: a 5-year survey of 157 patients', Military Medicine, vol. 169, no. 9, Sep, pp. 723-727.

Özkaya, N., Nordin, M. and Goldsheyder, D.L.D. (2012) Fundamentals of Biomechanics. Equilibrium, Motion, and Deformation, 3rd edition, New York, Dordrecht, Heidelberg, London: Springer.

Panagiotopoulou, O., Kupczik, K. and Cobb, S.N. (2011) 'The mechanical function of the periodontal ligament in the macaque mandible: a validation and sensitivity study using finite element analysis', Journal of Anatomy, vol. 218, no. 1, pp. 75-86.

Pankratov, A. and Robustova, T. (2001) 'A classification of mandibular fractures', Stomatologia M, vol. 2, pp. 29-31.

Parascandolo, S., Spinzia, A., Parascandolo, S., Piombino, P. and Califano, L. (2010) 'Two load sharing plates fixation in mandibular condylar fractures: biomechanical basis',

Journal of cranio-maxillo-facial surgery : official publication of the European Association for Cranio-Maxillo-Facial Surgery, vol. 38, no. 5, Jul, pp. 385-390.

Patil, P.M. (2012) 'Un-erupted lower third molars and their influence on fractures of the mandibular angle and condyle', British Journal of Oral and Maxillofacial Surgery, vol. 50, no. 5, pp. 443-446.

Peck, C.C., Langenbach, G.E.J. and Hannam, A.G. (2000) 'Dynamic simulation of muscle and articular properties during human wide jaw opening', Archives of Oral Biology, vol. 45, p. 969.

Pell, G.J. and Gregory, T. (1942) 'Report on a ten-year study of a tooth division technique for the removal of impacted teeth', American Journal of Orthodontics, vol. 28, p. 660.

Peltier, L.F. (1990) Fractures: A History and Iconography of Their Treatment. Norman orthopedic series, No. 1, San Francisco: Norman Publishing.

Pietrzak, G., Curnier, A., Botsis, J., Scherrer, S., Wiskott, A. and Belser, U. (2002) 'A nonlinear elastic model of the periodontal ligament and its numerical calibration for the study of tooth mobility', Computer Methods in Biomechanics and Biomedical Engineering, vol. 5, pp. 91-100.

Pini, M., Wiskott, H.W.A., Scherrer, S.S., Botsis, J. and Belser, U.C. (2002) 'Mechanical characterization of bovine periodontal ligament', Journal of Periodontal Research, vol. 37, p. 237-244.

Pogrel, M.A. and Kaban, L. (1989) 'Mandibular fracture', in Habal, A. (ed.) Facial Fractures, Toronto: B.C. Decker.

Qudah, M.A., Al-Khateeb, T., Bataineh, A.B. and Rawashdeh, M.A. (2005) 'Mandibular fractures in Jordanians: a comparative study between young and adult patients', Journal of cranio-maxillo-facial surgery : official publication of the European Association for Cranio-Maxillo-Facial Surgery, vol. 33, no. 2, Apr, pp. 103-106.

Rai, S. and Pradhan, R. (2011) 'Tooth in the line of fracture: its prognosis and its effects on healing', Indian Journal of Dental Research, vol. 22, no. 3, pp. 495-496.

Rajkumar, K., Ramen, S., Chowdhury, R. and Chattopadhyay, P. (2009) 'Mandibular third molars as a risk factor for angle fractures: a retrospective study.', Journal of Maxillofacial and Oral Surgery, vol. 8, no. 3, pp. 237-240.

Ramli, R., Abdul Rahman, R., Abdul Rahman, N., Abdul Karim, F., Krsna Rajandram, R., Mohamad, M.S.F., Mat Nor, G. and Sohadi, R.U.R. (2008) 'Pattern of maxillofacial injuries in motorcyclists in Malaysia', Journal of Craniofacial Surgery, vol. 19, no. 2, Mar, pp. 316-321.

Ramos, A., Completo, A., Relvas, C., Mesnard, M. and Simões, J.A. (2011) 'Straight, semi-anatomic and anatomic TMJ implants: the influence of condylar geometry and bone

fixation screws', Journal of cranio-maxillo-facial surgery : official publication of the European Association for Cranio-Maxillo-Facial Surgery, vol. 39, no. 5, Jul, pp. 343-350.

Reilly, D. and Burstein, A. (1975) 'The elastic and ultimate properties of compact bone tissue', Journal of Biomechanics, vol. 8, pp. 393-405.

Reitzik, M., Lownie, J.F., Cleaton-Jones, P. and Austin, J. (1978) 'Experimental fractures of monkey mandibles', International Journal of Oral Surgery, vol. 7, pp. 100-103.

Rhea, I.T., Rao, P.M. and Neovelline, R.A. (1999) 'Helical CT and three-dimensional CT of facial and orbital injury', Radiologic Clinics of North America, vol. 37, pp. 489-513.

Rho, J.Y., Ashman, R.B. and Turner, C.H. (1993) 'Young's modulus of trabecular and cortical bone material: ultrasonic and microtensile measurements', Journal of Biomechanics, vol. 26, pp. 111-119.

Roth, F.S., Kokoska, M.S., Awwad, E.E., Martin, D.S., Olson, G.T., Hollier, L.H. and Hollenbeak, C.S. (2005) 'The identification of mandible fractures by helical computed tomography and panorex tomography', Journal of Craniofacial Surgery, vol. 16, pp. 3940-3949.

Rowe, N.L. (1968) 'Fractures of the facial skeleton in children', Journal of Oral Surgery, vol. 26, no. 8, Aug, pp. 505-515.

Rowe, N.L. (1969) 'Fractures of the jaws in children', Journal of Oral Surgery, vol. 27, no. 7, Jul, pp. 497-507.

Rowe, N.L. (1971) 'The history of the treatment of maxillo-facial trauma', Annals of the Royal College of Surgeons of England, vol. 49, no. 5, Nov, pp. 329-349.

Rowe, N.L. and Killey, H.C. (1968) Fractures of the facial skeleton, London: Livingstone.

Sacknoff, R., Novelline, R.A., Rhea, J.T., Lawrason, J.N. and Rao, P.M. (1997) 'Mandibular fracture not shown by axial computed tomography: Benefit of computed reformation', Emergency Radiology, vol. 4, no. 2, pp. 109-111.

Sadler, T.W. (1994) Langman's Medical Embryology, 7th edition, Baltimore, Maryland: Williams and Wilkins.

Safdar, N. and Meechan, J.G. (1995) 'Relationship between fractures of the mandibular angle and the presence and state of eruption of the lower third molar', Oral Surgery Oral Medicine, Oral Pathology, Oral Radiology, and Endodontics, vol. 79, no. 6, pp. 680-684.

Sakr, K., Farag, I.A. and Zeitoun, I.M. (2006) 'Review of 509 mandibular fractures treated at the University Hospital, Alexandria, Egypt', British Journal of Oral and Maxillofacial Surgery, vol. 44, no. 2, Apr, pp. 107-111.

Salem, J.E., Lilly, G.E., Cutcher, J.L. and Steiner, M. (1968) 'Analysis of 523 mandibular fractures', Oral Surgery Oral Medicine and Oral Pathology, vol. 26, no. 3, Sep, pp. 390-395.

Sammarco, G.J., Burstein, A.H., Davis, W.L. and Frankel, V.H. (1971) 'The biomechanics of torsional fractures: The effect of loading on ultimate properties', Journal of Biomechanics, vol. 4, pp. 113-117.

Sanchez, G. M. and Meltzer, E. S. (2012) The Edwin Smith Papyrus: Updated Translation of the Trauma Treatise and Modern Medical Commentaries, Atlanta, Georgia: Lockwood Press.

Sane, J., Lindqvist, C. and Kontio, R. (1988) 'Sports-related maxillofacial fractures in a hospital material', International Journal of Oral and Maxillofacial Surgery, vol. 17, no. 2, Apr, pp. 122-124.

Sasaki, R.O.H., Kumasaka, A., Ando, T., Nakamura, K., Ueki, T., Okada, Y., Asanami, S., Chigono, Y., Ichinokawa, Y., Satomi, T., Matsuo, A. and Chiba, H. (2012) 'Analysis of the pattern of maxillofacial fracture by five departments in Tokyo: a review of 674 cases', Oral Science International, vol. 6, no. 1, pp. 1-7.

Savoldelli, C., Bouchard, P.-O., Loudad, R., Baque, P. and Tillier, Y. (2012) 'Stress distribution in the temporo-mandibular joint discs during jaw closing: a high-resolution three-dimensional finite-element model analysis', Surgical and Radiologic Anatomy, vol. 34, no. 5, Jul, pp. 405-413.

Sawhney, C.P. and Ahuja, R.B. (1988) 'Faciomaxillary fractures in north India. A statistical analysis and review of management', British Journal of Oral and Maxillofacial Surgery, vol. 26, no. 5, Oct, pp. 430-434.

Schneider, D.C. and Nahum, A.M. (1974) 'Impact studies of facial bones and skull', Proceedings of the 16th Stapp Car Crash Conference, SAE No. 720966, p. 204.

Schön, R., Roveda, S.I. and Carter, B. (2001) 'Mandibular fractures in Townsville, Australia: incidence, aetiology and treatment using the 2.0 AO/ASIF miniplate system', British Journal of Oral and Maxillofacial Surgery, vol. 39, no. 2, Apr, pp. 145-148.

Schuchardt, K., Schwenzer, N., Rottke, B. and Lentkodt, J. (1966) 'Ursachen Häufigkeit und Lokalisation der Frakturen des Desichtsschädels', Fortschritte der Kiefer- und Gesichts-Chirurgie, vol. 11, pp. 1-6.

Schuller-Götzburg, P., Pleschberger, M., Rammerstorfer, F.G. and Krenkel, C. (2009) '3D-FEM and histomorphology of mandibular reconstruction with the titanium functionally dynamic bridging plate', International Journal of Oral and Maxillofacial Surgery, vol. 38, no. 12, Dec, pp. 1298-1305.

Schwartz-Dabney, C.L. and Dechow, P.C. (2003) 'Variations in Cortical Material Properties Throughout the Human Dentate Mandible', American Journal of Physical Anthropology, vol. 120, pp. 252-277.

Simsek, S., Simsek, B., Abubaker, A.O. and Laskin, D.M. (2007) 'A comparative study of mandibular fractures in the United States and Turkey', International Journal of Oral and Maxillofacial Surgery, vol. 36, no. 5, May, pp. 395-397.

Sinn, D., Hill, S. and Watson, S. (1987) 'Mandibular fractures', in Foster, C. and Sherman, J. (ed.) Surgery of facial bone fractures, Churchill Livingstone.

Smith, R.J. (1983) 'The mandibular corpus of female primates: taxonomic, dietary and allometric correlates of interspecific variations in size and shape', American Journal of Physical Anthropology, vol. 61, pp. 315-330.

Spencer, A.J.M. (2004) Continuum Mechanics, Mineola, New York: Dover Publications, Inc.

Sperber, G. (2001), in Craniofacial development, Hamilton (ON): BC Decker Inc.

Spiessl, B. and Schrol, K. (1989) 'Classification of fractures', in Spiessl, B. (ed.) Internal fixation of the mandible, New York: Springer-Verlag.

Standring, S. (2008) 'Mandible', in Standring, S. (ed.) Gray's Anatomy: the Anatomical Basis of Clinical Practice, 40th edition, Edinburgh: Churchill Livingstone/Elsevier.

Sterne, J.A.C. and Egger, M. (2001) 'Funnel plots for detecting bias in meta-analysis: Guidelines on choice of axis', Journal of Clinical Epidemiology, vol. 54, pp. 1046-1055.

Stylogianni, L., Arsenopoulos, A. and Patrikiou, A. (1991) 'Fractures of the facial skeleton in children', British Journal of Oral and Maxillofacial Surgery, vol. 29, no. 1, Feb, pp. 9-11.

Subhashraj, K. (2009) 'A study on the impact of mandibular third molars on angle fractures', Journal of Oral and Maxillofacial Surgery, vol. 67, no. 5, pp. 968-972.

Subhashraj, K., Nandakumar, N. and Ravindran, C. (2007) 'Review of maxillofacial injuries in Chennai, India: a study of 2748 cases', British Journal of Oral and Maxillofacial Surgery, vol. 45, no. 8, Dec, pp. 637-639.

Subhashraj, K., Ramkumar, S. and Ravindran, C. (2008) 'Pattern of mandibular fractures in Chennai, India', British Journal of Oral and Maxillofacial Surgery, vol. 46, no. 2, Mar, pp. 126-127.

Sugiura, T., Yamamoto, K., Murakami, K., Kawakami, M., Kang, Y.-B., Tsutsumi, S. and Kirita, T. (2009) 'Biomechanical analysis of miniplate osteosynthesis for fractures of the atrophic mandible', Journal of Oral and Maxillofacial Surgery, vol. 67, no. 11, Nov, pp. 2397-2403.

Szucs, A., Bujtar, P., Sandor, G. and Barabas, J. (2010) 'Finite element analysis of the human mandible to assess the effect of removing an impacted third molar', Journal of the Canadian Dental Association, vol. 76, p. a72.

Takada, H., Abe, S., Tamatsu, Y., Mitarashi, S., Saka, H. and Ide, Y. (2006) 'Three-dimensional bone microstructures of the mandibular angle using micro-CT and finite element analysis: Relationship between partially impacted mandibular third molars and angle fractures', Dental Traumatology, vol. 22, no. 1, pp. 18-24.

Tang, Z., Tu, W., Zhang, G., Chen, Y., Lei, T. and Tan, Y. (2012) 'Dynamic simulation and preliminary finite element analysis of gunshot wounds to the human mandible', Injury, vol. 43, no. 5, May, pp. 660-665.

Tevepaugh, D.B. and Dodson, T.B. (1995) 'Are mandibular third molars a risk factor for angle fractures? A retrospective cohort study.', Journal of Oral And Maxillofacial Surgery, vol. 53, no. 6, pp. 646-649.

Thaller, S.R. and Mabourakh, S. (1991) 'Pediatric mandibular fractures', Annals of Plastic Surgery, vol. 26, no. 6, Jun, pp. 511-513.

Thangavelu, A., Yoganandha, R. and Vaidhyanathan, A. (2010) 'Impact of impacted mandibular third molars in mandibular angle and condylar fractures', International Journal of Oral and Maxillofacial Surgery, vol. 39, no. 2, pp. 136-139.

Thorén, H., Snall J., Hallermann W., Kormi E. and Tornwall J. (2008) 'Policy of Routine Titanium Miniplate Removal After Maxillofacial Trauma', Journal of Oral and Maxillofacial Surgery, vol. 66, no. 9, pp. 1901-1904.

Thorén, H., Iizuka, T., Hallikainen, D. and Lindqvist, C. (1992) 'Different patterns of mandibular fractures in children. An analysis of 220 fractures in 157 patients', Journal of cranio-maxillo-facial surgery: official publication of the European Association for Cranio-Maxillo-Facial Surgery, vol. 20, no. 7, Oct, pp. 292-296.

Turner, M.J., Clough, R.W., Martin, H.C. and Topp, L.C. (1956) 'Stiffness and deflection analysis of complex structures', Journal of Aeronautical Science, vol. 23, pp. 805-823.

Ugboko, V.I., Oginni, F.O. and Owotade, F.J. (2000) 'An investigation into the relationships between mandibular third molars and angle fractures in Nigerians', British Journal of Oral andMaxillofacial Surgery, vol. 38, no. 5, pp. 427-429.

University of Virginia, Department of Materials Science and Engineering, (2010) 'MSE 2090: Introduction to the Science and Engineering of Materials. Chapter 8. Failure.', [Online] Available at: people.virginia.edu/~lz2n/mse209

Vajgel, A., Camargo, I.B., Willmersdorf, R.B., de Melo, T.M., Laureano Filho, J. and Vasconcellos, R.J. (2013) 'Comparative finite element analysis of the biomechanical stability of 2.0 fixation plates in atrophic mandibular fractures', Journal of Oral and Maxillofacial Surgery, vol. 71, no. 2, Feb, pp. 335-342.

van Beek, G.J. and Merkx, C.A. (1999) 'Changes in the pattern of fractures of the maxillofacial skeleton', International Journal Of Oral and Maxillofacial Surgery, vol. 28, no. 6, Dec, pp. 424-428.

Van Hoof, R.F., Merkx, C.A. and Stekelenburg, E.C. (1977) 'The different patterns of fractures of the facial skeleton in four European countries', International Journal of Oral Surgery, vol. 6, pp. 3-11.

Venugopal, M.G., Sinha, R., Menon, P.S., Chattopadhyay, P.K. and Roy Chowdhury, S.K. (2010) 'Fractures in the maxillofacial region: a four year retrospective study', Medical Journal, Armed Forces India, vol. 66, no. 1, pp. 14-17.

Vetter, J.D., Topazian, R.G., Goldberg, M.H. and Smith, D.G. (1991) 'Facial fractures occurring in a medium-sized metropolitan area: recent trends', International Journal of Oral and Maxillofacial Surgery, vol. 20, no. 4, Aug, pp. 214-216.

Vignjevic, R., Morris, A.J. and Belagundu, A.D. (1998) 'Towards high fidelity fiinite element analysis', Advances in Engineering Software, vol. 29, pp. 655-665.

Vollmer, D., Meyer, U., Joos, U., Vegh, A. and Piffko, J. (2000) 'Experimental and finite element study of the mandible', Journal of Cranio-Maxillofacial Surgery, vol. 28, pp. 91-96.

Wagner, A., Krach, W., Schicho, K., Undt, G., Ploder, O. and Ewers, R. (2002) 'A 3-dimensional finite-element analysis investigating the biomechanical behavior of the mandible and plate osteosynthesis in cases of fractures of the condylar process', Oral Surgery, Oral Medicine, Oral Pathology, Oral Radiology and Endodontics, vol. 94, no. 6, Dec, pp. 678-686.

Walden, R.E., Wohlgemuth, P.R. and Fitz-Gibbon, J.H. (1956) 'Fractures of the Facial Bones', American Journal of Surgery, p. 92.

Wang, H., Ji, B., Jiang, W., Liu, L., Zhang, P., Tang, W., Tian, W. and Fan, Y. (2010) 'Three-dimensional finite element analysis of mechanical stress in symphyseal fractured human mandible reduced with miniplates during mastication', Journal of Oral and Maxillofacial Surgery, vol. 68, no. 7, Jul, pp. 1585-1592.

Ward-Booth, P., Schendel, S.A. and Hausamen, J.-E. (2006) Maxillofacial Surgery, 2nd edition, London: Churchill Livingstone.

Watanabe, P.C.A., Alonso, M.B.C.C., Monteiro, S.A.C., Tiossi, R. and Issa, J.P.M. (2009) 'Morphodigital study of bone quality in the mandibular angle in patients with third molar impacted', Anatomical Science International, vol. 84, no. 3, pp. 246-252.

Watts, D.C. (1989) 'Temperature dependence of the mechanical properties of human dentine', in Yettram, D.C. (ed.) Material Properties and Stress Analysis in Biomechanics, Manchester: Manchester University Press.

Weijs, W.A. (1981) 'Mechanical loading of the human jaw', Acta Morphologica Neerlando-Scandinavica, vol. 19, pp. 261-262.

Weijs, W.A. and Hillen, B. (1984a) 'Relationship between the physiological cross-section of the human jaw muscles and their cross-sectional area in computer tomograms', Acta Anatomica, vol. 118, pp. 129-138.

Weijs, W.A. and Hillen, B. (1984b) 'Relationships between masticatory muscle cross-section and skull shape', Journal of Dental Research, vol. 63, pp. 1154-1157.

Weijs, W.A. and Hillen, B. (1985b) 'Cross-sectional areas and estimated intrinsic strength of the human jaw muscles', Acta Morphologica Neerlando-Scandinavica, vol. 23, pp. 267-274.

Weijs, W.A. and Hillen, B. (1985b) 'Physiological cross-section of the human jaw muscles', Acta Anatomica, vol. 121, pp. 31-35.

Weiner, D., Murray, R., Huang, H. and Milzman, D. (2012) 'Presence of third molars and rates of mandible fractures after punched-in face', Canadian Journal of Emergency Medicine, vol. 14, p. S42.

Werkmeister, R., Fillies, T., Joos, U. and Smolka, K. (2005) 'Relationship between lower wisdom tooth position and cyst development, deep abscess formation and mandibular angle fracture', Journal of Cranio-Maxillofacial Surgery, vol. 33, no. 3, pp. 164-168.

Wescott, D.J. (2013) 'Biomechanics of Bone Trauma', Encyclopedia of Forensic Sciences, vol. 2, pp. 83-88.

Wilson, I.F., Lokeh, A., Benjamin, C.I., Hilger, P.A., Hamlar, D.D., Ondrey, F.G., Tashjian, J.H., Thomas, W. and Schubert, W. (2001) 'Prospective comparison of panoramic tomography (zonography) and helical computed tomography in the diagnosis and operative management of mandibular fractures', Plastic and Reconstructive Surgery, vol. 107, pp. 1369-1375.

Wolujewicz, M.A. (1980) 'Fractures of the mandible involving the impacted third molar tooth: An analysis of 47 cases', British Journal of Oral Surgery, vol. 18, no. 2, pp. 125-131.

Wood, S.A., Strait, D.S., Dumont, E.R., Ross, C.F. and Grosse, I.R. (2011) 'The effects of modeling simplifications on craniofacial finite element models: The alveoli (tooth sockets) and periodontal ligaments', Journal of Biomechanics, vol. 44, pp. 1831-1838.

World Health Organization (1977) International Classification of Diseases Index: Manual for the International Statistical Classification of Diseases, Ninth edition, Geneva: WHO Press.

Xu, H.H., Smith, D.T., Jahanmir, S., Romberg, E., Kelly, J.R., Thompson, V.P. and Rekow, E.D. (1998) 'Indentation damage and mechanical properties of human enamel and dentine', Journal of Dental Research, vol. 77, pp. 472-480.

Yadav, S., Tyagi, S., Puri, N., Kumar, P. and Kumar, P. (2013) 'Qualitative and quantitative assessment of relationship between mandibular third molar and angle fracture on North Indian population: A clinico-radiographic study', European Journal of Dentistry, vol. 7, no. 2, pp. 212-217.

Yamada, T., Sawaki, Y., Tohnai, I., Takeuchi, M. and Ueda, M. (1998) 'A study of sports-related mandibular angle fracture: relation to the position of the third molars', Scandinavian Journal of Medicine and Science in Sports, vol. 8, no. 2, pp. 116-119.

Yamamoto, K., Kuraki, M., Kurihara, M., Matsusue, Y., Murakami, K., Horita, S., Sugiura, T. and Kirita, T. (2010) 'Maxillofacial fractures resulting from falls', Journal of Oral and Maxillofacial Surgery, vol. 68, no. 7, Jul, pp. 1602-1607.

Yamamoto, K., Matsusue, Y., Murakami, K., Horita, S.I., Matsubara, Y., Sugiura, T. and Kirita, T. (2011) 'Maxillofacial fractures due to work-related accidents', Journal of cranio-maxillo-facial surgery : official publication of the European Association for Cranio-Maxillo-Facial Surgery, vol. 39, no. 3, Apr, pp. 182-186.

Zachariades, N. and Papavassiliou, D. (1990) 'The pattern and aetiology of maxillofacial injuries in Greece. A retrospective study of 25 years and a comparison with other countries', Journal of cranio-maxillo-facial surgery: official publication of the European Association for Cranio-Maxillo-Facial Surgery, vol. 18, no. 6, Aug, pp. 251-254.

Zachariades, N., Papavassiliou, D. and Koumoura, F. (1990) 'Fractures of the facial skeleton in children', Journal of cranio-maxillo-facial surgery : official publication of the European Association for Cranio-Maxillo-Facial Surgery, vol. 18, no. 4, May, pp. 151-153.

Zachariades, N., Papavassiliou, D., Papademetriou, I. and Koundouris, I. (1983) 'Fractures of the facial skeleton in Greece. A retrospective study covering 1791 cases in 10 years', Journal of Maxillofacial Surgery, vol. 11, no. 3, Jun, pp. 142-144.

Zachariades, N., Papavassiliou, D., Triantafyllou, D., Vairaktaris, E., Papademetriou, I., Mezitis, M. and Rapidis, A. (1984) 'Fractures of the facial skeleton in the edentulous patient', Journal of Maxillofacial Surgery, vol. 12, no. 6, Dec, pp. 262-266.

Zachar, M.R., Labella, C., Kittle, C.P., Baer, P.B., Hale, R.G. and Chan, R.K. (2013) 'Characterization of mandibular fractures incurred from battle injuries in Iraq and Afghanistan from 2001-2010', Journal of Oral and Maxillofacial Surgery, vol. 71, no. 4, Apr, pp. 734-742.

Zhou, H.-H., Ongodia, D., Liu, Q., Yang, R.-T. and Li, Z.-B. (2013) 'Incidence and pattern of maxillofacial fractures in children and adolescents: a 10 years retrospective cohort study', International Journal of Pediatric Otorhinolaryngology, vol. 77, no. 4, Apr, pp. 494-498.

Zhu, S.-J., Choi, B.-H., Kim, H.-J., Park, W.-S., Huh, J.-Y., Jung, J.-H., Kim, B.-Y. and Lee, S.-H. (2005) 'Relationship between the presence of un-erupted mandibular third molars and fractures of the mandibular condyle', International Journal of Oral and Maxillofacial Surgery, vol. 34, no. 4, pp. 382-385.

Zimmermann, E.A., Gludovatz, B., Schaible, E., Busse, B. and Ritchie, R.O. (2014) 'Fracture resistance of human cortical bone across multiple length-scales at physiological strain rates', Biomaterials, vol. 35, pp. 5472-5481.

Zix, J.A., Schaller, B., Lieger, O., Saulacic, N., Thorén, H. and Iizuka, T. (2011) 'Incidence, aetiology and pattern of mandibular fractures in central Switzerland', Swiss Medical Weekly, vol. 141, p. w13207.

Appendices

Appendix 1

Use of the companion disc.

The accompanying companion disc contains additional information which is not essential but may aid the understanding the thesis.

The disc contains a single file which requires Adobe Reader v. XI or later. The file is arranged as a portfolio of information. The structure is as follows:

Companion disc file structure

- **Non-linear dynamic analyses**
    - Animations (Cyst and third molar)
        - Cystic lesions
            - Angle impact
            - Symphyseal impact
        - Un-erupted third molars
    - Animations (Punch)
        - Parasymphyseal punch
            - High energy
            - Low energy
        - Body punch
            - High energy
            - Low energy
        - Angle Punch
            - High energy
            - Karate energy
            - Low energy
        - Ramus punch
            - High energy
            - Karate energy
            - Low energy
        - Symphyseal punch
            - High energy
            - Karate energy
            - Low energy

- **3D model folder**

Appendix 2

Basic elasticity

This section introduces some mathematical and engineering concepts that are important to the understanding of this thesis. It is not intended to be an exhaustive exposition of continuum mechanics. Readers interested in a more comprehensive understanding of the concepts presented here should consult standard texts, several of which are mentioned in the bibliography.

Stress and strain

When a load is applied to any material it deforms. Material behaviour may be described by a load vs. deformation curve.

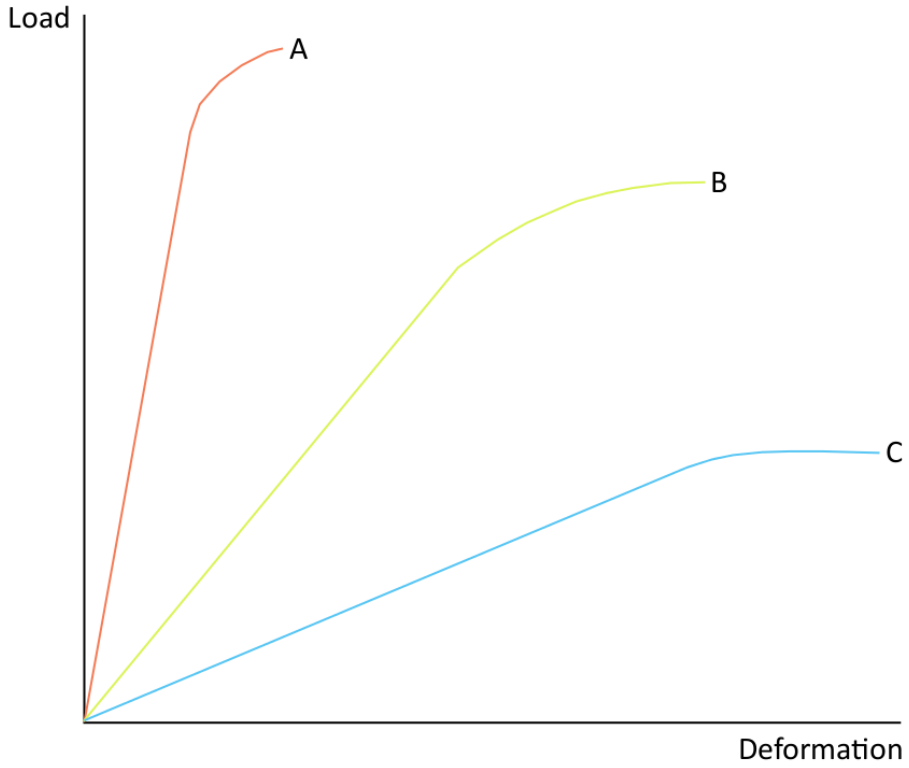

Load vs. deformation curve for a theoretical material. Adapted from Wescott, 2013

The graph above shows the load vs. deformation curve for three idealized materials. If we assume that they all refer to bone then A would represent a brittle bone i.e. showing little deformation, C a ductile bone (showing significant deformation on loading) and B would represent a bone with properties midway between the two.

The load vs. deformation curve cannot accurately describe material behaviour as force is related to application area and deformation (or displacement) is related to specimen length. A better way to understand material properties is to examine a stress vs. strain graph which diminishes the effects of sample size.

The amount of deformation relative to the original material length is known as engineering (or Cauchy) strain.

$$\varepsilon_e = \frac{\Delta L}{L}$$

The mathematical definition of strain. ε= strain, L= length, and ΔL= change in length.

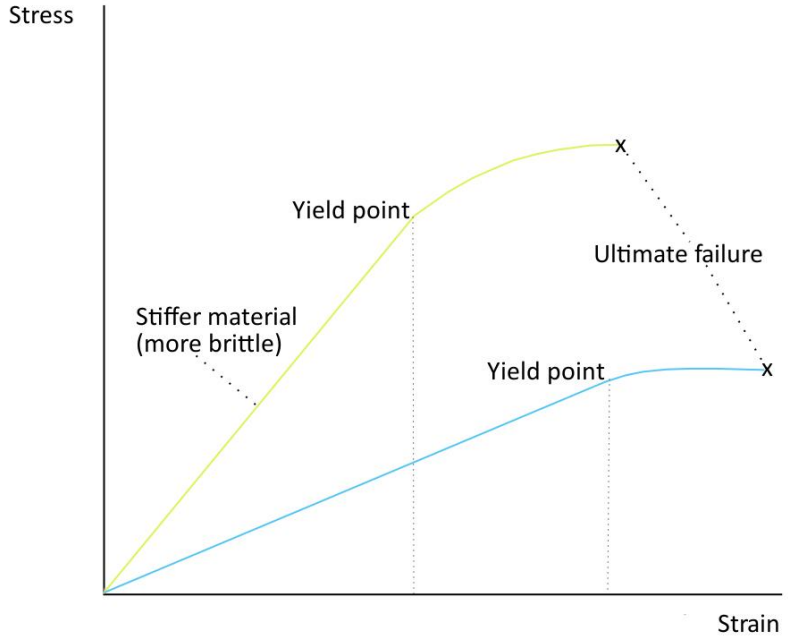

Stress vs. strain curve for two theoretical materials. Adapted from Wescott, 2013

Stress is defined as force per unit area. Where the area is the original cross-sectional area of the material this is known as engineering (or Cauchy) stress.

$$\sigma_e = \frac{F}{A_0}$$

The mathematical definition of stress (engineering).

When the final cross-sectional area of the material is taken into consideration, this is known as true stress and in this case the stress vs. strain curve will differ.

If the strain disappears when the stress is removed then the material is said to behave elastically. If, on the other hand, permanent deformation occurs when the stress is

removed then plastic deformation is said to have taken place. Excess strain will cause material failure regardless of the stress level.

The gradient of the curve at any point is known as the modulus. Young's modulus (E), also known as the elastic modulus, is defined by the slope of the linear portion of the curve. It can be seen that both curves in have a linear portion and a non-linear portion. The junction between the two is known as the yield point. On a microscopic level this point represents slippage between the layers of atoms and molecules leading to permanent deformation.

In the linear portion, the stress and strain increase in a proportional manner, and the material behaves elastically on loading and unloading. Hooke's law describes the stress (σ) and strain (ε) relationship in the elastic region.

$$E\varepsilon = \sigma$$

Hooke's law.

Materials which are loaded in one direction will undergo strains parallel and perpendicular to the load direction. This maybe expressed as the Poisson ratio (ν). This is the ratio of lateral strain (ε_{lat}) to longitudinal strain (ε_{long}).

$$\nu = -\frac{\varepsilon_{lat}}{\varepsilon_{long}}$$

Poisson's ratio

For most biological hard tissues, including bone, the Poisson ratio is approximately 0.3.

In general, a deformation resulting in <2% strain will be within the elastic limit. When greater load is applied a yield point is encountered and permanent deformation begins

to occur. In cortical bone the yield strain has been estimated as approximately 6800με (Carter, 1984). The yield stress is approximately 130MPa in tension. At these points, micro-cracks occur in the hydroxyapatite and collagen fibres are disrupted. Collagen fibres are responsible for the tensile properties of bone whereas the hydroxyapatite forms the compressive strength.

Eventually, bone under increasing tension or compression will undergo failure. This frequently manifests clinically as fracture. The ultimate strain of bone (the point of failure for a material with brittle properties) is approximately 10000-15000με in tension. The ultimate stress varies according to whether the bone is in tension (140MPa), compression (200MPa) or shear (65MPa) (Carter, et al., 1981). As a result, bony fracture is most likely to occur along shear planes. These run at approximately 45 degrees from normal compressive and tensile stresses.

The area under the stress vs. strain curve is known as the energy absorbed per unit volume. The area under the elastic region of the curve is elastically absorbed and that under the plastic region is the energy absorbed plastically. The total energy is also known as the strain energy density represents the total work done in deforming the material. Strain energy density has been used by several authors performing biological 3DFEA to determine the energy required to deform structures.

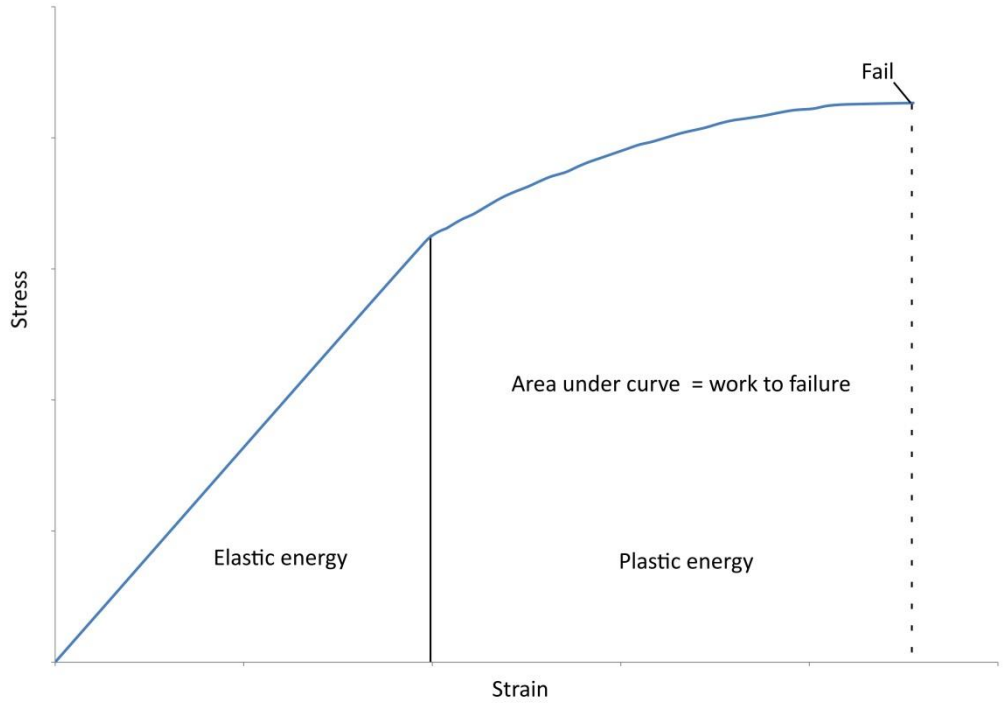

Stress vs. strain graph showing the derivation of work to failure (strain energy density). Adapted from Wescott, 2013

Measuring performance

Performance is a term borrowed from engineering, but frequently applied to biological systems. It refers to the mechanical efficiency or strength of a specific system. In reference to biological structures such as bone it can refer to the stress which it can withstand without deformation (which may cause system failure) or catastrophic material failure. Cortical bone has been described as failing under a ductile model of fracture (Nalla, et al., 2003) although Hansen, et al. (2008) noted a ductile-to-brittle transition, which was strain-rate related, in tensile and compressive tests to failure.

The von Mises formula was developed to predict yielding of isotropic ductile materials such as metals. Under this criterion, failure occurs when the von Mises stress equals the ultimate stress of the material. Whilst some have noted that this criterion is not very realistic for determining failure in bone (Doblaré, et al., 2004) von Mises stress (σ_{vm})(also referred to as the equivalent stress) has been used throughout biological literature to predict bony failure. Keyak and Rossi (2000) found that when isotropic material properties were used, von Mises criterion was the most accurate for fracture location prediction in cortical bone. This was even the case when the differences in compressive and tensile stress were accounted for. This same accuracy was not found in cancellous bone (Fenech and Keaveny, 1999).

In terms of the determination of fracture location, Keyak and Rossi (2000) found that the predicted location of the fracture was often a function of the failure criterion employed.

The maximum principal stress criterion (Rankine criterion (σ_1)) has been used by some authors to describe the brittle failure of bone. Failure is said to occur when the maximum principal stress in a system reaches the value of the maximum strength at the elastic limit in uniaxial tension. Keyak and Rossi (2000) used the criterion to determine the ultimate fracture load in femora and found errors of upto 30%.

The biological structure of bone results in its viscoelastic properties (Fan and Rho, 2003). As a result of this it has been suggested that strain rate may need to be taken into account in the ideal failure criterion, in addition to those of a material that fractures in a quasi-brittle manner. It is clear that there is no ideal failure criterion for bone loaded under impact conditions at present, therefore strain energy density, von Mises stress and von Mises strain (taken to mean equivalent stress and strain respectively) and strain rate were used in this thesis to measure performance.

Appendix 3

Introduction to finite element analysis

Three-dimensional finite element analysis (3DFEA) is a commonly used engineering technique. It is used to simulate the response of a physical system to loading. Physical systems under investigation are not limited to buildings or automobile crash analysis. 3DFEA may be applied to biological systems as the same governing principles apply to all structures.

With our current understanding, biological systems are impossible to model exactly, partly because they are understood incompletely and partly because of the high level of complexity required. As such 3DFEA models represent abstractions of systems. Such abstractions may require simplifying assumptions to be made.

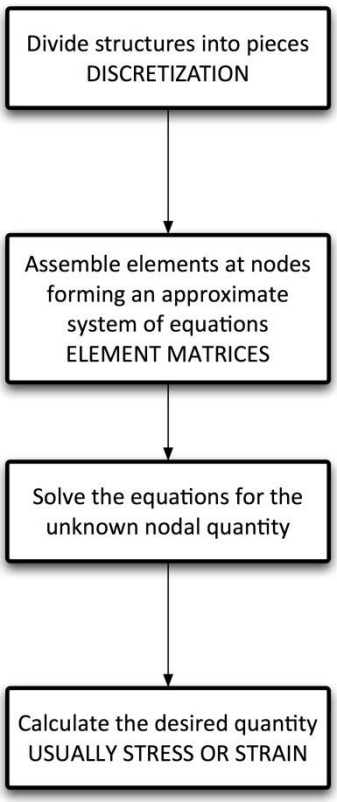

The process of finite element analysis.

The finite element method is a discretization technique. The FE model is a mathematical interpretation of a physical entity. The mathematical model is composed of disjoint components of much simpler geometry called finite elements.

The response of the mathematical model is calculated by assembling the elements to produce a result that should closely approximate the true value. Results of analyses are frequently displayed (post-processed) graphically using colour contour or vector maps which may be various calculations of stress, strain, displacement or force.

In order to obtain meaningful results and allow the subsequent correct interpretation, quality control systems and sound engineering judgement are required (Adams, 2008). Finite element solvers will, in most cases, solve any problem that has been input correctly. It does not give the researcher any insight into any flaws in the data input or output, therefore it is important to make sure the research question is clearly defined and that the model produced is specific to the question. Additionally, it is important point to remember that rarely in any biological analysis does one get the chance to use the exact material properties. Loads, boundary conditions or geometry, are rarely exact, although the finite element solver will give an exact answer.

Appendix 4

Embryology

The mandible develops from a mesenchymal collection, known as the mandibular prominence (1st pharyngeal arch), which is recognisable when the embryo is approximately 4½ weeks old (Sadler, 1994). It lies caudal to the stomatodeum. The pharyngeal arches have a core composed of mesenchymal tissue covered externally by ectoderm and lined internally by endoderm. The core also contains cells of neural crest origin, which develop into skeletal components, and the remaining tissue (mesoderm) gives rise to the musculature.

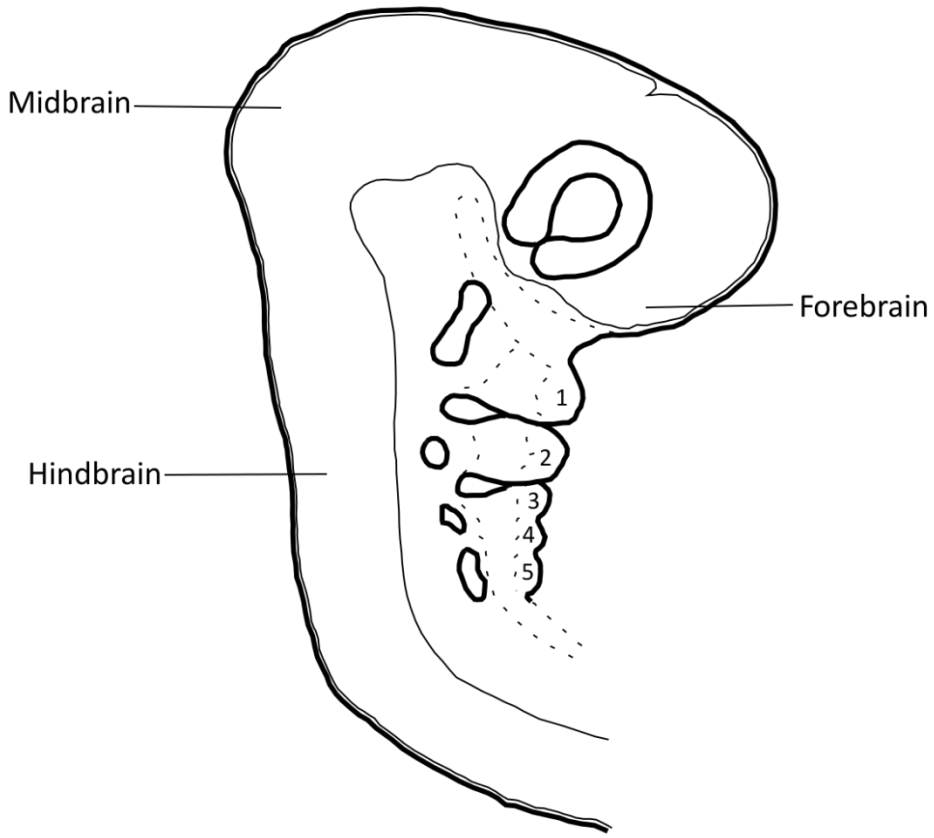

Representation of the human embryo at 4½ weeks. Numbers 1 to 5 represent the pharyngeal arches. Arch number 1 contains Meckel's cartilage, which forms a scaffold for mandibular development (Adapted from Sadler, 1994).

Each arch has a skeletal component, a muscular component, a nerve component, and an arterial component. In the case of the first arch, the skeletal component is Meckel's cartilage, which is formed from chondrification in the mesoderm. The cartilage forms the malleus, the anterior ligament of malleus, the sphenomandibular ligament, the lingual of the mandible, the *ossa mentalis*. The mandible itself forms around the cartilage, ossifying in membrane in the 6th week. The remaining cartilage has usually disappears early after birth. Postnatal growth occurs by endochondral apposition occurring at the condylar cartilages, contributing to an increase in ramus height, and the posterior ramus and alveolar ridges by intramembranous ossification (Sperber, 2001). The effect of this is that the mandible starts from a relative retrognathic position at birth to occupy a more prognathic position in the adult.

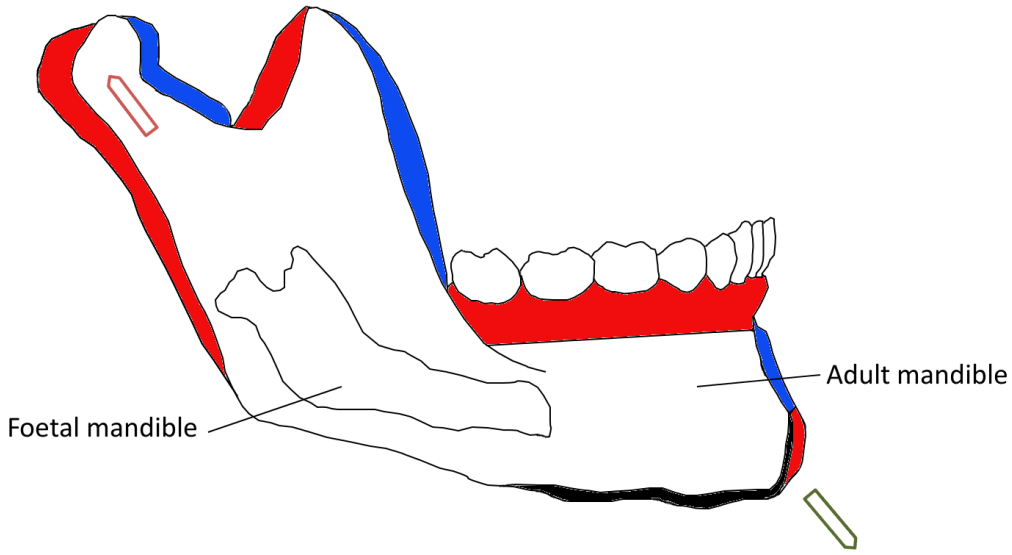

Adult mandible with foetal mandible superimposed. Red and green arrows show postero-superior and antero-inferior growth relative to the cranial base, respectively. Red areas are areas of bone deposition and blue areas represent bone resorption. (Adapted from Sperber, 2001)

The muscular components of the first pharyngeal arch form the muscles of mastication i.e. (temporalis, masseter, medial and lateral pterygoids), the mylohyoid muscle, the anterior belly of the digastric muscle, tensor palatini and tensor tympani. The trigeminal nerve supplies the muscles of mastication via the mandibular branch.

Adult mandibular anatomy

Osteology

The mandible is composed of two halves at birth, with a connecting fibrous joint which ossifies at the end of the first year resulting in a roughly, 'U'-shaped bone. It has an anterior convexity in the horizontal plane and ascends posteriorly into two rami where it is attached by a ligament to the base of the skull. An external surface (or labio-buccal surface) lies adjacent to the lower lip, and an internal (or lingual) surface adjacent to the tongue. At the most anterior aspect of the mandible in the midline of the external surface is the mandibular symphysis, which is frequently marked by a median ridge. Either side of the median ridge are the mental tubercles.

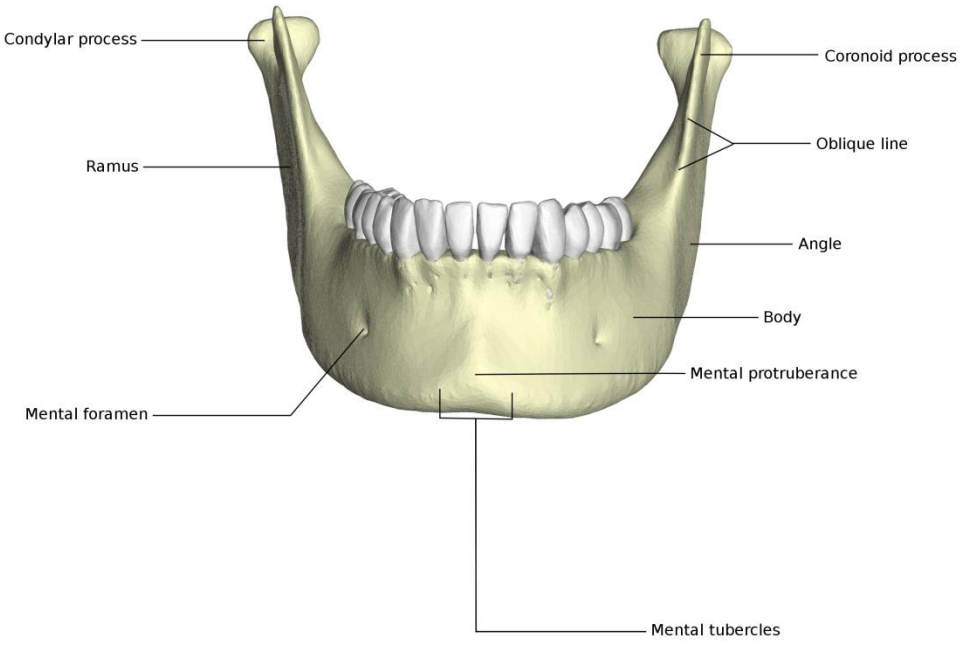

The bony landmarks of the mandible (labio-buccal surface).

Between the mental tubercles and the median ridge is the triangle-shaped mental protuberance. The chin itself is composed of the mental tubercles and the mental protuberance. Joining the mental tubercles near the midline and the oblique line postero-lateral to the molar teeth is the external oblique ridge. The alveolar portion of the mandible lies in the upper border of the mandible and encloses the teeth within the lingual and buccal plates of bone.

On the lingual aspect of the lower border of the mandible lies a depression for the anterior belly of the digastric muscle, just lateral to the midline.

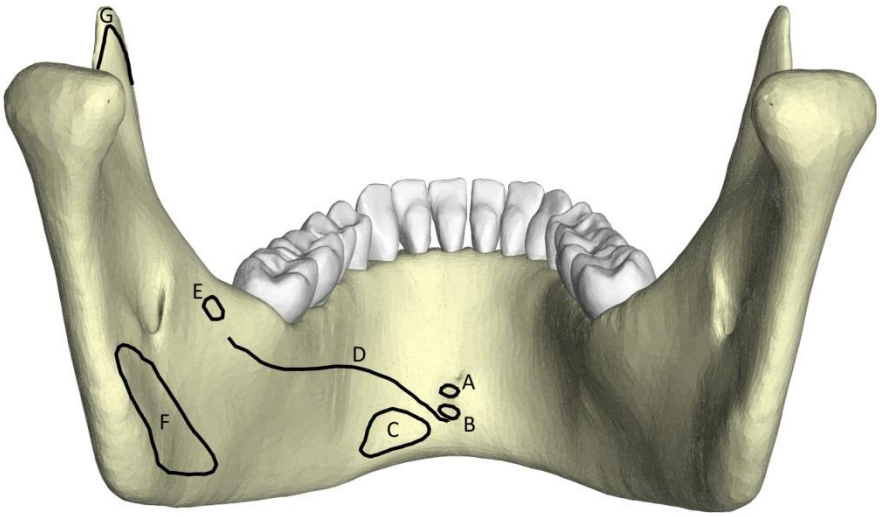

The muscular insertions of the mandible (lingual aspect). A = genioglossus; B= geniohyoid; C= anterior belly of digastric; D= mylohyoid; E= pterygomandibular raphe; F= medial pterygoid; G= temporalis (Adapted from Mc Minn, et al., 1993)

In the midline on the lingual (internal) surface lie two small protuberances, the genial tubercles (or mental spines). These indicate the attachment of genioglossus superiorly and geniohyoid inferiorly. The genial or lingual foramen is a canal that opens above the genial tubercles and contains a branch of the lingual artery. The mylohyoid line is a thin, oblique ridge that lies approximately 1cm below the alveolar crest of the mandible in the third molar region. It extends anteriorly as far as the mandibular symphysis where its prominence diminishes. The line forms the attachment of the mylohyoid muscle.

Below the mylohyoid line is the mylohyoid groove, extending from the ramus of the mandible and contains the mylohyoid neurovascular bundle. The submandibular fossa contains the submandibular gland which lies below the mylohyoid line. The sublingual gland lies in a concavity called the sublingual fossa on the lingual surface of the mandible above the mylohyoid muscle.

The mandibular canal, containing the mental neurovascular bundle, runs through the ramus and body of the mandible, starting at the mental foramen. This foramen lies in a variable position below, anterior or posterior to the premolar teeth (Mc Minn, 1994). Posteriorly, the mandibular foramen, which lies on the medial aspect of the ramus of the mandible, provides the exit for the mandibular nerve from the mandible. Supero-medial to the mandibular foramen lies a small projection (or tongue) of bone called the lingula. The spheno-mandibular ligament is inserted in to lingula from its origin on the spine of the sphenoid. This ligament is neither stretched nor compressed in physiological movements of the mandible and functions as an accessory ligament of the temporomandibular joint.

The ramus is a quadrilateral extension of the mandible. It has been described as having superior, inferior, anterior and posterior borders and two processes (coronoid and condylar). The inferior aspect of the ramus and the angle of the mandible are continuous. The angle is slightly everted in males, giving a more square jaw and is inverted in females (Standring, 2008). The posterior aspect of the ramus is continuous with the condylar process and joins the ramus through a bony projection known as the condylar neck. The majority of the head is composed of cancellous bone with a thin cortical covering. Fibrocartilage covers the area that articulates with the base of the skull. The antero-medial aspect of the head contains a small depression (the pterygoid fovea) to which the superior and inferior head of the lateral pterygoid muscles are inserted (Standring, 2008).

With increasing age there are a number of changes that take place in the mandible. These are more pronounced when there has been loss of the dentition and the mandible has undergone atrophy. There have been many suggestions in the literature that the gonial angle (i.e. the angle between the ramus and body of the mandible, also

called the mandibular angle) changes with age. Casey and Emrich, (1988) reviewed the current literature at the time and found that many well-known anatomy texts made statements regarding the widening of the angle with age, but their review of research literature was conflicting. Five articles reported a widening of the angle and six found no evidence for this. Their own study failed to show any increase in angle. A more recent study by Chole, et al. (2013) suggested that whilst there may be gonial angle changes associated with gender, there was no significant association with age or dental status. One change that certainly occurs with the loss of teeth is the atrophy of the alveolus due to loss of function. This leads to a reduction in bone height in the normally dentate region. This may occur to such an extent that the bone height in the body of the mandible may have a cross-sectional area approximating the condylar neck.

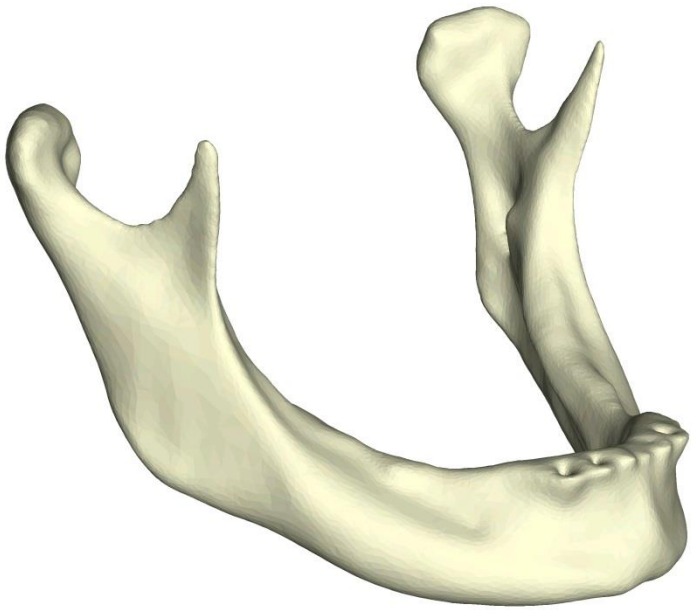

The atrophic edentulous mandible. Note that the extraction sockets from relatively recent extractions are still visible anteriorly.

Musculature

Four paired muscles, frequently described as the muscles of mastication, are attached to the ramus and angle of the mandible. These are the masseter, medial pterygoid, lateral pterygoid and temporalis. These muscles are the primary movers of the mandible.

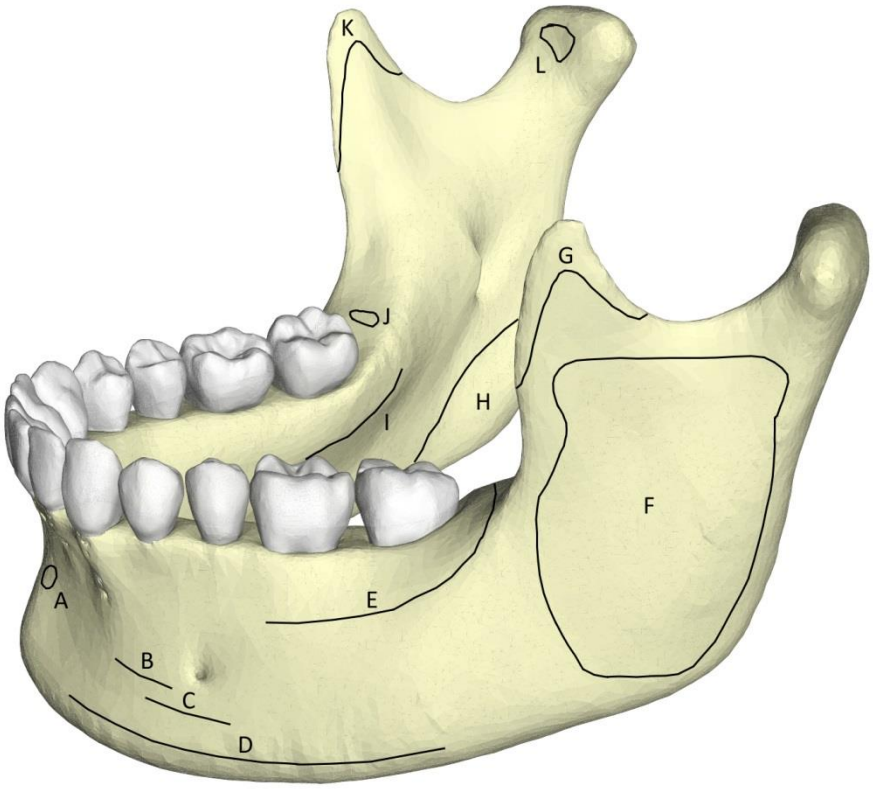

The muscular insertions of the mandible. A = mentalis; B= depressor labii inferioris; C= depressor anguli oris; D= platysma; E= buccinator; F= masseter; G= temporalis; H= medial pterygoid; I= mylohyoid; J= pterygomandibular raphe (sites of muscle insertions were adapted from Mc Minn, et al., 1993)

Tooth morphology

Humans have two successive generations of teeth known as the deciduous (primary) dentition and the permanent (secondary) dentition. Teeth develop from ectodermal and mesodermal components in the sixth week. Adult teeth begin to erupt into the mouth at approximately six years. The complete adult dentition is composed of 32 teeth arranged as eight teeth in each quadrant of the mouth (Sadler, 1994).

The crown of the tooth refers to that area which lies above the gingival margin in the healthy condition. It is composed of dentine covered with a layer of hard translucent enamel of approximately 2mm thick. The root is composed of the portion of the tooth that lies below the gingival margin. The crown and the root meet at the cervical margin. The root is composed mostly of dentine covered with cementum, and is surrounded by the alveolar bone of the osseous tooth socket. The cementum of the root is significantly thinner than the enamel covering the dentine of the crown. The cementum is attached to the alveolus by a connective tissue bridge known as the periodontal ligament. This ligament, composed mainly of collagen fibres is approximately 0.2mm wide.

Material properties of mandibular biological structures

The hard tissue of mandibular biological structures include, enamel, dentine, cementum, and bone. The associated soft tissue structures include the dental pulp, vascular supply, lymphatic drainage and periodontal ligament. In this section, the dental hard tissues will be discussed. The periodontal ligament will also be discussed insofar as it relates to the proposed study.

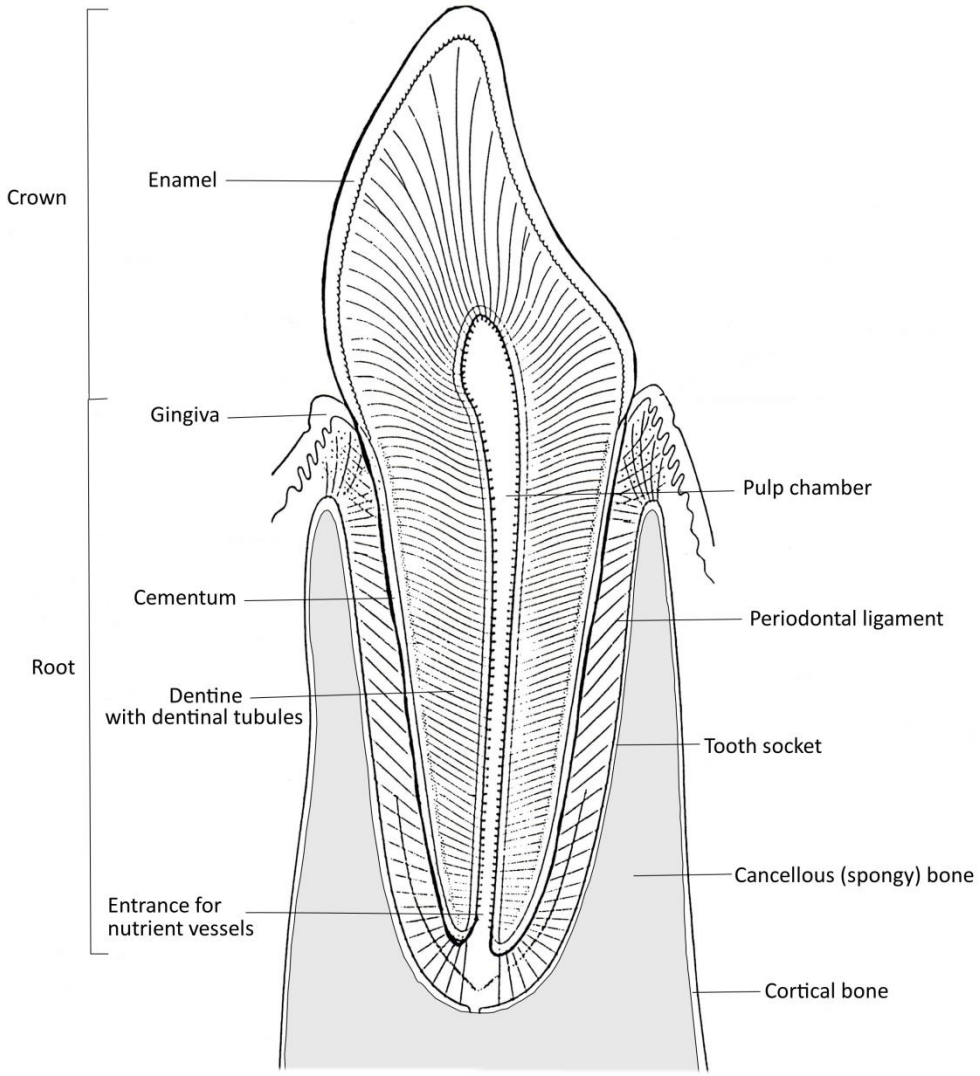

Anatomy of an adult tooth. Note that the diagram is not in proportion. Figure adapted from student anatomy notes, United Medical and Dental Hospitals of Guy's and St. Thomas' Hospitals, 1989.

Enamel

Enamel is a highly mineralized tissue. It contains crystalline apatites (95-96% by weight) and 1% organic matrix. It covers the crown of the teeth reaching up to 2.5mm over the cusp tips and tapering at the cervical margins (Standring, 2008). Structurally the enamel is composed of prisms which extend from the dentinal surface to just below the external enamel surface. The highly organized and complexly orientated prisms give enamel its anisotropic properties.

The elastic modulus for enamel (Young's modulus) is very high, reflecting its place as the hardest tissue in the body. Estimates have been made at between 81.4GPa (Craig, et al., 1961) and 130GPa (Moroi, et al., 1993). It behaves in a brittle-elastic manner (Xu, et al., 1998). Enamel has no repair mechanism meaning that once tooth substance is lost it must be repaired artificially.

Dentine

The majority of the substance of the tooth is composed of dentine. This hard-tissue is more mineralized than bone but less than enamel. A structural feature is the presence of dentinal tubules. Around the dentinal tubules is a collagenous organic matrix in which mineral is deposited. The tubules themselves enclose the cytoplasmic process of an odontoblast whose cell body lies on the surface of the dental pulp. Around the odontoblast, but still within the dentinal tubule, lies peritubular dentine. This is distinguished from normal dentine (intertubular dentine) by being more mineralized and having less collagen in its matrix.

The mechanical properties of dentine have been investigated by many authors (Duncanson and Korostoff, 1975; Korostoff, et al., 1975). The elastic modulus of dentine is not as high as that of enamel at standard room temperature; however, it is known to vary significantly with temperature in a similar way to bone (Bonfield and Li, 1968; Bonfield and Tully, 1982). This is important as the temperature in the oral cavity may vary from -10^{o}C to 60^{0}C depending on the temperature of ingested foods.

Temperature	0	23	37	50
Elastic modulus (E)	15.2	13.94	13.26	12.06

The change in Young's Modulus of dentine with temperature (uni-axial compression). (Watts, 1989).

The tubular structure of dentine results in its anisotropic properties. Despite this it is much less anisotropic than bone. It also possesses elastic and visco-elastic properties (Korostoff, et al., 1975).

Unlike enamel, dentine is formed throughout life and has the ability to repair itself.

Cementum

Cementum is the dental hard tissue, which covers the root of teeth. It is the closest dental hard tissue to bone. In terms of composition it is 50% mineral by weight with the predominant mineral being hydroxyapatite. However, unlike bone it is avascular. New layers of cementum are formed throughout life and may reach over a millimetre in thickness with advancing age (Standring, 2008).

The periodontal ligament

The periodontal ligament (PDL) functions as support for the teeth. It also plays a role in the eruption of teeth. The ligament itself is 0.2mm wide and contains cells associated with the maintenance of the alveolar bone. The ligament fibres are mainly composed of collagen with a small volume of oxytalan fibres connecting alveolar bone and cementum.

The PDL is viscoelastic and its properties vary with the mode of loading (Pietrzak, et al., 2002; Pini, et al., 2002). The elastic modulus of the PDL has been calculated as between $1x10^{-5}$ GPa and $3x10^{-5}$ GPa (Pietrzak, et al., 2002).

Bone

Material properties

The presence of mineral salts in bone accounts for the hardness. Bone is homogeneous and anisotropic i.e. its physical properties vary in location and direction. This is particularly apparent in the mandible.

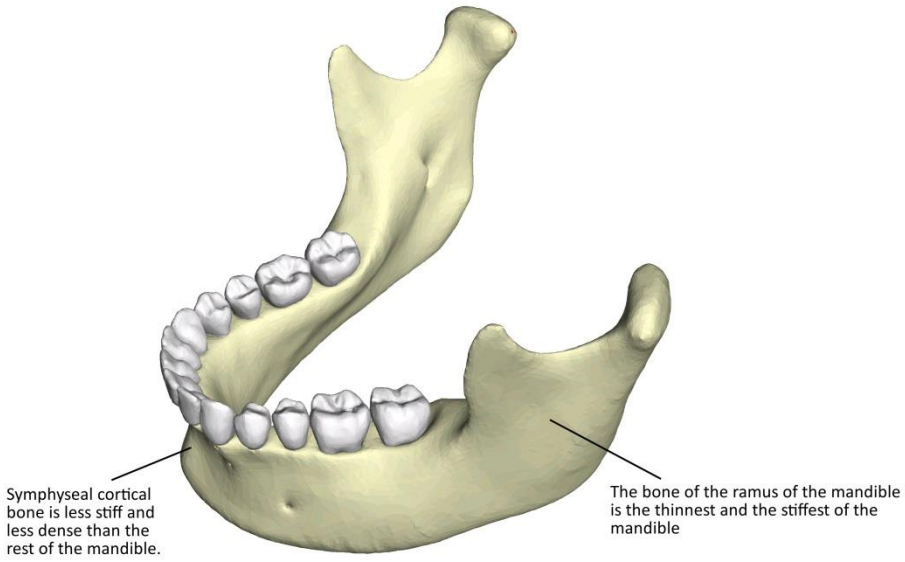

The variation of the properties of mandibular bone with site (Schwartz-Dabney and Dechow, 2003).

Bone has a mass density of between 1800 and 1900kg/m^3 and is strongest in compression (Carter, 1984). Cortical bone is weakest in shear with a failure stress of approximately 70MPa as opposed to 200MPa in compression and 140MPa in tension (Carter, 1984). The strength and elastic modulus of cancellous bone is dependent on its density (Hayes and Bouxsein, 1997).

Architecture

Bone may be described as a composite material. It has an organic matrix consisting mainly of collagen and other non-collagen fibres. Embedded within this organic matrix is an inorganic component primarily composed of hydroxyapatite crystals. The tissue is vascularized, supplying nutrition to hyaline cartilage cells and other connective tissue components. The bone cells themselves are unable to derive their nutrition via this

mechanism. There are small bone canaliculi which are connected to Haversian canals, which contain small capillaries (Huston, 2013).

Bone is formed in concentric layers (or lamellae) around capillaries. The capillaries and Haversian systems are connected by anastomosing vessels known as Volkman's canals.

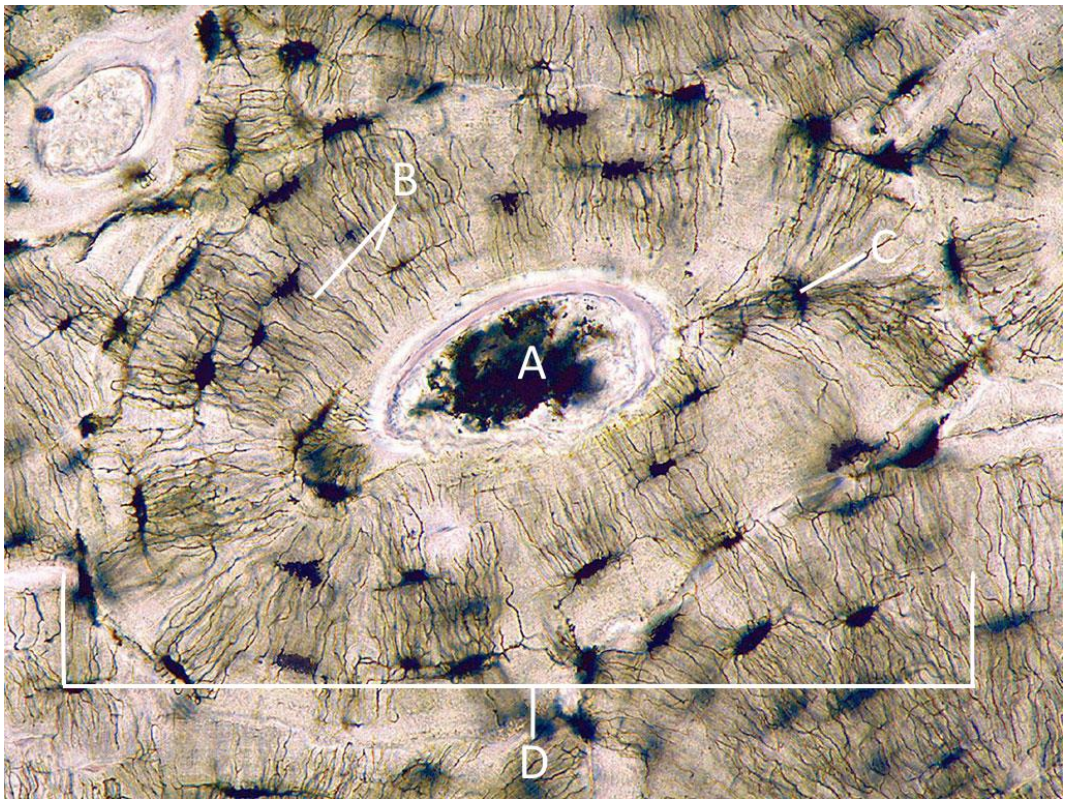

A photomicrograph of a section of bone. Label A represents a Haversian canal, B are canaliculi, C represents a lacuna which encloses the bone cell (osteocyte), and D is the osteon composed of Haversian canal surrounded by concentric lamellae. Image used with permission Copyright ©Cea1.com – Human Body Anatomy 2014

Bone has two macroscopic forms, cortical and cancellous. Cortical bone is hard, but less so than the dental hard tissues enamel and dentine. Cancellous bone (also described as trabecular or spongy) has lattice-like structure which readily adapts to loading. It has a density of between 5% and 70% of that of cortical bone. Despite the macroscopic differences between the two types of bone, microscopically there are none.

Cancellous bone is filled with marrow, although this is not part of the bone itself. The marrow has haemopoietic activity. This is lost with age as the initial red marrow is gradually replaced with yellow fatty marrow.

The periosteum is a layer of fibrous tissue, which covers the outer surface of cortical bone. In addition to providing nutrition to the underlying bone via fine periosteal vessels, it has osteogenic potential, which is of benefit in fracture healing.

Appendix 5

Mandibular fracture classifications

There are many classifications of fractures. Classifications may be general, applying to all bony fractures or specific to a bone or regions of a bone. A good anatomical classification system should clearly identify the involved region, and if possible the complexity of the pattern of the fracture. A clinical classification system may be more demanding, additionally aiming to inform the end-user of the severity of the injury and possible treatment therapies. Whether clinical or anatomical, all classification systems should be logical, systematic and easy to use. Mandibular fractures have been classified in many ways, both globally and regionally. Examples of classification schemes are shown below. The list is not exhaustive.

- Classification according to the macroscopic appearance of the fracture:
    - Linear or Comminuted
        - Determined by a single fracture or multiple fragments
    - Open or closed
        - Determined by the presence of communication with the exterior of the body
    - Complete or greenstick or torus/buckle
- Classification according to the relationship of the teeth (Kazanjian and Converse, 1974):
    - Class I: teeth both sides of fracture
    - Class II: teeth one side of fracture
    - Class III: edentulous

- Classification according to various anatomical sub-sites of fracture (Dingman and Natvig, 1964; Sinn, et al., 1987; Pogrel and Kaban, 1989; Buitrago-Tellez, et al., 2008). The anatomical sub-sites have included:
    - Condyle
    - Ramus
    - Coronoid
    - Angle
    - Body
    - Horizontal ramus
    - Parasymphysis
    - Canine region
    - Symphysis
- Classification of sub-sites:
    - Condyle (Lindahl, 1977; Spiessl and Schrol, 1989; Loukota, et al., 2005; Maclennan, 1952)
- According to the effect of muscle action:
    - Favourability
    - Stability
    - Displacement

Some classification systems are purely methods of coding, which may be useful for service and finance planning e.g. the International Statistical Classification of Diseases and Related Health Problems (ICD).

Most of the existing mandibular fracture classification systems have problems accurately describing high energy, multi-fragmentary injuries. Additionally, only one classification system has been validated, making comparisons between studies difficult.

The classification system of Buitrago, et al. (2008, pp. 1087) is based on the AO system and aims to "record the precise location of an osseous injury, displacement degree, fragmentation, presence of condylar head luxation or mandibular atrophy". It is comprehensive and has been extensively validated; however, its complexity means that reliability and accuracy may be problematic.

ICD-9 code	Fracture type; region
802.20, 802.30	Closed, open fracture of mandible
• 802.21, 802.31	• Closed, open fracture of mandible; condylar process
• 802.22, 802.32	• Closed, open fracture of mandible; subcondylar
• 802.23, 802.33	• Closed, open fracture of mandible; coronoid process
• 802.24, 802.34	• Closed, open fracture of mandible; ramus
• 802.25, 802.35	• Closed, open fracture of mandible; angle of jaw
• 802.26, 802.36	• Closed, open fracture of mandible; symphysis
• 802.27, 802.37	• Closed, open fracture of mandible; alveolar border
• 802.28, 802.38	• Closed, open fracture of mandible; body

Classification of fractured mandibles (World Health Organization, 1977). This has been superseded by the ICD-10 classification.

Appendix 6

What is a fracture?

The term “fracture” may describe different events depending on the context in which it is used. In the field of engineering, a fracture may be defined as “the separation of a body into pieces due to stress, at temperatures below the melting point” (University of Virginia, Department of Materials Science and Engineering, 2010). Materials may be roughly divided in to those, which fracture in a brittle manner, and those, which fracture in a ductile manner. Materials such as bone do not fit into a single category.

Ductile fracture may be differentiated from brittle fracture by its ability to undergo significant plastic deformation. This does not occur to any significant extent in brittle failure. The manner in which cracks initiate and propagate also differ. In ductile fracture, cracks will extend slowly in response to increased stress whereas brittle fractures grow rapidly. On the macroscopic level, there is no permanent deformation in brittle fracture. Ductile fracture characteristically leaves a dull, often fibrous-looking surface.

Both ductile and brittle fractures require energy to extend the initial crack. The energy required to extend the fracture is also known as the elastic strain energy. A crack will propagate until the end of the affected body is reached or the energy required for crack extension exceeds the strain energy released.

The term fracture, when used clinically in reference to hard-tissues such a bone, enamel, dentine or cementum, implies a complete or incomplete break in the continuity of the structure.

Traumatic injuries to bone will result in reversible deformation when the loading force is small and within the elastic limit. When the load is further increased, plastic deformation occurs which is irreversible. This has been described as a plastic fracture i.e.

there has been bending or acute angulation of the bone without macroscopic cortical bone disruption.

Another form of fracture is the torus or buckle. This refers to a fracture of the cortex on the side under compression with an intact adjacent cortex. This differs from greenstick fracture, which is a disruption of the cortex on the tension side of the fracture only.

The reference to “sides” of a bony cortex is in fact misleading as the cortex is composed of a single surface.

Clinically, fractures are usually visualized radiographically, although occasionally “open fractures,” allow direct visualization. In general, when a fracture is diagnosed radiographically, what is really being assessed is fragment displacement. When fragments are displaced in opposite directions, a radiolucent line, representing the less dense tissue space appears. When fragments override each other, there is increased radio-opacity. However, clearly, a fracture may occur when there is no discernible displacement and in such cases, other modalities such as CT, MRI or even nuclear medicine may be required to detect an occult fracture.

Bony fracture in most clinical cases will lead to a reduction in performance and occasionally failure of the associated system. Equally, in some cases, the performance loss is so minimal that the fracture may be left to heal without surgical intervention.

Appendix 7

Meta-analysis (random effects results)

Ascending ramus

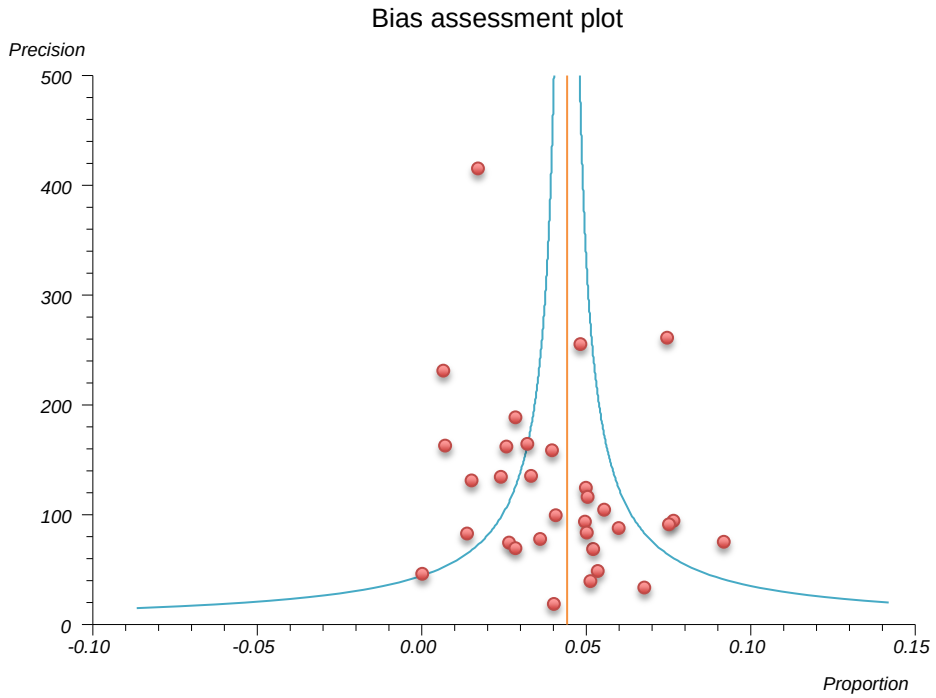

Ascending ramus bias assessment plot.

Author	Effect Size (Proportion) and 95% Confidence Interval (exact)			% Weight
	Point Estimate	Lower Limit	Upper Limit	Random
Abdullah, et al., 2013	0.026455	0.008644	0.060654	2.764228
Adebayo, et al., 2003	0.049462	0.03161	0.073296	3.353174
Adi, et al., 1990	0.05538	0.038874	0.076181	3.488149
Al Ahmed, et al., 2004	0.053333	0.023304	0.102382	2.567572
Al-Khateeb and Abdullah, 2007	0.051852	0.028634	0.085469	3.033068
Andersson, et al., 1984	0.032051	0.021727	0.045441	3.620071
Bither, et al., 2008	0.059671	0.040323	0.084576	3.374516
Elgehani, et al., 2009	0.033083	0.020847	0.049661	3.507671
Ellis, et al., 1985	0.048015	0.040785	0.056107	3.831323
Eskitaşcıoğlu, et al., 2009	0.015015	0.004893	0.03469	3.169453
Eskitaşcıoğlu, et al., 2013	0.02844	0.019404	0.040127	3.660764
Ferreira, et al., 2004	0.076358	0.057551	0.09893	3.516528
Gandhi, et al., 2011	0.006263	0.001293	0.018193	3.36758
Hall and Ofodile, 1991	0.028409	0.009287	0.065049	2.705305
Joshi, et al., 2013	0.05102	0.016771	0.115058	2.172136
Kadkhodaie, 2006	0.016834	0.012597	0.022017	3.830238
Le, et al., 2001	0.04	0.001012	0.203517	0.962965
Martins, et al., 2011	0.013699	0.001663	0.048607	2.543583
Mijiti, et al., 2014	0.07496	0.055595	0.098436	3.485032
Oji, 1998	0	0	0.084084	1.372654
Olafsson, 1984	0.05	0.030368	0.076982	3.246928
Sakr, et al., 2006	0.025572	0.015465	0.039647	3.547599
Salem, et al., 1968	0.049813	0.035822	0.067217	3.573519

Simsek, et al., 2007 (a)	0.035714	0.016459	0.066712	2.984625
Simsek, et al., 2007 (b)	0.039385	0.028409	0.053053	3.649028
Subhashraj, et al., 2007	0.091797	0.068229	0.120199	3.398847
Subhashraj, et al., 2008	0.040632	0.024256	0.063458	3.32898
Walden, et al., 1956	0.05035	0.03551	0.069027	3.534166
Yamamoto K et al. 2010	0.023952	0.012436	0.041465	3.388818
Yamamoto, et al., 2011	0.067416	0.025141	0.14098	2.079151
Zachariades, et al., 1990	0.074411	0.067171	0.082169	3.865539
Zhou, et al., 2013	0.006944	0.000842	0.024859	3.076786

Ascending ramus fracture results.

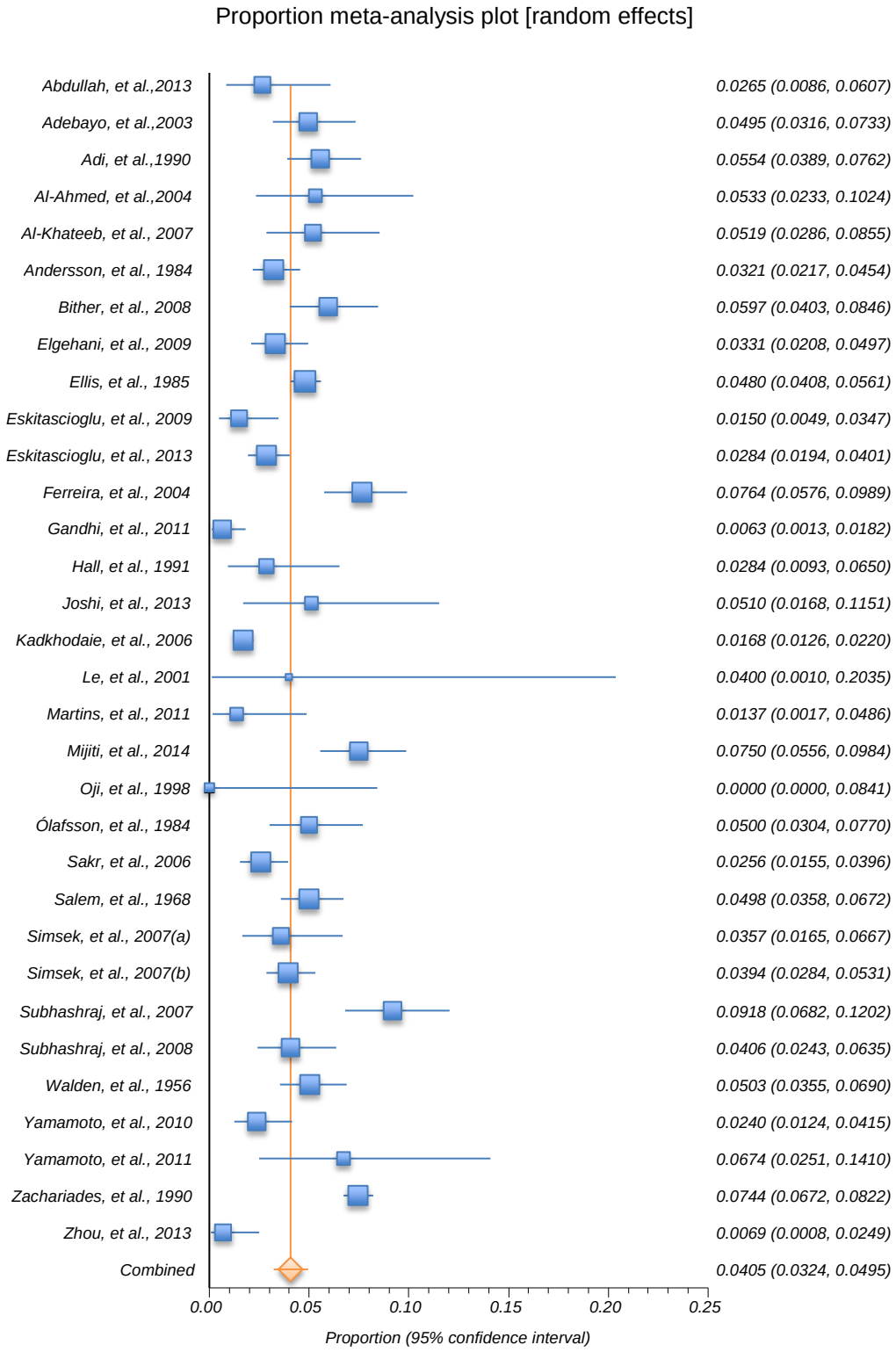

Ascending ramus Forest plot (random effects).

Angle

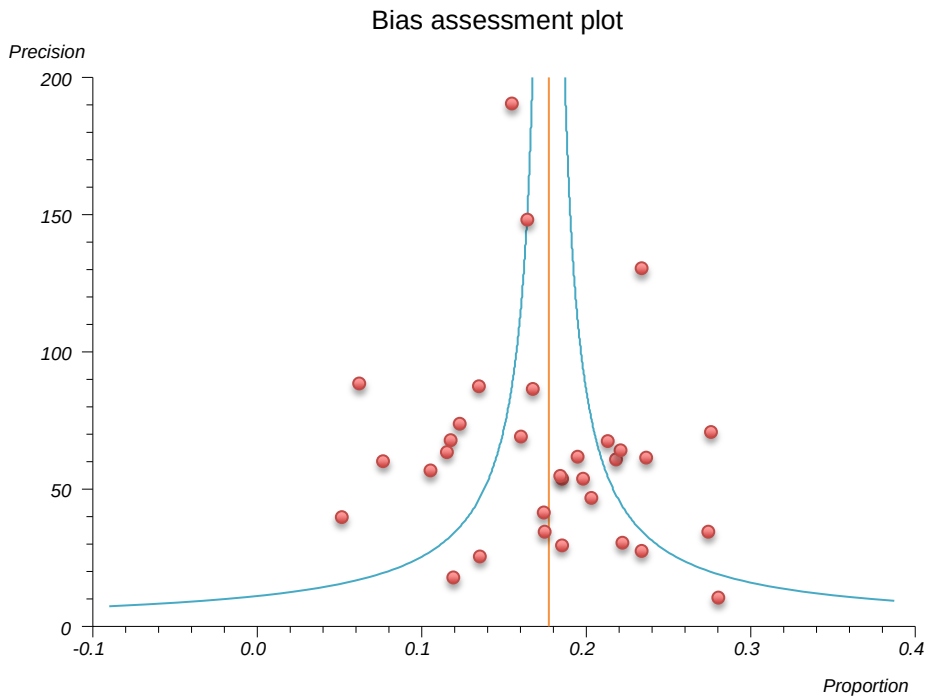

Angle bias assessment plot.

Author	Effect Size (Proportion) and 95% Confidence Interval (exact)			% Weight
	Point Estimate	Lower Limit	Upper Limit	Random
Abdullah, et al., 2013	0.174603	0.123342	0.236375	2.845119
Adebayo, et al., 2003	0.184946	0.150681	0.223277	3.333914
Adi, et al., 1990	0.19462	0.164449	0.227676	3.441289
Al Ahmed, et al., 2004	0.233333	0.168225	0.309277	2.674148
Al-Khateeb and Abdullah, 2007	0.174074	0.130796	0.22467	3.072445
Andersson, et al., 1984	0.134615	0.113392	0.158167	3.544643
Bither, et al., 2008	0.197531	0.163036	0.235753	3.351003
Elgehani, et al., 2009	0.218045	0.187219	0.251397	3.456682
Ellis, et al., 1985	0.233355	0.218618	0.248592	3.706955
Eskitaşcıoğlu, et al., 2009	0.105105	0.074308	0.143138	3.185042
Eskitaşcıoğlu, et al., 2013	0.166972	0.145296	0.190463	3.576211
Ferreira, et al., 2004	0.160059	0.133308	0.189794	3.463654
Gandhi, et al., 2011	0.183716	0.150035	0.221357	3.345454
Hall and Ofodile, 1991	0.221591	0.162569	0.290235	2.794315
Joshi, et al., 2013	0.05102	0.016771	0.115058	2.317742
Kadkhodaie, 2006	0.163807	0.150917	0.177337	3.706131
Le, et al., 2001	0.28	0.120717	0.493877	1.110758
Martins, et al., 2011	0.184932	0.12555	0.25754	2.653013
Mijiti, et al., 2014	0.122807	0.098145	0.151084	3.438829
Oji, 1998	0.119048	0.039806	0.256317	1.541027
Olafsson, 1984	0.202632	0.163354	0.246613	3.248208
Sakr, et al., 2006	0.220727	0.19139	0.252299	3.488058
Salem, et al., 1968	0.212951	0.185109	0.242919	3.508349
Simsek, et al., 2007 (a)	0.27381	0.219724	0.333302	3.032015
Simsek, et al., 2007 (b)	0.275696	0.248736	0.303931	3.567122
Subhashraj, et al., 2007	0.117188	0.090628	0.148259	3.370434
Subhashraj, et al., 2008	0.115124	0.086929	0.148578	3.31449
Walden, et al., 1956	0.236364	0.205665	0.269255	3.477518
Yamamoto K et al. 2010	0.061876	0.042425	0.086682	3.362432
Yamamoto, et al., 2011	0.134831	0.071655	0.223682	2.231384
Zachariades, et al., 1990	0.154403	0.144328	0.164896	3.732883
Zhou, et al., 2013	0.076389	0.04849	0.113371	3.108734

Angle results.

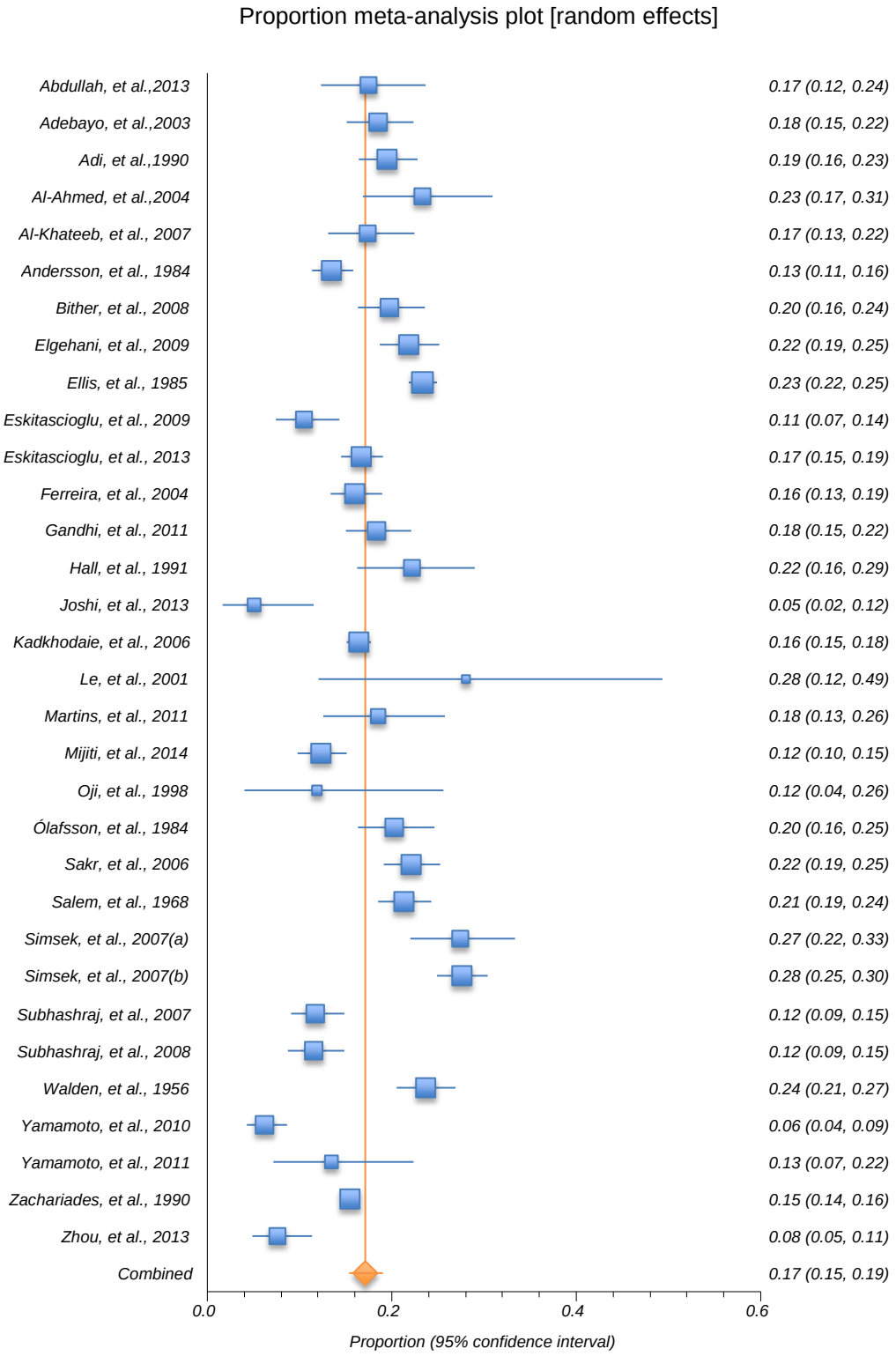

Angle Forest plot (random effects).

Body

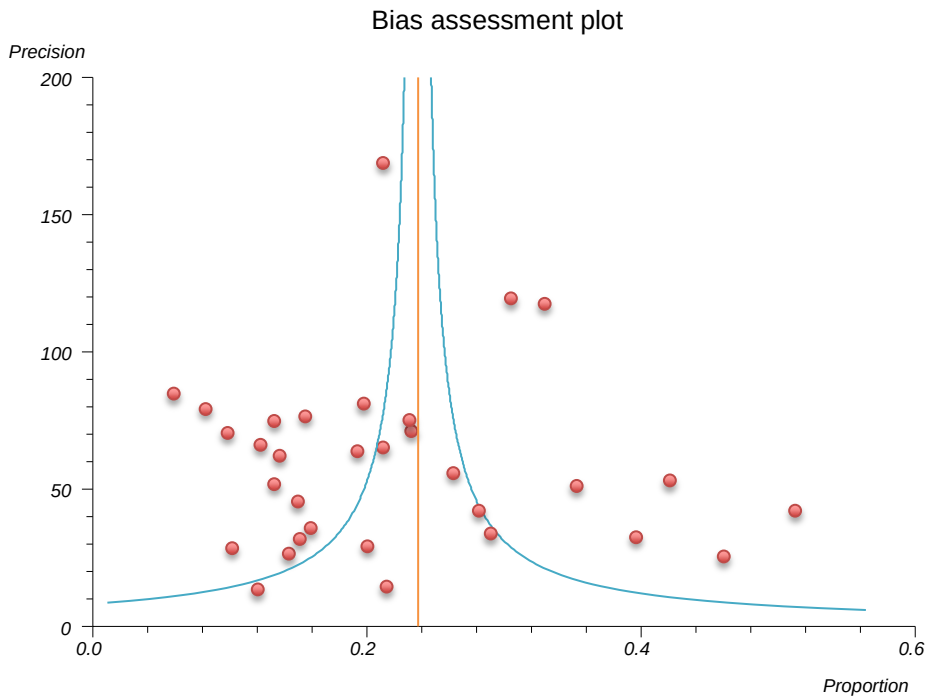

Body bias assessment plot.

Author	Effect Size (Proportion) and 95% Confidence Interval (exact)			% Weight
	Point Estimate	Lower Limit	Upper Limit	Random
Abdullah, et al., 2013	0.15873	0.10973	0.218778	3.053573
Adebayo, et al., 2003	0.511828	0.465369	0.558136	3.234013
Adi, et al., 1990	0.262658	0.228733	0.298817	3.269097
Al Ahmed, et al., 2004	0.2	0.139194	0.273036	2.981042
Al-Khateeb and Abdullah, 2007	0.396296	0.337527	0.457368	3.142043
Andersson, et al., 1984	0.231838	0.205147	0.260227	3.301523
Bither, et al., 2008	0.135802	0.10661	0.16951	3.239696
Elgehani, et al., 2009	0.192481	0.163184	0.224537	3.274008
Ellis, et al., 1985	0.329385	0.312911	0.34618	3.349965
Eskitaşcıoğlu, et al., 2009	0.132132	0.097675	0.173296	3.182844
Eskitaşcıoğlu, et al., 2013	0.197248	0.174009	0.222133	3.311176
Ferreira, et al., 2004	0.132159	0.107627	0.159927	3.276223
Gandhi, et al., 2011	0.098121	0.072989	0.128341	3.237855
Hall and Ofodile, 1991	0.460227	0.384981	0.536835	3.032591
Joshi, et al., 2013	0.142857	0.08036	0.22806	2.810232
Kadkhodaie, 2006	0.304953	0.288747	0.321529	3.349727
Le, et al., 2001	0.12	0.025465	0.31219	1.915417
Martins, et al., 2011	0.150685	0.096907	0.219205	2.971685
Mijiti, et al., 2014	0.352472	0.315051	0.39129	3.26831
Oji, 1998	0.214286	0.10296	0.368116	2.309734
Olafsson, 1984	0.281579	0.236897	0.329701	3.204927
Sakr, et al., 2006	0.211306	0.182473	0.242451	3.283929
Salem, et al., 1968	0.154421	0.13011	0.181299	3.290281
Simsek, et al., 2007 (a)	0.289683	0.234465	0.349925	3.126924
Simsek, et al., 2007 (b)	0.230548	0.205273	0.257355	3.308408
Subhashraj, et al., 2007	0.082031	0.059759	0.109266	3.246111
Subhashraj, et al., 2008	0.058691	0.038693	0.084816	3.227508
Walden, et al., 1956	0.420979	0.384482	0.458131	3.280609
Yamamoto K et al. 2010	0.121756	0.094427	0.15364	3.243475
Yamamoto, et al., 2011	0.101124	0.047293	0.183302	2.764238
Zachariades, et al., 1990	0.211038	0.199613	0.222812	3.357438
Zhou, et al., 2013	0.149306	0.110208	0.195798	3.155399

Body results.

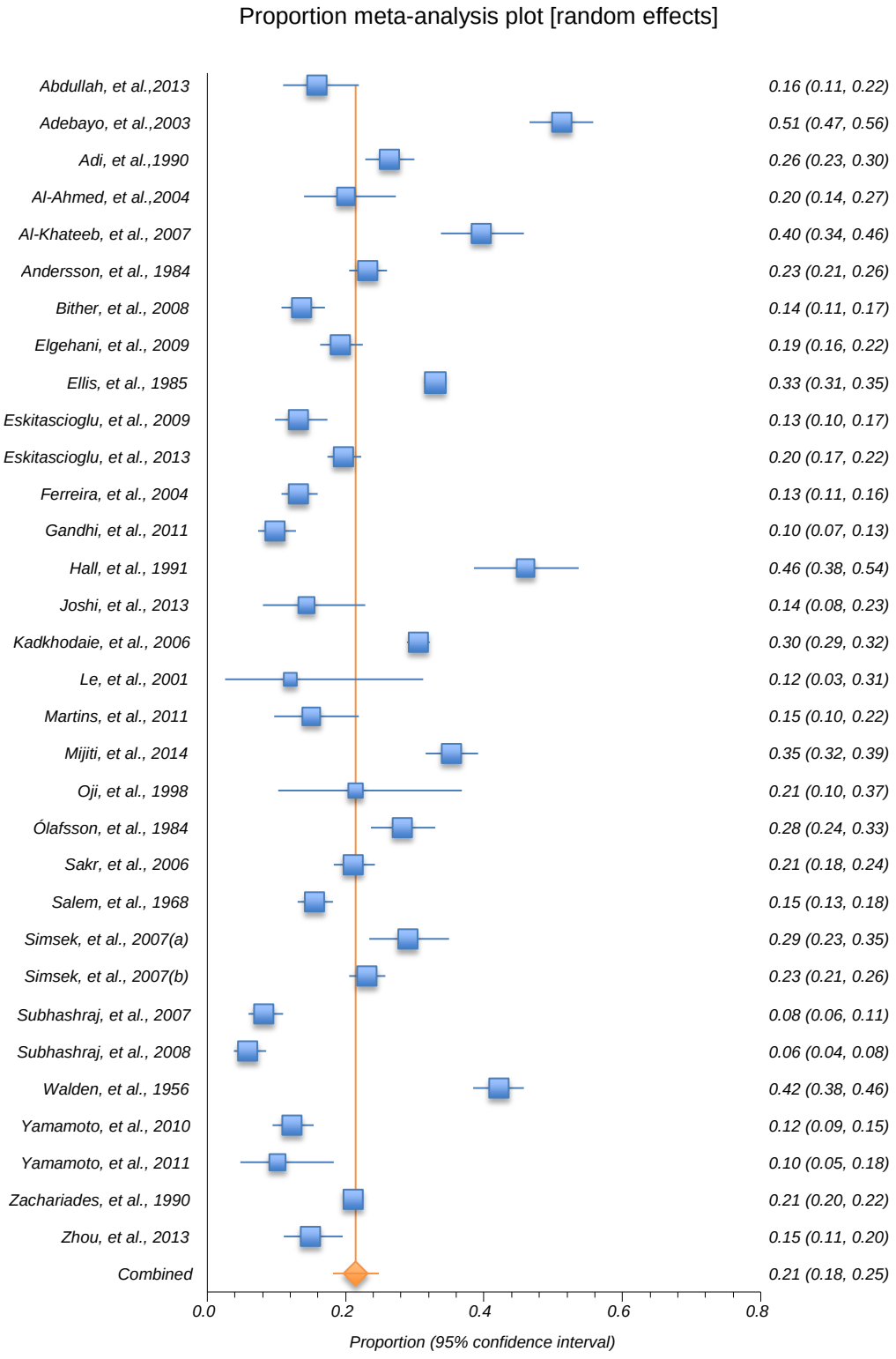

Body Forest plot (random effects).

Parasymphysis/Symphysis

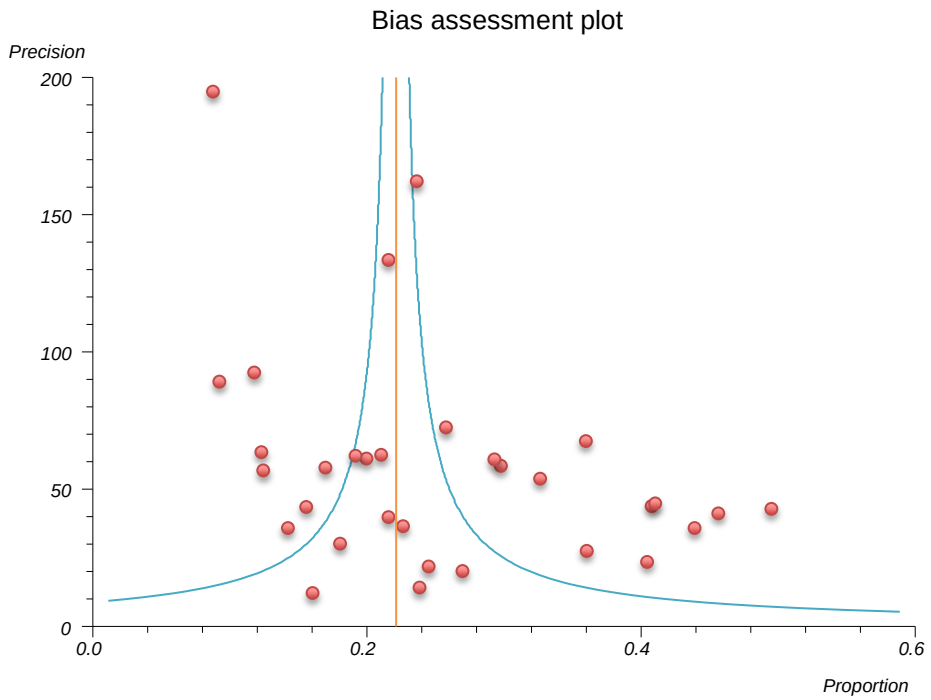

Parasymphysis/symphysis bias assessment plot.

Author	Effect Size (Proportion) and 95% Confidence Interval (exact)			% Weight
	Point Estimate	Lower Limit	Upper Limit	Random
Abdullah, et al., 2013	0.359788	0.291414	0.432638	3.072493
Adebayo, et al., 2003	0.122581	0.094178	0.155886	3.216627
Adi, et al., 1990	0.191456	0.16149	0.224335	3.244267
Al Ahmed, et al., 2004	0.18	0.1221	0.250978	3.013606
Al-Khateeb and Abdullah, 2007	0.155556	0.114468	0.204394	3.143578
Andersson, et al., 1984	0.117521	0.097585	0.139899	3.269704
Bither, et al., 2008	0.407407	0.363374	0.452574	3.221112
Elgehani, et al., 2009	0.326316	0.290767	0.363415	3.248126
Ellis, et al., 1985	0.087068	0.077411	0.097505	3.307511
Eskitaşcıoğlu, et al., 2009	0.438438	0.3844	0.493582	3.176091
Eskitaşcıoğlu, et al., 2013	0.359633	0.331097	0.38893	3.277256
Ferreira, et al., 2004	0.209985	0.179972	0.242536	3.249866
Gandhi, et al., 2011	0.494781	0.449115	0.540512	3.219659
Hall and Ofodile, 1991	0.142045	0.094081	0.202507	3.055514
Joshi, et al., 2013	0.244898	0.163643	0.34213	2.872718
Kadkhodaie, 2006	0.215604	0.201214	0.230534	3.307325
Le, et al., 2001	0.16	0.045379	0.360828	2.079925
Martins, et al., 2011	0.40411	0.323783	0.488409	3.005969
Mijiti, et al., 2014	0.199362	0.168769	0.232816	3.243648
Oji, 1998	0.238095	0.120516	0.394502	2.441127
Olafsson, 1984	0.123684	0.092311	0.161061	3.193618
Sakr, et al., 2006	0.297443	0.264759	0.331744	3.255915
Salem, et al., 1968	0.292653	0.261371	0.325465	3.260897
Simsek, et al., 2007 (a)	0.22619	0.176048	0.282897	3.131487
Simsek, et al., 2007 (b)	0.257445	0.231121	0.285147	3.275092
Subhashraj, et al., 2007	0.410156	0.367201	0.454155	3.226172
Subhashraj, et al., 2008	0.455982	0.408903	0.503653	3.211488
Walden, et al., 1956	0.092308	0.07211	0.115941	3.25331
Yamamoto K et al. 2010	0.169661	0.137827	0.205451	3.224093
Yamamoto, et al., 2011	0.269663	0.181032	0.374173	2.834241
Zachariades, et al., 1990	0.235841	0.223938	0.248064	3.313322
Zhou, et al., 2013	0.215278	0.16922	0.267299	3.15424

Parasymphysis/symphysis results.

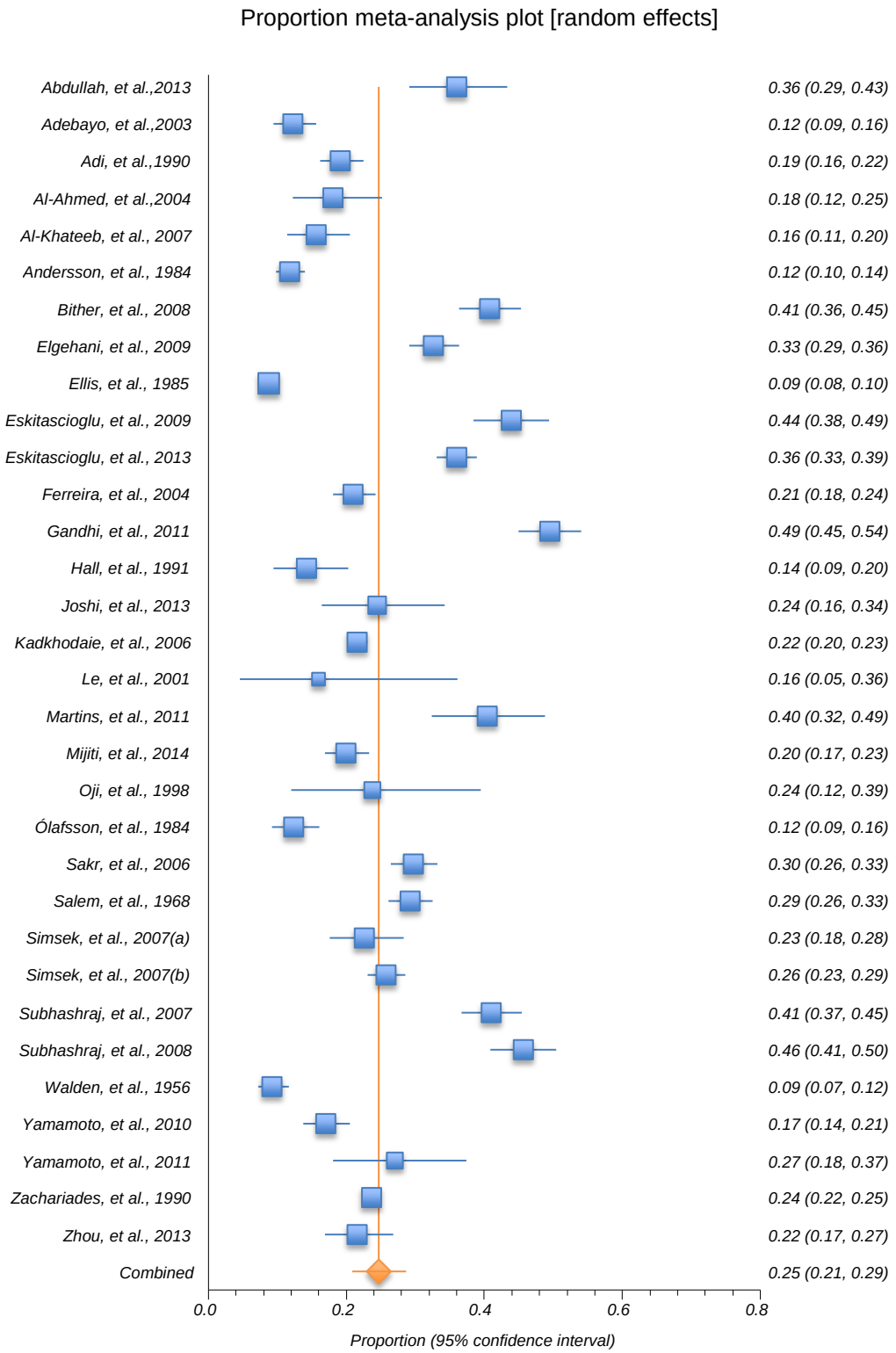

Parasymphysis/symphysis Forest plot (random effects).

Alveolus

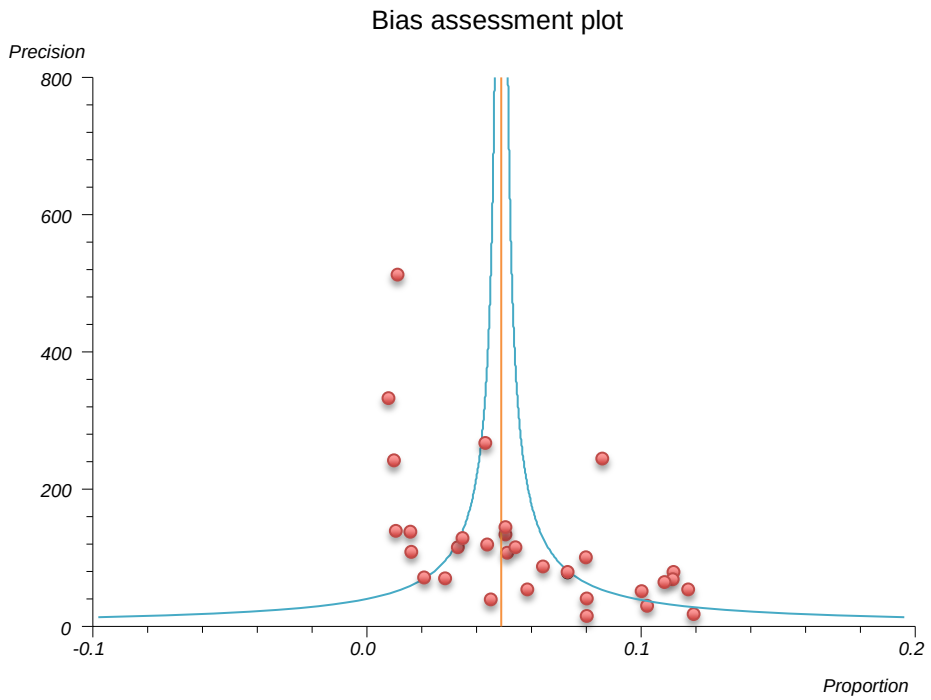

Alveolus bias assessment plot.

Author	Effect Size (Proportion) and 95% Confidence Interval (exact)			% Weight
	Point Estimate	Lower Limit	Upper Limit	Random
Abdullah, et al., 2013	0.058201	0.029409	0.10175	2.961149
Adebayo, et al., 2003	0.073118	0.051165	0.100679	3.291394
Adi, et al., 1990	0.03481	0.021941	0.05223	3.359439
Al Ahmed, et al., 2004	0.08	0.04202	0.135574	2.837018
Al-Khateeb and Abdullah, 2007	0.1	0.06694	0.142155	3.119083
Andersson, et al., 1984	0.050214	0.037125	0.066217	3.423515
Bither, et al., 2008	0.032922	0.018932	0.052913	3.302327
Elgehani, et al., 2009	0.043609	0.029397	0.062032	3.36907
Ellis, et al., 1985	0.010883	0.007549	0.015176	3.521436
Eskitaşcıoğlu, et al., 2009	0.117117	0.084621	0.156611	3.194467
Eskitaşcıoğlu, et al., 2013	0.050459	0.038235	0.065176	3.442816
Ferreira, et al., 2004	0.111601	0.088942	0.137687	3.373421
Gandhi, et al., 2011	0.073069	0.05142	0.100158	3.298781
Hall and Ofodile, 1991	0.028409	0.009287	0.065049	2.924758
Joshi, et al., 2013	0.102041	0.050028	0.17966	2.562173
Kadkhodaie, 2006	0.043056	0.036172	0.050821	3.520948
Le, et al., 2001	0.08	0.00984	0.260306	1.431496
Martins, et al., 2011	0.020548	0.004258	0.058874	2.821339
Mijiti, et al., 2014	0.051037	0.035167	0.071288	3.357897
Oji, 1998	0.119048	0.039806	0.256317	1.875169
Olafsson, 1984	0.015789	0.005816	0.034049	3.235967
Sakr, et al., 2006	0.053836	0.038736	0.072591	3.388604
Salem, et al., 1968	0.079701	0.061918	0.100639	3.40117
Simsek, et al., 2007 (a)	0.015873	0.004341	0.04014	3.091565
Simsek, et al., 2007 (b)	0.007685	0.003323	0.015086	3.437271
Subhashraj, et al., 2007	0.111328	0.085417	0.141825	3.314709
Subhashraj, et al., 2008	0.108352	0.080978	0.141085	3.27892
Walden, et al., 1956	0.00979	0.003945	0.020067	3.382056
Yamamoto K et al. 2010	0.063872	0.044095	0.088975	3.309616
Yamamoto, et al., 2011	0.044944	0.01238	0.111092	2.492066
Zachariades, et al., 1990	0.085573	0.077839	0.093811	3.536781
Zhou, et al., 2013	0.010417	0.002153	0.030138	3.143578

Alveolus results.

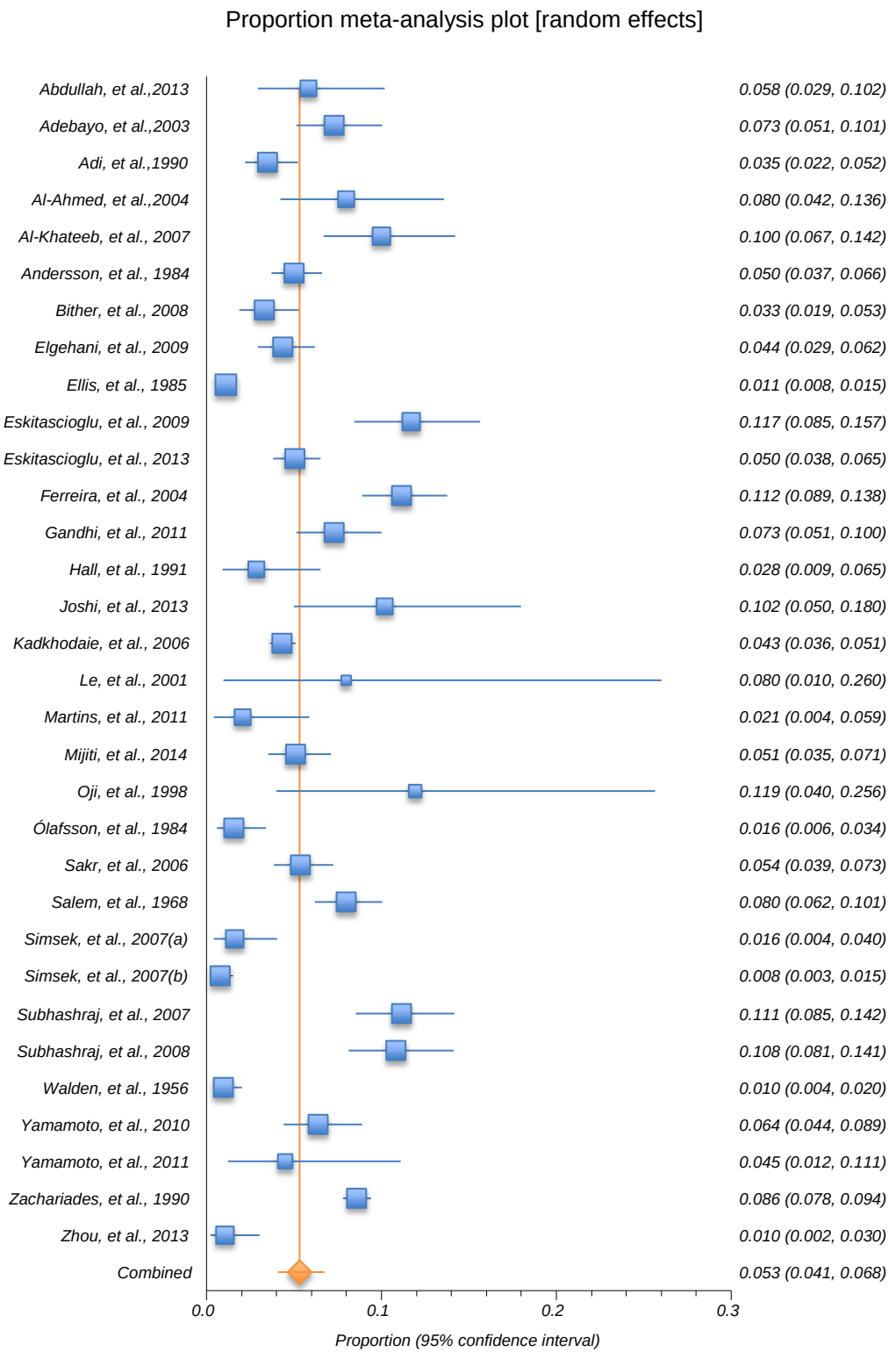

Alveolus Forest plot (random effects).

Meta-analysis (fixed effect results)

Condyle

Author	Effect Size (Proportion) and 95% Confidence Interval (exact)			% Weight
	Point Estimate	Lower Limit	Upper Limit	Fixed
Abdullah, et al., 2013	0.222222	0.165099	0.288274	0.780608
Adebayo, et al., 2003	0.058065	0.03861	0.083359	1.914544
Adi, et al., 1990	0.261076	0.227225	0.297176	2.600657
Al Ahmed, et al., 2004	0.253333	0.18593	0.330744	0.620378
Al-Khateeb and Abdullah, 2007	0.122222	0.085645	0.167346	1.113394
Andersson, et al., 1984	0.433761	0.401728	0.466211	3.84963
Bither, et al., 2008	0.166667	0.134617	0.202835	2.000822
Elgehani, et al., 2009	0.186466	0.157557	0.218189	2.736237
Ellis, et al., 1985	0.291293	0.275402	0.307576	12.838948
Eskitaşcıoğlu, et al., 2009	0.192192	0.151273	0.238684	1.372227
Eskitaşcıoğlu, et al., 2013	0.197248	0.174009	0.222133	4.482334
Ferreira, et al., 2004	0.309838	0.275261	0.346073	2.801972
Gandhi, et al., 2011	0.14405	0.113839	0.178734	1.972062
Hall and Ofodile, 1991	0.119318	0.075398	0.176593	0.727198
Joshi, et al., 2013	0.408163	0.309923	0.512107	0.406738
Kadkhodaie, 2006	0.255746	0.240436	0.27152	12.695152
Le, et al., 2001	0.32	0.149495	0.535001	0.10682
Martins, et al., 2011	0.226027	0.160983	0.302523	0.603944
Mijiti, et al., 2014	0.199362	0.168769	0.232816	2.580115
Oji, 1998	0.309524	0.176221	0.470861	0.176664
Olafsson, 1984	0.326316	0.279373	0.37599	1.565325
Sakr, et al., 2006	0.191117	0.163445	0.221266	3.056697
Salem, et al., 1968	0.210461	0.182749	0.240316	3.303205
Simsek, et al., 2007 (a)	0.15873	0.115885	0.209811	1.039441
Simsek, et al., 2007 (b)	0.189241	0.165872	0.214382	4.281019
Subhashraj, et al., 2007	0.1875	0.154601	0.224055	2.107642
Subhashraj, et al., 2008	0.221219	0.183411	0.262796	1.824158
Walden, et al., 1956	0.19021	0.16207	0.220932	2.94166
Yamamoto K et al. 2010	0.558882	0.514167	0.602899	2.062449
Yamamoto, et al., 2011	0.382022	0.281	0.49113	0.369762
Zachariades, et al., 1990	0.238735	0.226779	0.251007	19.880855
Zhou, et al., 2013	0.541667	0.48221	0.600257	1.187346

Condyle results.

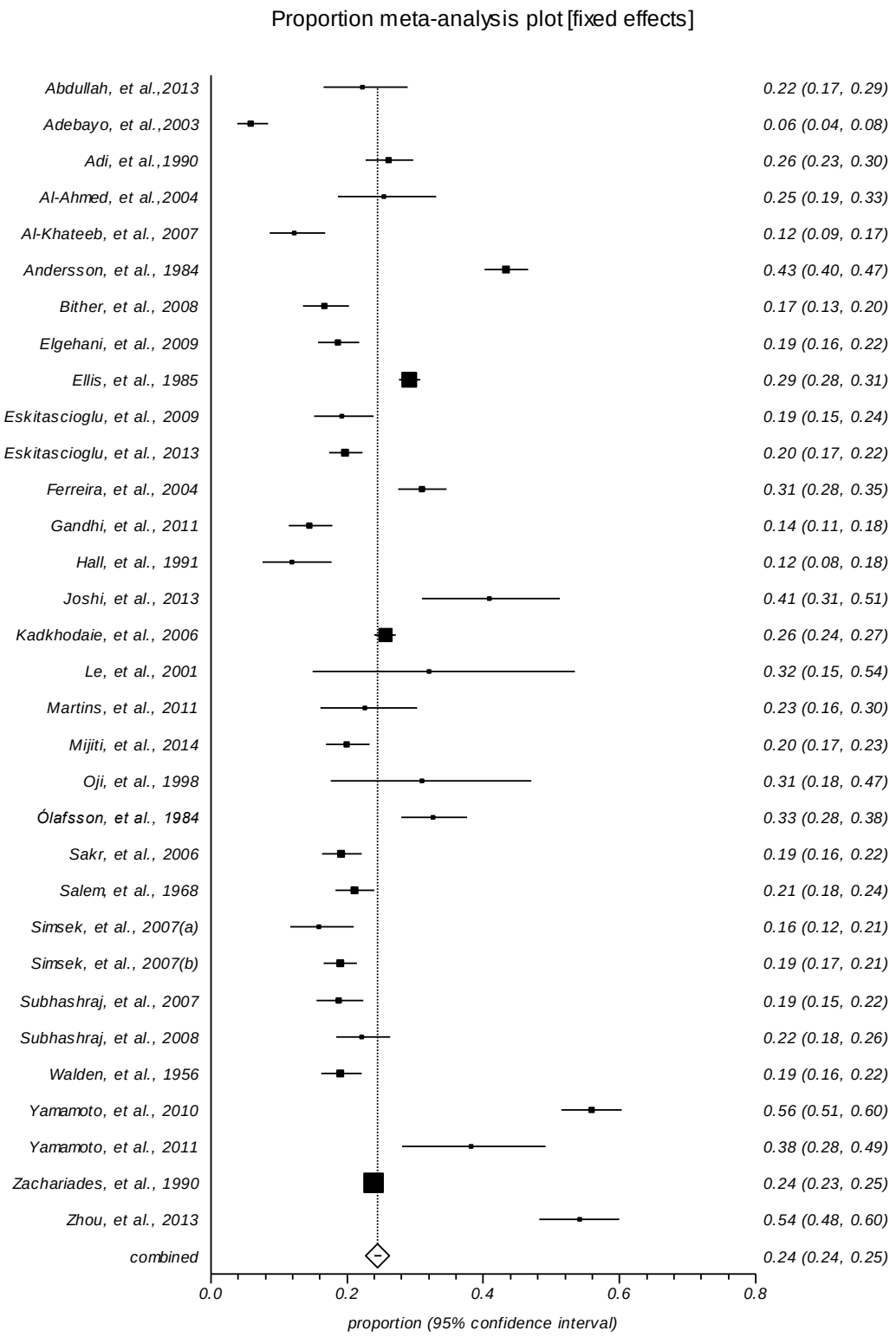
Proportion meta-analysis plot [fixed effects]
Abdullah, et al.,2013 0.22 (0.17, 0.29)
Adebayo, et al.,2003 0.06 (0.04, 0.08)
Adi, et al.,1990 0.26 (0.23, 0.30)
Al-Ahmed, et al.,2004 0.25 (0.19, 0.33)
Al-Khateeb, et al., 2007 0.12 (0.09, 0.17)
Andersson, et al., 1984 0.43 (0.40, 0.47)
Bither, et al., 2008 0.17 (0.13, 0.20)
Elgehani, et al., 2009 0.19 (0.16, 0.22)
Ellis, et al., 1985 0.29 (0.28, 0.31)
Eskitascioglu, et al., 2009 0.19 (0.15, 0.24)
Eskitascioglu, et al., 2013 0.20 (0.17, 0.22)
Ferreira, et al., 2004 0.31 (0.28, 0.35)
Gandhi, et al., 2011 0.14 (0.11, 0.18)
Hall, et al., 1991 0.12 (0.08, 0.18)
Joshi, et al., 2013 0.41 (0.31, 0.51)
Kadkhodaie, et al., 2006 0.26 (0.24, 0.27)
Le, et al., 2001 0.32 (0.15, 0.54)
Martins, et al., 2011 0.23 (0.16, 0.30)
Mijiti, et al., 2014 0.20 (0.17, 0.23)
Oji, et al., 1998 0.31 (0.18, 0.47)
Ólafsson, et al., 1984 0.33 (0.28, 0.38)
Sakr, et al., 2006 0.19 (0.16, 0.22)
Salem, et al., 1968 0.21 (0.18, 0.24)
Simsek, et al., 2007(a) 0.16 (0.12, 0.21)
Simsek, et al., 2007(b) 0.19 (0.17, 0.21)
Subhashraj, et al., 2007 0.19 (0.15, 0.22)
Subhashraj, et al., 2008 0.22 (0.18, 0.26)
Walden, et al., 1956 0.19 (0.16, 0.22)
Yamamoto, et al., 2010 0.56 (0.51, 0.60)
Yamamoto, et al., 2011 0.38 (0.28, 0.49)
Zachariades, et al., 1990 0.24 (0.23, 0.25)
Zhou, et al., 2013 0.54 (0.48, 0.60)
combined 0.24 (0.24, 0.25)
0.0
0.2
0.4
0.6
0.8
proportion (95% confidence interval)

Ascending ramus

Author	Effect Size (Proportion) and 95% Confidence Interval (exact)			% Weight
	Point Estimate	Lower Limit	Upper Limit	Fixed
Abdullah, et al., 2013	0.026455	0.008644	0.060654	0.780608
Adebayo, et al., 2003	0.049462	0.03161	0.073296	1.914544
Adi, et al., 1990	0.05538	0.038874	0.076181	2.600657
Al Ahmed, et al., 2004	0.053333	0.023304	0.102382	0.620378
Al-Khateeb and Abdullah, 2007	0.051852	0.028634	0.085469	1.113394
Andersson, et al., 1984	0.032051	0.021727	0.045441	3.84963
Bither, et al., 2008	0.059671	0.040323	0.084576	2.000822
Elgehani, et al., 2009	0.033083	0.020847	0.049661	2.736237
Ellis, et al., 1985	0.048015	0.040785	0.056107	12.838948
Eskitaşcıoğlu, et al., 2009	0.015015	0.004893	0.03469	1.372227
Eskitaşcıoğlu, et al., 2013	0.02844	0.019404	0.040127	4.482334
Ferreira, et al., 2004	0.076358	0.057551	0.09893	2.801972
Gandhi, et al., 2011	0.006263	0.001293	0.018193	1.972062
Hall and Ofodile, 1991	0.028409	0.009287	0.065049	0.727198
Joshi, et al., 2013	0.05102	0.016771	0.115058	0.406738
Kadkhodaie, 2006	0.016834	0.012597	0.022017	12.695152
Le, et al., 2001	0.04	0.001012	0.203517	0.10682
Martins, et al., 2011	0.013699	0.001663	0.048607	0.603944
Mijiti, et al., 2014	0.07496	0.055595	0.098436	2.580115
Oji, 1998	0	0	0.084084	0.176664
Olafsson, 1984	0.05	0.030368	0.076982	1.565325
Sakr, et al., 2006	0.025572	0.015465	0.039647	3.056697
Salem, et al., 1968	0.049813	0.035822	0.067217	3.303205
Simsek, et al., 2007 (a)	0.035714	0.016459	0.066712	1.039441
Simsek, et al., 2007 (b)	0.039385	0.028409	0.053053	4.281019
Subhashraj, et al., 2007	0.091797	0.068229	0.120199	2.107642
Subhashraj, et al., 2008	0.040632	0.024256	0.063458	1.824158
Walden, et al., 1956	0.05035	0.03551	0.069027	2.94166
Yamamoto K et al. 2010	0.023952	0.012436	0.041465	2.062449
Yamamoto, et al., 2011	0.067416	0.025141	0.14098	0.369762
Zachariades, et al., 1990	0.074411	0.067171	0.082169	19.880855
Zhou, et al., 2013	0.006944	0.000842	0.024859	1.187346

Ascending ramus results.

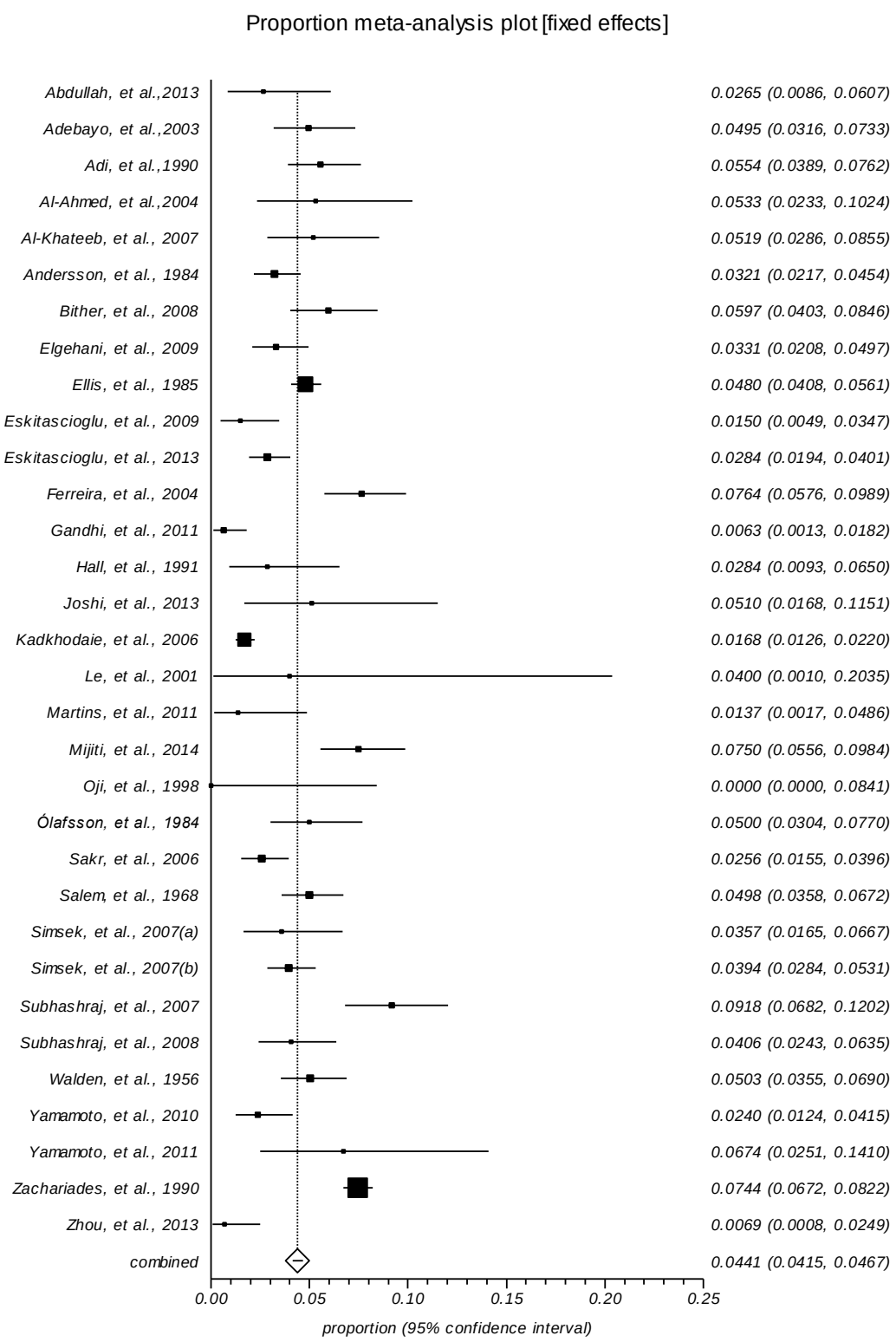
Proportion meta-analysis plot [fixed effects]
Abdullah, et al.,2013 0.0265 (0.0086, 0.0607)
Adebayo, et al.,2003 0.0495 (0.0316, 0.0733)
Adi, et al.,1990 0.0554 (0.0389, 0.0762)
Al-Ahmed, et al.,2004 0.0533 (0.0233, 0.1024)
Al-Khateeb, et al., 2007 0.0519 (0.0286, 0.0855)
Andersson, et al., 1984 0.0321 (0.0217, 0.0454)
Bither, et al., 2008 0.0597 (0.0403, 0.0846)
Elgehani, et al., 2009 0.0331 (0.0208, 0.0497)
Ellis, et al., 1985 0.0480 (0.0408, 0.0561)
Eskitascioglu, et al., 2009 0.0150 (0.0049, 0.0347)
Eskitascioglu, et al., 2013 0.0284 (0.0194, 0.0401)
Ferreira, et al., 2004 0.0764 (0.0576, 0.0989)
Gandhi, et al., 2011 0.0063 (0.0013, 0.0182)
Hall, et al., 1991 0.0284 (0.0093, 0.0650)
Joshi, et al., 2013 0.0510 (0.0168, 0.1151)
Kadkhodaie, et al., 2006 0.0168 (0.0126, 0.0220)
Le, et al., 2001 0.0400 (0.0010, 0.2035)
Martins, et al., 2011 0.0137 (0.0017, 0.0486)
Mijiti, et al., 2014 0.0750 (0.0556, 0.0984)
Oji, et al., 1998 0.0000 (0.0000, 0.0841)
Ólafsson, et al., 1984 0.0500 (0.0304, 0.0770)
Sakr, et al., 2006 0.0256 (0.0155, 0.0396)
Salem, et al., 1968 0.0498 (0.0358, 0.0672)
Simsek, et al., 2007(a) 0.0357 (0.0165, 0.0667)
Simsek, et al., 2007(b) 0.0394 (0.0284, 0.0531)
Subhashraj, et al., 2007 0.0918 (0.0682, 0.1202)
Subhashraj, et al., 2008 0.0406 (0.0243, 0.0635)
Walden, et al., 1956 0.0503 (0.0355, 0.0690)
Yamamoto, et al., 2010 0.0240 (0.0124, 0.0415)
Yamamoto, et al., 2011 0.0674 (0.0251, 0.1410)
Zachariades, et al., 1990 0.0744 (0.0672, 0.0822)
Zhou, et al., 2013 0.0069 (0.0008, 0.0249)
combined 0.0441 (0.0415, 0.0467)
0.00
0.05
0.10
0.15
0.20
0.25
proportion (95% confidence interval)

Angle

Author	Effect Size (Proportion) and 95% Confidence Interval (exact)			% Weight
	Point Estimate	Lower Limit	Upper Limit	Fixed
Abdullah, et al., 2013	0.174603	0.123342	0.236375	0.780608
Adebayo, et al., 2003	0.184946	0.150681	0.223277	1.914544
Adi, et al., 1990	0.19462	0.164449	0.227676	2.600657
Al Ahmed, et al., 2004	0.233333	0.168225	0.309277	0.620378
Al-Khateeb and Abdullah, 2007	0.174074	0.130796	0.22467	1.113394
Andersson, et al., 1984	0.134615	0.113392	0.158167	3.84963
Bither, et al., 2008	0.197531	0.163036	0.235753	2.000822
Elgehani, et al., 2009	0.218045	0.187219	0.251397	2.736237
Ellis, et al., 1985	0.233355	0.218618	0.248592	12.838948
Eskitaşcıoğlu, et al., 2009	0.105105	0.074308	0.143138	1.372227
Eskitaşcıoğlu, et al., 2013	0.166972	0.145296	0.190463	4.482334
Ferreira, et al., 2004	0.160059	0.133308	0.189794	2.801972
Gandhi, et al., 2011	0.183716	0.150035	0.221357	1.972062
Hall and Ofodile, 1991	0.221591	0.162569	0.290235	0.727198
Joshi, et al., 2013	0.05102	0.016771	0.115058	0.406738
Kadkhodaie, 2006	0.163807	0.150917	0.177337	12.695152
Le, et al., 2001	0.28	0.120717	0.493877	0.10682
Martins, et al., 2011	0.184932	0.12555	0.25754	0.603944
Mijiti, et al., 2014	0.122807	0.098145	0.151084	2.580115
Oji, 1998	0.119048	0.039806	0.256317	0.176664
Olafsson, 1984	0.202632	0.163354	0.246613	1.565325
Sakr, et al., 2006	0.220727	0.19139	0.252299	3.056697
Salem, et al., 1968	0.212951	0.185109	0.242919	3.303205
Simsek, et al., 2007 (a)	0.27381	0.219724	0.333302	1.039441
Simsek, et al., 2007 (b)	0.275696	0.248736	0.303931	4.281019
Subhashraj, et al., 2007	0.117188	0.090628	0.148259	2.107642
Subhashraj, et al., 2008	0.115124	0.086929	0.148578	1.824158
Walden, et al., 1956	0.236364	0.205665	0.269255	2.94166
Yamamoto K et al. 2010	0.061876	0.042425	0.086682	2.062449
Yamamoto, et al., 2011	0.134831	0.071655	0.223682	0.369762
Zachariades, et al., 1990	0.154403	0.144328	0.164896	19.880855
Zhou, et al., 2013	0.076389	0.04849	0.113371	1.187346

Angle results.

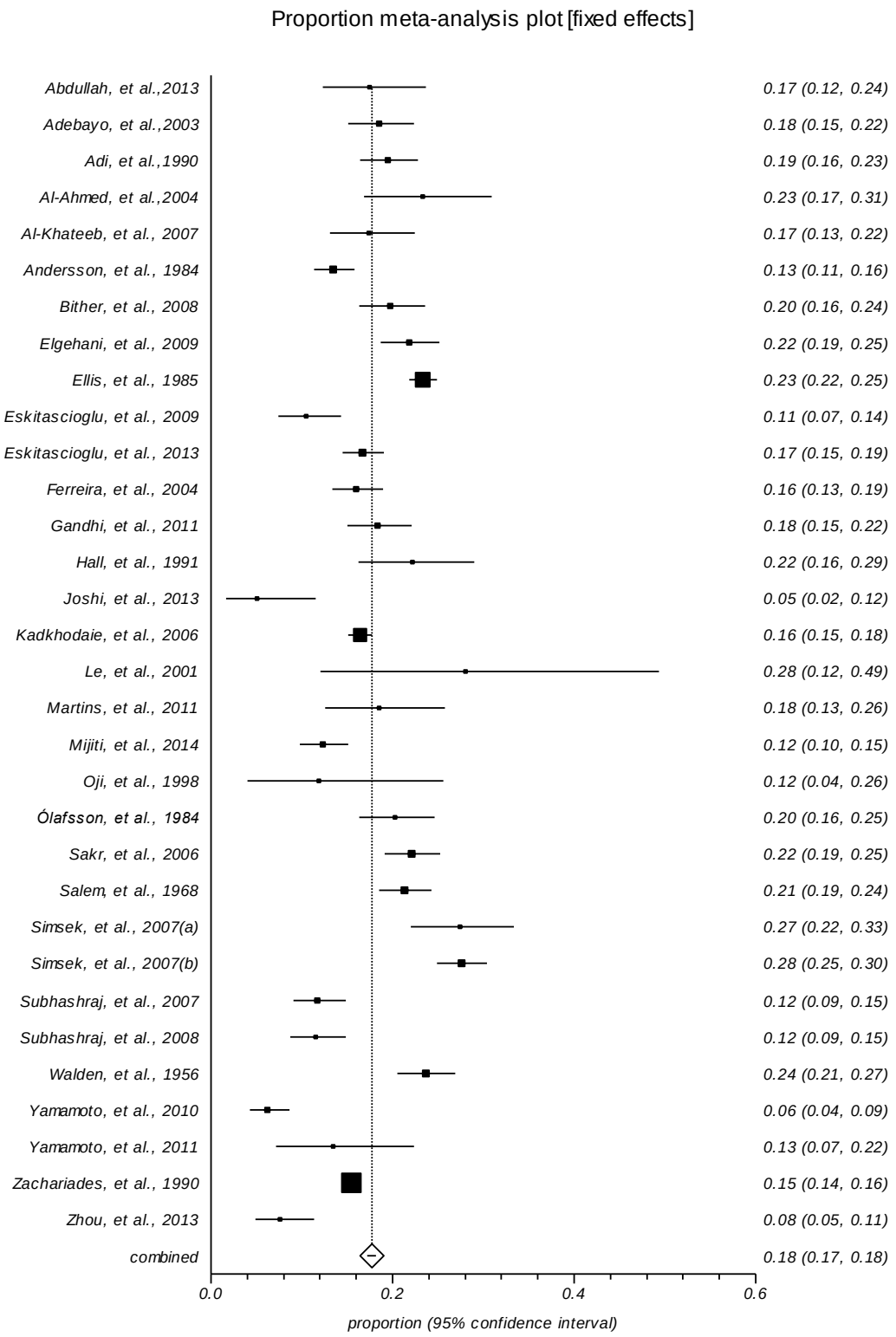
Proportion meta-analysis plot [fixed effects]
Abdullah, et al.,2013 0.17 (0.12, 0.24)
Adebayo, et al.,2003 0.18 (0.15, 0.22)
Adi, et al.,1990 0.19 (0.16, 0.23)
Al-Ahmed, et al.,2004 0.23 (0.17, 0.31)
Al-Khateeb, et al., 2007 0.17 (0.13, 0.22)
Andersson, et al., 1984 0.13 (0.11, 0.16)
Bither, et al., 2008 0.20 (0.16, 0.24)
Elgehani, et al., 2009 0.22 (0.19, 0.25)
Ellis, et al., 1985 0.23 (0.22, 0.25)
Eskitascioglu, et al., 2009 0.11 (0.07, 0.14)
Eskitascioglu, et al., 2013 0.17 (0.15, 0.19)
Ferreira, et al., 2004 0.16 (0.13, 0.19)
Gandhi, et al., 2011 0.18 (0.15, 0.22)
Hall, et al., 1991 0.22 (0.16, 0.29)
Joshi, et al., 2013 0.05 (0.02, 0.12)
Kadkhodaie, et al., 2006 0.16 (0.15, 0.18)
Le, et al., 2001 0.28 (0.12, 0.49)
Martins, et al., 2011 0.18 (0.13, 0.26)
Mijiti, et al., 2014 0.12 (0.10, 0.15)
Oji, et al., 1998 0.12 (0.04, 0.26)
Ólafsson, et al., 1984 0.20 (0.16, 0.25)
Sakr, et al., 2006 0.22 (0.19, 0.25)
Salem, et al., 1968 0.21 (0.19, 0.24)
Simsek, et al., 2007(a) 0.27 (0.22, 0.33)
Simsek, et al., 2007(b) 0.28 (0.25, 0.30)
Subhashraj, et al., 2007 0.12 (0.09, 0.15)
Subhashraj, et al., 2008 0.12 (0.09, 0.15)
Walden, et al., 1956 0.24 (0.21, 0.27)
Yamamoto, et al., 2010 0.06 (0.04, 0.09)
Yamamoto, et al., 2011 0.13 (0.07, 0.22)
Zachariades, et al., 1990 0.15 (0.14, 0.16)
Zhou, et al., 2013 0.08 (0.05, 0.11)
combined 0.18 (0.17, 0.18)
0.0
0.2
0.4
0.6
proportion (95% confidence interval)

Body

Author	Effect Size (Proportion) and 95% Confidence Interval (exact)			% Weight
	Point Estimate	Lower Limit	Upper Limit	Fixed
Abdullah, et al., 2013	0.15873	0.10973	0.218778	0.780608
Adebayo, et al., 2003	0.511828	0.465369	0.558136	1.914544
Adi, et al., 1990	0.262658	0.228733	0.298817	2.600657
Al Ahmed, et al., 2004	0.2	0.139194	0.273036	0.620378
Al-Khateeb and Abdullah, 2007	0.396296	0.337527	0.457368	1.113394
Andersson, et al., 1984	0.231838	0.205147	0.260227	3.84963
Bither, et al., 2008	0.135802	0.10661	0.16951	2.000822
Elgehani, et al., 2009	0.192481	0.163184	0.224537	2.736237
Ellis, et al., 1985	0.329385	0.312911	0.34618	12.838948
Eskitaşcıoğlu, et al., 2009	0.132132	0.097675	0.173296	1.372227
Eskitaşcıoğlu, et al., 2013	0.197248	0.174009	0.222133	4.482334
Ferreira, et al., 2004	0.132159	0.107627	0.159927	2.801972
Gandhi, et al., 2011	0.098121	0.072989	0.128341	1.972062
Hall and Ofodile, 1991	0.460227	0.384981	0.536835	0.727198
Joshi, et al., 2013	0.142857	0.08036	0.22806	0.406738
Kadkhodaie, 2006	0.304953	0.288747	0.321529	12.695152
Le, et al., 2001	0.12	0.025465	0.31219	0.10682
Martins, et al., 2011	0.150685	0.096907	0.219205	0.603944
Mijiti, et al., 2014	0.352472	0.315051	0.39129	2.580115
Oji, 1998	0.214286	0.10296	0.368116	0.176664
Olafsson, 1984	0.281579	0.236897	0.329701	1.565325
Sakr, et al., 2006	0.211306	0.182473	0.242451	3.056697
Salem, et al., 1968	0.154421	0.13011	0.181299	3.303205
Simsek, et al., 2007 (a)	0.289683	0.234465	0.349925	1.039441
Simsek, et al., 2007 (b)	0.230548	0.205273	0.257355	4.281019
Subhashraj, et al., 2007	0.082031	0.059759	0.109266	2.107642
Subhashraj, et al., 2008	0.058691	0.038693	0.084816	1.824158
Walden, et al., 1956	0.420979	0.384482	0.458131	2.94166
Yamamoto K et al. 2010	0.121756	0.094427	0.15364	2.062449
Yamamoto, et al., 2011	0.101124	0.047293	0.183302	0.369762
Zachariades, et al., 1990	0.211038	0.199613	0.222812	19.880855
Zhou, et al., 2013	0.149306	0.110208	0.195798	1.187346

Body results.

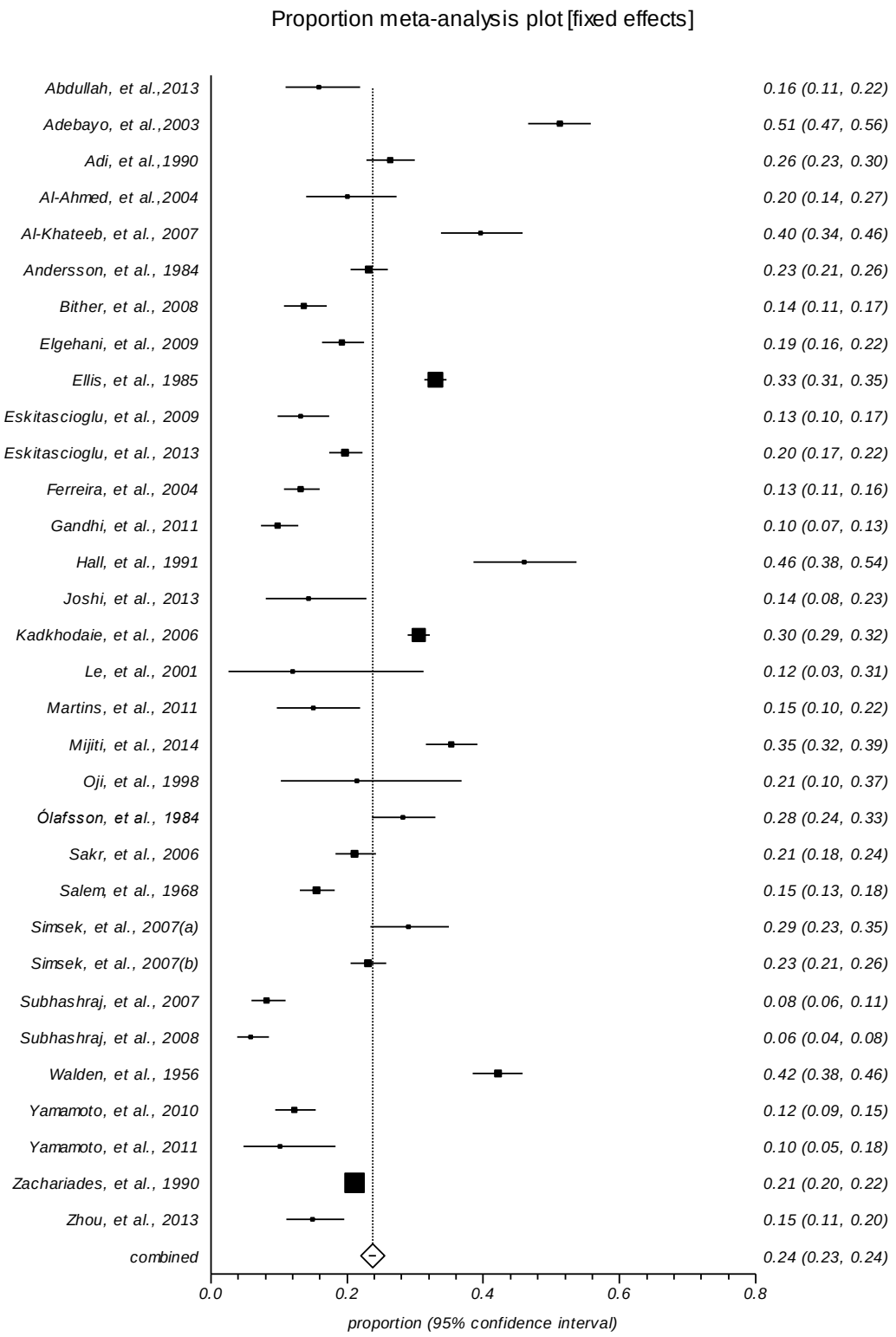
Proportion meta-analysis plot [fixed effects]
Abdullah, et al.,2013 0.16 (0.11, 0.22)
Adebayo, et al.,2003 0.51 (0.47, 0.56)
Adi, et al.,1990 0.26 (0.23, 0.30)
Al-Ahmed, et al.,2004 0.20 (0.14, 0.27)
Al-Khateeb, et al., 2007 0.40 (0.34, 0.46)
Andersson, et al., 1984 0.23 (0.21, 0.26)
Bither, et al., 2008 0.14 (0.11, 0.17)
Elgehani, et al., 2009 0.19 (0.16, 0.22)
Ellis, et al., 1985 0.33 (0.31, 0.35)
Eskitascioglu, et al., 2009 0.13 (0.10, 0.17)
Eskitascioglu, et al., 2013 0.20 (0.17, 0.22)
Ferreira, et al., 2004 0.13 (0.11, 0.16)
Gandhi, et al., 2011 0.10 (0.07, 0.13)
Hall, et al., 1991 0.46 (0.38, 0.54)
Joshi, et al., 2013 0.14 (0.08, 0.23)
Kadkhodaie, et al., 2006 0.30 (0.29, 0.32)
Le, et al., 2001 0.12 (0.03, 0.31)
Martins, et al., 2011 0.15 (0.10, 0.22)
Mijiti, et al., 2014 0.35 (0.32, 0.39)
Oji, et al., 1998 0.21 (0.10, 0.37)
Ólafsson, et al., 1984 0.28 (0.24, 0.33)
Sakr, et al., 2006 0.21 (0.18, 0.24)
Salem, et al., 1968 0.15 (0.13, 0.18)
Simsek, et al., 2007(a) 0.29 (0.23, 0.35)
Simsek, et al., 2007(b) 0.23 (0.21, 0.26)
Subhashraj, et al., 2007 0.08 (0.06, 0.11)
Subhashraj, et al., 2008 0.06 (0.04, 0.08)
Walden, et al., 1956 0.42 (0.38, 0.46)
Yamamoto, et al., 2010 0.12 (0.09, 0.15)
Yamamoto, et al., 2011 0.10 (0.05, 0.18)
Zachariades, et al., 1990 0.21 (0.20, 0.22)
Zhou, et al., 2013 0.15 (0.11, 0.20)
combined 0.24 (0.23, 0.24)
0.0
0.2
0.4
0.6
0.8
proportion (95% confidence interval)

Parasymphysis/Symphysis

Author	Effect Size (Proportion) and 95% Confidence Interval (exact)			% Weight
	Point Estimate	Lower Limit	Upper Limit	Fixed
Abdullah, et al., 2013	0.359788	0.291414	0.432638	0.780608
Adebayo, et al., 2003	0.122581	0.094178	0.155886	1.914544
Adi, et al., 1990	0.191456	0.16149	0.224335	2.600657
Al Ahmed, et al., 2004	0.18	0.1221	0.250978	0.620378
Al-Khateeb and Abdullah, 2007	0.155556	0.114468	0.204394	1.113394
Andersson, et al., 1984	0.117521	0.097585	0.139899	3.84963
Bither, et al., 2008	0.407407	0.363374	0.452574	2.000822
Elgehani, et al., 2009	0.326316	0.290767	0.363415	2.736237
Ellis, et al., 1985	0.087068	0.077411	0.097505	12.838948
Eskitaşcıoğlu, et al., 2009	0.438438	0.3844	0.493582	1.372227
Eskitaşcıoğlu, et al., 2013	0.359633	0.331097	0.38893	4.482334
Ferreira, et al., 2004	0.209985	0.179972	0.242536	2.801972
Gandhi, et al., 2011	0.494781	0.449115	0.540512	1.972062
Hall and Ofodile, 1991	0.142045	0.094081	0.202507	0.727198
Joshi, et al., 2013	0.244898	0.163643	0.34213	0.406738
Kadkhodaie, 2006	0.215604	0.201214	0.230534	12.695152
Le, et al., 2001	0.16	0.045379	0.360828	0.10682
Martins, et al., 2011	0.40411	0.323783	0.488409	0.603944
Mijiti, et al., 2014	0.199362	0.168769	0.232816	2.580115
Oji, 1998	0.238095	0.120516	0.394502	0.176664
Olafsson, 1984	0.123684	0.092311	0.161061	1.565325
Sakr, et al., 2006	0.297443	0.264759	0.331744	3.056697
Salem, et al., 1968	0.292653	0.261371	0.325465	3.303205
Simsek, et al., 2007 (a)	0.22619	0.176048	0.282897	1.039441
Simsek, et al., 2007 (b)	0.257445	0.231121	0.285147	4.281019
Subhashraj, et al., 2007	0.410156	0.367201	0.454155	2.107642
Subhashraj, et al., 2008	0.455982	0.408903	0.503653	1.824158
Walden, et al., 1956	0.092308	0.07211	0.115941	2.94166
Yamamoto K et al. 2010	0.169661	0.137827	0.205451	2.062449
Yamamoto, et al., 2011	0.269663	0.181032	0.374173	0.369762
Zachariades, et al., 1990	0.235841	0.223938	0.248064	19.880855
Zhou, et al., 2013	0.215278	0.16922	0.267299	1.187346

Parasymphysis/symphysis results.

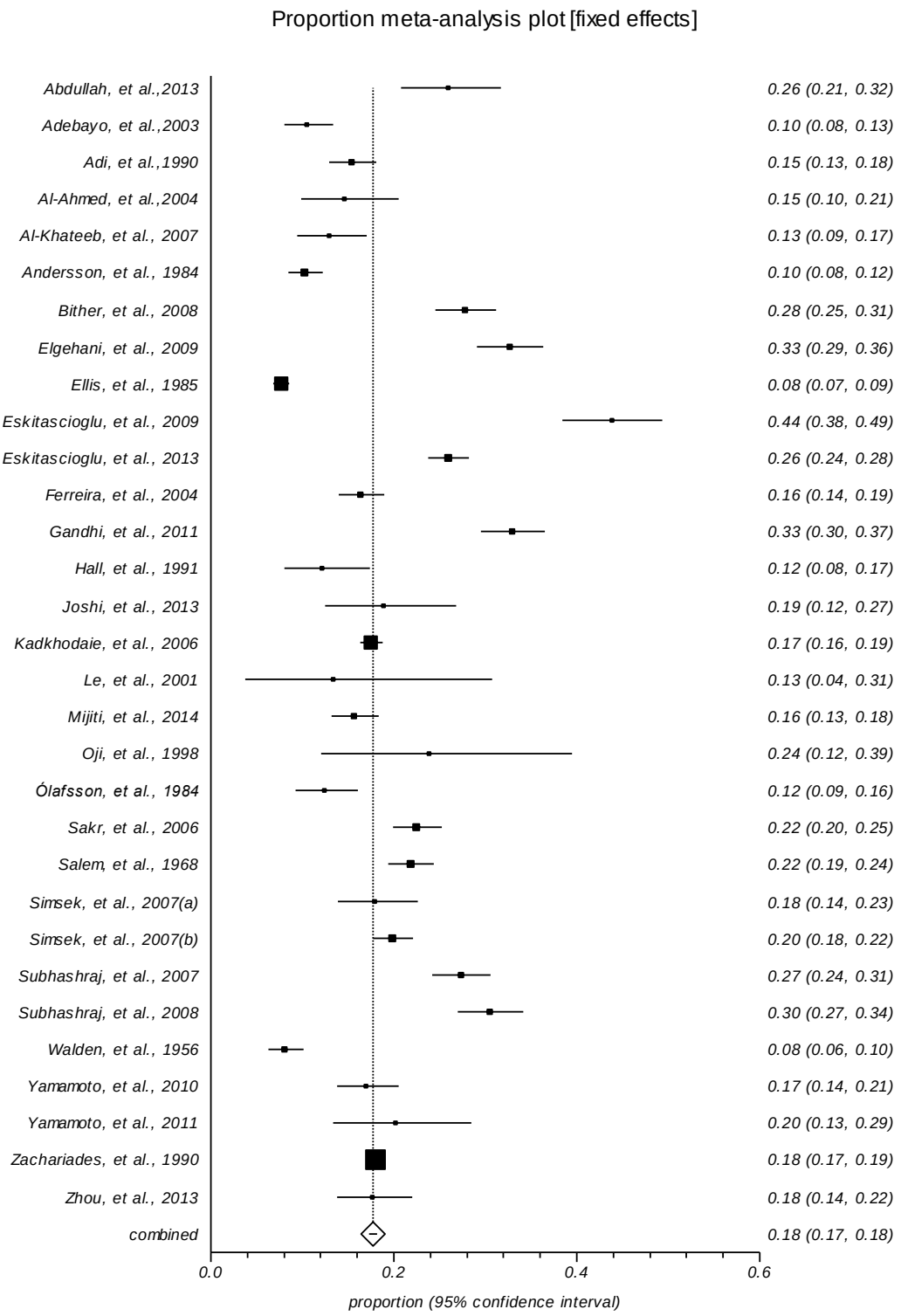
Proportion meta-analysis plot [fixed effects]
Abdullah, et al.,2013 0.26 (0.21, 0.32)
Adebayo, et al.,2003 0.10 (0.08, 0.13)
Adi, et al.,1990 0.15 (0.13, 0.18)
Al-Ahmed, et al.,2004 0.15 (0.10, 0.21)
Al-Khateeb, et al., 2007 0.13 (0.09, 0.17)
Andersson, et al., 1984 0.10 (0.08, 0.12)
Bither, et al., 2008 0.28 (0.25, 0.31)
Elgehani, et al., 2009 0.33 (0.29, 0.36)
Ellis, et al., 1985 0.08 (0.07, 0.09)
Eskitascioglu, et al., 2009 0.44 (0.38, 0.49)
Eskitascioglu, et al., 2013 0.26 (0.24, 0.28)
Ferreira, et al., 2004 0.16 (0.14, 0.19)
Gandhi, et al., 2011 0.33 (0.30, 0.37)
Hall, et al., 1991 0.12 (0.08, 0.17)
Joshi, et al., 2013 0.19 (0.12, 0.27)
Kadkhodaie, et al., 2006 0.17 (0.16, 0.19)
Le, et al., 2001 0.13 (0.04, 0.31)
Mijiti, et al., 2014 0.16 (0.13, 0.18)
Oji, et al., 1998 0.24 (0.12, 0.39)
Ólafsson, et al., 1984 0.12 (0.09, 0.16)
Sakr, et al., 2006 0.22 (0.20, 0.25)
Salem, et al., 1968 0.22 (0.19, 0.24)
Simsek, et al., 2007(a) 0.18 (0.14, 0.23)
Simsek, et al., 2007(b) 0.20 (0.18, 0.22)
Subhashraj, et al., 2007 0.27 (0.24, 0.31)
Subhashraj, et al., 2008 0.30 (0.27, 0.34)
Walden, et al., 1956 0.08 (0.06, 0.10)
Yamamoto, et al., 2010 0.17 (0.14, 0.21)
Yamamoto, et al., 2011 0.20 (0.13, 0.29)
Zachariades, et al., 1990 0.18 (0.17, 0.19)
Zhou, et al., 2013 0.18 (0.14, 0.22)
combined 0.18 (0.17, 0.18)
0.0
0.2
0.4
0.6
proportion (95% confidence interval)

Alveolus

Author	Effect Size (Proportion) and 95% Confidence Interval (exact)			% Weight
	Point Estimate	Lower Limit	Upper Limit	Fixed
Abdullah, et al., 2013	0.058201	0.029409	0.10175	0.780608
Adebayo, et al., 2003	0.073118	0.051165	0.100679	1.914544
Adi, et al., 1990	0.03481	0.021941	0.05223	2.600657
Al Ahmed, et al., 2004	0.08	0.04202	0.135574	0.620378
Al-Khateeb and Abdullah, 2007	0.1	0.06694	0.142155	1.113394
Andersson, et al., 1984	0.050214	0.037125	0.066217	3.84963
Bither, et al., 2008	0.032922	0.018932	0.052913	2.000822
Elgehani, et al., 2009	0.043609	0.029397	0.062032	2.736237
Ellis, et al., 1985	0.010883	0.007549	0.015176	12.838948
Eskitaşcıoğlu, et al., 2009	0.117117	0.084621	0.156611	1.372227
Eskitaşcıoğlu, et al., 2013	0.050459	0.038235	0.065176	4.482334
Ferreira, et al., 2004	0.111601	0.088942	0.137687	2.801972
Gandhi, et al., 2011	0.073069	0.05142	0.100158	1.972062
Hall and Ofodile, 1991	0.028409	0.009287	0.065049	0.727198
Joshi, et al., 2013	0.102041	0.050028	0.17966	0.406738
Kadkhodaie, 2006	0.043056	0.036172	0.050821	12.695152
Le, et al., 2001	0.08	0.00984	0.260306	0.10682
Martins, et al., 2011	0.020548	0.004258	0.058874	0.603944
Mijiti, et al., 2014	0.051037	0.035167	0.071288	2.580115
Oji, 1998	0.119048	0.039806	0.256317	0.176664
Olafsson, 1984	0.015789	0.005816	0.034049	1.565325
Sakr, et al., 2006	0.053836	0.038736	0.072591	3.056697
Salem, et al., 1968	0.079701	0.061918	0.100639	3.303205
Simsek, et al., 2007 (a)	0.015873	0.004341	0.04014	1.039441
Simsek, et al., 2007 (b)	0.007685	0.003323	0.015086	4.281019
Subhashraj, et al., 2007	0.111328	0.085417	0.141825	2.107642
Subhashraj, et al., 2008	0.108352	0.080978	0.141085	1.824158
Walden, et al., 1956	0.00979	0.003945	0.020067	2.94166
Yamamoto K et al. 2010	0.063872	0.044095	0.088975	2.062449
Yamamoto, et al., 2011	0.044944	0.01238	0.111092	0.369762
Zachariades, et al., 1990	0.085573	0.077839	0.093811	19.880855
Zhou, et al., 2013	0.010417	0.002153	0.030138	1.187346

Alveolus results.

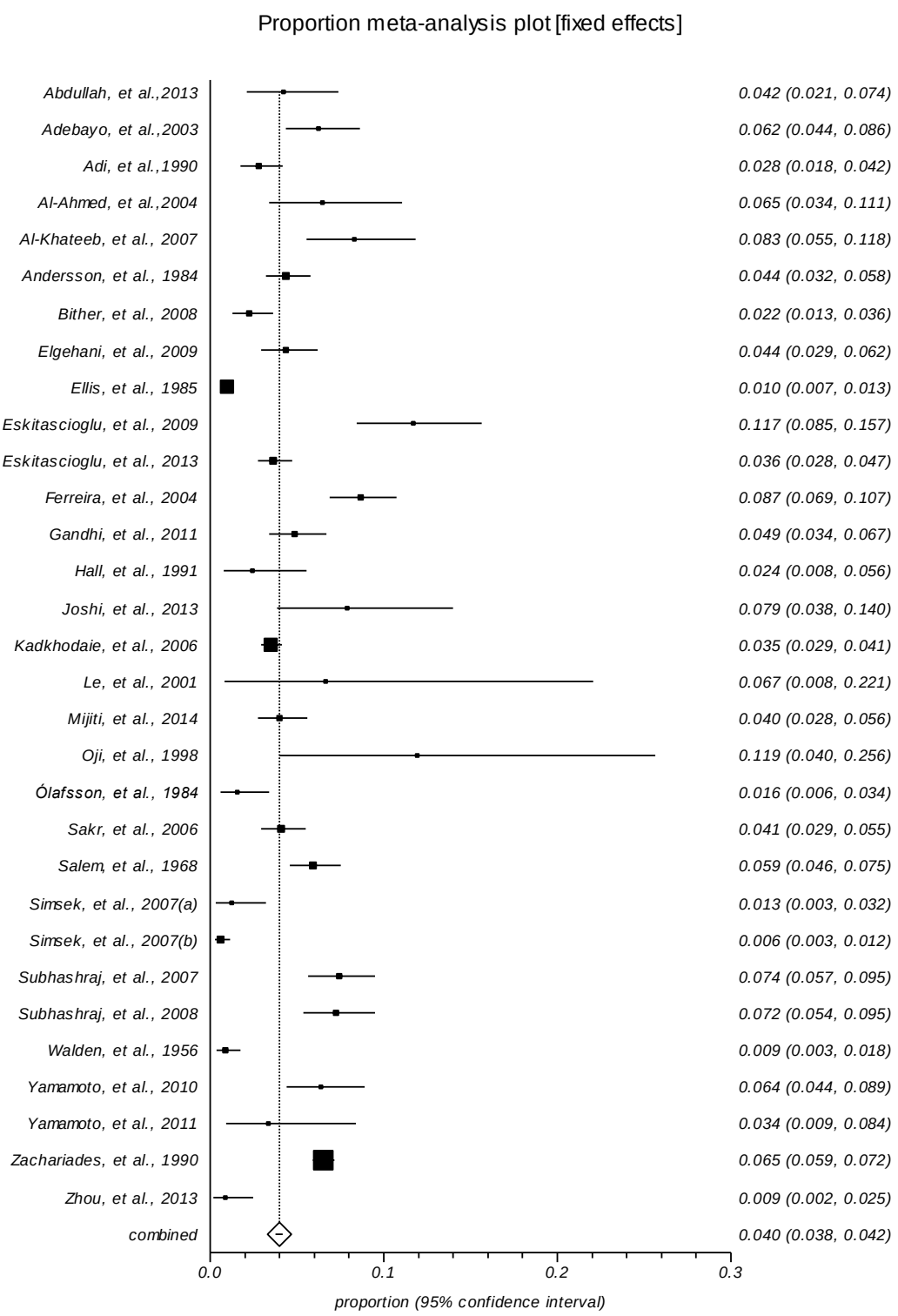
Proportion meta-analysis plot [fixed effects]
Abdullah, et al.,2013 0.042 (0.021, 0.074)
Adebayo, et al.,2003 0.062 (0.044, 0.086)
Adi, et al.,1990 0.028 (0.018, 0.042)
Al-Ahmed, et al.,2004 0.065 (0.034, 0.111)
Al-Khateeb, et al., 2007 0.083 (0.055, 0.118)
Andersson, et al., 1984 0.044 (0.032, 0.058)
Bither, et al., 2008 0.022 (0.013, 0.036)
Elgehani, et al., 2009 0.044 (0.029, 0.062)
Ellis, et al., 1985 0.010 (0.007, 0.013)
Eskitascioglu, et al., 2009 0.117 (0.085, 0.157)
Eskitascioglu, et al., 2013 0.036 (0.028, 0.047)
Ferreira, et al., 2004 0.087 (0.069, 0.107)
Gandhi, et al., 2011 0.049 (0.034, 0.067)
Hall, et al., 1991 0.024 (0.008, 0.056)
Joshi, et al., 2013 0.079 (0.038, 0.140)
Kadkhodaie, et al., 2006 0.035 (0.029, 0.041)
Le, et al., 2001 0.067 (0.008, 0.221)
Mijiti, et al., 2014 0.040 (0.028, 0.056)
Oji, et al., 1998 0.119 (0.040, 0.256)
Ólafsson, et al., 1984 0.016 (0.006, 0.034)
Sakr, et al., 2006 0.041 (0.029, 0.055)
Salem, et al., 1968 0.059 (0.046, 0.075)
Simsek, et al., 2007(a) 0.013 (0.003, 0.032)
Simsek, et al., 2007(b) 0.006 (0.003, 0.012)
Subhashraj, et al., 2007 0.074 (0.057, 0.095)
Subhashraj, et al., 2008 0.072 (0.054, 0.095)
Walden, et al., 1956 0.009 (0.003, 0.018)
Yamamoto, et al., 2010 0.064 (0.044, 0.089)
Yamamoto, et al., 2011 0.034 (0.009, 0.084)
Zachariades, et al., 1990 0.065 (0.059, 0.072)
Zhou, et al., 2013 0.009 (0.002, 0.025)
combined 0.040 (0.038, 0.042)
0.0
0.1
0.2
0.3
proportion (95% confidence interval)

Summary results

Anatomical location of fracture	Effect size (Prevalence)	95% Confidence interval Fixed
Angle	0.177	(0.172- 0.182)
Body	0.237	(0.231 - 0.242)
Condyle	0.245	(0.239 - 0.250)
Dentoalveolar	0.049	(0.046 - 0.052)
Symphyseal/Parasymphyseal	0.221	(0.216 - 0.226)
Ascending ramus	0.044	(0.042 - 0.047)

Appendix 8

Bias indicators

	Condyle	Ascending ramus fracture	Angle	Body	Parasymphysis	Alveolus
Non-combinability of studies						
Moment-based estimate of between studies variance	0.0399	0.0094	0.0152	0.0499	0.0364	0.0184
Bias indicators						
Begg-Mazumdar	Kendall's tau = 0.2989 P = 0.0181	Kendall's tau = 0.0924 P = 0.4785	Kendall's tau = 0.0.1647 P = 0.1884	Kendall's tau = 0.2 P = 0.1185	Kendall's tau = 0.0.1226 P = 0.3442	Kendall's tau = 0.1785 P = 0.1647
Harbord	0.6080 (92.5% CI = -3.7640 to 4.9800) P = 0.7991	-1.167892 (92.5% CI = -3.0851 to 0.7297) P = 0.2635	-0.2078 (92.5% CI = -2.8191 to 2.4034) P = 0.8841	-1.3771 (92.5% CI = -5.9129 to 3.1587) P = 0.5793	2.7520 (92.5% CI = -1.0908 to 6.5947) P = 0.1963	0.7169 (92.5% CI = -1.9666 to 3.4004) P = 0.6254

Appendix 9

How does the pattern of stress and strain differ in the atrophic human mandible on loading?

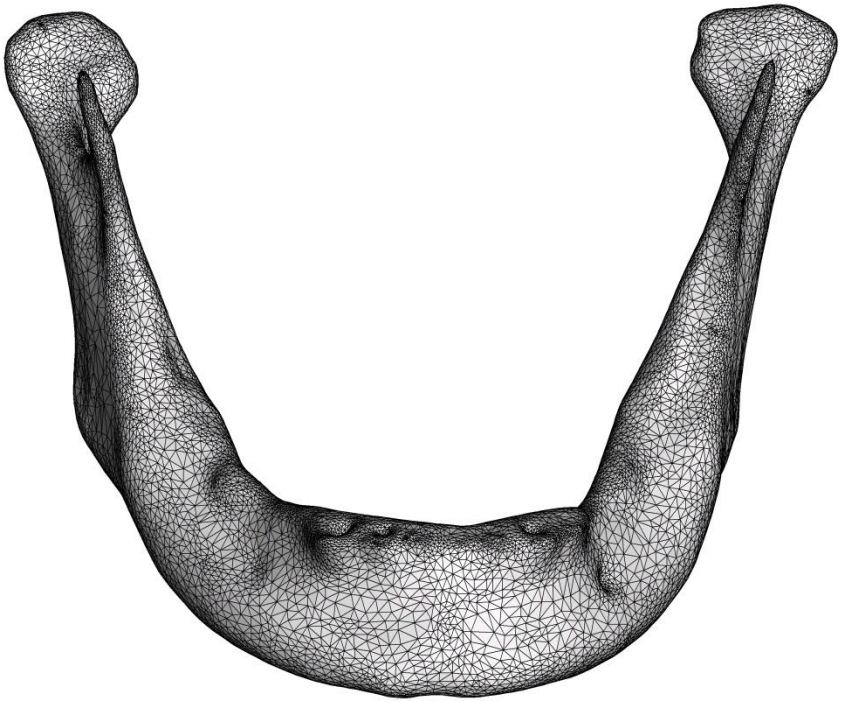

An STL model of an atrophic edentulous mandible made using a modified female VHP dataset. The anterior teeth were removed from the original scan data.

The atrophic edentulous mandibular model had similar gross geometry to the dentate mandible in that both were 'U'-shaped with proximal vertical extensions. With the resorption of the majority of the alveolar portion of the mandible the sampled zone was in a similar place to the dentate mandible i.e. placed halfway between the superior and inferior cortex on the buccal and lingual sides of the mandible. Examination of the colour contour plots showed similar buccal and lingual cortical signatures to those obtained in the dentate mandible. There were areas of high stress at the condylar head and neck bilaterally, with the right being greater than the left. The loading area showed high stress on the buccal and lingual aspect. There were increased areas of stress at the

contra-lateral buccal and lingual body. Peaks and troughs occurred roughly in the same anatomical positions in response to loading in the equivalent region. This would suggest that the cortical strain pattern was more a function of the geometry of the mandible rather than the material properties. Material properties might have changed the magnitude of the response but geometry was primarily responsible for the strain/stress disposition.

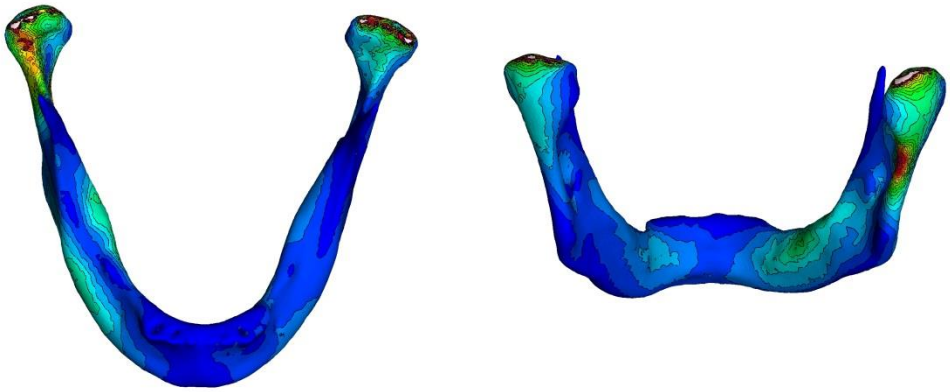

Colour contour maps of von Mises strain (ε_{vm}) showing the buccal and lingual aspects of cortex.

Buccal cortical strain in the atrophic mandible.

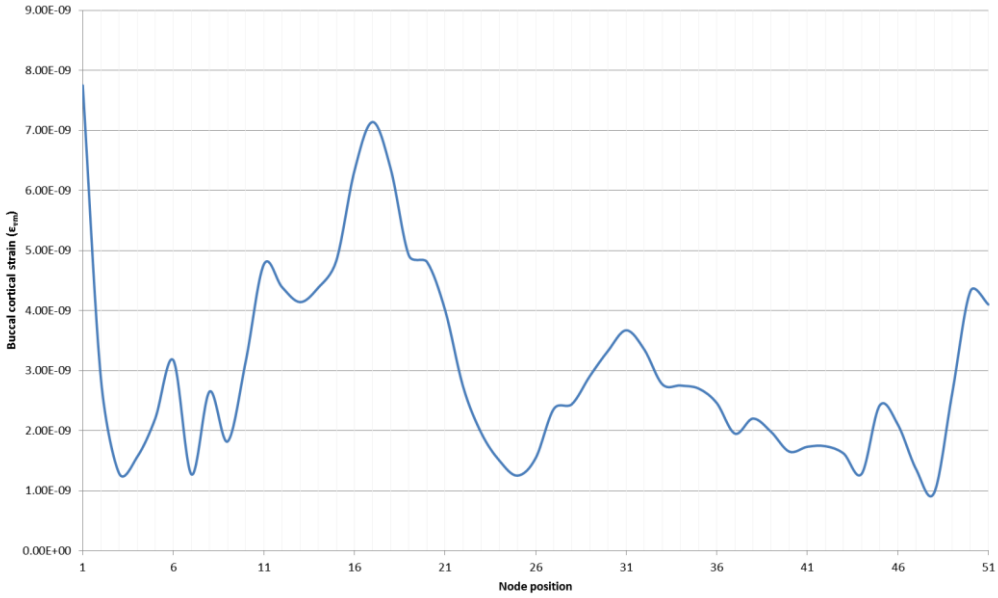

Graph of buccal cortical strain (ε_{vm}) in the atrophic mandible subjected to a physiological load in the region of the mandibular body. Strain at each node position is noted.

Buccal cortical strain results.

Node number	*Buccal ε_{vm}*
1	0.0063
2	0.0029
3	0.0016
4	0.0018
5	0.0024
6	0.0031
7	0.0017
8	0.0023
9	0.0018
10	0.0028
11	0.004
12	0.004
13	0.004
14	0.0043
15	0.005
16	0.0061
17	0.0066
18	0.0059
19	0.0047
20	0.0045
21	0.0035
22	0.0024
23	0.0017
24	0.0013
25	0.0012
26	0.0015
27	0.0023
28	0.0024
29	0.0028
30	0.0033
31	0.0034
32	0.0032
33	0.003
34	0.0026
35	0.0026
36	0.002
37	0.0022
38	0.002
39	0.0017
40	0.0017
41	0.0016
42	0.0015
43	0.0012
44	0.0021
45	0.0018
46	0.0014
47	0.0012
48	0.0027
49	0.0044
50	0.0039

Lingual cortical strain in the atrophic mandible.

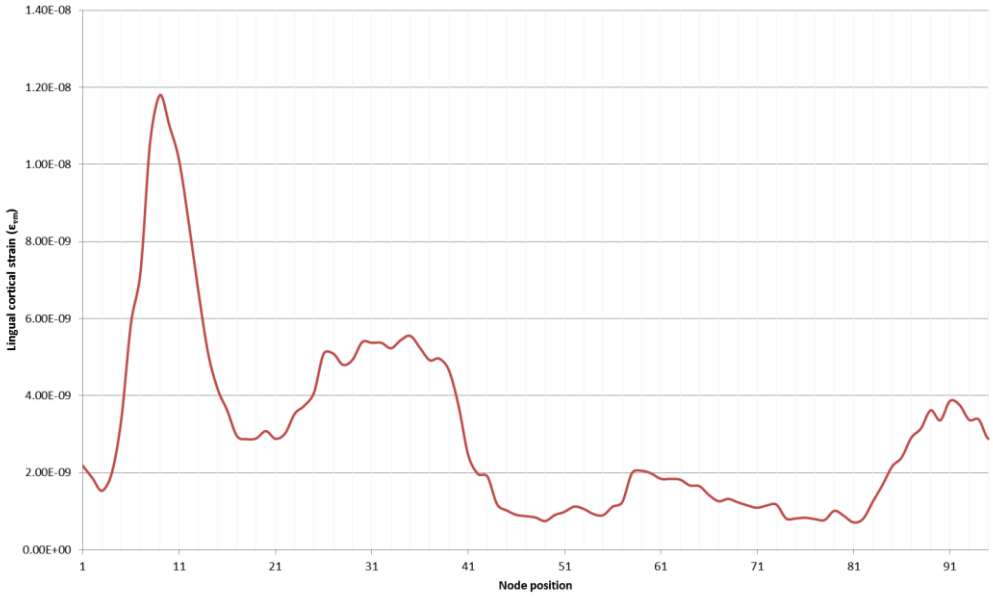

Graph of lingual cortical strain (ε_{vm}) in the atrophic mandible subjected to a physiological load in the region of the mandibular body. Strain at each node position is noted.

Lingual strain results

Node number	*Lingual ε_{vm}*
1	0.0019
2	0.00176
3	0.00177
4	0.00198
5	0.00337
6	0.00542
7	0.00661
8	0.00942
9	0.01033
10	0.00899
11	0.00867
12	0.00713
13	0.00597
14	0.0044
15	0.0036
16	0.00318
17	0.00237
18	0.00232
19	0.00256
20	0.00273
21	0.00248
22	0.00267
23	0.00316
24	0.00342
25	0.0036
26	0.00466
27	0.00464
28	0.00458
29	0.00449
30	0.00515
31	0.00522
32	0.00515
33	0.00482
34	0.00489
35	0.00509
36	0.00477
37	0.00433
38	0.00447
39	0.00405
40	0.0033
41	0.00223
42	0.00175
43	0.00164
44	0.00098
45	0.00089
46	0.00084
47	0.0008
48	0.00076
49	0.00075
50	0.00089
51	0.00095
52	0.0011
53	0.00103
54	0.00093
55	0.0009
56	0.00102
57	0.00114
58	0.00124
59	0.00216

60	0.00191
61	0.00191
62	0.0018
63	0.00188
64	0.0018
65	0.00168
66	0.0017
67	0.0014
68	0.00129
69	0.00131
70	0.00117
71	0.00106
72	0.00103
73	0.00096
74	0.00099
75	0.00061
76	0.00064
77	0.00076
78	0.00069
79	0.00069
80	0.00087
81	0.00084

82	0.00072
83	0.0007
84	0.00078
85	0.00107
86	0.00156
87	0.00201
88	0.00252
89	0.00272
90	0.00322
91	0.00328
92	0.00382
93	0.00332
94	0.00384
95	0.00384
96	0.00316
97	0.00318
98	0.00289
99	0.0031

Appendix 10

Tabulated results

Section 5.3.1

The effect of muscular contraction on buccal cortical von Mises stress

Contribution of individual muscles to buccal cortical stress (σ_{vm})(MPa)				
Node position	*Muscles*			
	Masseter	*Medial pterygoid*	*Temporalis*	*Lateral pterygoid*
1	1.87E-05	2.30E-05	4.59E-05	8.79E-06
2	2.52E-05	3.00E-05	7.41E-05	3.26E-06
3	2.69E-05	3.41E-05	8.97E-05	4.61E-06
4	2.50E-05	3.45E-05	9.76E-05	5.37E-06
5	1.83E-05	2.75E-05	8.34E-05	4.37E-06
6	1.25E-05	1.99E-05	6.30E-05	2.87E-06
7	7.89E-06	1.31E-05	4.04E-05	1.59E-06
8	5.69E-06	9.29E-06	2.47E-05	9.19E-07
9	4.72E-06	6.93E-06	1.41E-05	6.49E-07
10	3.95E-06	5.99E-06	8.59E-06	5.54E-07
11	4.06E-06	6.27E-06	5.76E-06	6.25E-07
12	3.43E-06	5.84E-06	2.63E-06	5.77E-07
13	3.77E-06	5.54E-06	2.19E-06	5.66E-07
14	3.16E-06	4.98E-06	3.12E-06	5.63E-07
15	3.07E-06	5.03E-06	4.38E-06	6.87E-07
16	2.90E-06	5.55E-06	5.64E-06	8.59E-07
17	2.73E-06	5.98E-06	6.83E-06	1.02E-06
18	2.75E-06	6.24E-06	8.39E-06	1.17E-06
19	3.39E-06	8.18E-06	1.12E-05	1.55E-06
20	2.46E-06	7.30E-06	9.31E-06	1.34E-06
21	2.29E-06	7.28E-06	9.68E-06	1.37E-06
22	1.96E-06	7.42E-06	9.81E-06	1.40E-06
23	1.63E-06	6.34E-06	8.28E-06	1.19E-06
24	1.09E-06	2.89E-06	3.78E-06	5.62E-07
25	1.04E-06	3.23E-06	4.17E-06	6.35E-07
26	1.26E-06	6.68E-06	8.45E-06	1.36E-06
27	1.18E-06	7.45E-06	9.51E-06	1.54E-06
28	9.78E-07	6.79E-06	8.43E-06	1.37E-06
29	1.06E-06	7.23E-06	8.43E-06	1.39E-06
30	9.26E-07	6.06E-06	6.88E-06	1.15E-06
31	8.25E-07	5.47E-06	7.05E-06	1.19E-06
32	8.82E-07	5.34E-06	5.65E-06	1.04E-06
33	9.73E-07	5.11E-06	4.42E-06	9.19E-07
34	1.09E-06	4.52E-06	3.15E-06	7.31E-07
35	1.27E-06	4.62E-06	2.10E-06	6.16E-07
36	1.47E-06	5.06E-06	1.46E-06	6.41E-07
37	1.95E-06	5.31E-06	1.50E-06	6.73E-07
38	2.28E-06	5.40E-06	3.75E-06	6.75E-07
39	2.26E-06	5.69E-06	6.59E-06	7.00E-07
40	2.27E-06	5.76E-06	8.87E-06	7.33E-07

41	2.53E-06	6.51E-06	1.25E-05	8.73E-07
42	3.07E-06	7.53E-06	1.79E-05	1.11E-06
43	3.73E-06	8.55E-06	2.30E-05	1.37E-06
44	6.89E-06	1.30E-05	3.83E-05	2.92E-06
45	1.09E-05	1.81E-05	5.41E-05	5.14E-06
46	1.47E-05	2.05E-05	6.10E-05	7.12E-06
47	1.83E-05	2.32E-05	6.87E-05	7.33E-06
48	1.82E-05	2.16E-05	6.00E-05	8.12E-06
49	1.42E-05	1.86E-05	4.16E-05	8.73E-06

The effect of muscular contraction on buccal cortical von Mises strain

Contribution of individual muscles to buccal cortical strain (ε_{vm})				
Node position	*Muscles*			
	Masseter	*Medial pterygoid*	*Temporalis*	*Lateral pterygoid*
1	1.80E-09	2.22E-09	4.43E-09	8.49E-10
2	2.44E-09	2.90E-09	7.15E-09	3.15E-10
3	2.60E-09	3.30E-09	8.67E-09	4.45E-10
4	2.42E-09	3.33E-09	9.43E-09	5.19E-10
5	1.76E-09	2.66E-09	8.05E-09	4.22E-10
6	1.20E-09	1.92E-09	6.09E-09	2.78E-10
7	7.62E-10	1.27E-09	3.90E-09	1.53E-10
8	5.50E-10	8.97E-10	2.38E-09	0.00E+00
9	4.56E-10	6.69E-10	1.36E-09	0.00E+00
10	3.81E-10	5.78E-10	8.29E-10	0.00E+00
11	3.92E-10	6.05E-10	5.56E-10	0.00E+00
12	3.31E-10	5.64E-10	2.54E-10	0.00E+00
13	3.64E-10	5.35E-10	2.11E-10	0.00E+00
14	3.06E-10	4.81E-10	3.02E-10	0.00E+00
15	2.96E-10	4.86E-10	4.23E-10	0.00E+00
16	2.80E-10	5.36E-10	5.45E-10	0.00E+00
17	2.64E-10	5.77E-10	6.60E-10	0.00E+00
18	2.66E-10	6.03E-10	8.10E-10	1.13E-10
19	3.28E-10	7.90E-10	1.09E-09	1.49E-10
20	2.38E-10	7.05E-10	8.99E-10	1.29E-10
21	2.22E-10	7.03E-10	9.35E-10	1.32E-10
22	1.89E-10	7.16E-10	9.47E-10	1.35E-10
23	1.57E-10	6.12E-10	8.00E-10	1.15E-10
24	1.05E-10	2.79E-10	3.66E-10	0.00E+00
25	1.00E-10	3.12E-10	4.03E-10	0.00E+00
26	1.21E-10	6.46E-10	8.16E-10	1.31E-10
27	1.14E-10	7.20E-10	9.19E-10	1.49E-10
28	0.00E+00	6.56E-10	8.15E-10	1.32E-10
29	1.02E-10	6.98E-10	8.14E-10	1.34E-10
30	0.00E+00	5.85E-10	6.65E-10	1.11E-10
31	0.00E+00	5.28E-10	6.81E-10	1.15E-10
32	0.00E+00	5.16E-10	5.46E-10	1.01E-10
33	0.00E+00	4.94E-10	4.27E-10	0.00E+00
34	1.05E-10	4.37E-10	3.04E-10	0.00E+00
35	1.23E-10	4.46E-10	2.03E-10	0.00E+00
36	1.42E-10	4.89E-10	1.41E-10	0.00E+00
37	1.89E-10	5.13E-10	1.45E-10	0.00E+00
38	2.21E-10	5.22E-10	3.62E-10	0.00E+00
39	2.18E-10	5.49E-10	6.37E-10	0.00E+00
40	2.20E-10	5.56E-10	8.56E-10	0.00E+00
41	2.45E-10	6.28E-10	1.21E-09	0.00E+00

42	2.96E-10	7.28E-10	1.73E-09	1.07E-10
43	3.60E-10	8.25E-10	2.22E-09	1.33E-10
44	6.65E-10	1.25E-09	3.70E-09	2.82E-10
45	1.05E-09	1.75E-09	5.23E-09	4.97E-10
46	1.42E-09	1.98E-09	5.90E-09	6.88E-10
47	1.77E-09	2.24E-09	6.64E-09	7.08E-10
48	1.76E-09	2.09E-09	5.80E-09	7.84E-10
49	1.37E-09	1.80E-09	4.01E-09	8.43E-10

The effect of muscular contraction on lingual cortical von Mises strain

Contribution of individual muscles to lingual cortical strain (ε_{vm})				
Node position	*Muscles*			
	Lat. pterygoid	*Med. pterygoid*	*Masseter*	*Temporalis*
1	5.96E-10	3.31E-09	1.19E-09	5.8E-09
2	4.19E-09	5.79E-09	2.42E-09	1.23E-08
3	1.1E-09	4.26E-09	2.2E-09	1.38E-08
4	1.76E-10	2.42E-09	1.47E-09	1.14E-08
5	1.59E-10	2.34E-09	1.31E-09	1.06E-08
6	2.88E-10	1.21E-09	9.4E-10	8.65E-09
7	3.26E-10	4.8E-10	4.46E-10	4.01E-09
8	2.35E-10	6.43E-10	3.94E-10	2.33E-09
9	2.03E-10	9.94E-10	2.77E-10	1.7E-09
10	1.82E-10	1.09E-09	2.9E-10	2.09E-09
11	1.54E-10	1.09E-09	3.29E-10	2.14E-09
12	1.2E-10	8.8E-10	4.11E-10	1.59E-09
13	0	4.11E-10	1.93E-10	6.38E-10
14	0	5.79E-10	3.16E-10	7.98E-10
15	0	5.3E-10	3.23E-10	5.12E-10
16	0	5.14E-10	3.6E-10	4.07E-10
17	0	5.03E-10	3.71E-10	3.54E-10
18	0	5.06E-10	3.26E-10	2.85E-10
19	0	5.56E-10	3.13E-10	2.63E-10
20	0	6.07E-10	2.99E-10	2.53E-10
21	0	6.02E-10	2.82E-10	2.14E-10
22	0	5.88E-10	2.88E-10	1.89E-10
23	0	6.45E-10	3.03E-10	2.37E-10
24	0	6.03E-10	3.19E-10	3.03E-10
25	0	5.59E-10	3.4E-10	3.95E-10
26	0	5.74E-10	3.58E-10	5.33E-10
27	1.01E-10	5.94E-10	3.52E-10	6.48E-10
28	1.1E-10	6.43E-10	3.12E-10	6.99E-10
29	1.27E-10	7.05E-10	3.03E-10	8.28E-10
30	1.52E-10	7.93E-10	3.02E-10	1.01E-09
31	1.73E-10	8.7E-10	2.88E-10	1.18E-09
32	1.95E-10	9.49E-10	2.9E-10	1.36E-09
33	2.04E-10	9.72E-10	2.57E-10	1.39E-09
34	1.93E-10	8.64E-10	2.33E-10	1.33E-09
35	1.87E-10	7.68E-10	2.03E-10	1.33E-09
36	1.74E-10	6.8E-10	1.79E-10	1.26E-09
37	1.53E-10	5.49E-10	1.5E-10	1.13E-09
38	1.64E-10	5.9E-10	1.29E-10	1.22E-09
39	1.57E-10	5.65E-10	0	1.19E-09
40	1.73E-10	6.48E-10	0	1.3E-09
41	1.8E-10	7.19E-10	0	1.33E-09
42	1.81E-10	7.65E-10	0	1.32E-09
43	1.82E-10	8.17E-10	0	1.29E-09
44	1.79E-10	8.52E-10	0	1.23E-09
45	1.74E-10	8.33E-10	0	1.17E-09

46	1.66E-10	8.24E-10	0	1.07E-09
47	1.59E-10	8.14E-10	1.03E-10	9.82E-10
48	1.31E-10	6.91E-10	1E-10	7.62E-10
49	1.21E-10	6.3E-10	1.04E-10	6.76E-10
50	1.04E-10	5.4E-10	1.01E-10	5.55E-10
51	0	4.9E-10	1.1E-10	5E-10
52	0	5.03E-10	1.27E-10	4.35E-10
53	0	5.99E-10	1.47E-10	3.31E-10
54	0	6.05E-10	1.34E-10	2.14E-10
55	0	5.83E-10	1.18E-10	1.85E-10
56	0	5.44E-10	1.18E-10	1.98E-10
57	0	5.26E-10	1.28E-10	2.22E-10
58	0	5.46E-10	1.5E-10	2.58E-10
59	0	5.14E-10	1.59E-10	2.79E-10
60	0	4.47E-10	0	3.9E-10
61	1.33E-10	7.98E-10	2.99E-10	8.57E-10
62	1.24E-10	7.39E-10	2.65E-10	9.04E-10
63	1.59E-10	8.83E-10	2.11E-10	1.55E-09
64	2.11E-10	1.09E-09	1.4E-10	2.14E-09
65	3.03E-10	1.33E-09	1.71E-10	2.41E-09
66	4.14E-10	1.5E-09	2.76E-10	2.21E-09
67	5.38E-10	1.56E-09	3.37E-10	1.74E-09
68	5.55E-10	1.26E-09	3.64E-10	1.34E-09
69	5.09E-10	1.02E-09	4.38E-10	3.52E-09
70	4.43E-10	1.5E-09	7.33E-10	5.72E-09
71	2.35E-09	3.09E-09	1.33E-09	8.32E-09
72	4.63E-09	3.74E-09	1.47E-09	8.38E-09
73	7.96E-10	3.51E-09	1.3E-09	6.84E-09
74	1.3E-09	4.96E-09	1.8E-09	8.92E-09

The effect of muscular contraction on lingual cortical von Mises stress

Contribution of individual muscles to lingual cortical stress (σ_{vm})(MPa)				
Node position	*Muscles*			
	Lat. pterygoid	*Med. pterygoid*	*Masseter*	*Temporalis*
1	6.17E-06	3.43E-05	1.23E-05	6.00E-05
2	4.34E-05	6.00E-05	2.51E-05	1.27E-04
3	1.13E-05	4.41E-05	2.28E-05	1.43E-04
4	1.82E-06	2.51E-05	1.52E-05	1.18E-04
5	1.65E-06	2.43E-05	1.36E-05	1.10E-04
6	2.98E-06	1.25E-05	9.74E-06	8.96E-05
7	3.37E-06	4.97E-06	4.62E-06	4.15E-05
8	2.43E-06	6.65E-06	4.08E-06	2.41E-05
9	2.10E-06	1.03E-05	2.87E-06	1.76E-05
10	1.89E-06	1.13E-05	3.00E-06	2.17E-05
11	1.59E-06	1.13E-05	3.40E-06	2.21E-05
12	1.24E-06	9.11E-06	4.25E-06	1.64E-05
13	7.20E-07	4.25E-06	2.00E-06	6.61E-06
14	8.07E-07	5.99E-06	3.27E-06	8.27E-06
15	7.90E-07	5.49E-06	3.35E-06	5.30E-06
16	8.34E-07	5.32E-06	3.72E-06	4.21E-06
17	8.29E-07	5.20E-06	3.84E-06	3.66E-06
18	7.76E-07	5.24E-06	3.38E-06	2.95E-06
19	7.71E-07	5.76E-06	3.24E-06	2.72E-06
20	7.55E-07	6.28E-06	3.10E-06	2.62E-06
21	6.99E-07	6.23E-06	2.92E-06	2.21E-06
22	6.66E-07	6.09E-06	2.98E-06	1.96E-06
23	6.20E-07	6.68E-06	3.13E-06	2.45E-06
24	5.95E-07	6.24E-06	3.30E-06	3.14E-06
25	6.81E-07	5.79E-06	3.53E-06	4.09E-06
26	8.73E-07	5.94E-06	3.71E-06	5.52E-06
27	1.04E-06	6.15E-06	3.64E-06	6.71E-06

28	1.14E-06	6.66E-06	3.23E-06	7.24E-06
29	1.32E-06	7.30E-06	3.14E-06	8.57E-06
30	1.58E-06	8.21E-06	3.13E-06	1.04E-05
31	1.80E-06	9.00E-06	2.98E-06	1.22E-05
32	2.02E-06	9.83E-06	3.01E-06	1.41E-05
33	2.12E-06	1.01E-05	2.66E-06	1.43E-05
34	2.00E-06	8.95E-06	2.41E-06	1.38E-05
35	1.93E-06	7.95E-06	2.10E-06	1.37E-05
36	1.81E-06	7.04E-06	1.86E-06	1.30E-05
37	1.58E-06	5.68E-06	1.56E-06	1.17E-05
38	1.69E-06	6.10E-06	1.34E-06	1.27E-05
39	1.62E-06	5.85E-06	9.83E-07	1.23E-05
40	1.79E-06	6.71E-06	7.65E-07	1.35E-05
41	1.86E-06	7.45E-06	5.94E-07	1.38E-05
42	1.88E-06	7.92E-06	5.31E-07	1.37E-05
43	1.88E-06	8.45E-06	6.14E-07	1.34E-05
44	1.85E-06	8.82E-06	7.63E-07	1.28E-05
45	1.80E-06	8.62E-06	8.61E-07	1.21E-05
46	1.72E-06	8.53E-06	9.56E-07	1.11E-05
47	1.64E-06	8.43E-06	1.07E-06	1.02E-05
48	1.36E-06	7.15E-06	1.04E-06	7.89E-06
49	1.25E-06	6.52E-06	1.08E-06	7.00E-06
50	1.07E-06	5.59E-06	1.05E-06	5.74E-06
51	9.91E-07	5.07E-06	1.14E-06	5.17E-06
52	9.26E-07	5.21E-06	1.31E-06	4.50E-06
53	9.18E-07	6.20E-06	1.52E-06	3.43E-06
54	8.40E-07	6.27E-06	1.38E-06	2.21E-06
55	8.42E-07	6.03E-06	1.22E-06	1.91E-06
56	8.51E-07	5.64E-06	1.22E-06	2.05E-06
57	8.57E-07	5.45E-06	1.33E-06	2.30E-06
58	9.29E-07	5.65E-06	1.55E-06	2.67E-06
59	9.00E-07	5.32E-06	1.64E-06	2.89E-06
60	7.88E-07	4.63E-06	9.48E-07	4.04E-06
61	1.38E-06	8.26E-06	3.09E-06	8.88E-06
62	1.29E-06	7.65E-06	2.75E-06	9.36E-06
63	1.65E-06	9.15E-06	2.19E-06	1.60E-05
64	2.19E-06	1.12E-05	1.45E-06	2.22E-05
65	3.14E-06	1.38E-05	1.78E-06	2.50E-05
66	4.28E-06	1.56E-05	2.85E-06	2.29E-05
67	5.57E-06	1.61E-05	3.49E-06	1.80E-05
68	5.75E-06	1.30E-05	3.77E-06	1.39E-05
69	5.28E-06	1.06E-05	4.53E-06	3.65E-05
70	4.58E-06	1.55E-05	7.59E-06	5.92E-05
71	2.43E-05	3.20E-05	1.38E-05	8.61E-05
72	4.79E-05	3.87E-05	1.52E-05	8.68E-05
73	8.24E-06	3.63E-05	1.34E-05	7.08E-05
74	1.34E-05	5.14E-05	1.87E-05	9.23E-05

Section 5.3.2

Buccal cortical strain the edentulous and dentate state

Buccal strain($\mu\varepsilon_{vm}$)		
Node position	*Edentulous*	*Dentate*
1	6184.2	6275.3
2	7014.31	7135.3
3	6963.88	7077.7
4	5717.47	5796.8
5	3191.4	3211.2
6	1644.91	1643.2
7	1146.72	1165.6
8	1373.59	1409.8
9	1385.97	1424.9
10	1386.79	1427.3
11	1658.88	1715
12	1518.29	1591.6
13	1606.43	1651.1
14	1815.31	1787
15	2042.28	2013.4
16	2346.13	2319.8
17	2622.96	2600.9
18	2473.11	2480.5
19	2548.96	2577.4
20	1362.35	1384
21	951.71	977.6
22	431.81	456.8
23	234.25	265.5
24	239.87	265.9
25	308.74	328
26	867.84	873.5
27	1285.91	1288.8
28	1304.67	1310.2
29	1412.61	1419
30	1258.2	1260.8
31	1523.33	1517.3
32	1307.25	1263.9
33	1095.07	1057.3
34	944.38	941.7
35	894.77	894.4
36	873.77	890.7
37	833.47	863.5
38	828.18	853.8
39	845.73	867.6
40	851.49	871.7

41	894.07	916.1
42	960.24	985.2
43	955.59	982.6
44	999.69	1035.4
45	649.7	681.9
46	1088.95	1098.5
47	2495.74	2524.1
48	3469.07	3513.8
49	3608.53	3654.9

Lingual cortical strain the edentulous and dentate state

Lingual strain($\mu\varepsilon_{vm}$)		
Node position	*Edentulous*	*Dentate*
1	1152.7	1191.9
2	2138.61	2202.4
3	1903.94	1944.6
4	1235.01	1256.2
5	721.49	730.2
6	772.37	800.7
7	1166.04	1226.6
8	1858.1	1932
9	1913.89	1981.2
10	2069.22	2134.5
11	2497.64	2569.5
12	2582.97	2649.2
13	1006.09	1031.5
14	1756.38	1800
15	1660.61	1697.9
16	1828.22	1865.3
17	1923.91	1960.7
18	1708.18	1737.7
19	1632.4	1661.8
20	1499.26	1533.4
21	1457.31	1503.4
22	1590.97	1659.8
23	1466.78	1568.1
24	1955.69	1999.7
25	2613.74	2569.3
26	3297.14	3244.4
27	3780.42	3744.6
28	3791.44	3692.4

29	4093.54	3959.1
30	4105.96	4036.6
31	3710.14	3720.1
32	3352.67	3402.1
33	2728.2	2770.1
34	1848.75	1893
35	1023.75	1092.7
36	646.55	738.6
37	468.29	560.1
38	764.65	815.3
39	1187.8	1212.7
40	1695.59	1715.8
41	2172.15	2193.2
42	2517.49	2540.1
43	2672.7	2687.5
44	2950.1	2960.1
45	3032.5	3028.8
46	3092.18	3070.1
47	3072.77	2990.7
48	2706.61	2555.3
49	2562.57	2425.5
50	2278.22	2204.6
51	2244.8	2236.7
52	2157.36	2177.7
53	1855.03	1886.8
54	1243.32	1297.6
55	989.17	1033.8
56	1006.03	1031.6
57	1078.17	1098.4
58	1197.82	1218.7
59	1253.21	1275.5
60	755.23	773.9
61	2563.72	2616.5
62	2381.85	2430.9
63	2336.39	2383.8
64	2205.91	2256.3
65	2277.2	2335.2
66	2127.62	2189.5
67	1756.14	1816
68	700.46	736.2
69	790.43	795.3
70	1528.79	1541.6
71	2985.23	3028.2
72	3833.65	3891.4
73	3608.15	3659.5
74	4686.76	4744.5

Section 5.3.3

The effect of load position on buccal cortical strain

	Buccal strain ($\mu\varepsilon_{vm}$) at anatomical sub-site				
Node position	*Ramus*	*Angle*	*Body*	*Parasymphysis*	*Symphysis*
1	9047.9	8792.8	6275.3	5156.4	5888.6
2	9144.9	9667.3	7135.3	7382.9	7493.8
3	8157.9	9334.8	7077.7	8247.3	8588.7
4	5364.2	7258.2	5796.8	7878.3	8750
5	2295.6	3815.5	3211.2	5599.6	6847.4
6	3143.7	2540.8	1643.2	3590.8	4713.9
7	4377.4	3027.4	1165.6	1967	2854.7
8	4464	3543.4	1409.8	1183	1821.3
9	2710.4	3257	1424.9	894.5	1278.2
10	1963.2	3009.7	1427.3	837.5	1009.8
11	1647.8	3423	1715	944.2	1053.7
12	1262.4	2413.4	1591.6	805	996.1
13	1136.7	2154.3	1651.1	785.7	902.7
14	1090.9	2093.5	1787	820.8	790.5
15	1007.5	1961.4	2013.4	1049.7	839.8
16	933.7	1798.5	2319.8	1361.3	993.5
17	894.1	1658.3	2600.9	1671.2	1127.1
18	920.1	1673.1	2480.5	2001	1232.7
19	1205.1	2037.6	2577.4	2672.3	1714.1
20	1057.2	1569	1384	2259.2	1612.5
21	1074	1551.7	977.6	2172	1784.1
22	1118.1	1546.6	456.8	2122.3	2139.4
23	1115.8	1556	265.5	1511.7	2531.2
24	870	1254.5	265.9	620	844.9
25	918.8	1305.8	328	662.3	933.8
26	1420.8	1895.7	873.5	1039.7	2214.8
27	1560.8	2080.3	1288.8	681.6	1991
28	1375.3	1845.5	1310.2	359.3	1600.6
29	1310.1	1764.3	1419	335.6	1557.3
30	1104.4	1493.5	1260.8	406.1	1208
31	1266.9	1732.6	1517.3	594.2	1028.9
32	1015.6	1396.5	1263.9	605.4	943.6
33	871.3	1202.5	1057.3	635.9	848.6
34	713.2	993.2	941.7	738	707.8
35	580.7	817.9	894.4	913.9	714.3
36	524.7	741.2	890.7	1060.2	799.1
37	474.1	673	863.5	1104.7	846.6
38	439.5	633.2	853.8	1086.2	842.2
39	382.3	566.7	867.6	1122.3	860.7
40	338.3	513.8	871.7	1152	881.5
41	336.8	521.9	916.1	1332.3	1078.4
42	316.1	514.2	985.2	1577.3	1349.2
43	284.7	478.2	982.6	1779.2	1638.5
44	244.9	389.2	1035.4	2676.7	2817
45	565.5	609.5	681.9	3556	4356.1
46	1173.1	1494.2	1098.5	3854.3	5220.8
47	1705.8	2330.6	2524.1	4328.4	5990.2
48	1957.4	2838.1	3513.8	4645.5	5577.6
49	1743.8	2697.1	3654.9	4855.3	4704.1

The effect of load position on lingual cortical strain

	Lingual strain ($\mu\varepsilon_{vm}$) at anatomical sub-site				
Node position	*Ramus*	*Angle*	*Body*	*Parasymphysis*	*Symphysis*
1	1924.4	1276.1	1191.9	5320.5	8088.1
2	3134.8	1846.1	2202.4	9460.2	13688.1
3	2531.1	1317.1	1944.6	7466.3	9793.3
4	2463.5	1644.7	1256.2	4500.9	5470.1
5	3584.3	2497.5	730.2	3720	5034.6
6	2278.8	1869.8	800.7	2299.6	2723.5
7	1627	1243.9	1226.6	1065.2	1607
8	3084.6	2081.5	1932	969	1779.2
9	4448	3050.1	1981.2	707.1	2574.1
10	5354.7	3804.2	2134.5	637.9	2752.9
11	6368.6	4779.3	2569.5	568.5	2685.1
12	6305.9	5131.8	2649.2	752	2216.1
13	2648.2	2046.4	1031.5	634	1145.9
14	3642.1	3505.2	1800	743.5	1406
15	2853.7	3366.4	1697.9	778	1203.6
16	2385	3724.2	1865.3	878.2	1057.3
17	2069.1	3876	1960.7	893.6	919.2
18	1620.2	3297.1	1737.7	812.6	762.9
19	1524.9	3087	1661.8	776.4	733
20	1447.7	2819	1533.4	718.3	711.6
21	1400.6	2590.7	1503.4	677.1	677.5
22	1430.4	2632.3	1659.8	705.9	657.8
23	1464.5	2524.4	1568.1	616.4	697.9
24	1478.1	2643	1999.7	800.5	679.6
25	1474.2	2798.7	2569.3	1119.7	647.9
26	1451.6	2891.9	3244.4	1516.5	689
27	1372.4	2799	3744.6	1832.6	705.8
28	1252.4	2426	3692.4	1969.8	762.8
29	1225.8	2329.5	3959.1	2282.2	867.2
30	1258.3	2275.7	4036.6	2731.6	1038.3
31	1271.6	2156.8	3720.1	3091.9	1225.5
32	1380.3	2217.2	3402.1	3471.3	1440.4
33	1452	2112.1	2770.1	3694.8	1533
34	1475.1	2056.6	1893	3534.6	1514.1
35	1517.1	2033.3	1092.7	3148.8	1697.7
36	1488.6	1974	738.6	2556.4	1775.8
37	1345.8	1783.5	560.1	1819.6	1726.9
38	1432.9	1884.6	815.3	1240.1	2104.4
39	1409.3	1859.7	1212.7	547.9	2038.2
40	1555.8	2059.9	1715.8	269	2071.2
41	1694.7	2280.7	2193.2	430.2	1882.6
42	1764.7	2414.4	2540.1	737.7	1662.3
43	1740.3	2407.1	2687.5	915.7	1561.9
44	1755.9	2477.6	2960.1	1259.4	1375.4
45	1759.1	2507.8	3028.8	1385.2	1276
46	1696.5	2451.6	3070.1	1578.8	1144.2
47	1618.9	2361.8	2990.7	1640.4	1068.5
48	1375.2	2024.8	2555.3	1535.1	855.3
49	1339.9	1978.8	2425.5	1541.2	783.6
50	1196.5	1778.5	2204.6	1505.9	656.3
51	1195.3	1786	2236.7	1627.4	606.9

52	1152.3	1727.4	2177.7	1694.5	634.5
53	1018.8	1527.6	1886.8	1604.3	718.7
54	732.4	1096.7	1297.6	1212.7	694.3
55	601.6	906.2	1033.8	960	648.2
56	560.1	862.2	1031.6	939.4	633.8
57	547.2	859.8	1098.4	1053	692.6
58	580.9	925.8	1218.7	1206.2	805.1
59	554.3	904.3	1275.5	1331.4	882.5
60	268.6	456.1	773.9	1132.4	933.8
61	878.8	1539.7	2616.5	3099.8	1924.8
62	785.8	1399.7	2430.9	2860.2	1719.7
63	675.4	1289.8	2383.8	3044.4	1975
64	525.7	1113.5	2256.3	3316.1	2521.3
65	395.9	984	2335.2	3800.8	3188
66	220.2	711.3	2189.5	3917.6	3621.5
67	241.4	423.6	1816	3690.4	3803.9
68	541.8	468.5	736.2	2163.1	2971.2
69	856.3	1039.6	795.3	618.9	1759.4
70	1006.4	1423.1	1541.6	2152.2	2700.7
71	1119.5	1982.2	3028.2	5982.3	6633.5
72	1219.5	2305.7	3891.4	7728.5	8347.7
73	932.9	1926.3	3659.5	7648.6	8292.7
74	942.2	2328.5	4744.5	10870.2	11995.5

Section 5.3.4

The effect of load angulation on buccal cortical strain (symphyseal loading)

Buccal cortical strain ($\mu\varepsilon_{vm}$) at varying loading angulations			
	45 degrees	*90 degrees*	*135 degrees*
1	0.004206	0.005889	0.00669
2	0.00602	0.007494	0.006553
3	0.006639	0.008589	0.006847
4	0.006244	0.00875	0.006857
5	0.0043	0.006847	0.005571
6	0.002725	0.004714	0.003977
7	0.001415	0.002855	0.002628
8	0.000717	0.001821	0.001903
9	0.000478	0.001278	0.001535
10	0.000509	0.00101	0.001302
11	0.000549	0.001054	0.001416
12	0.000406	0.000996	0.00137
13	0.000355	0.000903	0.001171
14	0.000355	0.000791	0.000901
15	0.000497	0.00084	0.000759
16	0.000711	0.000994	0.000735
17	0.000941	0.001127	0.000693
18	0.001154	0.001233	0.00063
19	0.001556	0.001714	0.000881
20	0.001394	0.001613	0.000913
21	0.001384	0.001784	0.001239
22	0.001278	0.002139	0.001942
23	0.000615	0.002531	0.003116
24	0.001177	0.000845	0.001789
25	0.001989	0.000934	0.00129
26	0.002867	0.002215	0.0011
27	0.001941	0.001991	0.001385
28	0.001272	0.001601	0.001339
29	0.000979	0.001557	0.001409
30	0.000649	0.001208	0.001147
31	0.000505	0.001029	0.000979
32	0.000494	0.000944	0.000849
33	0.000566	0.000849	0.000637
34	0.000618	0.000708	0.000422
35	0.000855	0.000714	0.000243
36	0.001117	0.000799	0.00017
37	0.001261	0.000847	0.000241
38	0.001261	0.000842	0.000346
39	0.001291	0.000861	0.000411
40	0.001321	0.000881	0.000449
41	0.0015	0.001078	0.00039
42	0.001753	0.001349	0.00041
43	0.001965	0.001638	0.000499
44	0.003	0.002817	0.00103
45	0.004102	0.004356	0.002092
46	0.004617	0.005221	0.002969
47	0.005079	0.00599	0.004258
48	0.0053	0.005578	0.004025
49	0.005274	0.004704	0.002624

The effect of load angulation on lingual cortical strain (symphyseal loading)

Lingual cortical strain ($\mu\varepsilon_{vm}$) at varying loading angulations			
	45 degrees	*90 degrees*	*135 degrees*
1	0.004353	0.008088	0.00716
2	0.007992	0.013688	0.011465
3	0.00684	0.009793	0.007123
4	0.004544	0.00547	0.003512
5	0.003837	0.005035	0.003539
6	0.002743	0.002723	0.002325
7	0.00158	0.001607	0.003288
8	0.001631	0.001779	0.00371
9	0.000952	0.002574	0.004178
10	0.000688	0.002753	0.00418
11	0.000467	0.002685	0.004064
12	0.000515	0.002216	0.003257
13	0.000455	0.001146	0.001355
14	0.000548	0.001406	0.001871
15	0.000558	0.001204	0.001489
16	0.000616	0.001057	0.00123
17	0.000594	0.000919	0.001045
18	0.000513	0.000763	0.000802
19	0.000459	0.000733	0.000747
20	0.000392	0.000712	0.000709
21	0.000343	0.000678	0.000731
22	0.000347	0.000658	0.000767
23	0.000227	0.000698	0.000941
24	0.000438	0.00068	0.001121
25	0.000722	0.000648	0.001193
26	0.001028	0.000689	0.001278
27	0.001282	0.000706	0.001247
28	0.001429	0.000763	0.001144
29	0.001677	0.000867	0.001125
30	0.002052	0.001038	0.0011
31	0.002338	0.001225	0.000958
32	0.002608	0.00144	0.000862
33	0.002717	0.001533	0.000733
34	0.002524	0.001514	0.000489
35	0.002365	0.001698	0.00044
36	0.002174	0.001776	0.000597
37	0.001871	0.001727	0.000787
38	0.001827	0.002104	0.001301
39	0.001439	0.002038	0.001603
40	0.001158	0.002071	0.001973
41	0.000719	0.001883	0.002194
42	0.000423	0.001662	0.002361
43	0.000421	0.001562	0.00248
44	0.000735	0.001375	0.002597
45	0.000829	0.001276	0.002509
46	0.001066	0.001144	0.002446
47	0.001175	0.001069	0.002294
48	0.00116	0.000855	0.001787
49	0.001175	0.000784	0.0015
50	0.001207	0.000656	0.001242
51	0.00135	0.000607	0.001136
52	0.001455	0.000634	0.00099
53	0.00141	0.000719	0.000668
54	0.001069	0.000694	0.000346
55	0.000804	0.000648	0.000351
56	0.00076	0.000634	0.000412

57	0.000894	0.000693	0.000432
58	0.001044	0.000805	0.000495
59	0.00121	0.000883	0.000532
60	0.001133	0.000934	0.000328
61	0.003143	0.001925	0.00072
62	0.002939	0.00172	0.000685
63	0.00321	0.001975	0.000508
64	0.003541	0.002521	0.000761
65	0.004164	0.003188	0.001438
66	0.004428	0.003621	0.002228
67	0.00431	0.003804	0.00274
68	0.002744	0.002971	0.002785
69	0.000928	0.001759	0.002589
70	0.001373	0.002701	0.002927
71	0.005227	0.006634	0.004498
72	0.007105	0.008348	0.005067
73	0.007343	0.008293	0.004752
74	0.010573	0.011996	0.006527

The effect of load angulation on buccal cortical strain (body loading)

Buccal cortical strain ($\mu\varepsilon_{vm}$) at varying loading angulations			
	45 degrees	*90 degrees*	*135 degrees*
1	0.00625	0.00628	0.00758
2	0.00539	0.00714	0.0105
3	0.00505	0.00708	0.0116
4	0.0047	0.0058	0.011
5	0.00377	0.00321	0.00789
6	0.00279	0.00164	0.00505
7	0.002	0.00117	0.00301
8	0.00158	0.00141	0.0023
9	0.00133	0.00142	0.00204
10	0.00117	0.00143	0.0019
11	0.00126	0.00171	0.0023
12	0.00123	0.00159	0.00211
13	0.0011	0.00165	0.00208
14	0.000899	0.00179	0.00222
15	0.000859	0.00201	0.00277
16	0.00142	0.00232	0.00332
17	0.00172	0.0026	0.00253
18	0.00111	0.00248	0.00242
19	0.000758	0.00258	0.00292
20	0.00011	0.00138	0.00197
21	0.000444	0.000978	0.0018
22	0.000934	0.000457	0.00155
23	0.00117	0.000266	0.00131
24	0.000769	0.000266	0.000954
25	0.000844	0.000328	0.000985
26	0.00138	0.000874	0.00114
27	0.00156	0.00129	0.0012
28	0.00145	0.00131	0.00118
29	0.00153	0.00142	0.00113
30	0.00124	0.00126	0.00109
31	0.00116	0.00152	0.00137
32	0.00099	0.00126	0.00113
33	0.000731	0.00106	0.00105
34	0.000516	0.000942	0.000995
35	0.000388	0.000894	0.000947
36	0.000373	0.000891	0.000915

37	0.000445	0.000863	0.000806
38	0.000526	0.000854	0.000734
39	0.000586	0.000868	0.000706
40	0.000617	0.000872	0.000694
41	0.000553	0.000916	0.000848
42	0.000525	0.000985	0.00104
43	0.000485	0.000983	0.00121
44	0.000664	0.00104	0.00183
45	0.00153	0.000682	0.00238
46	0.00254	0.0011	0.00241
47	0.00401	0.00252	0.00283
48	0.00407	0.00351	0.00314
49	0.00281	0.00365	0.00367

The effect of load angulation on lingual cortical strain (body loading)

Lingual cortical strain ($\mu\varepsilon_{vm}$) at varying loading angulations			
	45 degrees	*90 degrees*	*135 degrees*
1	0.00561	0.00119	0.00656
2	0.0088	0.0022	0.0111
3	0.00523	0.00194	0.00775
4	0.00256	0.00126	0.00402
5	0.00282	0.00073	0.00308
6	0.00194	0.000801	0.00215
7	0.003	0.00123	0.00195
8	0.00358	0.00193	0.0013
9	0.00395	0.00198	0.00147
10	0.00398	0.00213	0.00143
11	0.00398	0.00257	0.00139
12	0.0033	0.00265	0.00159
13	0.0013	0.00103	0.00099
14	0.00193	0.0018	0.00129
15	0.00156	0.0017	0.00142
16	0.00136	0.00187	0.00173
17	0.00123	0.00196	0.0019
18	0.000948	0.00174	0.00181
19	0.000852	0.00166	0.00182
20	0.000747	0.00153	0.00178
21	0.000775	0.0015	0.00172
22	0.000871	0.00166	0.00181
23	0.000958	0.00157	0.00177
24	0.00127	0.002	0.00199
25	0.00151	0.00257	0.00242
26	0.00176	0.00324	0.00305
27	0.00194	0.00374	0.00349
28	0.00192	0.00369	0.00341
29	0.00206	0.00396	0.00363
30	0.0021	0.00404	0.00368
31	0.0018	0.00372	0.00353
32	0.00148	0.0034	0.00341
33	0.00105	0.00277	0.00296
34	0.000549	0.00189	0.00224
35	0.000365	0.00109	0.00166
36	0.000555	0.000739	0.00133
37	0.000723	0.00056	0.00105
38	0.00122	0.000815	0.00104
39	0.00159	0.00121	0.00101
40	0.00208	0.00172	0.00115
41	0.00246	0.00219	0.00129

42	0.00272	0.00254	0.00143
43	0.00287	0.00269	0.00144
44	0.00305	0.00296	0.00156
45	0.003	0.00303	0.0016
46	0.00295	0.00307	0.00164
47	0.0028	0.00299	0.00163
48	0.00225	0.00256	0.0015
49	0.00197	0.00243	0.00155
50	0.0017	0.0022	0.00147
51	0.00162	0.00224	0.00156
52	0.00149	0.00218	0.00161
53	0.00113	0.00189	0.00155
54	0.000644	0.0013	0.00124
55	0.000522	0.00103	0.00104
56	0.000577	0.00103	0.00101
57	0.000619	0.0011	0.00106
58	0.000692	0.00122	0.00119
59	0.00074	0.00128	0.00122
60	0.000348	0.000774	0.000924
61	0.00136	0.00262	0.00241
62	0.0013	0.00243	0.00217
63	0.00112	0.00238	0.00229
64	0.000936	0.00226	0.00255
65	0.00132	0.00234	0.00288
66	0.00194	0.00219	0.00295
67	0.00232	0.00182	0.00284
68	0.00235	0.000736	0.002
69	0.0022	0.000795	0.00186
70	0.00227	0.00154	0.00325
71	0.00298	0.00303	0.00652
72	0.00325	0.00389	0.00788
73	0.00307	0.00366	0.00738
74	0.00392	0.00474	0.0103

Section 5.4.1

The effect of load position on buccal cortical strain (non-linear analysis)

	Buccal strain ($\mu\varepsilon_{vm}$) at anatomical sub-site				
Node position	***Ramus***	***Angle***	***Body***	***Parasymphysis***	***Symphysis***
1	7034.2579	6898.8229	4983.1251	5779.9447	6822.1
2	7072.6099	7668.0935	5640.3927	7797.2187	8623.9
3	6060.8678	7178.8986	5487.9208	8299.207	9751.2
4	3692.8874	5286.7256	4335.3582	7487.0999	9474.1
5	1615.0221	2616.5317	2294.4403	5033.9629	6847.7
6	2378.3366	1852.4414	1177.9586	3105.0135	4454.1
7	3276.3604	2229.7735	857.5776	1668.1802	2579.4
8	3357.1083	2593.4375	1019.1772	1019.1439	1623.1
9	1978.6752	2361.9394	1026.7554	768.4459	1169.1
10	1401.5493	2180.1557	1033.2229	717.3407	954.8
11	1174.7858	2555.349	1249.9171	820.1628	1013.3
12	905.6323	1741.0024	1162.7688	706.7832	942.8
13	814.5394	1529.2211	1198.9535	684.8569	852.7
14	783.0681	1496.6703	1278.4051	697.298	751.6
15	720.2783	1403.1756	1427.301	877.7813	817.5
16	662.7356	1276.9266	1676.0118	1123.9801	972.9
17	633.6346	1176.6319	1908.8657	1361.7498	1106.7
18	657.2397	1190.0732	1758.0302	1633.135	1228.8
19	859.2484	1433.5659	1818.5769	2191.0172	1699
20	760.5864	1116.7052	999.3266	1852.868	1566.6
21	776.568	1110.2628	708.1096	1830.7771	1714.9
22	817.7667	1117.2764	342.5209	1832.5111	2018.5
23	832.2343	1147.4208	178.1289	1291.0443	2288.8
24	654.6632	935.9668	176.4232	546.0201	741.1
25	686.172	968.3062	212.3788	591.8153	851.7
26	1064.6151	1404.1459	598.5878	994.3671	2050.1
27	1164.6474	1536.3577	899.3224	743.6959	1893.7
28	1024.7362	1355.5952	911.8209	479.2297	1536.5
29	970.1398	1286.5351	983.0315	423.847	1516
30	818.5776	1088.4719	871.6157	369.4477	1175
31	945.8963	1271.1277	1059.8965	400.5199	1039.8
32	751.721	1017.0963	882.5229	439.0423	936.5
33	643.2244	874.7451	745.5198	484.6952	827
34	527.8216	724.5262	667.4449	554.5494	670.8
35	429.3669	596.183	637.6695	697.608	645.9
36	389.5445	542.4371	639.9517	823.579	719.6
37	353.5552	494.4496	633.4714	893.198	791.3
38	329.4725	466.8384	632.5691	900.5556	804.6
39	283.5221	413.4649	642.5354	945.416	825.5
40	249.945	373.5658	646.8606	977.6657	842.3
41	248.2562	379.0905	678.3023	1133.569	1015.9
42	230.2939	371.1098	730.1141	1348.2104	1253.8
43	205.0212	343.3272	731.0501	1537.5342	1516.9

44	166.8433	274.2211	815.1622	2494.3143	2764.5
45	381.6776	373.831	599.4656	3561.5592	4611.5
46	812.6028	980.4051	676.3731	4099.1074	6116.2
47	1200.8357	1583.3325	1621.5005	4292.1518	7284.3
48	1405.1849	2002.4277	2365.9543	4105.9866	7099.1
49	1282.4841	1960.7079	2527.1033	3695.9127	5663.3

The effect of load position on lingual cortical strain (non-linear analysis)

	Lingual strain ($\mu\varepsilon_{vm}$) at anatomical sub-site				
Node position	***Ramus***	***Angle***	***Body***	***Parasymphysis***	***Symphysis***
1	1601.4654	1039.2545	921.5983	5334.8334	8731.5
2	2682.6209	1609.3439	1828.0298	9565.3837	14958.1
3	1821.9283	953.3935	1656.1541	7132.1845	8852.3
4	1708.8547	1139.3314	1093.3888	4037.8993	4317.8
5	2554.0776	1764.6102	606.3749	3297.7128	3758.2
6	1534.3562	1270.9944	646.1316	1929.5529	2578.9
7	1267.5982	896.0779	936.345	851.0097	2711.7
8	2398.655	1612.2547	1443.7211	628.1231	2337.7
9	3432.2776	2348.5303	1477.1414	595.2098	2717.3
10	4127.35	2910.5385	1591.6997	593.7523	2687.5
11	4915.8773	3643.4618	1912.0045	612.7451	2504
12	4836.4841	3880.6138	1955.2357	757.0681	1986.2
13	1957.8949	1490.3294	753.8935	581.0433	1062.5
14	2738.2532	2621.4626	1328.7918	682.2967	1256.5
15	2130.3256	2527.8149	1260.3856	716.5378	1105.9
16	1762.2192	2807.1891	1387.7968	809.8754	1006.2
17	1518.4497	2929.5648	1463.0723	826.2406	900.5
18	1192.4044	2490.0563	1305.2514	762.1828	787.4
19	1125.2215	2323.2238	1251.4235	738.1715	782.6
20	1068.0312	2104.4117	1151.5022	689.8239	773.7
21	1042.413	1944.7281	1131.7979	641.589	728.5
22	1080.1348	2008.8291	1255.598	655.595	701.9
23	1078.4549	1867.6751	1161.0103	567.2627	720.4
24	1061.153	1904.5014	1439.7276	672.2338	673.1
25	1065.7118	2034.9495	1878.9843	921.934	654.2
26	1068.0182	2127.9249	2399.6677	1246.7193	735.8
27	1009.5352	2081.9792	2834.4457	1538.4642	793.9
28	929.1627	1809.4699	2794.1878	1653.3305	878.6
29	896.0369	1712.7837	3007.4175	1906.8513	997.7
30	924.0206	1667.8219	3015.7581	2272.951	1193.5
31	919.6146	1546.7745	2750.4562	2559.2869	1373.2
32	1001.7285	1591.341	2493.6539	2874.3978	1581.8
33	1058.7074	1519.1748	2028.2933	3073.2404	1668.6
34	1083.3312	1493.6173	1372.778	2948.7661	1650.6
35	1116.2925	1486.4396	809.1143	2637.7442	1755.7
36	1100.0236	1449.1125	548.2973	2155.8538	1781.8
37	998.5305	1311.1103	402.6996	1554.2926	1685
38	1068.3678	1393.4864	575.1722	1139.7374	2018.5
39	1051.5012	1373.9453	859.6793	607.9862	1955

40	1161.3423	1527.5764	1217.9688	357.0096	2038.1
41	1263.9832	1693.2982	1562.6936	231.5903	1908.1
42	1310.3881	1787.4779	1820.8981	346.9648	1725.1
43	1289.5868	1776.5463	1920.5497	455.2618	1656.3
44	1301.746	1829.8413	2132.2946	695.9731	1504.7
45	1309.2552	1860.2776	2200.9327	808.2233	1412.9
46	1273.3817	1829.9789	2249.5033	971.7299	1292.8
47	1227.5238	1778.1781	2223.3022	1055.509	1222.5
48	1038.1086	1507.2406	1875.7234	1026.4867	974.4
49	1023.7359	1490.6567	1803.9184	1076.0941	877.1
50	919.5167	1347.1143	1635.8352	1065.6485	723.3
51	920.3195	1356.8103	1670.6233	1166.8086	635.4
52	869.6136	1286.627	1594.5794	1218.9887	622.2
53	770.1426	1140.6566	1384.0403	1196.6971	680.4
54	559.8177	828.9661	960.8172	938.3444	661.3
55	460.1067	685.6646	767.111	751.958	641.8
56	427.6702	651.5917	772.3552	723.0384	620.5
57	422.3665	656.7755	833.2769	818.6172	655.9
58	447.2807	705.3154	919.8875	932.972	745.2
59	425.727	686.9541	958.3288	1034.3684	794.3
60	205.171	344.7439	574.2365	943.9023	869.1
61	665.2924	1153.8204	1955.845	2472.2044	1633.1
62	591.4203	1043.712	1813.1782	2283.9986	1453.1
63	514.2648	974.8223	1811.2709	2524.5833	1688.6
64	399.3775	839.918	1710.6359	2831.518	2203.3
65	304.4812	749.114	1793.0985	3409.9702	2933.5
66	171.8376	551.0575	1703.1338	3755.0555	3566.9
67	169.0187	332.805	1461.3549	3874.2045	4070.8
68	384.0987	288.2924	694.2726	2816.7225	3519.4
69	623.3181	705.5011	452.2097	1488.3942	2142.5
70	745.89	1000.2272	874.2055	573.0341	1398.2
71	856.6363	1453.3103	1980.407	3444.3298	4879.8
72	958.5835	1748.387	2742.33	5339.0698	7028.9
73	780.1587	1546.28	2829.058	6384.3048	8271.2
74	825.7072	2005.1915	3989.7859	13549.6277	19964.8

Section 5.4.2

The effect of load position on buccal cortical strain (non-linear analysis, non-physiological load)

	Buccal strain ($\mu\varepsilon_{vm}$) at anatomical sub-site			
Node position	***Symphysis***	***Parasymphysis***	***Body***	***Ramus***
1	0.5358	0.3843	0.3985	0.5578
2	1.1807	0.9301	0.8461	1.0607
3	1.4195	1.0955	0.9531	1.1126
4	1.645	1.1885	0.9172	0.8808
5	1.1543	0.7101	0.4012	0.2847
6	0.6969	0.3595	0.1443	0.4551
7	0.3209	0.1305	0.1329	0.7079
8	0.136	0.06	0.1396	0.6279
9	0.0723	0.032	0.1042	0.3275
10	0.0471	0.0241	0.0921	0.1469
11	0.044	0.0245	0.1135	0.0805
12	0.032	0.0191	0.1062	0.0512
13	0.0269	0.0211	0.1371	0.04
14	0.0243	0.0289	0.1718	0.0334
15	0.0319	0.0474	0.206	0.0308
16	0.0581	0.08	0.2148	0.03
17	0.0839	0.1225	0.2551	0.0329
18	0.1263	0.1975	0.2897	0.0382
19	0.2108	0.3125	0.2945	0.0623
20	0.1608	0.2261	0.0989	0.071
21	0.1854	0.1704	0.0564	0.0769
22	0.2169	0.1336	0.0263	0.0819
23	0.2521	0.0975	0.026	0.0772
24	0.0531	0.0106	0.0258	0.0596
25	0.0496	0.0087	0.0302	0.0663
26	0.2502	0.0146	0.0863	0.1318
27	0.22	0.0059	0.1431	0.1553
28	0.161	0.004	0.152	0.1361
29	0.1352	0.0068	0.1668	0.1309
30	0.0938	0.0103	0.1444	0.1008
31	0.0676	0.0201	0.1826	0.1176
32	0.0426	0.0196	0.1182	0.0694
33	0.027	0.0199	0.0894	0.0477
34	0.0158	0.0286	0.0823	0.0314
35	0.016	0.0413	0.0719	0.0206
36	0.0184	0.0466	0.0671	0.0161
37	0.0216	0.0388	0.0505	0.0119
38	0.0262	0.0356	0.0435	0.0099
39	0.0316	0.0397	0.0438	0.008
40	0.0371	0.0453	0.0456	0.0069
41	0.0555	0.0648	0.0552	0.0069
42	0.0948	0.1051	0.0738	0.0065

43	0.1336	0.134	0.0823	0.0059
44	0.3939	0.289	0.1106	0.0048
45	0.821	0.4782	0.0658	0.0075
46	0.9907	0.4959	0.0708	0.0444
47	1.0919	0.5104	0.231	0.1095
48	0.8295	0.4897	0.355	0.1455
49	0.5681	0.453	0.3423	0.123

The effect of load position on lingual cortical strain (non-linear analysis, non-physiological load)

	Lingual strain ($\mu\varepsilon_{vm}$) at anatomical sub-site			
Node position	***Symphysis***	***Parasymphysis***	***Body***	***Ramus***
1	1.2942	0.5937	0.0858	0.1306
2	1.832	0.9262	0.1786	0.1422
3	2.2375	1.2465	0.3455	0.3096
4	1.5884	1.0041	0.3527	0.4394
5	1.5934	0.9208	0.2294	0.5665
6	1.0669	0.7537	0.2857	0.486
7	0.4002	0.5133	0.3888	0.3324
8	0.2229	0.3818	0.4115	0.4178
9	0.2376	0.091	0.2606	0.5015
10	0.3021	0.0385	0.2633	0.6615
11	0.2633	0.0275	0.2604	0.7567
12	0.1823	0.0313	0.2518	0.7404
13	0.078	0.0202	0.0854	0.3531
14	0.0829	0.0219	0.1241	0.3837
15	0.0535	0.0192	0.108	0.2704
16	0.0397	0.0201	0.1202	0.2115
17	0.0293	0.0192	0.1263	0.1506
18	0.0198	0.0159	0.1038	0.0945
19	0.0163	0.0151	0.1027	0.0792
20	0.014	0.0146	0.1009	0.0709
21	0.0121	0.016	0.0972	0.0611
22	0.0113	0.0193	0.1017	0.0526
23	0.0133	0.0202	0.1492	0.0566
24	0.0139	0.0349	0.2304	0.0641
25	0.0167	0.0542	0.2772	0.0532
26	0.025	0.083	0.3406	0.0425
27	0.0306	0.0906	0.2928	0.042
28	0.0401	0.1125	0.3082	0.0409
29	0.0595	0.1433	0.309	0.0448
30	0.1015	0.2433	0.3946	0.0531
31	0.1492	0.2941	0.3435	0.0696
32	0.1865	0.3765	0.3362	0.0941
33	0.199	0.3747	0.2182	0.1212
34	0.2284	0.3747	0.1152	0.133
35	0.2543	0.2953	0.046	0.1406
36	0.2722	0.2289	0.0309	0.1426

37	0.234	0.1384	0.028	0.1226
38	0.2822	0.0707	0.0594	0.1422
39	0.2689	0.0122	0.1102	0.1494
40	0.2935	0.0041	0.1827	0.1788
41	0.2667	0.0086	0.2476	0.1997
42	0.2758	0.0198	0.3141	0.2286
43	0.2315	0.0297	0.3103	0.2081
44	0.1696	0.0496	0.3271	0.1924
45	0.1419	0.0568	0.317	0.1799
46	0.103	0.0638	0.2903	0.1494
47	0.0751	0.0633	0.2276	0.1159
48	0.0435	0.0626	0.2032	0.0914
49	0.0319	0.0538	0.1563	0.0728
50	0.02	0.0549	0.1428	0.0582
51	0.0156	0.0641	0.1435	0.0549
52	0.0143	0.0934	0.19	0.0603
53	0.0139	0.0857	0.1591	0.0459
54	0.0132	0.0561	0.0923	0.0256
55	0.0125	0.0403	0.0701	0.0168
56	0.0133	0.0404	0.0626	0.0139
57	0.0182	0.0417	0.0555	0.0131
58	0.026	0.0518	0.0637	0.0136
59	0.0339	0.0612	0.0687	0.0123
60	0.0514	0.0597	0.0421	0.0054
61	0.1558	0.2284	0.194	0.0205
62	0.1381	0.2156	0.1877	0.0184
63	0.1501	0.2055	0.1577	0.0149
64	0.2471	0.2873	0.1807	0.0113
65	0.3721	0.4	0.2198	0.0089
66	0.431	0.4569	0.2307	0.0052
67	0.3407	0.4151	0.2011	0.0053
68	0.2415	0.162	0.0623	0.0206
69	0.5659	0.2518	0.0941	0.0646
70	1.136	0.6745	0.2549	0.0978
71	1.634	1.0718	0.4473	0.1141
72	1.5101	1.0422	0.4653	0.1112
73	1.2702	0.8732	0.3721	0.0706
74	2.0661	1.4192	0.605	0.1037

The effect of load position on buccal cortical stress (non-linear analysis, non-physiological load)

	Buccal stress (σ_{vm})(MPa) at anatomical sub-site			
Node position	***Symphysis***	***Parasymphysis***	***Body***	***Ramus***
1	404.1272	324.243	331.4517	414.3793
2	738.8577	608.3267	564.4878	676.1435
3	862.9023	694.2292	619.958	702.8436
4	979.8281	742.4924	601.3634	582.4033
5	724.8134	494.3764	334.1891	278.9669

6	487.429	312.2702	201.2204	361.7262
7	292.747	192.3278	193.3365	492.4443
8	196.0712	155.3115	196.7029	450.8206
9	161.9208	140.7278	178.288	294.5686
10	148.6027	136.0316	172.0075	200.6484
11	146.9865	136.2891	183.1494	166.0642
12	140.7489	131.2753	179.3117	150.6961
13	137.9925	133.437	195.4023	144.88
14	136.3303	139.0641	213.4461	141.4357
15	140.7263	148.7087	231.2076	140.0616
16	154.3584	165.7144	236.1139	139.6363
17	167.8502	187.84	257.0928	141.1707
18	189.9048	226.8184	274.8573	143.9738
19	234.3012	287.2914	277.6358	156.6097
20	207.7708	241.6768	175.5594	161.072
21	220.5666	212.9269	153.4005	164.1379
22	236.9338	193.9117	137.4751	166.6729
23	255.3835	174.9403	137.2931	164.208
24	152.3645	113.3519	137.2005	155.0482
25	150.5391	102.3378	139.7769	158.6014
26	254.3245	124.7837	169.0128	192.6655
27	238.6899	76.7418	198.5214	204.8759
28	208.1678	56.3655	203.2467	194.8966
29	194.6374	86.9358	210.8484	192.1404
30	173.0839	111.3728	199.2191	176.5242
31	159.4119	132.5125	219.1427	185.3099
32	146.3524	132.0016	185.5885	160.1982
33	138.1199	132.3013	170.5807	148.8821
34	127.0379	138.8937	166.8797	140.402
35	127.3956	145.5788	161.4533	132.9159
36	130.7258	148.3332	158.9701	127.2396
37	134.0671	144.2723	150.3153	117.841
38	137.6707	142.6367	146.6952	109.2621
39	140.6646	144.741	146.8629	97.5151
40	143.5919	147.7223	147.7951	87.3829
41	153.4438	157.8984	152.843	87.4598
42	174.174	178.8919	162.5116	83.1045
43	194.6695	194.0034	166.9445	76.8372
44	330.7982	274.7428	181.7696	64.6523
45	552.0727	372.9178	158.9974	93.4212
46	639.6591	382.6729	166.6022	147.2542
47	692.8092	393.3206	248.0101	181.2053
48	559.5292	391.2932	311.7632	200.0169
49	430.3954	374.0035	304.9372	188.3474

The effect of load position on lingual cortical stress (non-linear analysis, non-physiological load)

	Lingual stress (σ_{vm})(MPa) at anatomical sub-site			
Node position	***Symphysis***	***Parasymphysis***	***Body***	***Ramus***
1	798.2967	433.7987	168.8517	192.1258
2	1076.999	606.0037	217.475	198.3016
3	1288.542	772.6515	304.8923	285.7644
4	953.7702	647.0265	309.3908	353.522
5	956.5235	603.7712	247.895	419.6319
6	684.7073	516.9478	275.1658	378.0274
7	344.518	392.1784	327.2703	299.8859
8	249.5594	323.1049	338.3883	342.0089
9	248.3469	171.866	259.76	385.2733
10	281.8431	143.3041	261.1509	468.2426
11	261.3502	137.9599	259.5347	517.7913
12	219.6779	139.9805	255.2575	509.815
13	164.8188	132.4405	168.5785	308.5613
14	167.4107	134.1748	188.7261	324.1453
15	152.0658	131.292	180.3333	265.118
16	144.8677	132.2838	186.6298	234.3975
17	139.3913	131.5071	189.7729	202.6287
18	131.9361	127.0112	178.0406	173.2914
19	127.5435	125.6126	177.5253	165.3024
20	123.468	124.7322	176.6166	160.9926
21	118.4513	127.2122	174.6393	155.8743
22	115.8827	131.6061	176.9663	151.4621
23	121.9569	132.4754	201.7244	153.5228
24	123.203	142.242	244.0419	157.4068
25	127.8089	152.2569	268.3631	151.794
26	136.6845	167.3265	301.2837	146.2101
27	140.0006	171.2729	276.5166	145.9614
28	145.0405	182.7207	284.4336	145.3574
29	155.1227	198.6641	284.8202	147.4051
30	176.9771	250.7501	329.3823	151.746
31	201.7856	277.1039	302.8331	160.3759
32	221.2035	319.9701	298.9906	173.1605
33	227.7771	319.0675	237.7222	187.2728
34	242.9181	319.0485	184.0935	193.3764
35	256.3728	277.7355	147.9964	197.3189
36	265.653	243.2906	140.1734	198.2864
37	245.8322	196.3004	138.5503	187.9354
38	270.8966	160.9994	155.0835	198.1144
39	264.0199	114.8794	181.5419	201.865
40	276.8152	60.4788	219.4114	217.1662
41	262.8896	103.847	253.1951	227.9961
42	267.6363	132.1726	287.6623	243.012
43	244.657	139.5756	285.7043	232.3473
44	212.5414	149.981	294.3613	224.2417
45	198.1055	153.7735	289.1399	217.7419
46	177.9214	157.3932	275.2934	201.9047
47	163.3353	157.1042	242.5376	184.4635

48	146.7942	156.7322	229.9241	171.6641
49	140.7817	152.118	205.5531	161.9992
50	132.5809	152.7209	198.531	154.3794
51	126.8325	157.5231	198.8663	152.6455
52	124.5245	172.7618	223.0819	155.4374
53	123.6692	168.7662	207.0038	147.9519
54	121.9772	153.3005	172.1323	137.0696
55	120.1669	145.0652	160.5594	128.365
56	122.1959	145.0986	156.6316	123.3323
57	130.362	145.7796	152.9473	121.4457
58	137.507	151.0389	157.1882	122.8619
59	141.8557	155.8919	159.8206	119.4124
60	150.8418	155.153	145.9731	70.7428
61	205.6827	243.232	225.2038	132.5473
62	196.4667	236.5024	221.864	129.0889
63	202.3874	231.1948	206.3099	125.1026
64	252.9257	273.6979	218.2409	115.9547
65	317.9133	332.3314	238.6527	103.8492
66	349.1448	362.3164	244.357	69.5931
67	306.1599	341.772	229.2735	70.2706
68	269.5184	222.1399	159.0299	130.7405
69	425.4951	267.135	175.467	157.791
70	716.1303	476.1135	257.5443	175.0622
71	974.1115	681.663	356.9503	183.5041
72	909.5157	666.2532	366.1121	181.9532
73	784.7343	578.3068	317.7167	160.8128
74	1201.813	865.1869	440.9817	178.7708

Appendix 11

A clinical case showing the use of FEA to model a fracture presenting clinically.

This section shows a comparison between the results of a modelled high kinetic energy impact to the symphyseal region and a clinical case. The picture below shows a reconstructed CT scan taken from a patient who suffered facial trauma as a result of a kick to the symphyseal region by a horse.

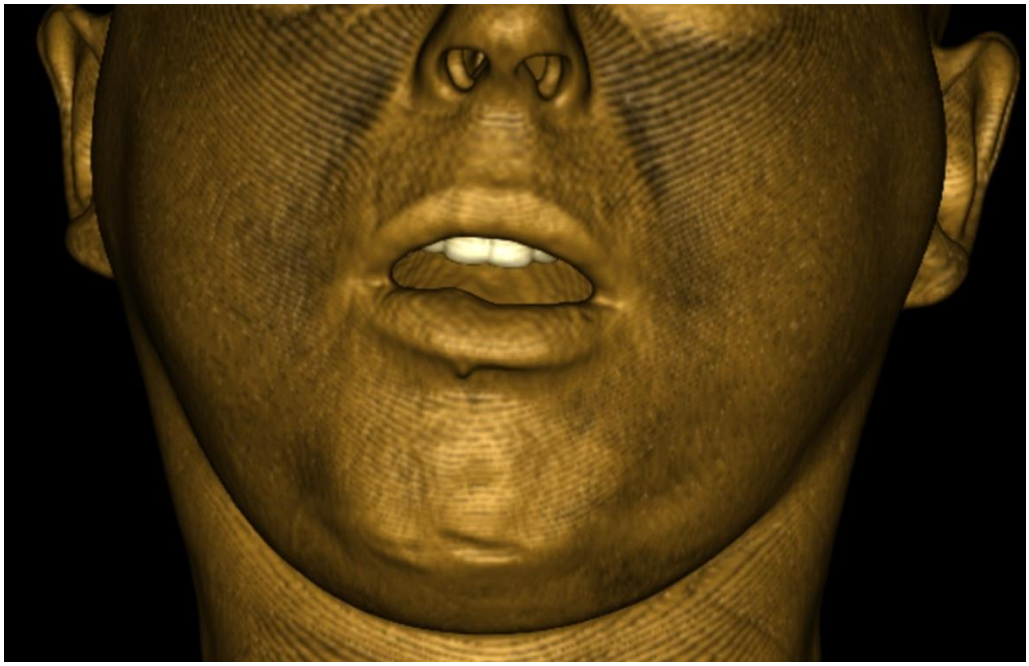

3D reconstruction of a CT of a patient who suffered a horse kick to the chin. (Used with the consent of the patient).

The unfortunate patient almost managed to avoid the kick and so did not receive the full impact. The only soft-tissue injury that the patient suffered was a 2.5cm horizontal laceration to the chin. The patient suffered bilateral fractures to the condylar necks and a linear fracture just to the patient's left of the symphysis. The FEA simulation of the injury suggests more fragmentation to the symphyseal region than is seen in the clinical case, although in the model there is no soft-tissue to absorb the impact energy. The pictures reinforce the impression that the sub-site location of mandibular fractures is determined by the point of impact. The energy of the impact determines how much damage is produced at these sub-sites. The clinical picture shows slightly more antero-

medial displacement of the condylar heads. This is due to the fact that the FE analysis shows only the first 1.0ms of impact (and there are no muscles represented in the model). The clinical CT (which was taken some time after the initial impact) shows the position of the condylar heads once the lateral pterygoid muscles have had time to act. There is also similarity of the angulation of the condylar neck fracture, with the fracture passing supero-inferiorly from lateral to medial. The results suggest that for this form of impact at least; the 3DFEA and simulation, using the element deletion algorithm, gives a reasonable impression of the clinical condition.

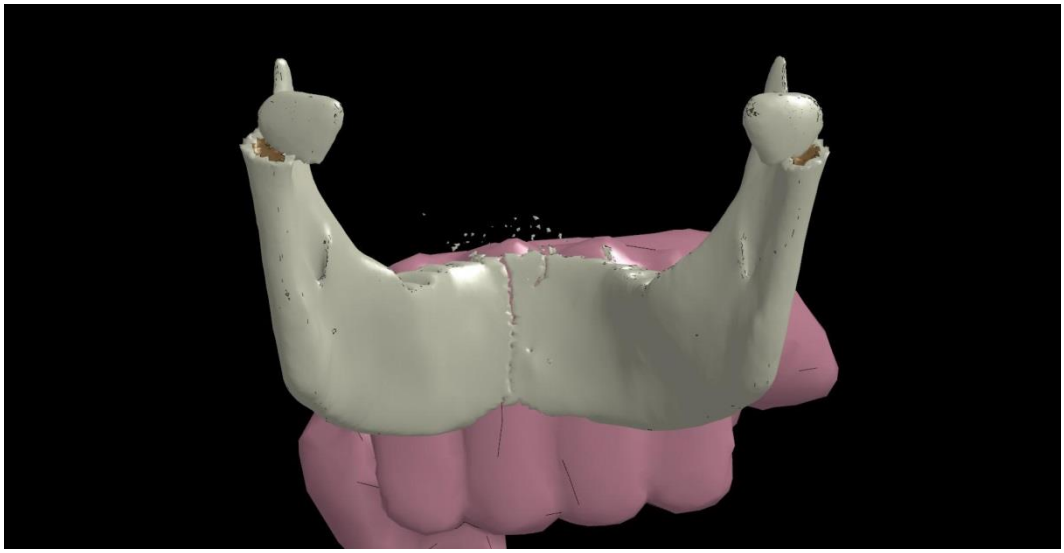

The FEA model (using the element deletion algorithm) of the mandible following an impact at the symphyseal region. Impact is at 1.0ms.

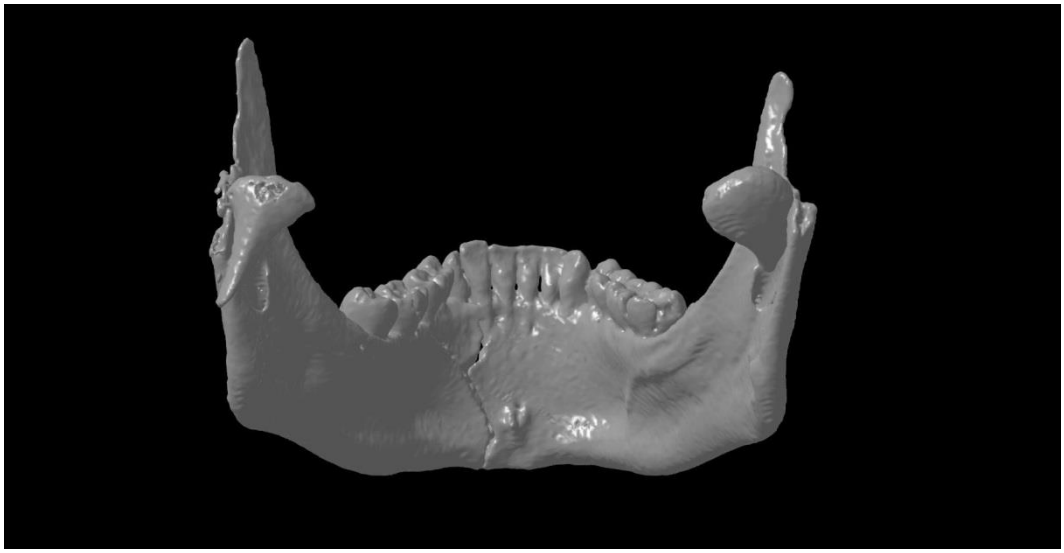

Reconstructed CT scan of a patient who suffered trauma to the symphyseal (chin) region. The mandible has been segmented from the remaining facial CT scan. The CT scan data was used with express consent of the patient.

Appendix 12

List of software and hardware used during this research

LS-DYNA (v 971)	www.ls-dyna.com
Strand7®	www.strand7.com
Enguage	digitizer.sourceforge.net
MIX 2.0	www.meta-analysis-made-easy.com
Mimics 14.1	www.materialise.com/mimics
Scan IP™	www.simpleware.com
Scan FE™	www.simpleware.com
+Scan CAD	www.simpleware.com
Osirix	www.osirix-viewer.com
Invesalius 3	cti.gov.br/invesalius/
LS-Pre-post	www.lstc.com/lspp
Irfanview	www.irfanview.com
Geomagic Studio	www.geomagic.com/en/products/studio
Paraview 3.8	www.paraview.org
GIMP 2.8	www.gimp.org
Adobe Photoshop®	www.adobe.com
Adobe Acrobat	www.adobe.com
Microsoft Word	www.microsoft.com
Microsoft Excel	www.microsoft.com
Papers	www.mekentosj.com

Analyses were performed on an Intel ® Core™ i7-4770 CPU@ 3.40GHz with 16GB memory, running Windows 7 64-bit (© 2007 Microsoft Corporation).

Analysis run-time

Each simulation was run for 1.0ms to achieve an impact time of the same duration. The mean computation time for the dynamic analyses was 56hrs 23mins.

Appendix 13

Electronic databases used in this research

Ovid Medline

Embase

PubMed

Scirus

Scopus

Google Scholar

Appendix 14

LS-DYNA reduced keyword file

```
$# LS-DYNA Keyword file created by LS-PrePost 3.2
*KEYWORD MEMORY=350000000 NCPU=4
*TITLE
*CONTROL_CONTACT
*CONTROL_ENERGY
*CONTROL_OUTPUT
*CONTROL_PARALLEL
*CONTROL_TERMINATION
*CONTROL_TIMESTEP
*DATABASE_ELOUT
*DATABASE_GLSTAT
*DATABASE_MATSUM
*DATABASE_NODOUT
*DATABASE_RBDOUT
*DATABASE_RCFORC
*DATABASE_BINARY_D3DUMP
*DATABASE_BINARY_D3PLOT
*DATABASE_BINARY_D3THDT
*DATABASE_EXTENT_BINARY
*BOUNDARY_SPC_SET
*SET_NODE_LIST
*BOUNDARY_SPC_SET
*SET_NODE_LIST
*CONTACT_ERODING_SURFACE_TO_SURFACE_MPP_ID
*SET_PART_LIST_TITLE
*CONTACT_ERODING_SURFACE_TO_SURFACE_MPP_ID
*SET_PART_LIST_TITLE
*SECTION_SOLID_TITLE
*MAT_PIECEWISE_LINEAR_PLASTICITY_TITLE
*SECTION_SOLID_TITLE
*SECTION_SOLID_TITLE
*MAT_PIECEWISE_LINEAR_PLASTICITY_TITLE
*PART
*SECTION_SOLID_TITLE
*SECTION_SOLID_TITLE
*INITIAL_VELOCITY_GENERATION
*DEFINE_TABLE_TITLE
*DEFINE_CURVE_TITLE
*ELEMENT_SOLID
*NODE
*END
```

Appendix 15

Sampled node positions

Lingual Node Positions

Node position	Node number
1	66947
2	40133
3	96434
4	41115
5	109081
6	57569
7	38274
8	66823
9	2863
10	66036
11	99613
12	80656
13	68702
14	100398
15	85719
16	9939
17	88175
18	56657
19	36916
20	737
21	28987
22	58496
23	89438
24	7615
25	76187
26	43146
27	101434
28	46645
29	39374
30	80778
31	30223
32	6246
33	33115
34	68533
35	108104
36	298
37	111833
38	39121
39	32727
40	99139
41	11311
42	71462
43	82036
44	61082
45	93164
46	104380
47	102012
48	102620
49	111174
50	10054
51	110185
52	22327
53	60621
54	49812
55	19478
56	79351
57	93726
58	32247
59	80180
60	84157
61	22710
62	33528
63	53369
64	81735
65	110241
66	42861
67	100830
68	63962
69	22373
70	91866
71	3873
72	76103
73	110516
74	13503

Buccal Node Positions

Node Positions	Actual Nodes
1	38932
2	63245
3	57990
4	25731
5	66328
6	98457
7	49226
8	37462
9	98338
10	94133
11	47551
12	89739
13	114930
14	86562
15	15126
16	76026
17	10033
18	84683
19	102009
20	125349
21	80502
22	121649
23	66001
24	87555
25	284
26	66259
27	48157
28	83408
29	99411
30	10560
31	2735
32	50029
33	7875
34	44231
35	24232
36	108295
37	98690
38	66479
39	63273
40	70032
41	84481
42	90808
43	79680
44	5876
45	70450
46	36655
47	24454
48	86992
49	80475

Appendix 16

Licences

Royalty Free License
http://support.turbosquid.com/entries/28757878

http://www.turbosquid.com/3d-models/maya-set-hands/481903,

Creative Commons Licence
https://creativecommons.org/licenses/by/3.0/legalcode

ISB 2015 Copyright

"Copyright Policy: By submitting the abstract, all authors confirm that: (1) they own the copyright and have not used copyrighted material without permission, and (2) the abstract has not been previously published or submitted elsewhere. By submitting the abstract, the authors transfer their copyright to the International Society of Biomechanics (ISB) pending acceptance of the abstract for presentation at the conference. In return, the ISB grants permission to the authors and to the Congress to publish the abstract in online repositories, provided that the abstract, and any reference to it, clearly identifies the ISB and the Congress where the abstract was presented. The authors also have permission to submit the work for journal publication. The copyright will be returned to the authors if the abstract is withdrawn before it is included in the proceedings".

Appendix 17

Review Protocol (Meta-analysis)

Review objective

The objective of this review is to determine the anatomical sub-site fracture frequency of the mandible as a result of trauma

Participants

Studies reporting the prevalence of mandibular sub-site fractures in humans as a result of trauma.

Interventions

All patients presenting with traumatically induce mandibular fractures, given conservative or surgical treatment.

Outcome

Any outcome related to mandibular fracture sub-site frequency that used the Dingman and Natvig classification system or one which could easily be mapped to it.

Study design

Prospective or retrospective case series reports will be examined. Retrospective reports must include all patients examined within the study period. A study must include at least a review of radiographic records of patients. Studies that include only patients that have undergone surgical treatment will be excluded due to the potential for bias. Database searches will be ineligible unless such a search includes a radiographic review. Studies that only include frequency data without details of the number of cases or number of

fractures will be excluded. For the purposes of the study, multiple fractures at different sub-sites in the same case will be counted. Eligible studies reporting several datasets (e.g. where the data has been sub-divided to perform another analysis) will have all data recombined into a single dataset.

Appendix 18

Symphyseal impact graphs

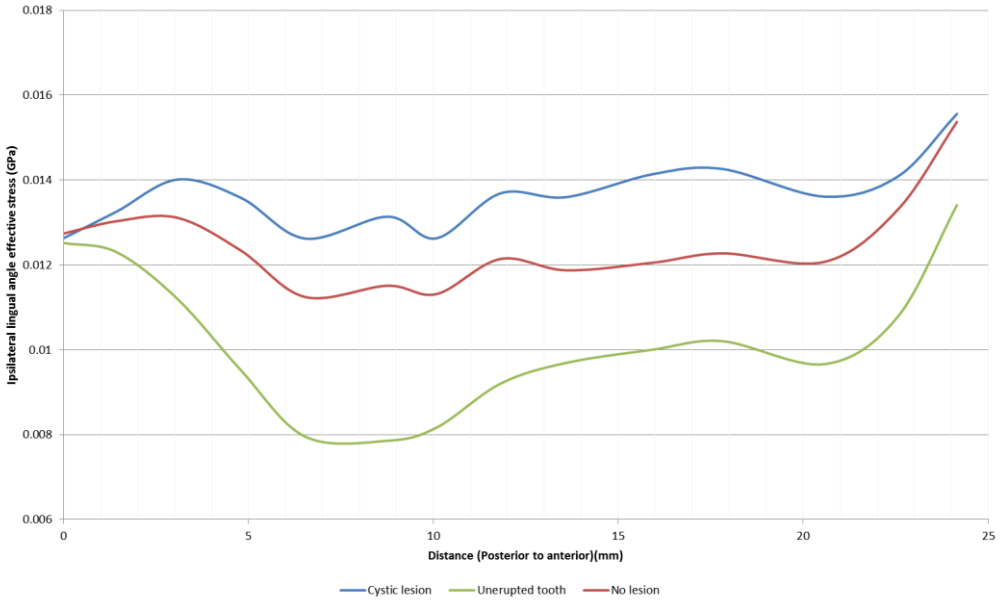

The figure shows the variation of right lingual angle cortical stress (σ_{vm})(GPa) for the node set following impact at the symphysis of the mandible. Three cases are considered, as shown. The same sample set is used in each case. The sample takes place at 0.2ms (i.e. just before the condylar neck fractures).

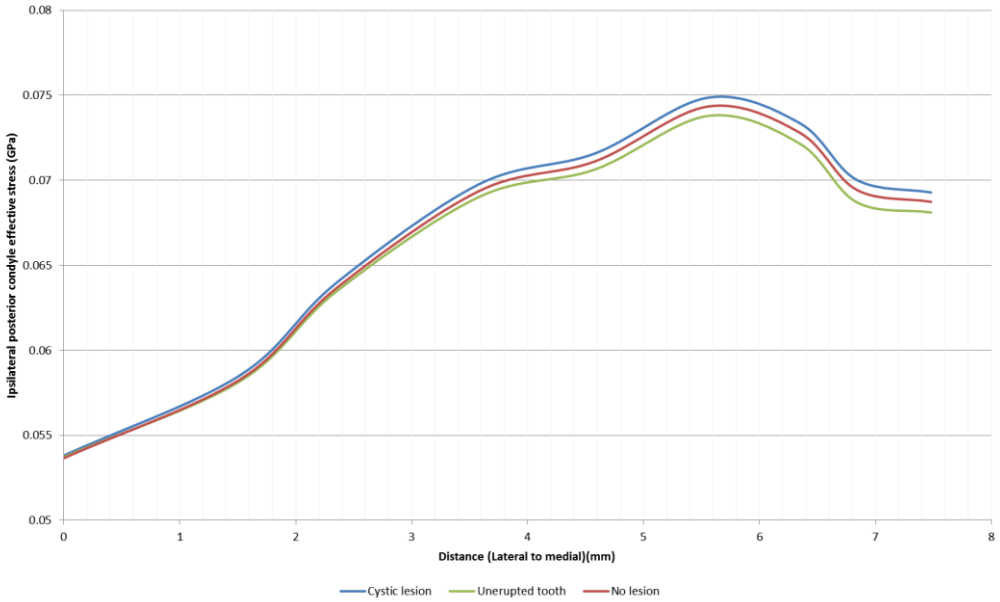

The figure shows the variation of right posterior condylar cortical stress (σ_{vm})(GPa) for the node set following impact at the symphysis of the mandible. Three cases are considered, as shown. The same sample set is used in each case. The sample takes place at 0.2ms (i.e. just before the condylar neck fractures).

Appendix 19

Data search exclusion criteria

Design	Letters related to mandibular trauma.
	Narrative reviews with no original data.
	Book chapters not reporting the original data source.
	Studies that failed to provide either raw numbers of the effect measures or prevalence estimates.
	Studies relating to facial fractures without detailed information on mandibular fractures.
	Studies reporting pathological fractures.
	Studies related to high-energy injuries resulting in severely comminuted fractures e.g. ballistic, explosions.
	Studies relating to only surgically treated fractures.
	Studies confined to a mandibular fractures in a single anatomical region e.g. Condyle and sub-condyle.
Data recorded	Studies not reporting sample size.
	Studies not employing and appropriate classification of mandibular anatomical fractures sub-classification.
	No data verification i.e. no examination of notes or radiographs by authors.